

L

ASSESSING POWER PLANT COOLING WATER INTAKE SYSTEM ENTRAINMENT IMPACTS

Prepared For:

California Energy Commission

Prepared By:

**JOHN STEINBECK, Tenera
Environmental Inc.**

**JOHN HEDGEPEETH, Tenera
Environmental Inc.**

**PETER RAIMONDI, Department of
Ecology and Evolutionary Biology,
University of California, Center for
Ocean Health, Long Marine Lab**

**GREGOR CAILLIET, Moss Landing
Marine Laboratories**

**DAVID MAYER, Tenera Environmental
Inc.**

CONSULTANT REPORT

OCTOBER 2007

CEC-700-2007-010

Prepared By:

Tenera Environmental Inc.
John Steinbeck
San Luis Obispo, California
Contract No. 700-05-002

Prepared For:

**CALIFORNIA ENERGY
COMMISSION**

Rick York
Project Manager

Paul Richins
Manager
ENVIRONMENTAL OFFICE

Terrence O'Brien
Deputy Director
ENERGY FACILITIES SITING DIVISION

B. B. Blevins
Executive Director

DISCLAIMER

This report was prepared as the result of work sponsored by the California Energy Commission. It does not necessarily represent the views of the Energy Commission, its employees, or the State of California. The Energy Commission, the State of California, its employees, contractors, and subcontractors make no warrant, express or implied, and assume no legal liability for the information in this report; nor does any party represent that the uses of this information will not infringe upon privately owned rights. This report has not been approved or disapproved by the California Energy Commission nor has the California Energy Commission passed upon the accuracy or adequacy of the information in this report.

ACKNOWLEDGEMENTS

It should be obvious that large studies like these require the coordinated work of many people. We would first like to thank the California Energy Commission, especially Rick York and Dick Anderson, for funding this study and recognizing the importance of publishing this work so it could be used by other researchers and decision makers. Thanks also to Duke Energy and Pacific Gas and Electric Company (PG&E) for the use of the data from the Duke Energy South Bay and Morro Bay power plants and the PG&E Diablo Canyon Power Plant. Special thanks go to James White and Brian Waters from Duke Energy, and Kathy Jones, Anne Jackson, Jim Kelly, and Bryan Cunningham from PG&E. We also want to thank Michael Thomas from the Central Coast Regional Water Quality Control Board who organized the Technical Workgroup that provided input on the Diablo Canyon and Morro Bay studies, which provided a model of cooperative science used in other studies throughout the state. More special thanks go to the Technical Workgroup members from various state and federal resource agencies and academia who provided valuable input on all three studies. Dr. John Skalski helped develop the models used in the assessments, and Drs. Roger Nisbet, Allen Stewart-Oaten, Alec MacCall, and others provided valuable input on various aspects of the studies. We want to thank Chris Ehrler and Jay Carroll from Tenera Environmental and Rick York and Joanna Grebel from the California Energy Commission for their editorial assistance with the report. We also received helpful comments on the final draft from Larry Barnthouse, Shane Beck, Kathleen Jones, Erika McPhee-Shaw, Roger Nisbet, and Pat Tenant. Finally we want to thank all of the scientists and technicians at Tenera Environmental who collected all of these data and processed the hundreds of samples collected from the three studies.

ABSTRACT

Steam electric power plants and other industrial facilities that withdraw cooling water from surface water bodies are regulated in the United States under Section 316(b) of the Clean Water Act of 1972. Of the industries regulated under Section 316(b), steam electric power plants represent the largest cooling water volumes with some large plant withdrawals exceeding 2 billion gallons per day. Environmental effects of cooling water withdrawal result from the impingement of larger organisms on screens that block material from entering the cooling water system and the entrainment of smaller organisms into and through the system. This paper focuses on methods for assessing entrainment effects (not impingement), and specifically, entrainment effects on ichthyoplankton. This report describes three studies that assessed entrainment at coastal power plants in California and discusses some of the considerations for the proper design and analysis of entrainment studies.

KEYWORDS

Once-through cooling, entrainment, impingement, Clean Water Act, 316(b), coastal power plants, marine life

TABLE OF CONTENTS

LIST OF TABLES	VII
LIST OF FIGURES	IX
EXECUTIVE SUMMARY	1
INTRODUCTION	5
METHODS	11
POWER PLANT DESCRIPTIONS.....	11
SOURCE WATER AND SOURCE POPULATION DEFINITIONS.....	13
SAMPLING.....	19
SELECTION OF TAXA FOR DETAILED ASSESSMENT.....	23
OTHER BIOLOGICAL DATA.....	28
DATA REDUCTION.....	29
SOURCE WATER ESTIMATES.....	32
IMPACT ASSESSMENT MODELS	32
RESULTS	51
SOUTH BAY POWER PLANT.....	51
MORRO BAY POWER PLANT.....	58
DIABLO CANYON POWER PLANT	68
DISCUSSION	83
GUIDELINES FOR ENTRAINMENT IMPACT ASSESSMENT.....	94
CONCLUSION.....	98
ACKNOWLEDGEMENTS	ERROR! BOOKMARK NOT DEFINED.
LITERATURE CITED	99

APPENDICES

- A. Variance Calculations for FH, AEL, and ETM models
- B. Mean larval fish concentrations by station in San Diego Bay
- C. Estimates of CIQ goby larvae at SBPP used in calculating ETM estimates of PE and annual estimate of proportional mortality (P_M).
- D. Estimates of KGB rockfish larvae at MBPP used in calculating ETM estimates of PE and annual estimate of proportional mortality (P_M).
- E. Estimates of KGB rockfish larvae at DCPD used in calculating ETM estimates of PE and annual estimate of proportional mortality (P_M).
- F. Regression estimates, onshore and alongshore current meter displacement, source water estimates, and estimates of the proportion of source water sampled (P_S) used in calculating ETM for KGB rockfish larvae at DCPD.

LIST OF TABLES

Table 1. Characteristics of the South Bay (SBPP), Morro Bay (MBPP), and Diablo Canyon (DCPP) power plants.....	13
Table 2. Source water body surface area and water volume at mean water level (MWL) by region for south San Diego Bay.....	17
Table 3. Volumes for Morro Bay and Estero Bay source water sub-areas.....	18
Table 4. Taxa used in assessments at South Bay (SBPP), Morro Bay (MBPP) and Diablo Canyon (DCPP) power plants.....	25
Table 5. Pigment groups of some preflexion rockfish larvae from Nishimoto (in-prep).	27
Table 6. Total annual entrainment estimates of larval fishes at South Bay Power Plant.....	52
Table 7. Results of fecundity hindcasting (FH) modeling for CIQ goby complex larvae entrained at South Bay Power Plant.	55
Table 8. Results of adult equivalent loss (AEL) modeling for CIQ goby complex larvae entrained at South Bay Power Plant.	56
Table 9. Estimates of proportional entrainment (PE) and proportion of source water population present for CIQ goby larvae at South Bay Power Plant entrainment and source water stations	58
Table 10. Summary of estimated South Bay Power Plant entrainment effects ..	58
Table 11. Total annual entrainment estimates of fishes and invertebrates at Morro Bay Power Plant	59
Table 12. Annual estimates of adult female kelp, gopher, and black-and-yellow (KGB) rockfish losses at Morro Bay Power Plant based on larval entrainment estimates using the fecundity hindcasting (FH) model.....	64
Table 13. Survival of the kelp, gopher, and black-and-yellow (KGB) rockfish complex larvae to an age of three years	65
Table 14. Annual estimates of adult kelp, gopher, and black-and-yellow (KGB) rockfish losses at Morro Bay Power Plant due to entrainment using the adult equivalent loss (AEL) model	66
Table 15. Estimates of KGB rockfish larvae at MBPP entrainment and source water stations.....	66
Table 16. Summary of estimated Morro Bay Power Plant entrainment effects. ..	67

Table 17. Fishes collected during Diablo Canyon Power Plant entrainment sampling.	69
Table 18. Diablo Canyon Power Plant entrainment estimates and standard errors for kelp, gopher, and black-and-yellow (KGB) rockfish complex.	71
Table 19. Diablo Canyon Power Plant fecundity hindcasting (FH) estimates for kelp, gopher, and black-and-yellow (KGB) rockfish complex	76
Table 20. Diablo Canyon Power Plant adult equivalent loss (AEL) estimates for kelp, gopher, and black-and-yellow (KGB) rockfish complex..	77
Table 21. Estimates used in calculating empirical transport model (ETM) estimates of proportional entrainment (PE) for kelp, gopher, and black-and-yellow (KGB) rockfish complex for Diablo Canyon Power Plant	78
Table 22. Onshore and alongshore current meter displacement used in estimating proportion of source water sampled (P_s)	80
Table 23. Results of entrainment monitoring and FH, AEL, and ETM modeling for 14 fishes at Diablo Canyon Power Plant.....	82

LIST OF FIGURES

Figure 1. Conceptual diagram of power plant cooling water systems at South Bay, Morro Bay, and Diablo Canyon Power Plants.....	6
Figure 2. Locations of Morro Bay (MBPP), Diablo Canyon (DCPP), and South Bay Power Plants (SBPP).....	10
Figure 3. Location of South Bay Power Plant entrainment (SB01) and source water stations and detail of power plant intake area.	12
Figure 4. Locations of Morro Bay Power Plant entrainment (Station 2) and source water stations.....	14
Figure 5. Locations of Diablo Canyon Power Plant (DCPP) entrainment stations and source water sampling grid.	15
Figure 6. Relative cumulative upcoast/downcoast and onshore/offshore current vectors from Diablo Canyon Power Plant	47
Figure 7. Monthly mean larval concentration of the <i>Clevelandia ios</i> , <i>Ilypnus gilberti</i> , and <i>Quietula y-cauda</i> (CIQ) goby complex larvae at SBPP	53
Figure 8. Length frequency distribution for CIQ goby complex larvae from the South Bay Power Plant entrainment station.....	54
Figure 9. Weekly mean larval concentration of kelp, gopher, and black-and-yellow (KGB) rockfish complex larvae at the Morro Bay Power Plant intake entrainment station.	61
Figure 10. Comparison of average concentrations of kelp, gopher, and black-and-yellow (KGB) rockfish complex larvae at the Morro Bay Power Plant intake, Morro Bay source water, and Estero Bay	62
Figure 11. Length frequency distribution for kelp, gopher, and black-and-yellow (KGB) rockfish complex larvae from the Morro Bay Power Plant entrainment station.	63
Figure 12. Weekly mean larval concentrations of kelp, gopher, and black-and-yellow (KGB) rockfish complex larvae at the Diablo Canyon Power Plant intake entrainment stations.....	71
Figure 13. Annual mean concentration (+/- 2 standard errors) for kelp, gopher, and black-and-yellow (KGB) rockfish complex larvae collected from surface plankton tows in DCPP Intake Cove.	72
Figure 14. Average concentration for kelp, gopher, and black-and-yellow (KGB) rockfish complex larvae in each of the 64 nearshore stations for DCPP.....	74

Figure 15. Length frequency distribution for kelp, gopher, and black-and-yellow (KGB) rockfish complex larvae measured from entrainment stations at Diablo Canyon Power Plant intake..... 75

EXECUTIVE SUMMARY

Steam electric power plants and other industries that withdraw cooling water from surface water bodies are regulated in the United States under Section 316(b) of the Clean Water Act of 1972. Of the industries regulated under Section 316(b), steam electric power plants have the largest cooling water volumes with some large plants exceeding 2 billion gallons per day. Environmental effects of cooling water withdrawal result from impingement of larger organisms on screens that block material from entering the cooling water system and the entrainment of smaller organisms into and through the system.

Concerns regarding the environmental effects of entrainment result from the large volume of cooling water potentially used by coastal power plants. In California, the 21 coastal power plants potentially withdraw up to 17 billion gallons of seawater per day. This process results in the loss of billions of aquatic organisms, including fishes, fish larvae and eggs, crustaceans, shellfish, and many other forms of aquatic life from California's coastal ecosystem each year. There has been increased focus on the effects of power plant cooling water intake systems because the biological resources of the world's oceans, and California's coast in particular, are in serious decline. Long-term declines, which started in the early 1970s, have occurred in 60 percent of the fishes for which landings are reported. Despite the potential contribution of cooling water withdrawal to these declines, recent studies have only been completed at a few of the California power plants (California Energy Commission 2005). Regulations for Section 316(b) of the Clean Water Act published in July 2004 (USEPA 2004) will result in new studies on the environmental effects of cooling water systems at many of the existing power plants in California and throughout the country. The results of these studies will help determine the environmental effects of cooling water withdrawal on biological communities.

While the assessment of impingement effects is relatively straightforward, the assessment of entrainment effects requires thoughtful consideration of all aspects of the study design. The difficulties in entrainment assessments arise from several factors. The organisms entrained include planktonic larvae of fishes and invertebrates that are difficult to sample and identify. The entrained larvae are also part of larger source water populations that may extend over large areas or be confined to limited habitats, making it difficult to determine the effects of entrainment losses. The early life histories of most fishes on the Pacific Coast are also poorly described, limiting the usefulness of demographic models for assessing entrainment effects. All of these factors make the assessment of cooling water system entrainment difficult. This report will present, by example, some of the considerations for the proper design and analysis of entrainment studies.

This report describes three studies for assessing entrainment at coastal power plants in California. They represent a range of marine and estuarine habitats: the South Bay Power Plant in south San Diego Bay and the Morro Bay and Diablo Canyon power plants in Central California. These studies used a multiple modeling approach for assessing entrainment effects. When appropriate life history information was available for a species, demographic modeling techniques were used to calculate the numbers of adults represented by the losses of fish eggs and larvae due to entrainment. The primary approach for assessment at these plants was the "Empirical Transport Model" (ETM), originally developed for use with power plants entraining water from rivers, and then adapted for use on the open coast and in estuaries in Southern California. The Empirical Transport Model uses the same principles as fishery management to estimate effects of fishing mortality on the sustainability of a stock. Just as fishery managers use catch and population size to estimate fishery mortality, the Empirical Transport Model requires estimates of both entrainment and source water larval populations. The source water population is the abundance of organisms at risk of entrainment as determined by biological and hydrodynamic/oceanographic data. The process of defining the source water and obtaining an estimate of its population varied among the three plants and also among species within studies. This paper will present the multiple modeling approaches used for power plant entrainment assessments, with the main focus being a comparison of the processes used to define the source water populations used in the Empirical Transport Modeling from the three power plants.

The results showed that standard demographic models were generally not usable with species found along the California coast due to the absence of life history information for most of them. The results for the Empirical Transport Model ranged from very small levels (<1.0 percent) of proportional mortality due to entrainment for wide ranging pelagic species such as northern anchovy to levels as high as 50 percent for fishes with more limited habitat that were spawned near power plant intake structures. The results of the Empirical Transport Model were generally consistent with the biology and habitat distributions of the fishes analyzed.

Based on experiences with these and other studies, the authors believe that a prescriptive approach to the design of entrainment assessments is not possible, and therefore, some general considerations are provided that might be helpful in the design, sampling, and analysis of entrainment impact assessments. These include ensuring that organisms that could be affected by entrainment are effectively sampled and that the sampling will account for any endangered, threatened, or other listed species that could be affected by entrainment. In addition to identifying species potentially affected, it is critical to determine the source water areas potentially affected, including the distribution of habitats that might be differentially affected by cooling water intake system (CWIS) entrainment. The sampling plan also needs to account for the design,

location, and hydrodynamics of the power plant intake structure. The sampling frequency should accommodate important species that might have short spawning seasons. This may require that the sampling frequency be seasonally adjusted based on presence of certain species. The relative effects of entrainment estimated by the ETM model should be much less subject to interannual variation than absolute estimates using “fecundity hindcasting” (FH), “adult equivalent loss” (AEL), or other demographic models. Therefore, if source water sampling is done along with entrainment sampling, then one year is a reasonable period of sampling for these studies. The size of the source water sampling area should be based on the hydrodynamics of the system. In a closed system, this may be the entire source water. In an open system, ocean or tidal currents and dispersion should be used to determine the appropriate sampling area for estimating daily entrainment mortality (PE) for the larger source water population.

Some practical considerations for sample collection and processing include adjusting the sample volume for the larval concentrations in the source waters. This is best done using preliminary sampling with the gear proposed for the study. Age of larvae are best determined using analysis of otoliths, but if this is not possible, be sure that length frequencies measured from the entrainment samples are realistic based on available life history and account for egg stages that would be subject to entrainment if fish eggs are not sorted and identified from the samples. This is easily accommodated in the Empirical Transport Model approach by adding the duration of the planktonic egg stage to the larval duration calculated from the otolith or length data.

Although the authors believe that the Empirical Transport Model is best approach for assessment, results from multiple models provide additional information for verifying results and for determining effects at the adult population level. One approach for assessment at the adult population level is through converting Empirical Transport Model results into an estimate of the habitat necessary to replace the production lost due to entrainment (“area of production foregone” [APF]). The area of production foregone is calculated by multiplying the area of habitat present within the estimated source water by the proportional entrainment mortality estimated from Empirical Transport Model. This approach may be useful for scaling restoration projects to help offset losses due to entrainment. The ETM can also be used to estimate the number of equivalent adults lost by entrainment by applying the mortality estimate to a survey of the standing stock. This can be compared with estimates from Fecundity Hindcast and Adult Equivalent Loss. When making these types of comparisons, it is important to hindcast or extrapolate the Fecundity Hindcast and Adult Equivalent Loss model estimates to the same age. This may not necessarily result in the same estimates from both models unless the data used in the two models are derived from a life table assuming a stable age distribution. The USEPA (2002) used Adult Equivalent Loss and another demographic

modeling approach, production foregone, to estimate the number of age-1 individuals lost due to power plant impingement and entrainment. The accuracy of estimates from any of these demographic models is subject to the underlying uncertainty in aging, survival, and fecundity estimates and population regulatory, behavioral, or environmental factors that may be operating on the subject populations at the time the life history data were collected.

Uncertainty associated with the Empirical Transport Model is primarily derived from sampling error that can be controlled by careful design using some of the guidelines provided in this report. With a good sampling design, the Empirical Transport Model provides a site-specific, empirically based approach to entrainment assessment that is a major improvement over demographic modeling approaches. In addition, the results can be used to estimate entrainment effects on other planktonic organisms, in estimating cumulative effects of multiple power plants and other sources of mortality, and in scaling restoration efforts to offset losses due to entrainment. The authors hope that the information in this report will assist others in the design and analysis of cooling water intake system assessments that will be required as a result of the recent publication of new rules for Section 316(b) of the Clean Water Act (USEPA 2004).

CHAPTER 1: INTRODUCTION

Steam electric power plants and other industries (for example, pulp and paper, iron and steel, chemical, manufacturing, petroleum refineries, and oil and gas production) use water from coastal areas for cooling resulting in impacts to the marine organisms occupying the affected water bodies. Industries that withdraw cooling water from surface water bodies are regulated in the United States under Section 316(b) of the Clean Water Act of 1972 [33 U.S. Code Section 1326(b)]. Section 316(b) requires "...that the location, design, construction, and capacity of cooling water intake structures reflect the best technology available for minimizing adverse environmental impacts." Of the industries regulated under section 316(b), steam electric power plants have the largest cooling water volumes ranging from tens of thousands to millions of cubic meters per day ($m^3 d^{-1}$) (Veil et al. 2003). A survey in 1996 reported that 44 percent of the power plants in the United States used a steam electric process involving once-through cooling (Veil 2000). Electricity is generated at these plants by heating purified water to create high-pressure steam, which is expanded in turbines that drive generators and produce electricity (Figure 1). After leaving the turbines, steam passes through a condenser where high volume cooling water flow cools and condenses the steam, which is then recirculated back through the system.

Regulatory guidance for complying with Section 316(b) that was first proposed by the U.S. Environmental Protection Agency (EPA) in 1976 was successfully challenged in the courts by a group of 58 utility companies in 1977 and never implemented (Bulleit 2000). As a result, Section 316(b) was implemented by the states using a broad range of approaches; some states developed fairly comprehensive programs while others never adopted any formal regulations (Veil et al. 2003). The EPA has recently published new regulations for 316(b) compliance (USEPA 2004) as part of the settlement of a lawsuit against the EPA by environmental groups headed by the Hudson Riverkeeper (Nagle and Morgan 2000). As a result of these new regulations, power plants throughout the United States are now required to reduce the environmental effects of their cooling water intake systems (CWIS).

The withdrawal of water by once-through cooling water systems has two major impacts on the biological organisms in the source water body: impingement and entrainment (Figure 1). Almost all power plants with once-through cooling employ some type of screening device to block large objects from entering the cooling water system (impingement). Fishes and other aquatic organisms large enough to be blocked by the screens may become impinged if the intake velocity exceeds their ability to move away. These organisms will remain impinged against the screens until intake velocity is reduced such that organisms can move away or the screen is backwashed to remove them. Some organisms are killed, injured, or weakened by impingement. Small

planktonic organisms or early life stages of larger organisms that pass through the screen mesh are entrained in the cooling water flow. These organisms are exposed to high velocity and pressure due to the cooling water pumps, increased temperatures and, in some cases, chemical treatments added to the cooling water flow to reduce biofouling.

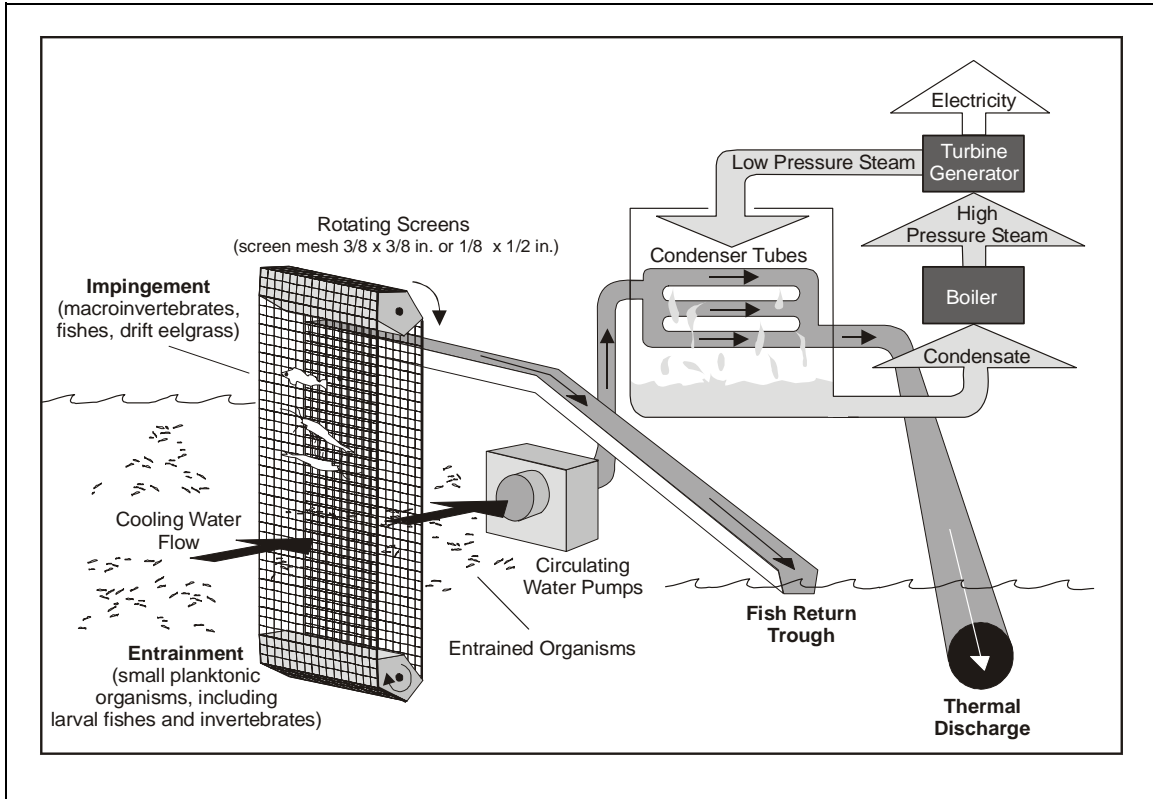


Figure 1. Conceptual diagram of power plant cooling water systems at South Bay, Morro Bay, and Diablo Canyon Power Plants, and relationship of impingement and entrainment processes to circulating water system. A fish return trough is present only at the South Bay Power Plant.

Most impingement and entrainment (316[b]) studies on CWIS effects at power plants were completed in the late 1970s and early 1980s using draft guidance issued by the EPA (USEPA 1977). More recently, many power plants throughout the country began to upgrade and expand their generating capacities due to increased demands for power. The California Energy Commission (Energy Commission), which had regulatory authority for these projects in California, required utility companies to determine the impacts of these CWIS changes. Although existing CWIS are regulated in California through National Pollution Discharge Eliminations System (NPDES) permits issued by the nine Regional Water Quality Control Boards (RWQCB) in the state, the projects done under the regulatory authority of the Energy Commission also required coastal zone permits under the California Coastal Act and therefore were conducted in compliance

with the California Environmental Quality Act (CEQA). The Energy Commission and the RWQCBs required new studies in anticipation of the publication of new EPA regulations, but also because data on CWIS impacts were not available for some of the plants and studies at other plants were usually over 20 years old. As a result, the authors had the opportunity in California to develop approaches to assessing CWIS impacts that might prove useful to researchers at power plants throughout the United States. These studies involved regulatory agency staff, scientists, consultants, and industry representatives, usually meeting and working under the heading of Technical Workgroups. This collaborative process was first used for studies at the Pacific Gas & Electric Company Diablo Canyon Power Plant and was initiated and directed by Michael Thomas at the Central Coast Regional Water Quality Control Board (CCRWQCB) (Ehrler et al. 2003). This process was also used on studies for plant repowering projects under Energy Commission and RWQCB review at the Moss Landing, Morro Bay, Potrero and Huntington Beach power plants.

This paper focuses on methods for assessing only entrainment effects (not impingement) and, specifically, entrainment effects on ichthyoplankton. Entrainment affects all types of planktonic organisms, but most studies do not assess holoplankton (phytoplankton and zooplankton that are planktonic for their entire life) because their broad geographic distributions and short generation times reduce the effects of entrainment on their populations. In contrast, the potential for localized effects on certain fish populations is much greater, especially for power plants located in riverine or estuarine areas where a large percentage of the local population may be at risk of entrainment (Barnthouse et al. 1988, Barnthouse 2000). Although the potential for similar effects exists for certain invertebrate meroplankton (for example, crab and clam larvae), taxonomy of early larval stages of many invertebrates is not sufficiently advanced to allow for assessments at the species level. The different larval stages of many invertebrates may also require different mesh sizes and sampling techniques that increase the costs and complexity of a study. In contrast, as a result of programs such as the California Coastal Oceanographic Fisheries Investigations (CalCOFI) program, operating since 1950, ichthyoplankton of the West Coast have been well described, and long-term data sets exist on the abundances of many larval fishes (Moser 1996).

The best-documented and most extensive 316(b) studies from the period of the late 1970s and early 1980s were from the Hudson River power plants (Barnthouse et al. 1988, Barnthouse 2000). Impacts of cooling water withdrawals from three plants were extensively studied using long-term, riverwide sampling and analyzed using mathematical models designed to predict the effects on striped bass and other fish populations. After many years of debate surrounding a lawsuit, the case was settled out of court. Two of the most important factors in laying the groundwork for the settlement were the converging estimates of the effects from different researchers and the

development of models that estimated conditional mortality from empirical data that reflected the “complex interactions of a host of factors” and helped identify the “relative importance of each component of the analysis” (Englert and Boreman 1988).

Numerous demographic modeling approaches have been proposed and used for projecting losses from CWIS impacts (Dey 2003). Equivalent adult (Horst 1975, Goodyear 1978), production foregone (Rago 1984), and variations of these approaches and models (Dey 2003) translate entrainment losses of egg and larval stages into equivalent units (adult fishes, biomass, and so forth) that otherwise would not have been lost to the population. Although these models are the most commonly used methods for CWIS assessment and were used by the EPA to support the new 316(b) regulations (USEPA 2004), there can be problems with their application and interpretation. The models require life history parameters (larval duration, survival, fecundity, and so forth) that are available for only a limited number of species, generally those managed for commercial or recreational fishing. Our experience has shown that on the California coast, taxa (the term ‘taxa’ [‘taxon’ singular] is used to refer to individual species or broader taxonomic categories that cannot be identified to species) that are usually entrained in highest numbers are small, forage fishes that have very limited life history information available.

However, these models are attractive because their interpretation appears to be straightforward since they convert larval forms into “equivalent units” that are more easily understood by the public, regulators, and managers. The estimates of numbers or biomass of fish from the models can also be added to losses from impingement and compared with commercial or recreational fishery data to provide cost estimates of the losses. Unfortunately, these interpretations are available for only a few taxa, there is usually no scale for determining the significance of the losses to the source water populations, and the studies are only done for a one- to two-year period, not accounting for inter-annual variation in larval abundances. The source water population is the abundance of organisms at risk of entrainment as determined by biological and hydrodynamic/oceanographic data.

Our assessments included a modified version of the Empirical Transport Model (ETM) (Boreman et al. 1978, 1981), which circumvented the problems with existing demographic modeling. This model was first developed for use with power plants entraining water from rivers, but MacCall et al. (1983) used the same general approach for entrainment assessments at power plants on the open coast and in estuaries in Southern California. In contrast to demographic models, it does not require detailed life history information. The ETM provides an estimate of the mortality caused by entrainment to a source water population independent of any other sources of mortality, such as conditional mortality (Ricker 1975). Inherent in this approach is the requirement

for an estimate of the source water population of larvae affected by entrainment. The ETM is based on the same principles used in fishery management to estimate effects of fishing mortality on a source water population or stock (Boreman et al. 1981, MacCall et al. 1983). Although not specifically required for calculating estimated losses, an estimate of the source water population is also required to provide a context for the losses estimated by demographic models.

The process of defining the source water and obtaining an estimate of its population varies among studies and among taxa within studies. This paper will present the multiple modeling approaches used for power plant entrainment assessments, with the main focus being a comparison of the processes used to define the source water populations used in the ETM modeling from three power plants in California, South Bay Power Plant (SBPP), Morro Bay Power Plant (MBPP), and Diablo Canyon Power Plant (DCPP), which represent a range of marine and estuarine habitats (Figure 2). This comparison allows us to compare the approaches and assess the influence of the source water on the proportional mortality of affected fish and invertebrate larval taxa.

The source water population definitions for the three studies were based on the hydrodynamic and biological characteristics of the water bodies where the facilities were located. This is necessary to characterize the sources of the water that is drawn into a power plant. This is fairly simple if the source of cooling water is a lake that is so well mixed that the larval concentrations are uniform. In this case the only necessary information to estimate the mortality on the larvae is the volume of the lake and the plant cooling water volume. In this simple example, the mortality is the ratio of the cooling water volume to the source water volume since the concentration of larvae entrained will be equal to the concentration in the source water. In the case of SBPP, samples were collected throughout the entire source water since the larval composition in the habitats within the south part of San Diego Bay were potentially different even though the source water volume for SBPP was treated as a closed system similar to the lake in the above example. The source water for MBPP included both bay and ocean components requiring biological sampling in both locations and calculations to include the effects of tides on the source water. The effects of ocean currents affected the source water potentially entrained for DCPP and the ocean component of the MBPP source water. As a result, the source water potentially affected by entrainment was much larger than the areas sampled for these two studies requiring additional measurements and modifications to the model. The many factors that need to be considered in the design of these kinds of studies can be examined by comparing the different approaches taken at the three facilities.

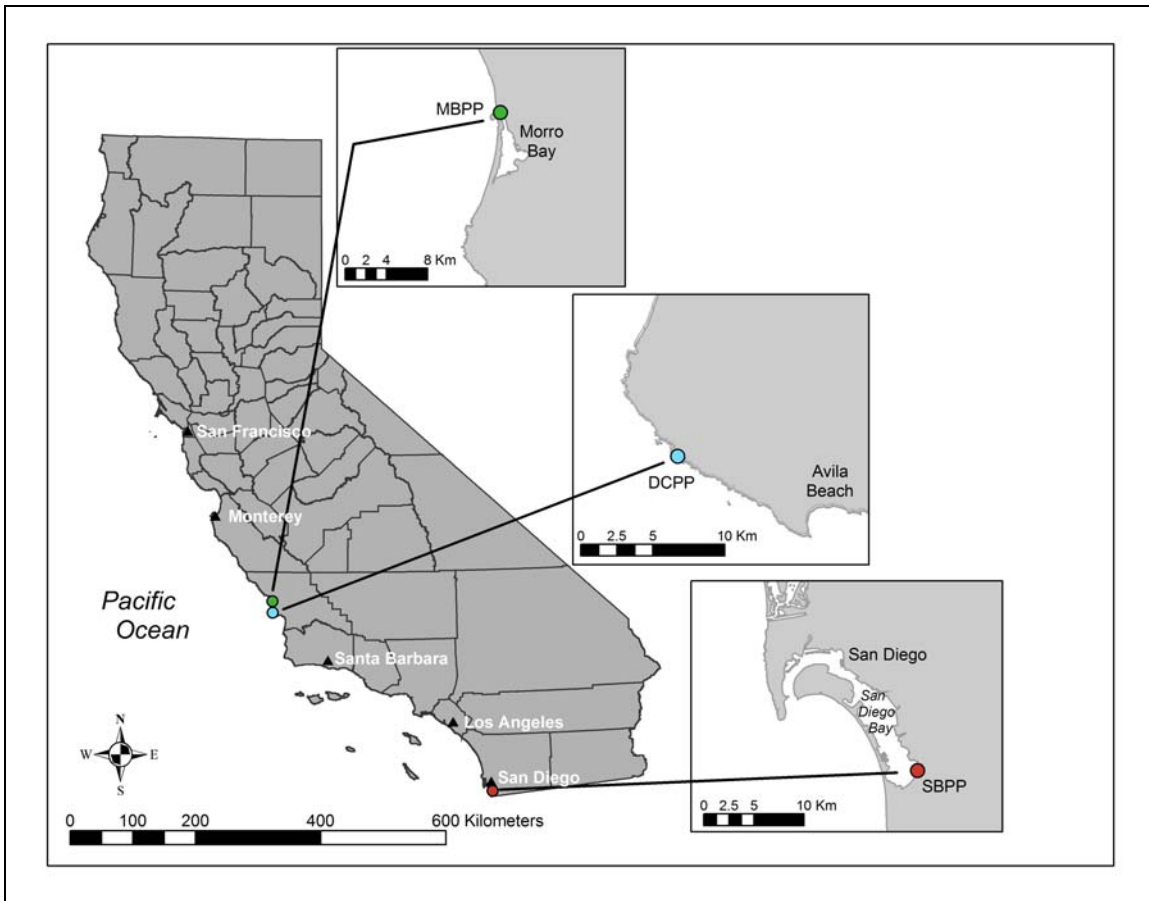


Figure 2. Locations of Morro Bay (MBPP), Diablo Canyon (DCPP), and South Bay power plants (SBPP).

During the course of these studies, the authors have modified the assessment approaches, and this process has continued as the authors have participated in additional, more recent studies. Therefore, one of the additional purposes of this paper is to present these more recent changes in assessment methods even though they may differ from methods presented in the three example studies.

The experiences resulting from these studies are especially pertinent with the recent publication of new rules for Section 316(b) of the Clean Water Act (USEPA 2004), and Energy Commission and California Coastal Commission (CCC) requirements for modernizing power plants in California. The new 316(b) rules require that information on the source water body be submitted as part of 316(b) compliance (40 CFR 125.95[b][2]). Although not stated in the new rules, it seems appropriate that CWIS impacts would be evaluated based on the source water body information. The Energy Commission and CCC have required this in recent studies and most likely will continue this practice. Hopefully the information in this paper will assist others in the design and evaluation of CWIS assessments that will be required under the new rules.

CHAPTER 2: METHODS

Power Plant Descriptions

The studies to be presented as examples were conducted at three power plants: SBPP, MBPP, and DCPD (Figure 2). The CWS for all three plants share several features: shoreline intake structures with stationary trash racks that consist of vertical steel bars to prevent larger objects and organisms from entering the system and traveling water screens (TWS) located behind the bar racks that screen out smaller organisms and debris from the system (Figure 1).

Entrainment occurs to organisms that pass through the smaller mesh of the TWS. These organisms are exposed to increased temperatures and pressures as they pass through CWS. The surfaces of the piping in the CWS can be covered with biofouling organisms that feed on organisms that pass through the system. Although studies have shown that there may be some survival after CWS passage (Mayhew et al. 2000), most of these studies were conducted at power plants in rivers and estuaries on the East Coast or in the Gulf of Mexico where biofouling was not recognized as a large problem compared with coastal environments. In addition, these studies only examined survival after passage through the system and did not include comparisons of intake and discharge concentrations where losses due to cropping should be factored into CWS survival. For example, during testing used to determine the appropriate entrainment sampling location, losses between the intake and discharge at the Moss Landing Power Plant sometimes exceeded 95 percent and were always greater than 50 percent (Pacific Gas and Electric Co. 1983). For these reasons, our assessments of CWS effects have assumed that entrained organisms experience 100 percent mortality.

The SBPP, operated by Duke Energy, is located on the southeastern shore of San Diego Bay in the city of Chula Vista, California, approximately 16 km north of the U. S. – Mexican border (Figure 3). The plant draws water from San Diego Bay for once-through cooling of its four electric generating units, which can produce a maximum of 723 MW (Table 1). With all pumps in operation, maximum water flow through the plant is 1,580 m³min⁻¹ (2.3 million m³d⁻¹).

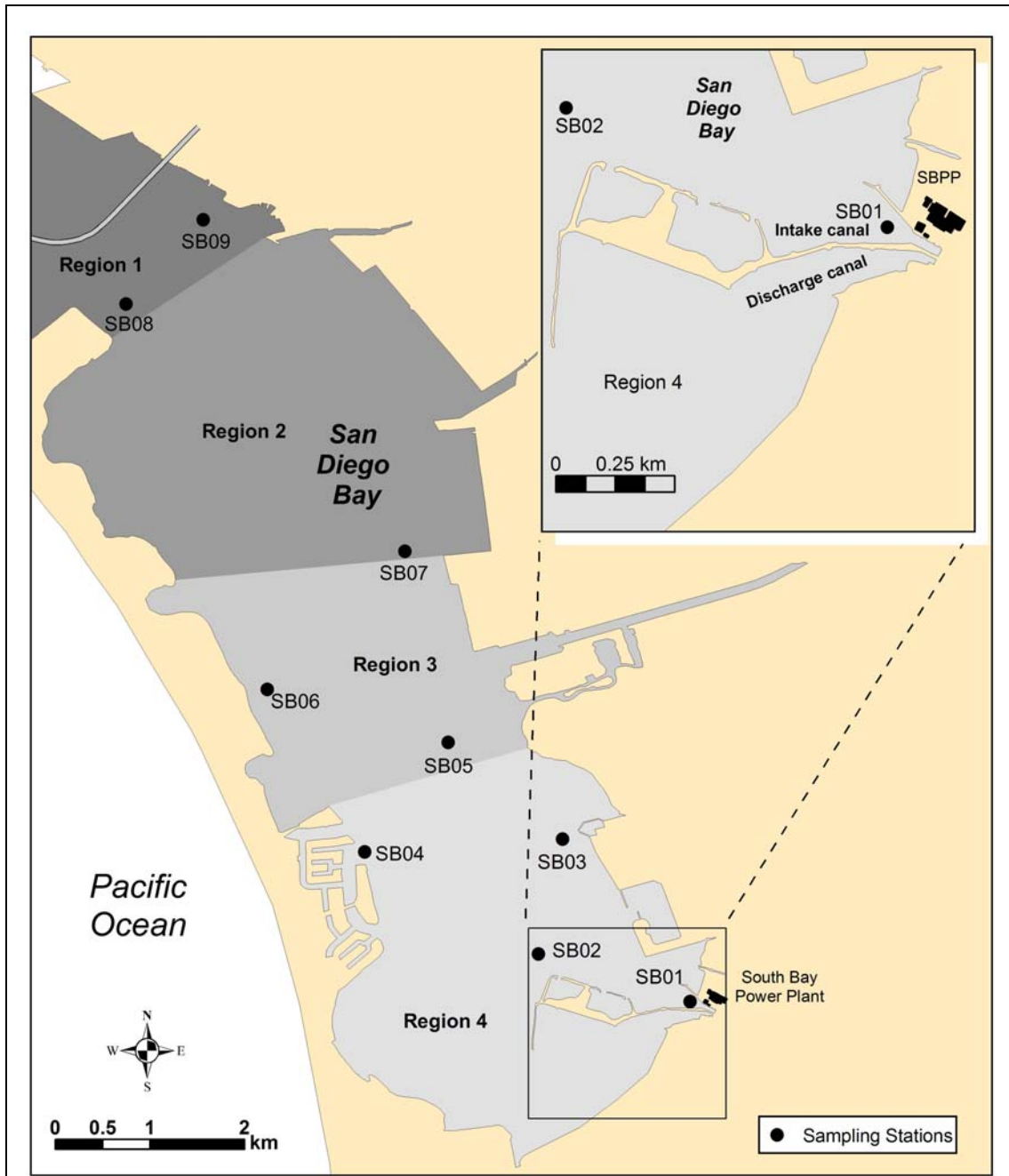


Figure 3. Location of South Bay Power Plant entrainment (SB01) and source water stations and detail of power plant intake area. Shaded areas represent regions of the bay used in calculating bay volumes.

The MBPP, operated by Duke Energy, is located on the northeastern shoreline of Morro Bay, which is approximately midway between San Francisco and Los Angeles, California (Figure 4). The plant draws water from Morro Bay for once-through cooling of its four electric generating units, which can produce a total of 1,002 MW (Table 1).

With all pumps in operation, water flow through the plant is 1,756 m³min⁻¹ (2.53 million m³d⁻¹). Morro Bay studies were done as part of the permitting requirements for an upgrade to the plant that result in a decrease in flow to 1,086 m³min⁻¹ (1.56 million m³d⁻¹). Therefore, all of the entrainment estimates and modeling were calculated using this flow rate.

Table 1. Characteristics of the South Bay (SBPP), Morro Bay (MBPP), and Diablo Canyon (DCPP) power plants.

Power Plant	Number of Power Generating Units	Total Maximum Megawatt (MW) Electric Output	Number of Circulating Water Pumps	Total Maximum Daily Flow (m ³)
SBPP	4	723	8 (2/unit)	2.3x10 ⁶
MBPP	4	1,002	8 (2/unit)	2.5x10 ⁶
DCPP	2	2,200	4 (2/unit)	9.7x10 ⁶

The DCPP, operated by Pacific Gas and Electric Company, is located on the open coast midway between the communities of Morro Bay and Avila Beach on the central California coast in San Luis Obispo County (Figure 5). The intake structure for the plant is located behind two breakwaters that protect it from waves and surge. The plant has two nuclear-fueled generating units that can produce a total of 2,200 MW (Table 1). With the main pumps and smaller auxiliary seawater system pumps in operation, total water flow through the plant is 6,731 m³min⁻¹ or (9.7 million m³d⁻¹).

Source Water and Source Population Definitions

The concept of defining the source water potentially affected by CWS operation is inherent in the assessment process but was not defined as a necessary component of a 316(b) assessment until the recent publication of the new 316(b) rules. The new rules require all existing power plants with CWS capacities greater than 189,000 m³d⁻¹ to complete a Comprehensive Demonstration Study that includes a qualitative description of the source water. A more detailed quantitative definition of source water is not necessary for demographic modeling approaches but is required to place calculated losses into context. The Empirical Transport Model (ETM) requires a more specific definition since the model calculates the conditional mortality due to entrainment on an estimate of the population of organisms in the source water that are potentially subject to entrainment.

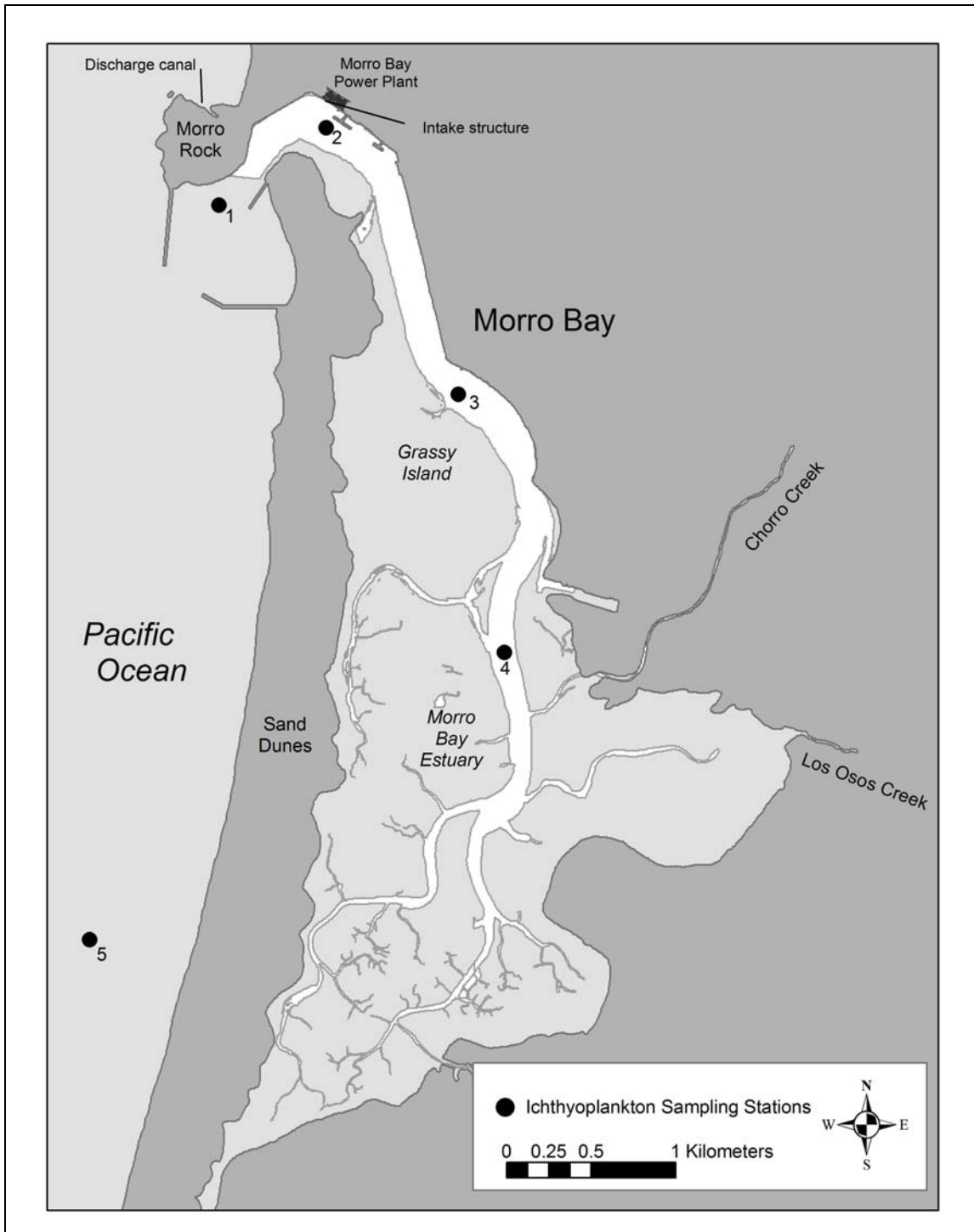


Figure 4. Locations of Morro Bay Power Plant entrainment (Station 2) and source water stations. White area depicts the main tidal channels in the bay, light gray areas are submerged at high tide, and dark gray areas are above the mean high tide line.

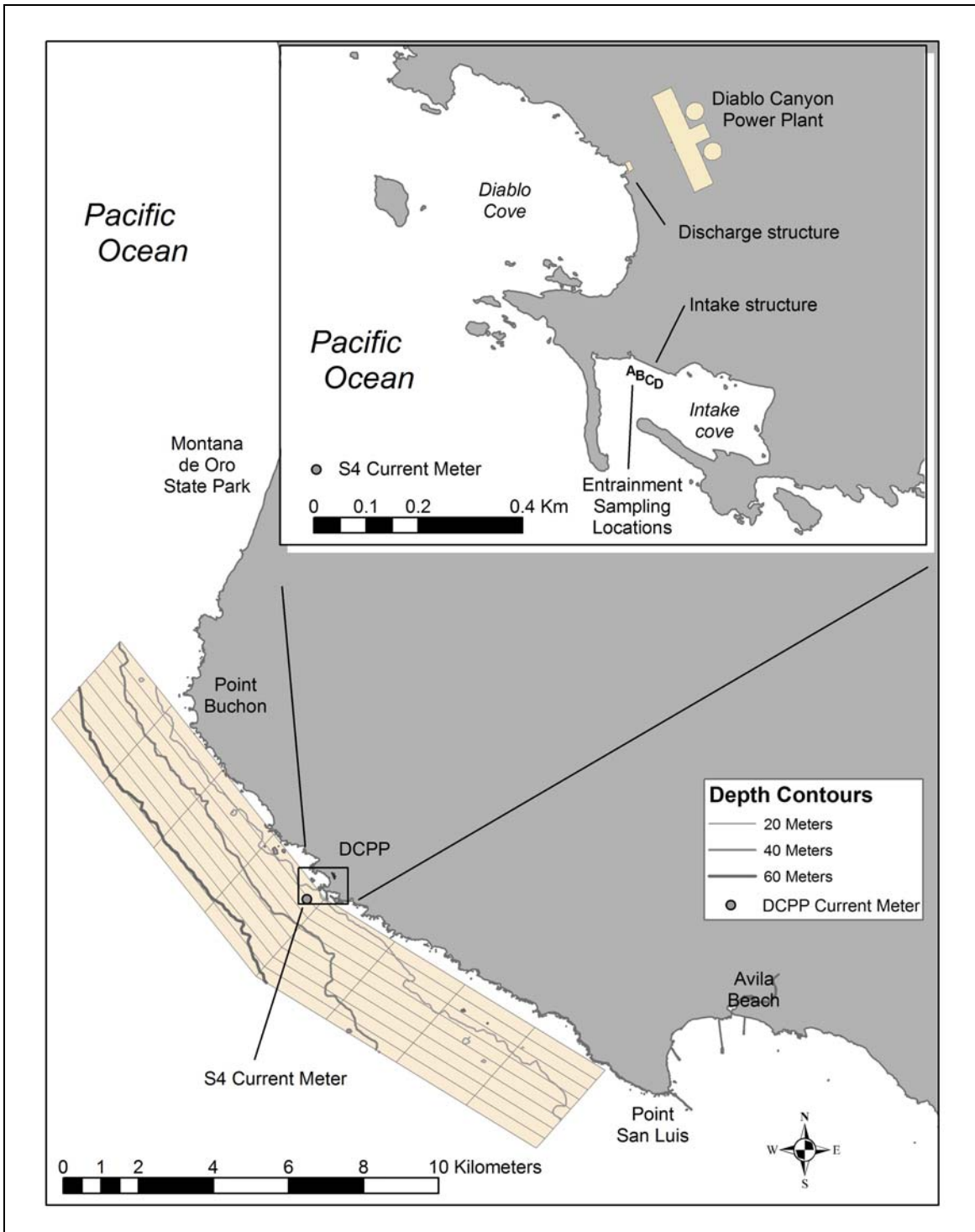


Figure 5. Locations of Diablo Canyon Power Plant (DCPP) entrainment stations (A, B, C, D, in insert) and source water sampling grid.

Critical to properly defining the source water for these studies was physical data that was collected either during the studies or from other sources to estimate the volume of the areas sampled and the total size of the source water. At SBPP and MBPP, hydrographic data collected for the study from several sources was used to estimate volume of the two water bodies. That volume was used as the total source water volume for SBPP. In addition to the volume of Morro Bay, current data from offshore and information on tides was used to estimate the total source water volume that included both bay and ocean components. Data from the same current meter used in the DCP study were used in the MBPP study to calculate an average current speed over the period of January 1, 1996 – May 31, 1999. Current direction was ignored in calculating the average speed. The current speed was used to estimate unidirectional displacement over the period that the larvae in the sampling area offshore from Morro Bay were exposed to entrainment (described below). At DCP, hydrographic data from National Oceanic and Atmospheric Administration was used to estimate the volumes of each of the 64 nearshore sampling stations (described below). In addition, data on alongshore and onshore current velocities were measured using an InterOceans S4 current meter positioned approximately 1 km west of the DCP intake at a depth of approximately 6 m (Figure 5). The direction in degrees true from north and speed in cm/s were estimated for each hour of the nearshore study grid survey periods. These data were used to estimate the size of the area that could have acted as a source for larvae in the nearshore sampling area (described below).

South Bay Power Plant

The SBPP draws ocean water from the southernmost end of San Diego Bay (Figure 3). Allen (1999) divided San Diego Bay into four eco-regions and defined the south and south-central eco-regions as the area from the Coronado Bridge to the southern end of San Diego Bay. Analyses of current patterns and tidal dispersion were used to justify the use of the south and south-central eco-regions (south of the Coronado Narrows) as an appropriate source volume for modeling the effects of entrainment by SBPP. These analyses were done by Dr. John Largier, formerly at Scripps Institute of Oceanography, and now at Bodega Marine Laboratory of the University of California at Davis, and Dr. David Jay, Oregon Health and Science University (Tenera Environmental 2004). The analysis of tidal currents measured at 18 locations throughout the interior of San Diego Bay showed that tidal currents exhibited a local maximum in the south bay at the Coronado Narrows and increased toward the bay mouth. Estimates of tidal dispersion were formed using data from the same 18 current meters, which showed spatial patterns generally similar to those from Largier (1995).

The results of Largier (1995) showed that tidal dispersion had a local maximum at the Coronado Narrows, consistent with the idea that the Narrows acts as the “mouth” of

south bay. South of the Narrows, currents and tidal dispersion are much reduced. Mixing throughout the south bay was estimated to take from one week to a month, typical of the period of time that the larvae were estimated to be exposed to entrainment. The results suggested that larvae are likely removed from the south bay primarily, but not exclusively, by dispersion and that advection may be dominant only during winter river-flow events. The analyses confirmed, quantitatively, Allen's (1999) definitions of eco-regions in San Diego Bay and helped verify the use of the Coronado Narrows as a logical seaward boundary for the SBPP source volume.

Since retention times in the south bay exceeded the average larval durations for most of the taxa examined, the source water was treated as a static volume. Volume was calculated as the volume of water below "mean water level" (MWL, the average of a large number of tidal observations) from the southern end of San Diego Bay northward to the Coronado Narrows (Figure 3). Computing the source volume required compiling the areas and volumes below fixed elevations (horizontal strata). Variations in tidal range required that the South Bay be divided into four regions, with tidal datum levels determined for each, either directly from a tide gauge in the region or by interpolation from adjacent gauges. Tide gauges were available in Regions 2, 3, and 4, whereas datum levels in Region 1 had to be determined by interpolation. Bathymetry for Regions 1 and 2 and the periphery of Regions 3 and 4 were obtained from the U.S. Navy and supplemented with data collected for this study. Estimates of the average concentrations of the organisms inside the bay were multiplied by the sum of the estimated volumes from the four areas (Table 2) to obtain estimates of the bay source water populations that were used in the calculations of mortality for the ETM.

Table 2. Source water body surface area and water volume at mean water level (MWL) by region for south San Diego Bay.

Region	Datum	Height (m)	Area (m ²)	Volume (m ³)
1	MWL	0.90	4,241,241	33,754,018
2	MWL	0.90	10,173,006	70,387,388
3	MWL	0.91	6,355,524	25,060,179
4	MWL	0.93	9,556,875	20,410,508
			30,326,646	149,612,092

Morro Bay Power Plant

The MBPP source water was divided into two sub-areas, bay water and nearshore coastal water, because the location of the intake structure near the harbor entrance entrained both bay and nearshore taxa (Figure 4). The source water for MBPP could not be treated as a static volume, such as the source water for SBPP, because of the location of the power plant intake near the harbor entrance, which made it subject to daily tidal

flows, and the smaller volume of the bay relative to an area such as San Diego Bay. To compensate for daily tidal movement past MBPP, the volume of the Morro Bay source water component was calculated as the sum of the bay's twice daily exchange of its 15.5 million m³ tidal prism, adjusted for tidal exchange, (mean high water to mean low water) and the bay's non-tidal volume of 5.4 million m³. The volume of the tidal prism was adjusted to account for the portion of the Morro Bay outflow that returned with the incoming tide. Since volume was used to estimate the total supply of entrained larvae, inclusion of the recirculated tidal prism volume would double count a portion of the larval supply and underestimate potential entrainment effects. This was accounted for using a tidal exchange ratio (TER), calculated for Morro Bay. The TER is the fraction of the total tidal exchange that consists of "new" water coming into the estuary, or water that did not leave the estuary on the previous tidal cycle (Largier et al. 1996). In Morro Bay, the "total tidal exchange" is synonymous with the tidal prism, except for the amount estimated by TER.

The TER is difficult to estimate from measurements because the currents that prevail outside any estuary mouth are complex and variable, and it is quite sensitive to processes inside and outside the estuary, especially complex currents, river inflow, and density stratification (Largier et al. 1996). However, a method was developed (Largier et al. 1996) that measures the TER from the change in salinity of water flowing in and out of the entrance of an estuary. Applying this method, the Morro Bay TER was calculated to be between 70 and 80 percent of the average daily tidal prism by Dr. David Jay (Tenera Environmental 2001). A TER of 75 percent was used in calculating the bay source water volume, which was equal to the twice-daily tidal exchange of the average tidal prism, adjusted for the TER, added to the bay's non-tidal volume. Estimates of the average concentrations of organisms from the stations inside the bay (Stations 1–4) were multiplied by this volume to obtain estimates of the bay source water populations (Table 3). Since tidal exchange was used in calculating the source volume for Morro Bay, the plant's intake flow volume was calculated over a complete daily tidal cycle of two highs and two lows, which was 24 hours and 50 minutes.

Table 3. Volumes for Morro Bay and Estero Bay source water sub-areas.

Area	Volume (m ³)
Morro Bay	15,686,663
Estero Bay Sampling Area	20,915,551

The area sampled outside Morro Bay in Estero Bay was treated as a static volume (Table 3) that was equal to the volume of Morro Bay uncorrected for tidal exchange. This

volume for Estero Bay was used because it represented the volume of water exchanged with the bay that could be subject to entrainment. Estimates of the average concentrations of the organisms from the station just inside the bay (Station 1) and the station down-coast (Station 5) were multiplied by this volume to obtain estimates of the Estero Bay populations in the area sampled. The total size of the source water beyond the area sampled was estimated using ocean current data. Morro Bay and Estero Bay larval estimates were calculated separately so that the large source volume in Estero Bay did not inflate the source water estimates for bay taxa that were in much lower abundances outside the bay.

Diablo Canyon Power Plant

The DCPD nearshore sampling was designed to only provide information on abundance and distribution in the vicinity of DCPD of larval fishes and the invertebrates selected for detailed assessment, since it was recognized that the actual source water would be much larger for some taxa and vary by taxa and seasonally due to changing oceanographic conditions. In establishing the nearshore sampling area, the authors considered that ocean currents in the area generally move both up and down the coast past DCPD. The currents also showed inshore/offshore oscillations, but these occurred less frequently and generally at a lower magnitude. The nearshore sampling area contained 64 stations or “cells” (Figure 5) that were centered on the Intake Cove at DCPD. The northern extent of the sampling area was near Point Buchon, and the southern half, a mirror image of the northern portion, extended to near Point San Luis. The shape of the sampling area reflected a slight bend (approximately 20°) in the coast at DCPD. The sampling area extended a distance of 8.7 km to both the north and south and an average distance of 3 km offshore. Regions inshore of the sampling area were in shallow water with partially submerged rocks, making the areas unsafe for boat operations and sampling. Volumes in each of the 64 cells were estimated using the surface area of the cell and the average depth based on available bathymetry data. The number of larvae in each cell was estimated by multiplying the average concentration during each survey by the volume of water sampled.

Sampling

Sampling at all three of the facilities was designed to provide estimates of both entrainment and source water concentrations that accounted for the differences in the cooling water volumes at the three plants and were representative of the range of habitats and organisms potentially affected by entrainment in each area. As a result of the differences among the three plants and funding available, the combined entrainment and source water sampling efforts ranged from five stations for the MBPP study to 68 stations for the DCPD study.

Sample collection methods were similar to those developed and used by CalCOFI in their larval fish studies (Smith and Richardson 1977). Sampling at all three plants was conducted using a bongo frame with two 71-cm diameter rings with plankton nets constructed of 333-micrometer mesh. Each net was fitted with a Dacron sleeve and a cod-end container to retain the organisms. Each net was equipped with a calibrated General Oceanics flowmeter, which allowed the calculation of the amount of water filtered. Net lengths varied according to the depth of the water sampled. Shorter nets, 1.8 m in length, were used for entrainment sampling in the shallower intake cove at DCP. Longer nets, 3.3 m in length, were used for all other sampling. All of the nets were lowered as close to the bottom as possible and retrieved using oblique or vertical tows to sample the entire water column. Once the nets were retrieved from the water, all of the collected material was rinsed into the codend. The target volume of each tow at both the entrainment and source water stations was 40-60 m³ for both nets combined. The sample volume was checked when the nets reached the surface, and the tow continued or started over if the target volume was not collected. The contents of both nets were either combined into one sample immediately after collection or treated as a single sample for analysis.

Entrainment sampling at all three plants was done in the waters outside the plant CWIS as close as possible to the intake structure bar racks. This sampling design assumed that the concentrations from the waters in front of the CWIS are the same as the concentrations in the cooling water flow. Sampling was done outside the CWIS because of the numerous problems involved in sampling inside the plant or at the discharge. Sampling inside the plant usually involves sampling with a pump that generally obtains a small volume relative to plankton nets in a given period of time. Although samples inside the CWIS may be well mixed, the cooling water flow inside the system is exposed to biofouling organisms that can significantly reduce the concentration of larval fish and other organisms. Sampling outside the plant also allowed entrainment samples to be used in characterizing source water populations. This was critical to the ETM calculations and allowed source water estimates to be calculated for taxa that may have only been collected from entrainment samples.

South Bay Power Plant

Entrainment and source water sampling was conducted monthly from January 2001 through January 2002 (Tenera Environmental 2004). Entrainment samples were collected from Station SB1 located in the SBPP intake channel (Figure 3). Each tow proceeded out the intake channel against the prevailing intake current. The intake channel was bounded by a separation dike to the south and a shallow mudflat to the north, and there was a constant current flow toward the intake structure. Therefore it was assumed that all of the water sampled at the entrainment station would be drawn through the SBPP

cooling water system. Entrainment samples were collected over a 24-hour period, with each period divided into six 4-hour sampling cycles. Two replicate tows were collected consecutively at the entrainment station during each cycle. Source water samples at Stations SB2-SB9 were collected from the same vessel during the remainder of each cycle (Figure 3). A single tow was completed at each of the source water stations during each of the six 4-hr cycles.

The stations for the SBPP study (Figure 3) were stratified to include four channel locations on the east side of the bay and four shallower locations on the west side of the bay. The source water stations ranged in depth from approximately -2 m mean lower low water (MLLW) at SB8 to -12 m MLLW at SB9. This station array was chosen to include a range of depths and adjacent habitats in south San Diego Bay that would characterize the larval fish composition in the source water. For example, stations on the east side of the bay were adjacent to salt marsh habitat and would tend to have a greater proportion of larvae from fishes with demersal eggs that spawned in salt marsh channels, such as gobies, while deeper channel stations in the northern end of the study area would tend to have more larvae of species that spawn in open water such as northern anchovy (*Engraulis mordax*).

Morro Bay Power Plant

Entrainment and source water sampling was conducted from December 1999 through December 2000 (Tenera Environmental 2001). Entrainment samples were collected weekly from in front of the MBPP intake structures (Station 2; Figure 4). Samples were collected over a continuous 24-hour period with each period divided into six 4-hour sampling cycles. Two tows were conducted during each cycle. During the same period, monthly source water samples were collected at four stations in addition to the entrainment station (Figure 4). Initially, source water surveys were collected twice per day during daylight hours on high and low tides, but after two months of sampling in February 2000, sample collection for source water surveys was expanded to cover the entire 24-hour period and was no longer linked to tidal cycle.

Fewer stations were sampled in the MBPP study relative to the SBPP study due to the smaller size of the estuary. Station 1 was located just inside the entrance to Morro Bay and was intended to characterize water from outside the bay that was subject to entrainment during incoming tides. Only two other source water stations (Stations 3 and 4) were located in Morro Bay because the areas that could be sampled in the south part of the bay were limited to narrow navigation channels. This was not considered to be a problem because of the large tidal prism relative to the size of the bay that resulted in shallower portions of the bay draining through the deeper navigation channels where the sampling occurred. Station 5 was located outside the bay approximately 4.7 km

down coast (or, south of the harbor mouth) and was intended to characterize open coastal taxa potentially subject to entrainment.

Diablo Canyon Power Plant

Collection of the DCPD entrainment samples occurred from October 1996 through June 1999 (Tenera Environmental 2000). This was the longest period of sampling among the three studies. The sampling was continued longer than one year because of El Niño conditions during the first year, which were agreed by the Technical Workgroup as not representative of normal conditions. Entrainment samples were collected once per week from four permanently moored sampling stations located directly in front of the intake structure that were sampled in a random order during eight three-hour cycles (Figure 5). Two samples were collected at each station during each cycle. The first nine surveys were collected with 505 µm mesh nets, but due to extrusion of larval fishes through the net mesh observed during these first few surveys, subsequent surveys were collected with 335 µm mesh.

The boundaries and shape of the nearshore sampling area were chosen to ensure that the area would be large enough to characterize the larvae from the fishes potentially influenced by the large volume of the DCPD CWIS and would be representative of the variety of nearshore habitats found in the area. These were the same reasons used to justify the large sampling effort (64 stations) relative to the SBPP and MBPP studies. Sampling of the nearshore study area occurred monthly from July 1997 through June 1999. Two randomly positioned stations within each of the 64 cells of the grid were sampled once each survey. The study grid was sampled continuously over 72 hours using a “ping-pong” transect to limit temporal and spatial biases in the sampling pattern and to optimize shipboard time. The starting cell (constrained to the 28 cells on the perimeter of the grid) and the initial direction of the transect (constrained to the two cells diagonally, adjacent to the starting cell) were selected at random. When the adjacent diagonal cell had previously been sampled, one of the two adjacent cells in the direction of travel was randomly selected to be sampled next. To minimize temporal variation between entrainment and study grid sampling, source water surveys were scheduled to bracket the 24-hour entrainment survey, overlapping by one day before and after the collection of entrainment samples.

Entrainment and nearshore sampling efforts did not start at the same times, and therefore the entire sampling period was divided into five analysis periods. All of the weekly entrainment samples from October 1996 through November 1998 were processed so this period was divided into two yearlong analysis periods. Results for these periods are not presented because they were only used to generate estimates directly from entrainment data. The nearshore sampling period was also divided into

two yearlong analysis periods. Only the entrainment samples collected during the sampling of the nearshore area were processed from December 1998 through June 1999 so entrainment data from July 1998 through June 1999 were used to generate model estimates for a fifth analysis period that could be directly compared with model estimates that incorporated data from the nearshore sampling area.

Selection of Taxa for Detailed Assessment

Although almost all planktonic forms (phyto-, zoo-, and ichthyoplankton) are affected by entrainment, these three studies and most other 316(b) studies have focused on a few organism groups, typically ichthyoplankton and zooplankton. The effects on phytoplankton and invertebrate holoplankton are typically not studied because their large abundances, wide distributions, and short generation times should make them less susceptible to CWIS impacts. The groups of organisms selected for assessment in these studies included larval fishes and larvae from commercially or recreationally important invertebrates such as Cancer spp. crabs and California spiny lobster (*Panulirus interruptus*).

The workgroup also looked at including kelp spores, fish eggs, squid paralarvae, and abalone and bivalve larvae in the assessment. The risk of a significant impact on adult kelp populations by entrainment of kelp spores was determined to be negligible due to the large number of spores produced along the coast. Additionally, it is not possible to identify the species of kelp based on gametes or spores. Fish eggs were not included because they are difficult to identify to species, and the most abundant fishes in these studies had egg stages that were not likely to be entrained; they either have demersal/adhesive eggs or are internally fertilized and extrude free-swimming larvae. Squid paralarvae are also unlikely to be entrained because they are competent swimmers immediately after hatching. Abalone larvae were not included because they are at low risk of entrainment and cannot be effectively sampled or identified during early life stages when they would be susceptible to entrainment (Tenera Environmental 1997). In addition, algal spores, fish eggs, and abalone and bivalve larvae would all require smaller mesh than the mesh used for ichthyoplankton and separate sampling efforts.

The final list of fish and invertebrates analyzed in each of the studies (Table 4) was determined by technical workgroups after all of the samples had been processed and data from the entrainment samples summarized. The assessments included taxa from the organism groups that were in highest abundance in the entrainment samples (generally those comprising up to 90 percent of the total abundance) and commercially or recreationally important fishes and invertebrates that were in high enough abundances to allow for their assessment. It was also realized that organisms having

local adult and larval populations (that is, source not sink species) were more important than species such as the northern lampfish (*Stenobranchius leucopsarus*), which is an offshore, deep-water species whose occurrence in entrainment was likely due to onshore currents that transported the larvae into coastal waters from their primary habitat. These 'sink species' were not included in the assessments.

Table 4. Taxa used in assessments at South Bay (SBPP), Morro Bay (MBPP), and Diablo Canyon (DCPP) power plants.

Scientific Name	Common Name
<u>SBPP</u> – taxa comprising 99 percent of total entrainment abundance	
<i>Clevelandia ios</i> , <i>Ilypnus gilberti</i> , <i>Quietula y-cauda</i>	CIQ goby complex
<i>Gillichthys mirabilis</i>	longjaw mudsucker
<i>Anchoa</i> spp.	anchovies
Atherinopsidae	silversides
<i>Hypsoblennius</i> spp.	combtooth blennies
<u>MBPP</u> – taxa comprising 90 percent of total entrainment abundance plus commercial taxa	
unidentified Gobiidae	gobies
<i>Leptocottus armatus</i>	Pacific staghorn sculpin
<i>Stenobranchius leucopsarus</i>	northern lampfish
<i>Quietula y-cauda</i>	shadow goby
<i>Hypsoblennius</i> spp.	combtooth blennies
<i>Sebastes</i> spp. V_De	KGB rockfishes
<i>Atherinopsis californiensis</i>	jacksmelt
<i>Clupea pallasii</i>	Pacific herring
<i>Genyonemus lineatus</i>	white croaker
<i>Scorpaenichthys marmoratus</i>	cabezon
<i>Cancer antennarius</i>	brown rock crab
<i>Cancer jordani</i>	hairy rock crab
<i>Cancer anthonyi</i>	yellow crab
<i>Cancer gracilis</i>	slender crab
<i>Cancer productus</i>	red rock crab
<i>Cancer magister</i>	Dungeness crab
<u>DCPP</u> – ten most abundant taxa plus commercial taxa	
<i>Sardinops sagax</i>	Pacific sardine
<i>Engraulis mordax</i>	northern anchovy
<i>Sebastes</i> spp. V / <i>S. mystinus</i>	blue rockfish complex
<i>Sebastes</i> spp. V_De/V_D_	KGB rockfish complex
<i>Oxylebius pictus</i>	painted greenling
<i>Artedius lateralis</i>	smoothhead sculpin
<i>Orthonopias triacis</i>	snubnose sculpin
<i>Scorpaenichthys marmoratus</i>	cabezon
<i>Genyonemus lineatus</i>	white croaker
<i>Cebidichthys violaceus</i>	monkeyface prickleback
<i>Gibbonsia</i> spp.	Clinid kelpfishes
<i>Rhinogobiops nicholsii</i>	blackeye goby
<i>Citharichthys</i> spp.	sanddabs
<i>Paralichthys californicus</i>	California halibut
<i>Cancer antennarius</i>	brown rock crab
<i>Cancer gracilis</i>	slender crab

The list of taxa reveals one of the problems with these studies. In some cases larvae cannot be identified to the species level and can only be identified into broader taxonomic groupings. Myomere and pigmentation patterns were used to identify many species; however, this can be problematic for some species. For example, sympatric members of the family Gobiidae share morphologic and meristic characters during early life stages (Moser 1996) making identification to the species level difficult. In the MBPP study the authors grouped those gobiids that were not identifiable to species into an “unidentified gobiid” category (that is, unidentified Gobiidae). In the SBPP study the authors were able to determine that the unidentified gobies were comprised of three species (Table 4). Larval combtooth blennies (*Hypsoblennius spp.*) can be easily distinguished from other larval fishes (Moser 1996). However, the three sympatric species along the central California coast cannot be distinguished from each other on the basis of morphometrics or meristics. These combtooth blennies were grouped into the “unidentified combtooth blennies” category (that is, *Hypsoblennius spp.*). Many rockfish species (*Sebastes spp.*) are closely related, and the larvae share many morphological and meristic characteristics, making it difficult to visually identify them to species (Moser et al. 1977, Moser and Ahlstrom 1978, Baruskov 1981, Kendall and Lenarz 1987, Moreno 1993, Nishimoto in prep.). Identification of larval rockfish to the species level relies heavily on pigment patterns that change as the larvae develop (Moser 1996). Of the 59 rockfishes known from California marine waters (Lea et al. 1999), at least five can be reliably identified to the species level as larvae (Laidig et al. 1995, Yoklavich et al. 1996): blue rockfish (*Sebastes mystinus*), shortbelly rockfish (*S. jordani*), cowcod (*S. levis*), bocaccio (*S. paucispinis*), and stripetail rockfish (*S. saxicola*). The *Sebastes* larvae collected could only be identified into broad sub-generic groupings based on pigment patterns; these larvae were grouped using information provided by Nishimoto (in prep.; Table 5). The use of these broad taxonomic categories presents problems in determining the most appropriate life history parameters to use in the demographic models. This involved calculating an average value or determining the most appropriate value from different sources and species.

Table 5. Pigment groups of some preflexion rockfish larvae from Nishimoto (in-prep).

The code for each group is based on the following letter designations:		
V_ = long series of ventral pigmentation (starts directly at anus)		De = elongating series of dorsal pigmentation (scattered melanophores after continuous ones)
V = short series of ventral pigmentation (starts 3-6 myomeres after anus)		d = develops dorsal pigmentation (1-2 or scattered melanophores)
D_ = long series of dorsal pigmentation (4 or more in a continuous line) extending to above anus		P = pectoral blade pigmentation
D = short series of dorsal pigmentation (4 or more in a continuous line) not extending to anus		p = develops pectoral pigmentation (1-2 or scattered melanophores)
CODE	SPECIES	COMMON NAME
V D	Long ventral series, short dorsal series, no pectoral pigment	
	<i>S. atrovirens</i>	kelp
	<i>S. chrysomelas</i>	black and yellow
	<i>S. maliger</i>	quillback
	<i>S. nebulosus</i>	China
	<i>S. semicinctus</i>	halfbanded
V De	Long ventral series, elongating dorsal series, pectoral pigment	
Or	<i>S. auriculatus</i>	brown
V DeP	<i>S. carnatus</i>	gopher
Or	<i>S. caurinus</i>	copper
V dep	<i>S. dalli</i>	calico
	<i>S. rastrelliger</i>	grass
V	Short ventral series, no dorsal series, no pectoral	
	<i>S. aleutianus</i>	rougeve
	<i>S. alutus</i>	Pacific Ocean perch
	<i>S. brevispinis</i>	silvergrey
	<i>S. cramerii</i>	darkblotched
	<i>S. diploproa</i>	splitnose
	<i>S. elongatus</i>	greenstriped
	<i>S. macdonaldi</i>	Mexican
	<i>S. miniatus</i>	vermilion
	<i>S. nigrocinctus</i>	tiger
	<i>S. proriger</i>	redstripe
	<i>S. rosaceus</i>	rosy
	<i>S. ruberrimus</i>	yelloweye
	<i>S. serriceps</i>	treefish
	<i>S. umbrosus</i>	honeycomb
	<i>S. wilsoni</i>	pygmy
	<i>S. zacentrus</i>	sharpchin

Other Biological Data

All of the assessment models required some life history information from a species to enable the calculation of entrainment effects. Age-specific survival and fecundity rates are required for the fecundity hindcasting (FH) and adult equivalent loss (AEL) demographic models. Calculation of FH requires egg and larval survivorship up to the age of entrainment plus estimates of lifetime fecundity, while AEL requires survivorship estimates from the age at entrainment to adult recruitment. Species-specific survivorship information (for example, age-specific mortality) from egg or larvae to adulthood was not available for many of the taxa considered in the assessments at the three plants. Life history information was gathered from the scientific literature and other sources. Uncertainty surrounding published life history parameters is seldom known and rarely reported, but the likelihood that it is very large needs to be considered when interpreting results from the demographic approaches for estimating entrainment effects. Accuracy of the estimated entrainment effects from demographic models such as FH and AEL depend on the accuracy of age-specific mortality and fecundity estimates. In addition, these data are unavailable for many species, limiting the application of these models to large numbers of species.

All three modeling approaches (FH, AEL, and ETM) required an age estimate of the entrained larvae. The larval ages were estimated using the length of the entrained larvae and an estimate of the larval growth rate for each species obtained from the scientific literature and other sources. The size range from the minimum to the average size of the larvae was used to calculate the average age of the entrained larvae that was used in the FH and AEL models, while the size range from the minimum to the maximum size of the larvae was used to calculate the maximum age of the entrained larvae and the period that the larvae were subject to entrainment for the ETM model. Minimum and maximum lengths used in these calculations were adjusted to account for potential outliers in the measurements by using the 1st and 99th percentile values in the calculations. These values were chosen based on examination of the distributions of the length measurements, and other values may be more appropriate for other studies or species depending upon the data. The size range was estimated for each taxon from a representative sample of larvae from the SBPP and MBPP studies, while all of the entrained larvae of the taxa selected for detailed assessment were measured from the DCP study. All of the measurements were made using a video capture system attached to a microscope and Optimas™ image analysis software.

Data Reduction

Entrainment Estimates

Estimates of daily larval entrainment for all ichthyoplankton and selected invertebrate larvae for all of the plants were calculated from data collected at the entrainment stations located directly in front of the power plant intake structures. Daily entrainment estimates were used to calculate daily incremental entrainment mortality estimates used in the ETM. Estimates of entrainment over annual study periods were used in the FH and AEL demographic modeling.

Daily entrainment estimates and their variances were derived from the mean concentration of larvae (number of larvae per cubic meter of water filtered) calculated from the samples collected during each 24-hour entrainment survey. These estimates were multiplied by the daily intake flow volume for each plant (MBPP and SBPP studies used engineering estimates of cooling water flow and DCPD used actual daily flow) to obtain the number of larvae entrained per day for each taxon as follows:

$$E_i = v_i \cdot \bar{\rho}_i, \quad (1)$$

where v_i = total intake volume for the survey day of the i th survey period, and $\bar{\rho}_i$ = average concentration for the survey day of the i th survey period.

Entrainment was estimated for the days within each weekly (MBPP and DCPD) or monthly survey period (SBPP). The number of days in each period was determined by setting the sampling date at the midpoint between sample collections. Daily cooling water intake volumes were then used to calculate entrainment for the study period by summing the product of the entrainment estimates and the daily intake volumes for each survey period. These estimates and their associated variances were then added to obtain annual estimates of total entrainment and variance for each taxon as follows:

$$E_T = \sum_{i=1}^n \left(\frac{V_i}{v_i} \right) E_i, \quad (2)$$

where

v_i = intake volume on the survey day of the i th survey period ($i=1, \dots, n$);

V_i = total intake volume for the i th survey period ($i=1, \dots, n$); and

E_i = the estimate of daily entrainment during the entrainment survey of the i th survey period.

with an associated variance of

$$\text{Var}(E_T) = \sum_{i=1}^n \left(\frac{V_i}{v_i} \right)^2 \text{Var}(E_i), \quad (3)$$

using the sampling variances of entrainment on the survey day of the i^{th} period, $\text{Var}(E_i)$. The daily sampling variance for SBPP and MBPP was calculated using the average concentrations from samples collected during each cycle, while the daily sampling variance for DCPD was calculated by treating each sampling cycle as a separate stratum using data from the four entrainment stations. Both methods underestimated the true variance because they did not incorporate the variance associated with the within-survey period variation and daily variations in intake flow due to waves, tide, and other factors not measured by the power plant. One hundred percent mortality was assumed for all entrained organisms.

For the study at DCPD, estimates of annual entrainment were scaled to better represent long-term trends by using ichthyoplankton data collected inside the Intake Cove at DCPD (Figure 5). These data were used to calculate an index of annual trends in larval abundance for the period of 1990 through 1998. This multi-year annualized index consisted of five months (February–June) of larval fish concentrations from 1990, six months (January–June) from 1991, and seven months (December–June) from all subsequent years. The estimated annual entrainment (ET) was adjusted to the long-term average using the following equation:

$$E_{\text{Adj-T}} = \left(\frac{\bar{I}}{I_i} \right) \cdot E_T, \quad (4)$$

where

$E_{\text{Adj-T}}$ = adjusted estimate of total annual entrainment to a long-term average, 1990–1998;

I_i = index value from DCPD Intake Cove surface plankton tows for each i^{th} year; and

\bar{I} = average index value from DCPD Intake Cove surface plankton tows, 1990–1998.

The abundances used in calculating the index were not expected to be representative of the abundances calculated from the DCPD entrainment data since they were only collected during five to seven months of the year in contrast to the entrainment sampling that occurred continuously from October 1996 through June 1999. The use of the index assumes that the difference in abundance is approximately equal over time, although the validity of this assumption probably varied among taxa. Variance for adjusted annual entrainment can then be expressed as follows:

$$\text{Var}(E_{Adj-T}) = \left(\frac{\bar{I}}{I_i}\right)^2 \cdot \text{Var}(E_T), \quad (5)$$

assuming the indices are measured without error. Ignoring the sampling error of the indices will underestimate the true variance but will qualitatively account for the change in scale associated with multiplying the annual entrainment estimate by a scalar. The variance of E_{Adj-T} , however, does not take into account the between-day, within-station variance, interannual variation, nor the variance associated with the indices used in the adjustment. Hence, the actual variance of the E_{Adj-T} estimate is likely to be greater than the value expressed above.

The Intake Cove surface tow index was assumed to have the following relationship:

$$E(I_i) = C \cdot E_i, \quad (6)$$

where

$E(I_i)$ = expected value of the index for the i th year;

E_i = entrainment for the i th year; and

C = proportionality coefficient.

If this relationship holds true and the differences over time are constant, then the inter-annual variance in the index has the following relationship:

$$\text{Var}(I_i) = C^2 \text{Var}(E_i). \quad (7)$$

Therefore, the coefficients of variation (CV) for I and E across n years have the following relationship:

$$CV(\bar{I}) = \frac{\sqrt{\text{Var}(I)}}{\bar{I}} = \frac{\sqrt{C^2 \text{Var}(E)}}{C\bar{E}} = CV(\bar{E}). \quad (8)$$

Hence, the CV for the Intake Cove surface tow index should be a measure of the CV for entrainment across years. In the case of E and I , variances include sampling errors that may not be equal. Therefore, the CV of I was used to estimate variation in entrainment across years.

The use of adjusted entrainment in FH and AEL models at DCPD provided results that better represented average long-term effects. Adjusted entrainment values were not used in calculating ETM results because the computation of ETM relies on a proportional entrainment (PE) ratio using estimates from paired entrainment and nearshore larval sampling. Moreover, if the assumptions of the ETM model are valid,

then the estimate already represents average long-term entrainment effects because the PE ratio should largely be a function of the ratio of the cooling water to source water volumes, which is constant if the plant is operating at full power compared to ichthyoplankton abundances that vary over time. This would especially be true if the PE were averaged over several taxa, assuming that the effects of larval behavior cancel across all the species. As a result, the use of adjusted entrainment in FH and AEL models also provided a better basis to compare results from all three models when they were converted into a common currency through the use of population or fishery stock assessments. This advantage of the ETM could be affected if actual cooling water flows varied considerably seasonally and among years.

Source Water Estimates

Average concentrations calculated from source water stations were used to estimate source water populations of species or taxa groups using the same method used for calculating entrainment estimates for each i^{th} survey period. At SBPP a single source water estimate was calculated, while at MBPP, separate estimates were calculated for Morro Bay and Estero Bay source water components.

At DCPD separate estimates were calculated for each of the 64 grid stations based on the depth and surface area of each station. In addition, an adjustment was made to the estimated number of larvae in the Row 1 cells of the study grid to help compensate for the inability to safely collect samples inshore of the grid (Figure 5). The estimated volume of water directly inshore of the study grid was multiplied by the concentration of larvae collected in the Row 1 cells, except for cells directly offshore from the power plant and the cell farthest upcoast, which is more offshore than the rest of the cells in Row 1 due to the bend in the coastline at Point Buchon. The adjustment was not done for the volume of water inshore of that cell because it would have added a substantial volume to that cell, and the composition and abundance would not have been representative of the other inshore areas. The average concentration from the entrainment stations was used for the areas inshore from the two cells directly offshore from the Intake Cove where entrainment samples were collected. The estimated number of larvae in each grid station and from the areas inshore of the grid was added to obtain an estimate of the sampled source water populations.

Impact Assessment Models

Demographic Approaches

Adult equivalent loss models (Goodyear 1978) evolved from impact assessments that compared power plant losses to estimates of adult populations or commercial fisheries

harvests. In the case of adult fishes impinged by intake screens, the comparison was relatively straightforward. To compare numbers of impinged sub-adults and juveniles and entrained larval fishes to adults, it was necessary to convert these losses to adult equivalents using demographic factors such as survival rates. Horst (1975) provided an early example of the equivalent adult model (EAM) to convert numbers of entrained early life stages of fishes to their hypothetical adult equivalency. Goodyear (1978) extended the method to include survival for several age classes of larvae.

Demographic approaches, exemplified by EAM, produce an absolute measure of loss beginning with simple numerical inventories of entrained or impinged individuals and increasing in complexity when the inventory results are extrapolated to estimate numbers of adult fishes or biomass. We used two related demographic approaches in assessing entrainment impacts at all three facilities: AEL (Goodyear 1978), which uses the larval losses to estimate the equivalent number of adult fishes that would not have been lost to the population, and FH (Horst 1975, Goodyear 1978, MacCall, pers. comm.), which estimates the number of adult females at the age of maturity whose reproductive output has been lost due to entrainment. The method is similar to the Egg Production Method described by Parker (1980, 1985) and implemented in Parker and DeMartini (1989) at San Onofre Nuclear Generating Station except they used only eggs to hindcast adult equivalents.

Both AEL and FH approaches require an estimate of the age at entrainment for each taxon that was estimated by dividing the difference between the smallest (represented by the 1st percentile value) and the average lengths of a representative sample of larvae measured from the entrainment samples by a larval growth rate obtained from the literature. This assumes that the period of vulnerability to entrainment starts when the larvae are either hatched or released and that the smallest larvae in the samples represent newly hatched or released larvae. This minimum value was checked against reported hatch and release sizes for the taxa analyzed in these studies and in most cases was less than these reported values.

Additionally, age-specific survival and fecundity rates are required for calculating FH and AEL. FH requires egg and larval survivorship up to the age of entrainment plus estimates of fecundity, age at maturity, and longevity, while AEL requires survivorship estimates from the age at entrainment to adult recruitment. Furthermore, to make estimation practical, the affected population is assumed to be stable and stationary, and age-specific survival and fecundity rates are assumed to be constant over time. In addition, the FH method assumes that all of the females instantaneously reach 100 percent maturity at the age of maturity.

Species-specific survivorship information from egg or larvae to adulthood was limited for many of the taxa considered in these studies. These rates when available were inferred from the literature along with estimates of uncertainty. Uncertainty surrounding published demographic parameters is seldom known and rarely reported, but the likelihood that it is very large needs to be considered when interpreting results from the demographic approaches for estimating entrainment effects. The ratio of the standard deviation to the mean (CV) was assumed to be 30 percent for all life history parameters used in the models for the SBPP and MBPP studies and 100 percent for the DCPD study. The larger CV was used at DCPD because it was the first study conducted, and the authors wanted to use a large CV to ensure that the confidence intervals adequately reflected the large degree of uncertainty associated with the estimates. The smaller CV used for SBPP and MBPP does not reflect increased confidence in the life history data, but the realization that the larger CV used at DCPD resulted in confidence intervals for the estimates that spanned several orders of magnitude minimizing their usefulness in the assessment.

Fecundity Hindcasting

The FH approach couples larval entrainment losses to adult fecundity using survivorship between stages to estimate the numbers of adult females at the age of maturity whose reproductive output has been lost due to entrainment, that is, hindcasting the numbers of adult females at the age of maturity effectively removed from the reproductively active population. Accuracy of the estimate of impacts using this model is dependent upon an accurate estimate of survival from parturition through the estimated average age at entrainment and total lifetime female fecundity. If it can be assumed that the adult population has been stable at some current level of exploitation and that the male:female ratio is constant at 50:50, then fecundity and mortality are integrated into an estimate of adult loss at the age of female maturity by converting entrained larvae back into adult females and multiplying by two to approximate the total number of equivalent adults at the age of female maturity.

A potential advantage of FH is that survivorship need only be estimated for a relatively short period of the larval stage (for example, egg to larval entrainment). The method requires age-specific mortality rates and fecundities to estimate equivalent adult losses. Furthermore, this method, as applied, assumes a 50:50 male:female ratio; hence the loss of a single female's reproductive potential was equivalent to the loss of two adult fish. Other assumptions included the following:

- Life history parameter values from the literature are representative of the population for the years and location of the study.

- Size of the stock does not affect survivorship or the rate of entrainment mortality (no density dependence).
- Reported values of egg mass were lifetime averages to calculate an unbiased estimate of lifetime fecundity.
- Total lifetime fecundity was accurately estimated by assuming that the mortality rate was uniform between age-at-maturity and longevity.
- “Knife-edge” recruitment into the adult population at the age of maturity.
- Loss of the reproductive potential of one female was equivalent to the loss of an adult female at the age of maturity.

The estimated number of females at the age of maturity whose lifetime reproductive potential was lost due to entrainment was calculated for each taxon as follows:

$$FH = \frac{E_T}{TLF \cdot \prod_{j=1}^n S_j}, \quad (9)$$

where

E_T = total entrainment estimate;

S_j = survival rate from parturition to the average age of the entrained larvae at the end of the j^{th} stage; and

TLF = average total lifetime fecundity (TLF) for females, equivalent to the average number of eggs spawned per female over their reproductive years.

While E_T was used in the modeling at SBPP and MBPP, E_{Adj-T} was used at DCP. In practice, survival was estimated by either one or several age classes, depending on the data source, to the estimated age at entrainment. The expected TLF was approximated by the following expression:

$$\begin{aligned} TLF &= \text{Average eggs/year} \cdot \text{Average number of years of reproductive life} \\ &= \text{Average eggs/year} \cdot \left(\frac{\text{Longevity} - \text{Age at maturation}}{2} \right). \end{aligned} \quad (10)$$

The number of years of reproductive potential was approximated as the midpoint between the ages of maturity and longevity. This approximation was based on the assumption of a linear uniform survivorship curve between these events (that is, a uniform survival rate). Total lifetime fecundity for the studies at SBPP was calculated by adding 1 to the difference between longevity and age-at-maturity. This was done to account for spawning during the two ages used in the calculation. For heavily exploited

species such as northern anchovy and sardine (*Sardinops sagax*), the expected number of years of reproductive potential may be much less than predicted using this assumption. Therefore, for the DCP study, the estimated longevity for heavily exploited fishes was based on the oldest observed individual caught by the fishery, rather than by the oldest recorded fish. If life table data are available for a taxon, then the lifetime fecundity should be estimated directly rather than using the approximation presented in Equation 10. The variance of FH was approximated by the Delta method (Seber 1982) and is presented in Appendix A.

Adult Equivalent Loss

The AEL approach uses abundance estimates of entrained or impinged organisms to project the loss of equivalent numbers of adults based on stage-specific survival and age-at-recruitment (Goodyear 1978). The primary advantage of this approach, and of FH, is that it translates power plant-induced early life-stage mortality into numbers of adult fishes, which are familiar units to resource managers. Adult equivalent loss does not require source water estimates of larval abundance in assessing effects. This latter advantage may be offset by the need to gather age-specific mortality rates to predict adult losses and the need for information on the adult population of interest for estimating population-level effects (that is, fractional losses). Other assumptions of AEL using data on survivorship from entrainment to recruitment into the fishery assume the following:

- Published values of life history parameters are representative of the fish population in the years and location for the specific study.
- If survivorship values from the literature are limited to single observations, values are assumed constant over time or representative of the mean survivorship.
- Survival rates used in the calculations are representative and constant for the life stage of the larvae or fish in the calculations.
- Size of the stock does not affect survivorship or the rate of entrainment mortality (no density dependence).

In some cases, survival rates estimated for a similar fish species were used. Should survivorship data from one species be substituted for another, then there is the following additional assumption:

- Values of survivorship for the two species are the same.

For fish species where larval survival data are missing, expected survival could be estimated using fecundity combined with juvenile and adult survival data. This approach requires the following additional assumption:

- The fish population is stationary in size such that each adult female contributes two new offspring to the population of adults during its lifetime.

Starting with the number of age class j larvae entrained, it is conceptually easy to convert the numbers to an equivalent number of adults lost at some specified age class using the following formula:

$$AEL = \sum_{j=1}^n E_j S_j, \quad (11)$$

where,

n = number of age classes;

E_j = estimated number of larvae lost per year in age class j ; and

S_j = survival rate for the j^{th} age class of the 1.. n classes between entrainment and adulthood.

In practice, survival was estimated by either one or several age classes, depending on the data source, from the estimated age at entrainment to recruitment into the fishery. Survivorship to recruitment, at an adult age, was apportioned into several age stages, and AEL was calculated as follows:

$$AEL = E_r \prod_{j=1}^n S_j, \quad (12)$$

where,

S_j = survival rate over the j^{th} age class.

The variance of AEL was approximated by the Delta method (Seber 1982) and is presented in Appendix A.

Alignment of FH and AEL Estimates

AEL and FH can be compared by assuming a stationary population where an adult female must produce two adults (that is, one male and one female). These two adults are products of survival and total lifetime fecundity (TLF) modeled by the following expression:

$$2 = S_{egg} \cdot S_{larvae} \cdot S_{adult} \cdot TLF, \quad (12)$$

which leads to the following:

$$S_{adult} = \frac{2}{TLF \cdot S_{egg} \cdot S_{larvae}}. \quad (13)$$

Substituting into the overall form of the following AEL equation:

$$AEL = E_T \cdot S_{adult}, \quad (14)$$

yields the following:

$$AEL = \frac{2(E_T)}{S_{egg} \cdot S_{larva} \cdot TLF}. \quad (15)$$

Assuming a 50:50 sex ratio, without independent survival rates, AEL and FH are deterministically related as $AEL \equiv 2FH$. The two estimates can be aligned so that female age at maturity is also the age of recruitment used in computing AEL. Otherwise, an alignment age can be accomplished by solving the simple exponential survival growth equation (Ricker 1975, Wilson and Bossert 1971):

$$N_t = N_0 \cdot e^{-Z(t-t_0)}, \quad (16)$$

by substituting numbers of either equivalent adults or hindcast females, their associated ages, and mortality rates into the equation where,

- N_t = number of adults at time t ;
- N_0 = number of adults at time t_0 ;
- Z = instantaneous rate of natural mortality; and
- t = age of hindcast animals (FH) or extrapolated age of animals (AEL).

This allows for the alignment of ages for a population under equilibrium in either direction so they are either hindcast or extrapolated to the same age such that $AEL \equiv 2FH$. Estimates of entrainment mortality calculated from AEL and FH approaches can be compared for similar time periods in taxa for which independent estimates are available for (1) survival from entrainment to the age at maturity, and (2) entrainment back to the number of eggs produced. This comparison serves as a method of cross-validating the two demographic models. Substantial differences between the model estimates may indicate that the population growth rate implied by the model parameters is unrealistically high or low.

FH estimates the number of females at the age of maturity whose reproductive output is lost. The total number of females N_F of all ages in the population can be estimated by the average fecundity as

$$N_F = \frac{E_T}{\bar{F} \cdot \prod_{j=1}^n S_j} \quad (17)$$

AEL can be extrapolated to all mature female ages and summed to make a comparison to $2 \cdot N_F$ using the preceding assumptions. The number of females whose reproductive output is lost in the population, N_F , will be greater than the females estimated by FH. The analogue, sum of extrapolated AEL over adult ages, will be greater than AEL and represents the number of adult males and females lost.

Empirical Transport Model

The ETM estimates conditional probability of mortality (P_M) associated with entrainment and requires an estimate of proportional entrainment (PE) as an input. Proportional entrainment is an estimate of the daily entrainment mortality on larval populations in the source water, independent of other sources of mortality. Following Ricker (1975), PE is an estimate of the conditional mortality rate. Proportional entrainment was calculated using the ratio of intake and source water abundances. In previous entrainment studies using the ETM method, intake concentrations were assumed from weighted population concentrations (Boreman et al. 1981). As proposed by the U.S. Fish and Wildlife Service (Boreman et al. 1978, 1981), ETM has been used to assess entrainment effects at the Salem Nuclear Generating Station in Delaware Bay, New Jersey and at other power stations along the east coast of the United States (Boreman et al. 1978, 1981; PSE&G 1993). Variations of this model have been discussed in MacCall et al. (1983) and used to assess impacts at the San Onofre Nuclear Generating Station (SONGS; Parker and DeMartini 1989).

The ETM estimates conditional mortality due to entrainment, while accounting for spatial and temporal variability in distribution and vulnerability of each life stage to cooling water withdrawals. The original form of the ETM incorporated many time-, space-, and age-specific estimates of mortality as well as information regarding spawning periodicity and larval duration (Boreman et al. 1978, 1981). Most of this information is limited or unknown for the taxa that were investigated for this study. Thus, the applicability of this form of the ETM will be limited by the absence of empirically derived or reported demographic parameters needed as input to the model. The approach used in these studies only requires an estimate of the time the larvae are susceptible to entrainment. By compounding the PE estimate over time, the ETM can be used to estimate entrainment over a period using assumptions about species-specific larval life histories, specifically the length of time in days that the larvae are in the water column and exposed to entrainment.

On each sampling day i , the conditional entrainment mortality can be expressed as follows:

$$PE_i = \frac{E_i}{N_i}, \quad (18)$$

where

E_i = total numbers of larvae entrained during a day during the i^{th} survey; and
 N_i = numbers of larvae at risk of entrainment, that is, abundance of larvae in the sampled source water during a day during the i^{th} survey.

Survival over one day = $1-PE_i$, and survival over the number of days (d) that the larvae are vulnerable to entrainment = $(1-PE_i)^d$, where d is estimated from the lengths of a representative sample of larvae collected over the entire study period. Values used in calculating PE are population estimates based on respective larval concentrations and volumes of the cooling water system flow and source water areas. The estimate of daily entrainment (E_i) was calculated using the methods described in this document. The abundance of larvae at risk in the source water during the i^{th} survey can be directly expressed as follows:

$$N_i = V_S \cdot \bar{\rho}_{N_i}, \quad (19)$$

where

V_S = the static volume of the source water (N); and

$\bar{\rho}_{N_i}$ = the average larval concentration in the source water during the i^{th} survey.

The authors note that the daily estimate of survival used by MacCall et al. (1983) and Boreman et al. (1981) is $S=e^{-PE}$, which assumes the Baranov catch equation, $E=FN$, where F corresponds to PE and N is the average population size (Ricker 1975). The authors' estimate of daily survival assumes that N is the population size prior to entrainment. In the authors' studies, the outcome is approximately the same regardless of the type of survival estimates because PE values were weighted by large populations. When entrainment becomes relatively large, it is recommended to use the Baranov-based estimate as in MacCall et al. (1983) because mortality estimates are reflective of average population size and also are larger.

In the SBPP and MBPP studies, the estimated volumes of source water bodies previously described were used to estimate the abundance using an average concentration based on

all of the samples from the source water for a given survey on a single day. At DCPD the equation to estimate PE for a day on which entrainment was sampled was:

$$PE = \frac{N_E}{N_G}, \quad (20)$$

where

N_E = estimated number of larvae entrained during the day, calculated as
 (estimated concentration of larvae in the water entrained that day) ×
 (design specified daily cooling water intake volume); and

N_G = estimate of larvae in nearshore sampling area that day, calculated as
 $\sum_{i=1}^{64} [(average\ concentration\ per\ cell) \cdot (cell\ volume)]$ for $i = 1, \dots, 64$ grid cells.

where the estimated cell concentrations were obtained from the 72-hour source water survey that contained the 24-hour entrainment sampling period. In addition, an adjustment was made to the estimated number of larvae in the Row 1 cells of the study grid to help compensate for the inability to safely collect samples inshore of the grid (Figure 5). The estimated volume of the water directly inshore of the study grid was multiplied by the concentration of larvae collected in the Row 1 cells, except for cells A1, D1, and E1, as described.

Regardless of whether the species has a single spawning period per year or multiple overlapping spawnings the estimate of total larval entrainment mortality can be expressed as the following:

$$P_M = 1 - \sum_{i=1}^n f_i (1 - P_S PE_i)^d, \quad (21)$$

where

PE_i = estimate of proportional entrainment for the i th survey ($i = 1, \dots, n$);
 P_S = proportion of sampled source water to total estimated source water;
 f_i = annual proportion of total larvae hatched during the i th survey; and
 d = estimated number of days that the larvae are exposed to entrainment.

To establish independent survey estimates, it was assumed that each new survey represented a new, distinct cohort of larvae that was subject to entrainment. Each of the surveys was weighted using the proportion of the total population at risk during the i th survey (f_i). In the original study plan and analyses for MBPP and DCPD studies, the

authors proposed to use the proportion of larvae entrained during each survey period as the weights for the ETM model. Weights were proposed to be calculated as follows:

$$f_i = \frac{E_i}{E_T}, \quad (22)$$

where E_i is estimated entrainment during the i^{th} survey, and E_T is estimated entrainment for the entire study period. This formulation conflicts with the formula for PE that uses the population in the source water during each survey to define the population at risk. If the weights are meant to represent the proportion of the population at risk during each survey, then the weights should be calculated as follows:

$$f_i = \frac{N_i}{N_T}, \quad (23)$$

where N_i is the source population spawned during the i^{th} survey, and N_T is the sum of the N_i s for the entire study period. Weights calculated using the entrainment estimates redefined the population at risk as the population entrained and represented a logical inconsistency in the model. Weights calculated using the source water estimates were used at SBPP and were used in final analyses of the data from the MBPP and DCPD studies in this paper.

The number of days that the larvae of a specific taxon were exposed to the mortality estimated by PE, was estimated using length data from a representative number of larvae from the entrainment samples. At SBPP, a single estimate of larval exposure was used in the calculations. The number of days (d) from hatching to entrainment was estimated by calculating the difference between the values of the 1st and upper 99th percentiles of the length measurements for each entrained larval taxon and dividing this range by an estimate of the larval growth rate for that taxon that was obtained from the scientific literature. The 1st and upper 99th percentiles were used to eliminate potential outlier measurements in the length data. In earlier studies at MBPP and DCPD, two estimates of d were calculated for each taxon and these were used to calculate two ETM estimates. The first estimate calculated d using the difference in length between the 1st and upper 99th percentiles and was used to represent the maximum number of days that the larvae were exposed to entrainment. The second estimate calculated d using the difference in length between the 1st percentile and the average length and was used to represent the average number of days that the larvae were exposed to entrainment.

The estimate of P_s in the ETM model is defined by the ratio of the area or volume of sampled source water to a larger area or volume containing the population of inference (Parker and DeMartini 1989). If an estimate of the larval (or adult) population in the

larger area is available, the value of P_s can be computed directly using the estimate of the larval or adult population in the sampling area, defined by Ricker (1975) as the proportion of the parental stock. If the distribution in the larger area is assumed to be uniform, then the value of P_s for the proportion of the population will be the same as the proportion computed using area or volume.

For the SBPP study, the entire source water was sampled ($P_s = 1.0$) and P_s was not incorporated in the ETM. At the MBPP, P_s was not incorporated in the ETM for fishes that were primarily associated with the estuarine habitats in Morro Bay. The P_s was included for fish and crab taxa whose adult distributions extended into the nearshore waters. Estimates of the population of inference for these taxa were unavailable; therefore, P_s was estimated using the distance the larvae could have traveled based on the duration of exposure to entrainment and current speed as follows:

$$P_s = \frac{L_G}{L_P}, \quad (24)$$

where

L_G = length of sampling area; and

L_P = length of alongshore current displacement based on the period (d) of larval vulnerability for a taxon.

The length of alongshore displacement was calculated using average current speed for the period of January 1, 1996 through May 31, 1999 from an InterOceans S4 current meter deployed at a depth of -6 m MLLW in approximately 30 m of water about 1 km west of the DCP Intake Cove, south of Morro Bay. The current direction was ignored in the calculations but was predominantly alongshore. The current speed was used to estimate unidirectional displacement over the period that the larvae were exposed to entrainment. The value of alongshore displacement (L_P) was compared with the alongshore length of the sampled waterbody (L_G). The distance between the west Morro Bay breakwater and Station 5 is 4.8 km; a value of 9.6 km (twice the distance) was used for L_G . This value was used because it places Station 5 in the center of the sampled water body.

For the MBPP study the authors presented only a single estimate of P_M for the taxa that used an adjustment for P_s in the ETM because any changes due to the increased duration were inversely proportional to the changes in P_s and resulted in nearly equal estimates of P_M . (The exponential model [MacCall et al. 1983], $1 - e^{-P_s P E t}$, gives equal estimates for P_s inversely proportional to t .) The estimate of the standard error is increased due to the

extended period of entrainment risk; so two estimates of the standard error were presented for these taxa.

The sampling for the DCPD study was also extrapolated to provide an estimate of entrainment effects outside the nearshore sampling area. Boreman et al. (1981) point out that if any members of the population are located outside the sampled area, then the ETM will overestimate the conditional entrainment mortality for the entire population. In their study of entrainment at SONGS, Parker and DeMartini (1989) incorporated the inference population (which was an extrapolation to the entire Southern California Bight from the coast to a depth of 75 m, an area extending about 500 km) directly into their estimate of PE. In the DCPD ETM analyses, PE was multiplied by the estimated fraction of the population in the nearshore sampling area (P_s). The size of the population affected by entrainment varied from relatively small (for example, the size of the sampling area) to very large (for example, fishery management units, zoogeographic range). For some species an area approximately the size of the study grid represented the population of inference and, in these cases, $P_s \approx 1$. For other species, the population of inference was larger than the study grid. The population of inference depended not only on the species, but also what appealed usefully to intuition, as a number of methods could be used for extrapolation. Therefore, the ETM was calculated over a range of values of P_s for each of the taxa selected for detailed assessment. The resulting curves were used to determine the ETM at any value of P_s . The curves were interpreted as a continuous probability function representing the risk of entrainment to the larvae at different values of P_s . Point estimates of P_M (and their ranges) were also calculated for each taxon.

The relationship between P_M and P_s was represented by the sets of curves for each of the taxa analyzed for DCPD. Two point estimates of P_s were also computed to account for the variation in the distribution of adult fishes included in the assessment. For offshore and subtidal taxa whose larval distribution extends to the offshore edge of the study grid, P_s was calculated as follows:

$$P_s = \frac{N_G}{N_P}, \quad (25)$$

where N_G is the number of larvae in the study grid, and N_P is the number of larvae in the population of inference. The numerator N_G , presented earlier in the calculation of PE, was calculated as follows:

$$N_G = \sum_{k=1}^{64} A_{G_k} \cdot \bar{D}_k \cdot \rho_{i,k}, \quad (26)$$

where

A_{G_k} = area of grid cell k;

\bar{D}_k = average depth of the k th grid cell; and

ρ_{ik} = concentration (per m^3) of larvae in k th grid cell during survey i .

N_P was estimated by an offshore and alongshore extrapolation of the study grid concentrations, using water current measurements. The following conceptual model was formulated to extrapolate larval concentrations (per m^3) offshore of the grid:

$$P_S = \frac{N_G}{N_P} = \frac{\sum_{j=1}^{K_G} L_{G_j} \cdot W_j \cdot \bar{D}_j \cdot \rho_j}{\sum_{j=1}^{K_P} L_{P_j} \cdot W_j \cdot \bar{D}_j \cdot \rho_j}, \quad (27)$$

where

L_{G_j} = alongshore length of grid in the j th stratum;

W_j = width of j th stratum;

L_{P_j} = alongshore length of population in j th stratum based on current data;

\bar{D}_j = average depth of j th stratum; and

ρ_j = average density of larvae in j th stratum.

For this model, the grid was subdivided into K_G alongshore strata (that is, $K_G=8$ rows in the grid) and the population into $K_P > K_G$ alongshore strata. This approach described discrete values in intervals of a continuous function. Therefore, to ease implementation, an essentially equivalent formula used grid cell concentrations during the i^{th} sampling period, $\rho_{i,k}$ for a linear extrapolation of density (# per m^2 calculated by multiplying $\rho_{i,k}$ by the cell depth) as a function of offshore distance, w :

$$P_{S_i} = \frac{N_{G_i}}{N_{P_i}} = \frac{N_{G_i}}{N_{G_i} \left(\frac{L_{P_i}}{L_G} \right) + L_{P_i} \int_{W_0}^{W_{max}} \rho(w) dw}, \quad (28)$$

where L_P = alongshore length of population in the i^{th} study period based on current displacement. The limits of integration are from the offshore margin of the study grid, W_0 , to a point estimated by the onshore movement of currents or where the density is zero or biologically limited, W_{max} . Note that this point will usually occur outside the study grid area and that the population number, N_P , is composed of two components that represent the alongshore extrapolation of the grid population and the offshore extrapolation of the alongshore grid population (Figure 5).

Alongshore and onshore current velocities used in the calculations were measured at a current meter positioned approximately 1 km west of the DCPPI intake at a depth of approximately 6 m (Figure 5). The direction in degrees true from north and speed in cm/s were estimated for each hour of the nearshore study grid survey periods. Figure 6 shows the results of current meter analysis in which hourly current vectors were first rotated orthogonal to the coast by 49 degrees west of north. The movement of water was then tracked during the period from April 1997 through June 1999. A total alongshore length can be calculated from these data using the maximum upcoast and downcoast current movement over the larval duration period prior to each survey period. The maximum upcoast and downcoast current vectors measured during each survey period were added together to obtain an estimate of total alongshore displacement. This contrasts with the approach for the MBPP where average current speed was used in calculating alongshore movement. Transport of larvae into the nearshore via onshore currents was also accounted for and used to set the limits of the offshore density extrapolation. Within this scenario, there were two subclasses:

1. For species in which the regression of density versus offshore distance had a negative slope, the offshore distance predicted where density was zero (that is, integral of zero) was calculated. The alongshore distance was calculated from the water current data.
2. For species in which the regression of density versus offshore distance had a slope of ≥ 0 , either the offshore distance from the water current data or an average distance based on the depth distribution of the adults offshore was used. Literature values (for example, CalCOFI) were used to place a limit on both the distance and density values used in the offshore extrapolation.

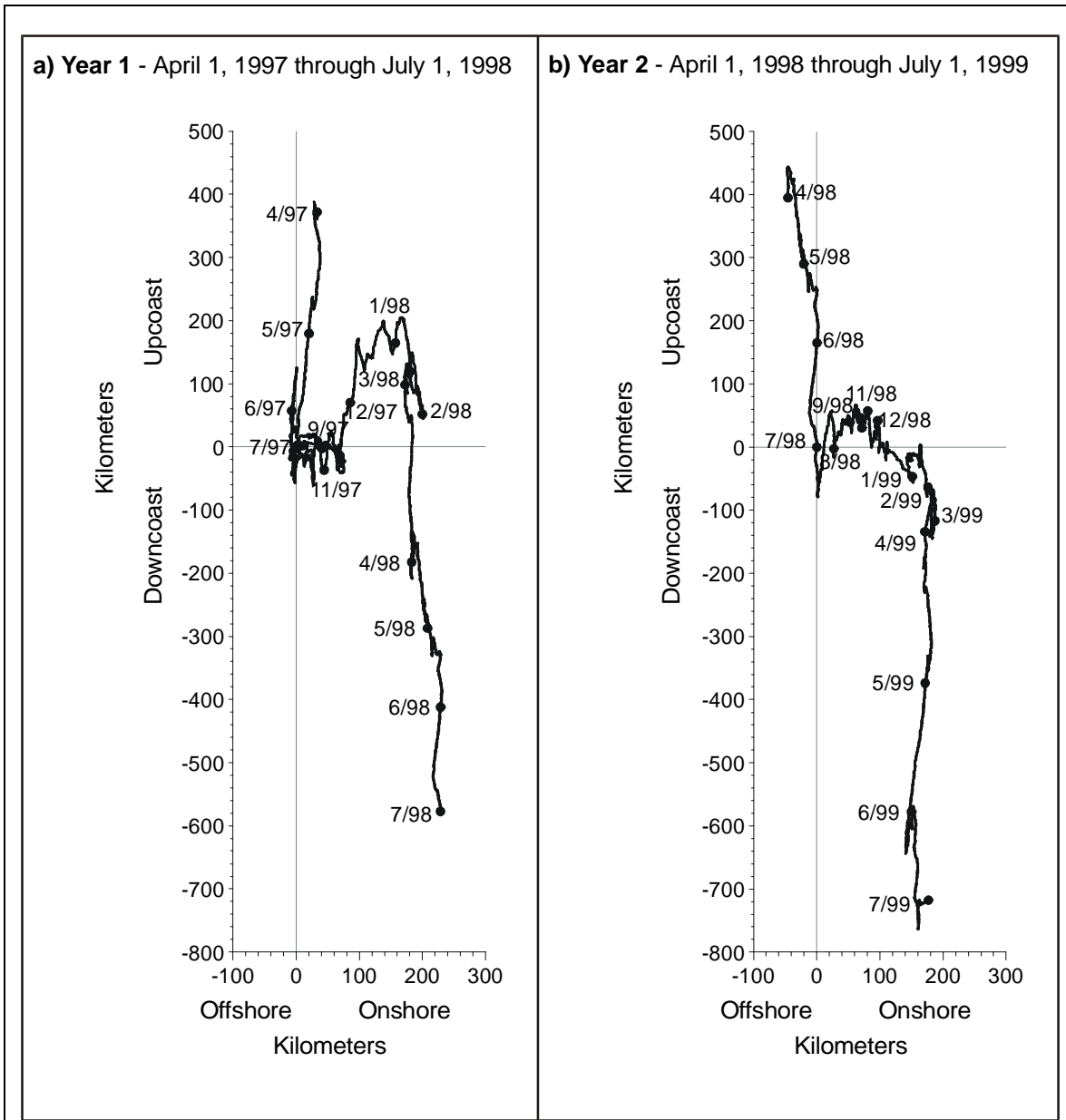


Figure 6. Relative cumulative upcoast/downcoast and onshore/offshore current vectors from current meter located approximately 1 km west of the Diablo Canyon Power Plant intake at a depth of 6 m. Dates on current vectors are the dates of each survey.

Parameter values needed in performing the extrapolation were obtained by using analysis of covariance based on all of the data from the surveys for the study period from July 1997 through June 1999. The following quadratic model was tested in the analysis:

$$\rho_{ij} = \alpha_i + \beta w_{ij} + \gamma w_{ij}^2 + \varepsilon_{ij}, \quad (29)$$

where

- ε_i = normally distributed error term with mean of zero;
- w_{ij} = distance for the i th observation in the j th survey;
- ρ_{ij} = larval density per m^2 for the i th observation in the j th survey; and
- α, β, γ = regression coefficients.

The following linear model produced a better fit in all cases:

$$\rho_{ij} = \alpha_i + \beta w_{ij} + \varepsilon_{ij}. \quad (30)$$

A common slope, β , for all surveys and unique intercepts, α_i , for each survey were derived from the model. It is reasonable to assume a common slope, but differences in abundance between surveys required fitting different intercepts.

Similar to the demographic models there are also assumptions associated with the ETM approach. Although there are fewer life history parameters necessary for the ETM, it shares with the demographic models the assumption that the life history data used to calculate the period the larvae are exposed to entrainment is representative of the population in the years and location for the specific study and accurately estimates the period of larval exposure. Since the ETM is only estimating the entrainment mortality on the population of larvae, assumptions regarding compensation would only be important in interpreting the effects on adult populations. An assumption inherent to all the models is that the sampling resulted in representative estimates of entrainment for the period surveyed. Additional assumptions of the ETM include the following:

- The sampling resulted in representative estimates of the source water populations of larvae susceptible to entrainment and that the PE estimated from the entrainment and source water population samples is representative of entrainment mortality during the survey period.
- The estimates of the source water population represent the proportion for the survey period (f_i) of total larval production.
- The samples during each survey period represent a new and independent cohort of larvae.

Although it would seem that there are also assumptions associated with the definition of the source water population relative to the population of inference, these assumptions become less critical if the ETM results are converted, for example, to “area of production

foregone" (APF). The APF is a useful method for converting the results of ETM into a context for resource managers and is presented in Chapter 4.

Variance calculations for PE are presented in Appendix A. Variance calculations for the estimate of P_M are not presented because of the different approaches and parameters that will be used in the ETM calculations for each study.

CHAPTER 3: RESULTS

Detailed results for an example taxon from each plant are presented to compare the modeling approaches for different source water body types. Results at SBPP are presented for the arrow, cheekspot, and shadow (*Clevelandia ios*, *Ilypnus gilberti*, and *Quietula y-cauda* [CIQ]) goby complex, which was the most abundant fish larvae collected during the study. At Morro Bay and Diablo Canyon, the kelp, gopher, and black-and-yellow (*S. atrovirens*, *S. carnatus*, and *S. chrysomelas* [KGB]) rockfish complex results provided illustrative data. These results provide example calculations for the FH and AEL models as well as for the ETM so that all three modeling approaches can be compared between sites.

The example taxa are indicative of the source water at the three study sites. Since SBPP used a fixed source water body volume, the ETM model for all of the taxa analyzed, including CIQ gobies, was calculated similarly. At MBPP, the ETM model for the taxa that were designated as primarily inhabitants of Morro Bay was calculated using a fixed source water volume using calculations identical to those for CIQ gobies for the SBPP study. Therefore, the authors decided to present the ETM results for the KGB rockfish at MBPP since the source water for this taxon included both the bay and a nearshore area, the size of which was estimated using current meter data. A similar approach was taken for the DCP study and, therefore, the results for the KGB rockfish complex are also presented for that study to provide a comparison with the results for MBPP.

South Bay Power Plant

A total of 23,039 larval fishes in 20 taxonomic categories ranging from ordinal to specific classifications were collected from 144 samples at the SBPP entrainment station (SB1) during monthly sampling from February 2001 through January 2002 (Table 6). These samples were used to estimate that total annual entrainment of fish larvae was 2.42×10^9 . Entrainment samples were dominated by gobies in the CIQ complex, which comprised about 76 percent of the total estimated entrainment. Five taxa evaluated for entrainment effects (Table 4) comprised greater than 99 percent of the total number of fish larvae entrained. No invertebrates were evaluated because only a single *Cancer* crab megalopae was collected.

The entrainment and source water stations extend over a distance of greater than 9 km in south San Diego Bay and include both channel and shallow mudflat habitats. Despite the differences in location and habitat, CIQ complex gobies were the most abundant fish larvae at all of the stations (Appendix B). Other fishes showed considerable variation in abundance among stations. For example, combtooth blennies (*Hypsoblennius* spp.) were much more abundant along the eastern shore north of SBPP where there are more piers

and other structures, whereas longjaw mudsuckers (*Gillichthys mirabilis*) were in highest abundance near the power plant. Overall, taxa richness generally increased from the entrainment station in the far south end of the bay to Station SB9 in the north.

Table 6. Total annual entrainment estimates of larval fishes at South Bay Power Plant based on monthly larval densities (sampled at Station SB1 from February 2001 through January 2002) and the plant’s designed maximum circulating water flows; $n=144$ tows at one station. Data and estimates for taxa comprising <0.01 percent of the composition not presented individually but lumped under other taxa.

Taxa	Common Name	Total Larvae Collected	Est. Total Annual Entrainment	Entrain. Percent Comp.	Entrain. Cum. Percent
CIQ goby complex	gobies	17,878	1,830,899,000	75.64	75.64
<i>Anchoa</i> spp.	bay anchovies	4,390	514,809,000	21.27	96.91
<i>Hypsoblennius</i> spp.	combtooth blennies	226	22,335,000	0.92	97.83
<i>Gillichthys mirabilis</i>	longjaw mudsucker	249	21,953,000	0.91	98.74
Atherinopsidae	silversides	140	14,521,000	0.60	99.34
<i>Syngnathus</i> spp.	pipefishes	101	10,013,000	0.41	99.75
<i>Acanthogobius flavimanus</i>	yellowfin goby	19	2,261,000	0.09	99.85
<i>Strongylura exilis</i>	Calif. needlefish	8	740,000	0.03	99.88
Sciaenidae	croakers	6	706,000	0.03	99.91
	Other 11 taxa	22	2,291,000	0.09	100.00
Total		23,039	2,420,528,000		

SBPP Results for CIQ Gobies

The following sections present results for demographic and empirical transport modeling of SBPP entrainment effects. All three modeling approaches are presented for the CIQ goby complex. CIQ goby larvae were most abundant at the entrainment station during June and July (Figure 7). Brothers (1975) indicated that the peak spawning period for arrow goby occurred from November through April, while spawning in cheekspot and shadow goby was more variable and can occur throughout the year. A peak spawning period for shadow goby in June and July of Brothers’ (1975) study corresponds to the increased larval abundances during those months in this study.

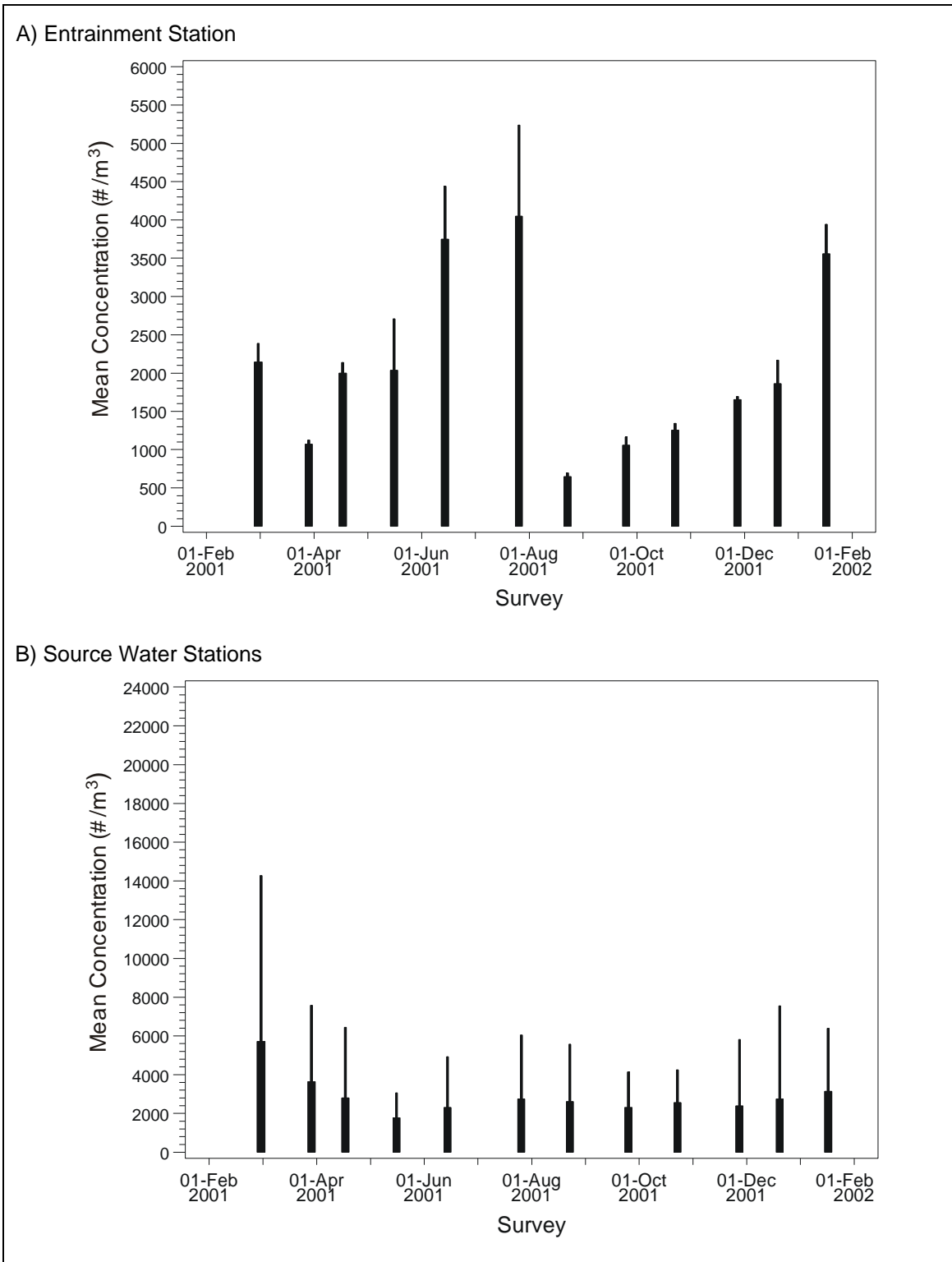


Figure 7. Monthly mean larval concentration (standard error shown at top of dark bars) of the *Clevelandia ios*, *Ilypnus gilberti*, and *Quietula y-cauda* (CIQ) goby complex larvae at SBPP; A) intake entrapment station and B) source water stations.

The ETM required an estimate of the length of time the larvae are susceptible to entrainment. The length frequency distribution for a representative sample of CIQ goby larvae showed that the majority of larvae were recently hatched based on the reported hatch size of 2–3 mm (Moser 1996) (Figure 8). The mean length of the collected CIQ goby larvae was 3.1 mm and the difference between the lengths of the 1st (2.2 mm) and 99th (5.8 mm) percentile values were used with a growth rate of 0.16 mm^{-d} estimated from Brothers (1975) to determine that CIQ goby larvae were vulnerable to entrainment for 22.9 days. The growth rate of 0.16 mm^{-d} was determined using Brothers (1975) reported transformation lengths for the three species and an estimated transformation age of 60 d.

The comprehensive comparative study of the three goby species in the CIQ complex by Brothers (1975) also provided the necessary life history information for both FH and AEL demographic models and shows how life history data from the scientific literature are used in the modeling.

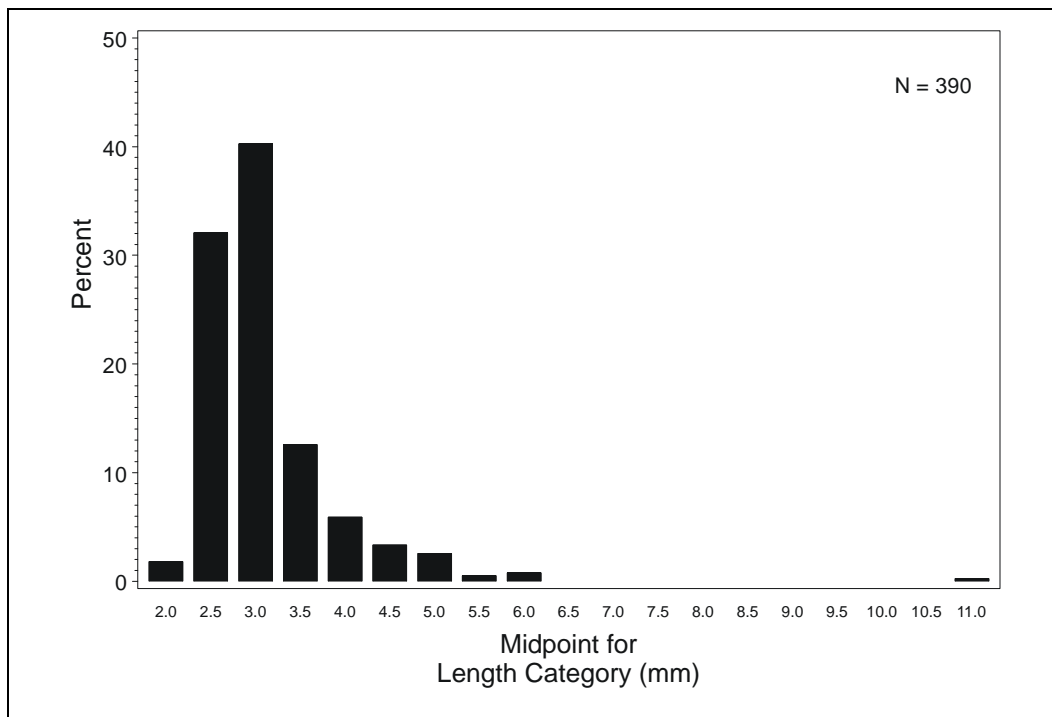


Figure 8. Length frequency distribution for *Clevelandia ios*, *Ilypnus gilberti*, and *Quietula y-cauda* (CIQ) goby complex larvae from the South Bay Power Plant entrainment station.

Fecundity Hindcasting

The annual entrainment estimate for CIQ gobies was used to estimate the number of adult females at the age of maturity whose reproductive output was lost due to entrainment (Table 7). No estimates of egg survival for gobies were available, but

because goby egg masses are demersal (Wang 1986) and parental care, usually provided by the adult male, is common in the family (Moser 1996), egg survival is probably high and was assumed to be 100 percent. Average larval mortality of 99 percent over the two months between hatching and transformation for the three species of CIQ gobies from Brothers (1975) was used to estimate a daily survival rate of 0.931 as follows: $0.931 = (1 - 0.99)^{(6/365.25)}$. Mean length and length of the first percentile (2.2 mm) were used with the growth rate of $0.16 \text{ mm} \cdot \text{d}^{-1}$ to estimate a mean age at entrainment of 5.8 d. Survival to average age at entrainment was then estimated as $0.931^{5.8} = 0.659$. An average batch fecundity estimate of 615 eggs was based on calculations from Brothers (1975) on size-specific fecundities for the three species. Brothers (1975) found eggs at two to three stages of development in the ovaries; therefore, an estimate of 2.5 spawns per year was used in calculating FH ($615 \text{ eggs/spawn} \times 2.5 \text{ spawns/year} = 1,538 \text{ eggs/year}$). The TLF for the studies at SBPP was calculated by adding 1 to the difference between the average ages of maturity (1.0) and longevity (3.3) from Brothers (1975) to account for spawning of a portion of the population during the first year. The FH model was used to estimate that the number of adult females at the age of maturity whose lifetime reproductive output was entrained through the SBPP circulating water system was 1,085,000 (Table 7). The standard error for the entrainment estimate was used to estimate a confidence interval based on just the sampling variance that was considerably less than a confidence interval for the estimate calculated using an assumed CV of 30 percent for all of the life history parameters.

Table 7. Results of fecundity hindcasting (FH) modeling for CIQ goby complex larvae entrained at South Bay Power Plant. The upper and lower estimates are based on a 90 percent confidence interval of the mean. FH was recalculated using the upper and lower confidence interval estimates for total entrainment.

	Estimate	Estimate Std. Error	FH Lower Estimate	FH Upper Estimate	FH Range
FH Estimate	1,085,000	1,880,000	63,000	18,782,000	18,719,000
Total Entrainment	1.83×10^9	21,725,000	961,000	1,209,000	248,000

Adult Equivalent Loss

Three survival components were used to estimate AEL. These were 1) larval survival from the age of entrainment to the age of settlement, 2) survival from settlement to age 1, and 3) from age 1 to the average female age. Larval survival from average age at entrainment through settlement at 60 days was estimated as $0.931^{60-5.8} = 0.021$ using the same daily survival rate used in formulating FH. Brothers (1975) estimated that

mortality in the first year following settlement was 91 percent for arrow, 66–74 percent for cheekspot, and 62–69 percent for shadow goby. These estimates were used to calculate a daily survival rate of 0.995 as follows:

$$0.995 = \frac{(1 - 0.91)^{1/(365.25-60)} + (1 - 0.70)^{1/(365.25-60)} + (1 - 0.65)^{1/(365.25-60)}}{3}$$

This value was used to calculate a finite survival of 0.211 for the first year following settlement as follows: $0.211 = 0.995^{(365.25-60)}$. Adult daily survival from one year through the average female age of 1.71 years from life table data for the three species provided by Brothers (1975) was estimated as 0.99. This value was used to calculate a finite survival of 0.195 as follows: $0.195 = (0.99)^{((1.71 \times 365.25) - 365.25)}$. The product of the three survival estimates and the entrainment estimate were used to estimate that the number of larvae entrained through the SBPP circulating water system number were equivalent to the loss of 1,580,000 adult CIQ gobies (Table 8). The standard error for the entrainment estimate was used to estimate a confidence interval based on just the sampling variance that was considerably less than a confidence interval for the estimate calculated using an assumed CV of 30 percent for all of the life history parameters.

Table 8. Results of adult equivalent loss (AEL) modeling for CIQ goby complex larvae entrained at South Bay Power Plant. The upper and lower estimates are based on a 90 percent confidence interval of the mean. AEL was recalculated using the upper and lower confidence interval estimates for total entrainment.

	Estimate	Estimate Std. Error	AEL Lower Estimate	AEL Upper Estimate	AEL Range
AEL Estimate	1,580,000	2,739,000	91,300	2.74x10 ⁷	2.73x10 ⁷
Total Entrainment	1.83x10 ⁹	2.17x10 ⁷	1,399,000	1,760,000	361,000

Empirical Transport Model

The ETM estimates for CIQ gobies were calculated using the data in Appendix C and a larval duration of 22.9 days. Average larval concentrations from the entrainment and source water sampling were multiplied by the cooling water and source water volumes, respectively, to obtain the estimates that were used in calculating PE estimate for each survey. Weights were calculated by multiplying the source water estimate for each survey by the number of days in the survey period. Estimates for the surveys were summed and the proportion (f_i) for each survey calculated.

Daily mortality (PE_i) estimates ranged from 0.004 to 0.025 for the 12 surveys with an average value of 0.012 (Table 9). This average PE was similar to the volumetric ratio of

the cooling water system to source water volumes (0.015), which was bounded by the range of PE_i estimates. PE_i estimates equal to the volumetric ratio would indicate that the CIQ goby larva were uniformly distributed throughout the source water and were withdrawn by the power plant at a rate approximately equal to that ratio. The small range in both the PE_i estimates and the values of f_i indicate that goby larvae were present in the source water throughout the year. The largest fractions of the source water population occurred in the February ($f_i = 0.2165$) and July ($f_i = 0.1064$) surveys, which was consistent with the spawning periods for arrow and shadow gobies, respectively. June and July surveys also had the highest entrainment station concentrations resulting in higher PE_i estimates for those surveys (Figure 7).

Results for Other Taxa

The modeling results for other taxa selected for detailed assessment showed that both demographic modeling approaches could be calculated only for the CIQ goby complex (Table 10) due mainly to a lack of larval survival estimates for the life stages between larvae and adult. The alignment of the $2*FH$ and AEL estimates would have been improved by extrapolating AEL to the age of maturity rather than the average female age of 1.7 years. Differences in the FH model results among taxa were generally proportional to entrainment estimates as shown by decreasing $2*FH$ estimates for the top four taxa. As the results for the ETM model show, proportional effects of entrainment on the source populations vary considerably for the five taxa and do not reflect differences in entrainment estimates, but the combination of larval concentrations at entrainment and source water stations. The ETM estimates of P_M ranged from 0.031 (3.1 percent) to 0.215 (21.5 percent), with the estimated effects being lowest for combtooth blennies and highest for CIQ gobies and longjaw mudsuckers.

Table 9. Estimates of proportional entrainment (PE) and proportion of source water population present for CIQ goby larvae at South Bay Power Plant entrainment and source water stations from monthly surveys conducted from February 2001 through January 2002.

Survey Date	PE Estimate	Proportion of Source Population for Period (<i>f</i>)
28-Feb-01	0.0057	0.2165
29-Mar-01	0.0045	0.0977
17-Apr-01	0.0109	0.0491
16-May-01	0.0175	0.0475
14-Jun-01	0.0247	0.0620
26-Jul-01	0.0225	0.1064
23-Aug-01	0.0038	0.0675
25-Sep-01	0.0070	0.0704
23-Oct-01	0.0075	0.0661
27-Nov-01	0.0105	0.0773
20-Dec-01	0.0103	0.0584
17-Jan-02	0.0173	0.0811
Average =	0.0118	

Table 10. Summary of estimated South Bay Power Plant entrainment effects based on fecundity hindcasting (FH), adult equivalent loss (AEL), and empirical transport (ETM) estimates of proportional mortality (P_m) models. The FH estimate is multiplied by 2 to test the relationship that $2 \cdot FH \approx AEL$.

Taxa	Entrainment Estimate	% Source Numbers	2*FH	AEL	P_M
CIQ goby complex	1.83×10^9	76.75	2,170,000	1,580,000	0.215
anchovies	5.15×10^8	15.12	214,000	*	0.105
combtooth blennies	2.23×10^7	5.93	21,500	*	0.031
longjaw mudsucker	2.19×10^7	0.17	2,960	*	0.171
silversides	1.45×10^7	0.65	*	*	0.146

* Information unavailable to compute model estimate.

Morro Bay Power Plant

A total of 30,270 larval fishes in 87 taxonomic categories ranging from ordinal to specific classifications was collected from 609 samples at the MBPP entrainment station during weekly sampling from January 2000 through December 2000 (Table 11). These data were used to estimate total annual entrainment of fish larvae at 5.08×10^8 . Entrainment samples were dominated by unidentified gobies, which comprised 77 percent of the total estimated entrainment of fish larvae. The top seven taxa comprising greater than 90

percent of the total and three other commercially or recreationally important fishes in the top 95 percent (white croaker *Genyonemus lineatus*, Pacific herring *Clupea pallasii*, and cabezon *Scorpaenichthys marmoratus*) were evaluated for entrainment effects along with six species of *Cancer* crab megalopae (Table 4) (results for *Cancer* crab not presented).

Table 11. Total annual entrainment estimates of fishes and invertebrates at Morro Bay Power Plant based on weekly larval densities sampled at Station 2 (n=609 tows) from January to December 2000 and the plant's maximum circulating water flows. Data and estimates for taxa comprising <0.01 percent of the composition are not presented individually but lumped as other taxa.

Taxon	Common Name	Total Collected	Estimated Annual # of Entrained Larvae	Percent of Total	Cumulative Percent
Gobiidae unid.	gobies	22,964	393,261,000	77.37	77.37
<i>Leptocottus armatus</i>	Pacific staghorn sculpin	1,129	17,321,000	3.41	80.78
<i>Stenobranchius leucopsarus</i>	northern lampfish	1,018	14,549,000	2.86	83.64
<i>Quietula y-cauda</i>	shadow goby	845	13,504,000	2.66	86.30
<i>Hypsoblennius</i> spp.	combtooth blennies	572	10,042,000	1.98	88.27
<i>Sebastes</i> spp. V_De	KGB rockfishes	360	6,407,000	1.26	89.53
<i>Atherinopsis californiensis</i>	jacksmelt	384	6,266,000	1.23	90.76
<i>Rhinogobiops nicholsi</i>	blackeye goby	226	3,778,000	0.74	91.51
<i>Gillichthys mirabilis</i>	longjaw mudsucker	186	3,286,000	0.65	92.15
<i>Lepidogobius lepidus</i>	bay goby	181	3,233,000	0.64	92.79
<i>Clupea pallasii</i>	Pacific herring	242	3,030,000	0.60	93.39
<i>Scorpaenichthys marmoratus</i>	cabezon	171	2,888,000	0.57	94.54
Atherinopsidae unid.	silversides	163	2,720,000	0.54	95.08
<i>Atherinops affinis</i>	topsmelt	153	2,575,000	0.51	95.58
<i>Sebastes</i> spp. V	rockfishes	150	2,453,000	0.48	96.07
<i>Tarletonbeania crenularis</i>	blue lanternfish	142	2,213,000	0.44	96.50
<i>Engraulis mordax</i>	northern anchovy	155	2,136,000	0.42	96.92
larval fish - damaged	larval fish - damaged	74	1,283,000	0.25	97.18
<i>Gibbonsia</i> spp.	clinid kelpfish	98	1,141,000	0.22	97.40
<i>Bathymasteridae</i> unid.	ronquils	67	1,119,000	0.22	97.62
Cottidae unid.	sculpins	59	1,009,000	0.20	97.82
<i>Artedius lateralis</i>	smoothhead sculpin	46	739,000	0.15	97.96
<i>Oligocottus</i> spp.	sculpin	40	620,000	0.12	98.09
Stichaeidae unid.	pricklebacks	41	616,000	0.12	98.21
Chaenopsidae unid.	tube blennies	31	551,000	0.11	98.32
<i>Cebidichthys violaceus</i>	monkeyface eel	28	505,000	0.10	98.41
<i>Bathylagus ochotensis</i>	popeye blacksmelt	28	495,000	0.10	98.51
	59 other taxa	483	7,564,000	2.93	100.00
Total Larvae		30,270	508,296,000		

Species composition for entrainment at MBPP was much more diverse than the results from SBPP. This may have resulted from the more frequent weekly sampling at MBPP and the location of the power plant near the entrance to the bay relative to the back bay location of SBPP. Entrainment was dominated by fishes that primarily occur as adults in the bay, such as gobies, but also included numerous fishes that are more typically associated with nearshore coastal habitats, such as rockfish and cabezon.

MBPP Results for the KGB Rockfish Complex

Detailed results and details on the data used in the three modeling approaches at MBPP are presented for the KGB larval rockfish complex. KGB rockfish had the sixth highest estimated entrainment (6,407,000) or 1.3 percent of the total larval fishes (Table 11). Consistent with the annual spawning period for most rockfishes (Parrish et al. 1989), larvae occurred in entrainment samples from January through June with the highest abundances in April (Figure 9). Results from source water surveys showed the same abundance peaks seen in samples collected at the MBPP intake station (Figure 10). Although not collected every month, KGB rockfish larvae were collected from all of the stations inside Morro Bay during the April survey. They reached their greatest concentration at the Estero Bay Station 5 during the May survey when they were less common at the stations inside Morro Bay.

The length frequency distribution for a representative sample of KGB rockfish larvae showed a relatively narrow size range of 3.4 to 5.4 mm (1st and 99th percentile values = 3.5 and 5.1) with an average size of 4.3 mm (Figure 11). These results indicate that most of the larvae are less than the maximum reported size at extrusion of 4.0–5.5 mm (Moser 1996) and are therefore subject to entrainment for a relatively short period. There are no studies on the larval growth rates for the species in the KGB rockfish complex, so a larval growth rate of 0.14 mm^{-d} from brown rockfish (Love and Johnson 1999, Yoklavich et al. 1996) was used in estimating that the average age at entrainment was 5.5 d, and the maximum age at entrainment, based on the 99th percentile values, was 11.3 d.

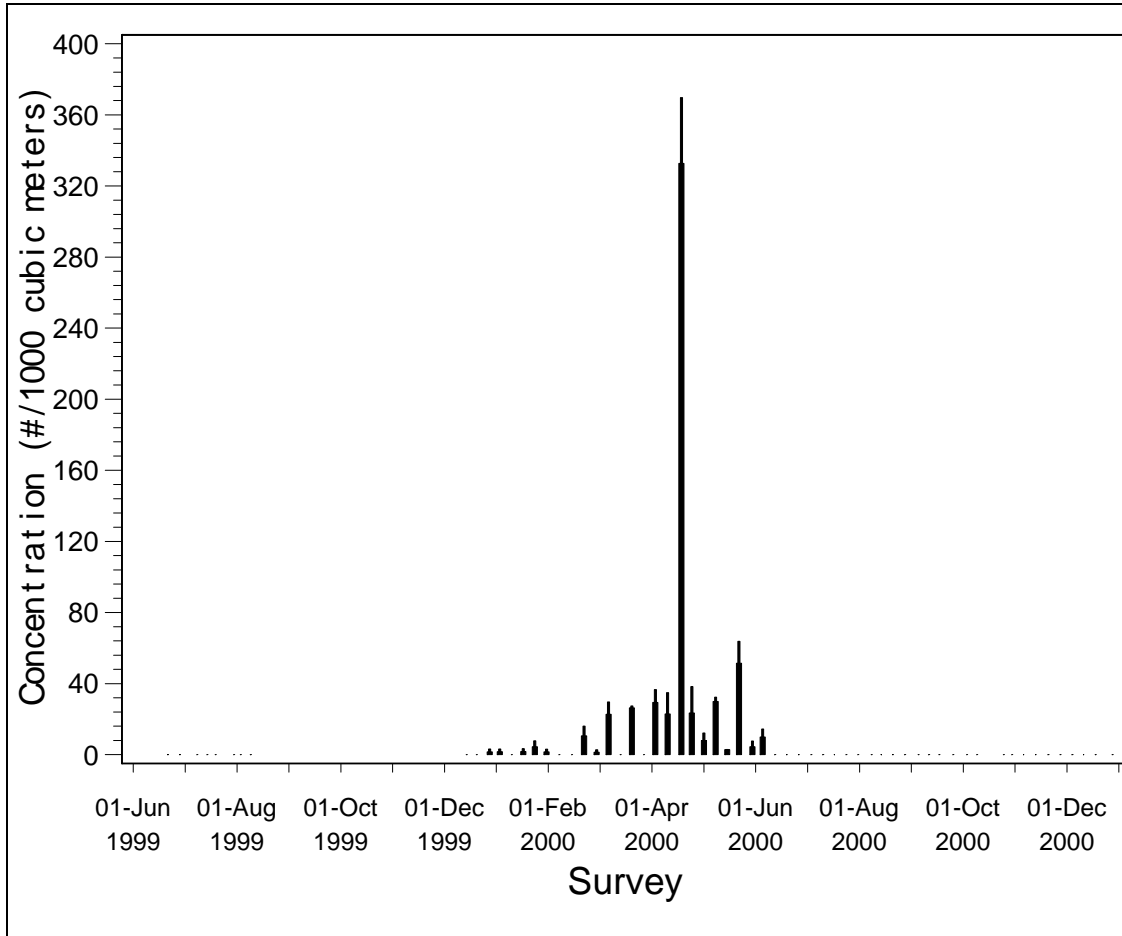


Figure 9. Weekly mean larval concentration of kelp, gopher, and black-and-yellow (KGB) rockfish complex larvae at the Morro Bay Power Plant intake entrainment station.

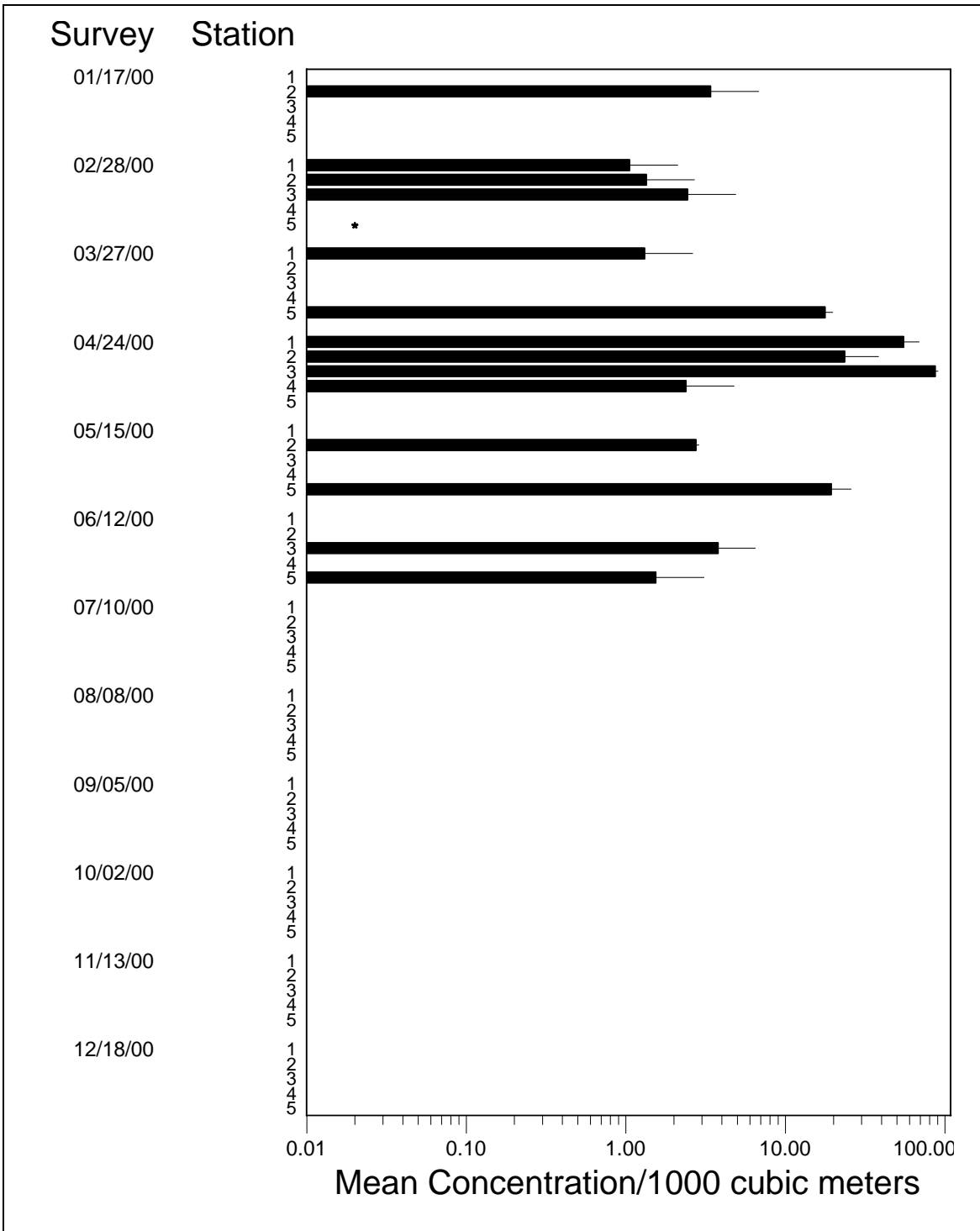


Figure 10. Comparison of average concentrations of kelp, gopher, and black-and-yellow (KGB) rockfish complex larvae at the Morro Bay Power Plant intake (Station 2), Morro Bay source water (Stations 1, 3, and 4), and Estero Bay (Station 5) from January 2000 through December 2000 with standard error indicated (+1 SE). Entrainment data only plotted for paired surveys. *No samples were collected during February 2000 at Station 5. Note that data are plotted on a log₁₀ scale.

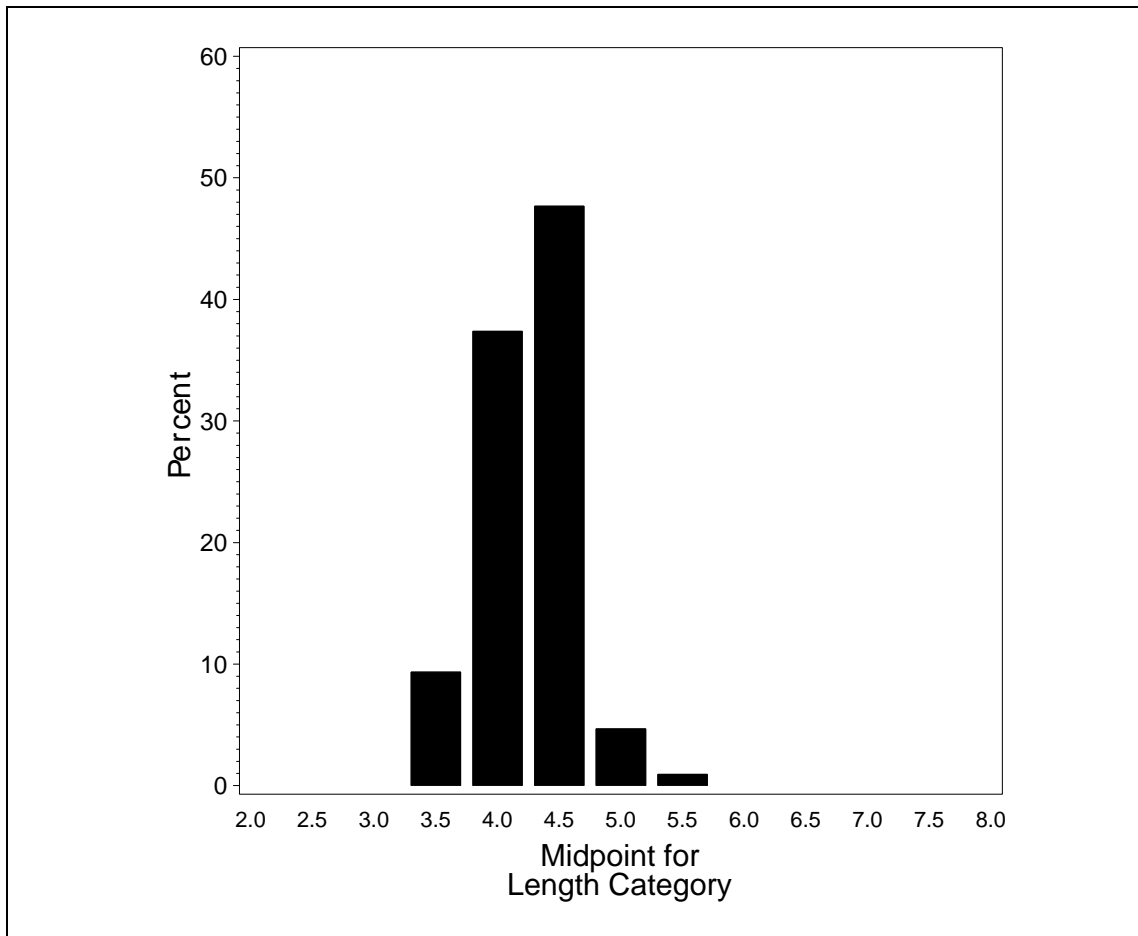


Figure 11. Length frequency distribution for kelp, gopher, and black-and-yellow (KGB) rockfish complex larvae from the Morro Bay Power Plant entrainment station.

Fecundity Hindcast Model

Total annual larval entrainment for KGB rockfish was used to estimate the number of adult females at the age of maturity whose reproductive output was lost due to entrainment (Table 12). The parameters required for formulation of FH estimates for KGB rockfishes were compiled from references on different rockfish species. Rockfishes are viviparous and release larvae once per year. A finite survival rate of 0.463 for the larvae from time of release to the average age at entrainment was estimated using an instantaneous mortality rate of 0.14/day from blue rockfish (Mary Yoklavich, NOAA/NMFS/PFEG, Pacific Grove, CA, pers. comm. 1999) over 5.5 days ($0.463 = e^{-0.14 \times 5.5}$). An average annual fecundity estimate of 213,000 eggs per female was used in calculating FH (DeLacy et al. 1964: 52,000-339,000; MacGregor 1970: 44,118-104,101 and

143,156-182,890; Love and Johnson 1999: 80,000-760,000). Estimates of five years as the age at maturity and 15 years for longevity were used in calculating FH (Burge and Schultz 1973, Wyllie Echeverria 1987, Lea et al. 1999). The model estimated that the reproductive output of 13 adult females at the age on maturity was entrained by the MBPP (Table 12). Variation due to sampling error had only a small effect on the range of estimates.

Adult Equivalent Loss

Total annual MBPP entrainment of KGB rockfish was used to estimate the number of equivalent adults theoretically lost to the population. The parameters required for formulation of AEL estimates for KGB rockfish were derived from data on larval blue rockfish survival. Survivorship of KGB rockfishes from parturition to an estimated recruitment age of three years was partitioned into six stages (Table 13). The estimate of AEL was calculated assuming the entrainment of a single age class having the average age of recruitment. The estimated number of equivalent adults corresponding to the number of larvae that would have been entrained by the proposed MBPP combined-cycle intake was 23 (Table 14). The uncertainty of the AEL estimate due to sampling error was very small.

Although the FH and AEL estimates were very close to the theoretical relationship of $2FH \equiv AEL$, the AEL was only extrapolated to age three. The estimate would decrease by extrapolating to five years, the age of maturity used in the FH calculations.

Table 12. Annual estimates of adult female kelp, gopher, and black-and-yellow (KGB) rockfish losses at Morro Bay Power Plant based on larval entrainment estimates using the fecundity hindcasting (FH) model for the January through December 2000 data. Upper and lower estimates represent the changes in the model estimates that result from varying the value of the corresponding parameter in the model.

	Estimate	Estimate Std. Error	Upper FH Estimate of	Lower FH Estimate	FH Range
FH Estimate	13	8	37	5	32
Entrainment	6,407,000	189,000	14	12	2

Table 13. Survival of the kelp, gopher, and black-and-yellow (KGB) rockfish complex larvae to an age of three years, based on blue rockfish (*Sebastes mystinus*) data.

Lifestage	Day (Start)	Day (End)	Instantaneous Natural Daily Mortality (Z)	Lifestage Survival (S)
Early larval 1	0	5.5	0.14	0.463
Early larval 2	5.5	20	0.14	0.131
Late larval	20	60	0.08	0.041
Early juvenile	60	180	0.04	0.008
Late juvenile	180	365	0.0112	0.126
Pre-recruit	365	1,095	0.0006	0.645

Note: Survival was estimated from release as $S = e^{(-Z)(\text{Day}(\text{end})-\text{Day}(\text{Start}))}$. Daily instantaneous mortality rates (Z) for blue rockfish larvae were used to calculate KGB larval survivorship and were provided by Mary Yoklavich (NOAA/NMFS/PFEG, Pacific Grove, CA, pers. comm. 1999). Annual instantaneous mortality was assumed as 0.2/year after two-year average age of entrainment was estimated as 5.5 days based on average size at entrainment and a growth rate of 0.14 mm/day (0.006 in./day) (Yoklavich et al. 1996).

Empirical Transport Model

The estimated P_M value for the KGB rockfish complex was 0.027 (2.7%) for the period of entrainment risk applied in the model (11.3 days) (Table 15) (All of the data used in the ETM calculations are in Appendix D). The model included an adjustment for P_s (0.088) because this taxon occupies nearshore habitats that extend well beyond the sampling areas. The value of P_s was computed by using alongshore distance of the sampled source water area (9.6 km) and dividing it by the alongshore distance the larvae could have traveled during the 11.3 day larval duration at an average current speed of 11.3 cm/s. The PE estimates ranged from 0 to 0.3097 (Table 15). Although the largest PE estimate occurred for the January survey, the largest fraction of the population was collected during the April survey ($f_i = 0.7218$) when the PE estimate was an order of magnitude lower.

Table 14. Annual estimates of adult kelp, gopher, and black-and-yellow (KGB) rockfish losses at Morro Bay Power Plant due to entrainment using the adult equivalent loss (AEL) model for the January through December 2000 data. Upper and lower estimates represent the changes in the model estimates that result from varying the value of the corresponding parameter in the model.

	Estimate	Estimate Std. Error	Upper AEL Estimate	Lower AEL Estimate	AEL Range
AEL Estimate	23	15	69	8	61
Total Entrainment	6,407,000	189,000	24	22	2

Table 15. Estimates of KGB rockfish larvae at MBPP entrainment and source water stations from monthly surveys conducted from January 2000 through December 2000 used in calculating empirical transport model (ETM) estimates of proportional entrainment (PE) and annual estimate of proportional mortality (P_M). The daily cooling water intake volume used in calculating the entrainment estimates was 1,619,190 m³, and the volume of the source water used in calculating the source water population estimates was 15,686,663 m³. Bay volume = 20,915,551 m³. The larval duration used in the calculations was 11.28 days. More detailed data used in the calculations are presented in Appendix E.

Survey Date	Bay PE	Offshore PE	Total PE	Proportion of Source Population for Period (f)
17-Jan-00	0.3097	0	0.3097	0.0099
28-Feb-00	0.1052	0.0988	0.0509	0.0239
27-Mar-00	0	0	0	0.1076
24-Apr-00	0.0533	0.0661	0.0295	0.7218
15-May-00	0.3785	0.0220	0.0208	0.1197
12-Jun-00	0	0	0	0.0169
10-Jul-00	0	0	0	0
8-Aug-00	0	0	0	0
5-Sep-00	0	0	0	0
2-Oct-00	0	0	0	0
27-Nov-00	0	0	0	0
18-Dec-00	0	0	0	0
	$\bar{x} = 0.0705$	$\bar{x} = 0.0156$	$\bar{x} = 0.0342$	

Results for Other Taxa

The modeling results for other taxa selected for detailed assessment showed that both demographic models could only be used with about half of the fishes analyzed (Table

16). Differences in the demographic model results among taxa were generally proportional to the differences in entrainment estimates as shown by the decreasing 2*FH estimates for the six fishes analyzed. An exception was KGB rockfishes that had lower model estimates in proportion to their entrainment due to the longer lifespan and later age of maturity of this taxa group relative to the other fishes analyzed. The ETM estimates of P_M for the analyzed fishes ranged from 0.025 (2.5 percent) to 0.497 (49.7 percent) with the estimated effects being lowest for fishes with source populations that extended outside the bay into nearshore areas. The highest estimated effects occurred for combtooth blennies that are commonly found as adults among the fouling communities on the piers and structures that are located along the waterfront near the MBPP intake.

Table 16. Summary of estimated Morro Bay Power Plant entrainment effects based on fecundity hindcasting (FH), adult equivalent loss (AEL), and empirical transport (ETM) estimates of proportional mortality (P_M) models. The FH estimate is multiplied by 2 to test the relationship that 2·FH = AEL. ETM model (P_M) calculated using nearshore extrapolation of source water population.

Taxon	Common Name	Total Entrainment	2*FH	AEL	P_M
Gobiidae	unidentified gobies	3.9×10^8	796,000	268,000	0.116
<i>Leptocottus armatus</i>	Pacific staghorn sculpin	1.7×10^7	*	*	0.051
<i>Stenobranchius leucopsarus</i>	northern lampfish	1.5×10^7	*	*	0.025
<i>Quietula y-cauda</i>	shadow goby	1.3×10^7	12,700	7,440	0.028
<i>Hypsoblennius</i> spp.	combtooth blennies	1.0×10^7	8,720	8,080	0.497
<i>Sebastes</i> spp. V_De	KGB rockfishes	6.4×10^6	26	*	0.027
<i>Atherinopsis californiensis</i>	jacksmelt	6.3×10^6	*	*	0.217
<i>Genyonemus lineatus</i>	white croaker	3.0×10^6	106	*	0.043
<i>Clupea pallasii</i>	Pacific herring	3.0×10^6	86	532	0.164
<i>Scorpaenichthys marmoratus</i>	cabezon	2.9×10^6	*	*	0.025

* - Information unavailable to compute model estimate.

Diablo Canyon Power Plant

There were 97,746 larval fishes identified and enumerated from the 4,693 entrainment samples processed for the DCPD study (Table 17). These were placed into 178 different taxonomic categories ranging from ordinal to specific classifications. This list of taxa was much more diverse than the studies at SBPP and MBPP due to length of the sampling effort, number of samples collected, and greater variety of habitats found in the area around the DCPD. The taxa in highest abundance were those whose adults were generally found close to shore, in shallow water. One exception was the thirteenth most abundant taxon, the northern lampfish, whose adults are found midwater and to depths of 3,000 m (Miller and Lea 1972). Fourteen fish taxa (Table 4) were selected for detailed assessment using the FH, AEL, and ETM approaches based on their numerical abundance in the samples and their importance in commercial or recreational fisheries.

There were 43,785 larval fishes identified and enumerated from the 3,163 samples processed from the nearshore sampling area. These comprised 175 different taxa ranging from ordinal to specific levels of classification. Adults of these taxa live in a variety of habitats, from intertidal and shallow subtidal to deep-water and pelagic habitats. The taxa in highest abundance in the nearshore sampling area were those whose adults were typically pelagic or subtidal; the more intertidally or nearshore distributed species were found in lower abundance in the sampling area.

DCPD Results for the KGB Rockfish Complex

Larval rockfishes in the KGB complex showed distinct seasonal peaks of abundance at the DCPD intake structure, with their greatest abundance tending to occur between March and July (Figure 12). An El Niño began developing during the spring of 1997 (NOAA 1999) and was detected along the coast of California in fall of that year (Lynn et al. 1998). This may have slightly affected the density in 1998 compared with the previous year. The El Niño event did not affect seasonal peaks in abundance between years; during both periods KGB rockfish larvae first starting appearing in February, reached peak abundances in April and May, and were not present following late-July.

Table 17. Fishes collected during Diablo Canyon Power Plant entrainment sampling. Fishes comprising less than 0.4 percent of total not shown individually but lumped under “other taxa”.

Taxon	Common Name	Count	Percent of Total	Cumulative Percent
<i>Sebastes</i> spp. V_De (KGB rockfish complex)	rockfishes	17,576	18.0	18.0
<i>Gibbonsia</i> spp.	clinid kelpfishes	9,361	9.6	27.6
<i>Rhinogobiops nicholsi</i>	blackeye goby	7,658	7.8	35.4
<i>Cebidichthys violaceus</i>	monkeyface eel	7,090	7.3	42.6
<i>Artedius lateralis</i>	smoothhead sculpin	5,598	5.7	48.4
<i>Orthonopias triacis</i>	snubnose sculpin	4,533	4.6	53.0
<i>Genyonemus lineatus</i>	white croaker	4,300	4.4	57.4
Cottidae unid.	sculpins	3,626	3.7	61.1
Gobiidae unid.	gobies	3,529	3.6	64.7
<i>Engraulis mordax</i>	northern anchovy	3,445	3.5	68.3
Stichaeidae unid.	pricklebacks	2,774	2.8	71.1
<i>Sebastes</i> spp. V (blue rockfish complex)	rockfishes	2,731	2.8	73.9
<i>Stenobranchius leucopsarus</i>	northern lampfish	2,326	2.4	76.3
<i>Sardinops sagax</i>	Pacific sardine	2,191	2.2	78.5
<i>Scorpaenichthys marmoratus</i>	cabezon	1,938	2.0	80.5
<i>Oligocottus</i> spp.	sculpins	1,708	1.7	82.2
Bathymasteridae unid.	ronquils	1,336	1.4	83.6
<i>Oxylebius pictus</i>	painted greenling	1,133	1.2	84.8
<i>Oligocottus maculosus</i>	tidepool sculpin	1,035	1.1	85.8
<i>Liparis</i> spp.	snailfishes	900	0.9	86.7
Chaenopsidae unid.	tube blennies	817	0.8	87.6
Pleuronectidae unid.	righteye flounders	698	0.7	88.3
<i>Clinocottus analis</i>	wooly sculpin	683	0.7	89.0
<i>Sebastes</i> spp. V_D	rockfishes	656	0.7	89.7
<i>Ruscarius creaseri</i>	roughcheek sculpin	633	0.6	90.3
<i>Artedius</i> spp.	sculpins	623	0.6	90.9
<i>Lepidogobius lepidus</i>	bay goby	541	0.6	91.5
<i>Bathylagus ochotensis</i>	popeye blacksmelt	497	0.5	92.0
<i>Paralichthys californicus</i>	California halibut	378	0.4	92.4
<i>Parophrys vetulus</i>	English sole	361	0.4	92.8
<i>Sebastes</i> spp.	rockfishes	357	0.4	93.1
Osmeridae unid.	smelts	356	0.4	93.5
<i>Neoclinus</i> spp.	fringeheads	352	0.4	93.9
	144 other taxa	6,006	6.1	100.0
	Total Larvae	97,746		

There were 17,863 larval KGB rockfishes identified from 774 of samples collected at the DCPD intake structure between October 1996 and June 1999, representing 20 percent of the entrainment samples collected and processed during that period. Annual estimated numbers of KGB rockfish larvae entrained at DCPD varied relatively little between the 1996–97 Analysis Period 1 (268,000,000) and the 1997–98 Analysis Period 2 (199,000,000) (Table 18). An approximation of 95 percent confidence intervals (± 2 std. errors) for the two estimates overlap, indicating that the differences between them were probably not statistically significant and that entrainment of KGB rockfish larvae was relatively constant between years.

Estimates of annually entrained KGB rockfish larvae were adjusted (Table 18) to the long-term average DCPD Intake Cove surface plankton tow index, calculated as the ratio between the nine-year average of DCPD Intake Cove sampling (Figure 13) and the average annual index estimated from these same tows during the year being adjusted. Average indices for 1997 and 1998 were 0.070 and 0.065 larvae/m³, respectively, and the long-term average index for 1990 through 1998 was 0.072 larvae/m³. Thus, the ratios used to adjust the 1997 and 1998 estimates of larvae entrained were 1.03 and 1.13, respectively, indicating that larval density was slightly lower than the long-term average during those years. Adjustments resulted in estimates of 275,000,000 entrained KGB rockfish larvae for 1996–97 Analysis Period 1 and 222,000,000 for 1997–98 Analysis Period 2 (Table 18). The same trends in overall abundance as noted for unadjusted entrainment values were apparent in the adjusted values; namely, larval KGB rockfish abundance changed little between analysis periods. Annual estimates of abundance during the study period were low relative to the long-term average index of larval abundance from the Intake Cove plankton tows as indicated by the index ratios greater than one.

Larval KGB rockfishes generally occurred in the nearshore sampling area with similar seasonality to that observed at the DCPD intake structure with peak abundance occurring in May of both 1998 and 1999 (Figure 12). There were 5,377 KGB rockfish larvae identified from 701 samples representing 23 percent of the nearshore sampling area samples collected and processed from July 1997 through June 1999. The mean concentrations in May of each sampling year were very similar (1998: 0.29/m³; 1999: 0.28/m³), indicating little change in abundance between the El Niño and subsequent La Niña years. The pattern of abundances in the nearshore sampling area differed between years with larger abundances of larvae in the sampling cells closest to shore during 1999 (Figure 14b). Regression analyses of the data for the two sampling periods showed declining abundances with increasing distance offshore (negative slope) for the 1999 period and almost no change with increasing distance offshore for the 1998 period (Appendix F).

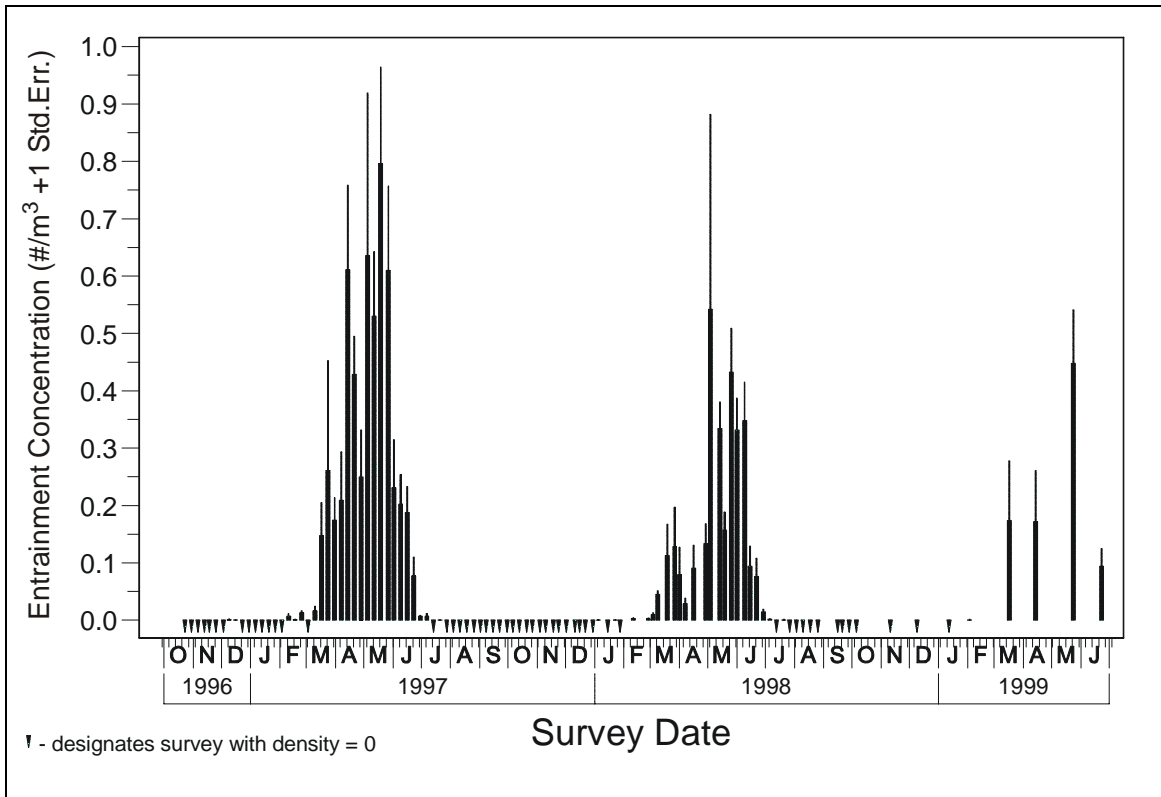


Figure 12. Weekly mean larval concentrations of kelp, gopher, and black-and-yellow (KGB) rockfish complex larvae at the Diablo Canyon Power Plant intake entrainment stations. Dark bars represent mean concentration, and thinner bars represent one standard error.

Table 18. Diablo Canyon Power Plant entrainment estimates (E_T) and standard errors for kelp, gopher, and black-and-yellow (KGB) rockfish complex. E_{Adj-T} refers to the number entrained after adjustment to a long-term mean density. Note: The results for Analysis Periods 2 and 3 are the same because the overlap between the periods occurred during the peak larval abundances of KGB rockfish larvae.

<i>Analysis Period</i>	E_T	$SE(E_T)$	E_{Adj-T}	$SE(E_{Adj-T})$
1) Oct 1996 – Sept 1997	268,000,000	24,000,000	275,000,000	24,700,000
2) Oct 1997 – Sept 1998	199,000,000	25,900,000	222,000,000	28,900,000

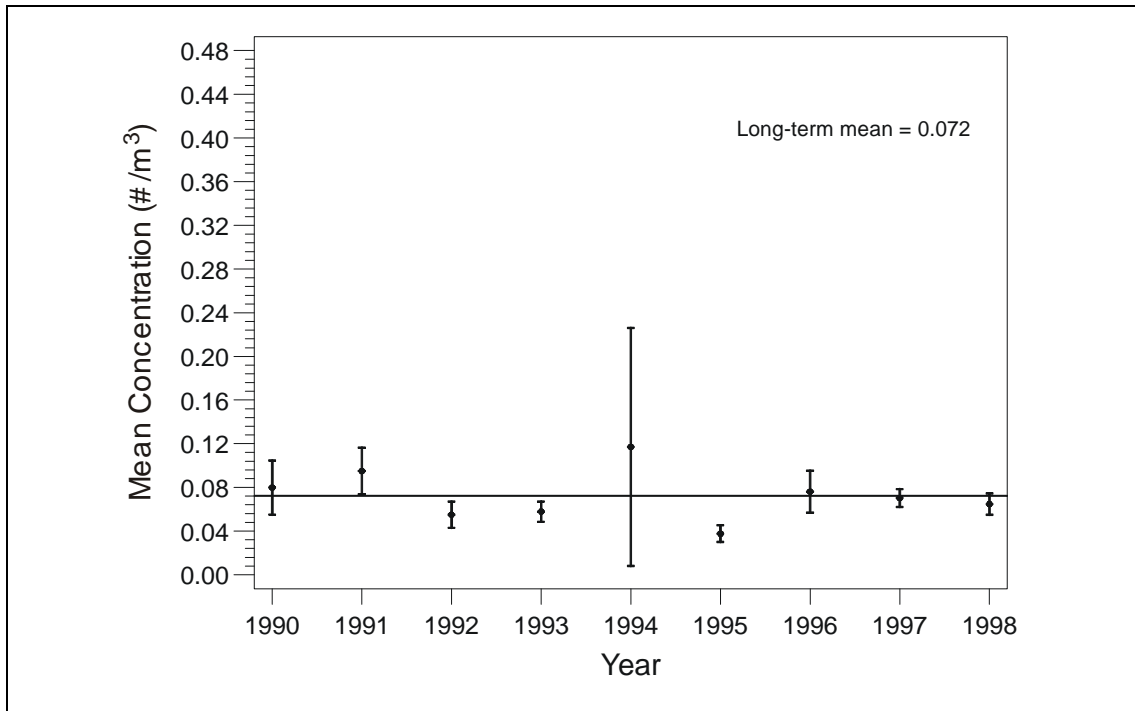


Figure 13. Annual mean concentration (+/- 2 standard errors) for kelp, gopher, and black-and-yellow (KGB) rockfish complex larvae collected from surface plankton tows in DCPD Intake Cove. Data were collected from December through June for every year except 1990 when only data from February through June were collected. The horizontal line is the long-term mean for all years combined.

Standard lengths of all measured KGB rockfish larvae collected at the DCPD intake structure between October 1996 and June 1999 (9,926 larvae) ranged from 2.4 to 8.0 mm (mean = 4.2 mm) (Figure 15). The lengths of entrained KGB larvae, excluding the largest 1 percent and smallest 1 percent of all measurements, ranged from 3.3 to 5.6 mm. Similar to the KGB assessment at Morro Bay, a growth rate of 0.14 mm/d (Mary Yoklavich, NOAA / NMFS / PFEG, Santa Cruz, CA, pers. comm. 1999) was used to estimate the age of entrained larvae. Assuming that the size of the smallest 1 percent represents post-extrusion larvae that are aged zero days (d), then the estimated ages of entrained larvae ranged from zero up to ca. 16.4 d post-extrusion for the size of the largest 1 percent of the larvae. The estimated average age of KGB larvae entrained at DCPD was 6.4 d post-extrusion. The reported extrusion size for species in this complex ranges from 4.0–5.5 mm (Moser 1996).

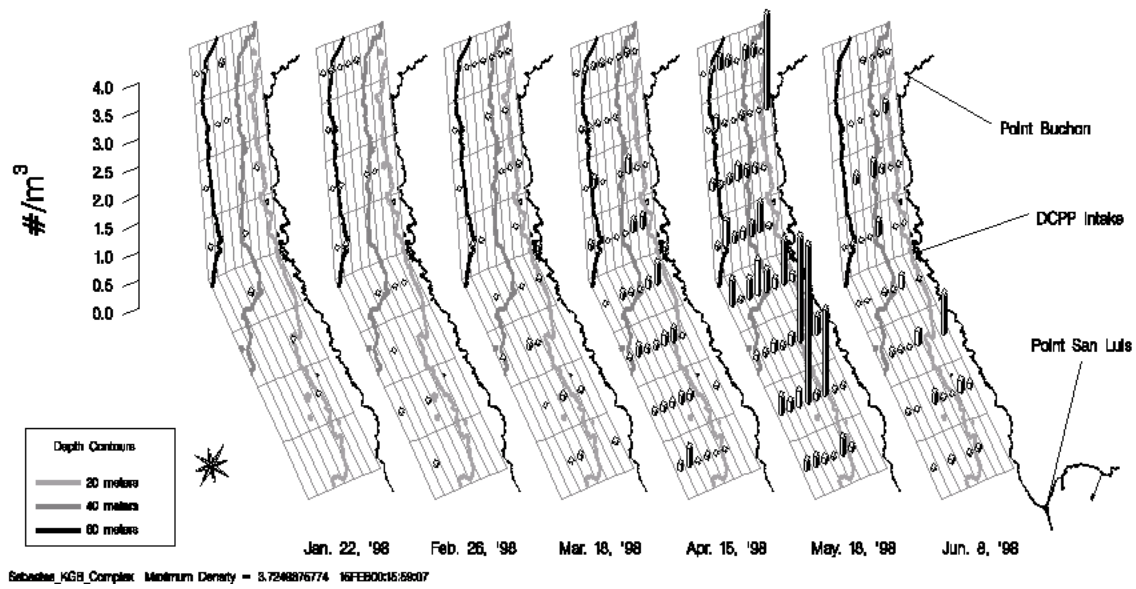
Fecundity Hindcasting

The same life history parameter values used for the MBPP study (Table 13) were also used to calculate FH estimates for the KGB rockfish complex for the DCPD study.

Average age at entrainment was estimated as 6.2 d. This was calculated by subtracting the value of the 1st percentile value of the lengths (3.3 mm) from the mean length at entrainment (4.2 mm) and dividing by the larval growth rate for brown rockfish of 0.14 mm/d (Love and Johnson 1999; Yoklavich et al. 1996) that was also used in the MBPP study. The survival rate of the KGB larvae from size at entrainment to size at recruitment into the fishery was partitioned into six stages from parturition to recruitment using the same approach presented for the MBPP study (Table 19). The survival rate from extrusion to the average age at entrainment using data from blue rockfish was estimated as 0.419 ($0.419 = e^{(-0.14)(6.2)}$).

The estimated number of adult KGB rockfish females at the age of maturity whose reproductive output was been lost due to entrainment was 617 for the 1996–97 period and 497 for the 1997–98 period (Table 19). The similarity between the estimates was a direct result of the similarity between adjusted entrainment estimates for the two periods. Low FH estimates resulted from the relatively high fecundity of adults and young average entrainment age estimated for larvae in this complex and not including other sources of mortality such as losses due to fishing in the model. The variation in the entrainment estimate had very little effect on the model estimates relative to the variation resulting from the life history parameters.

A) January 1998 – June 1998 surveys



B) January 1999 – June 1999 surveys

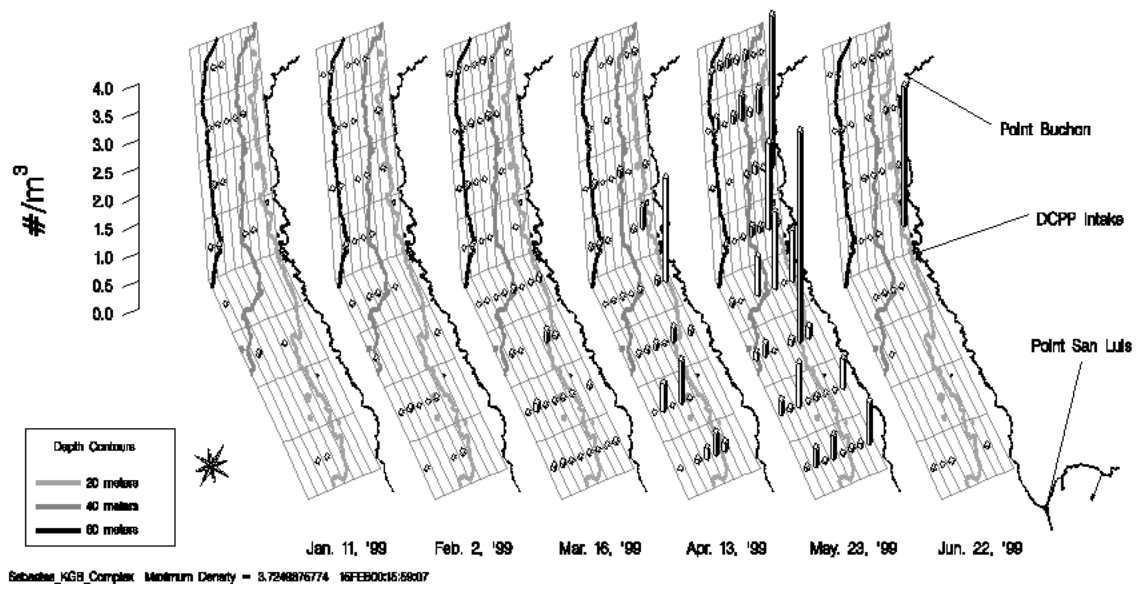


Figure 14. Average concentration for kelp, gopher, and black-and-yellow (KGB) rockfish complex larvae in each of the 64 nearshore stations for surveys done from A) January 1998 through June 1998, and B) January 1999 through June 1999 for Diablo Canyon Power Plant. Surveys done in other months are not shown because there were few or no KGB rockfish complex larvae collected.

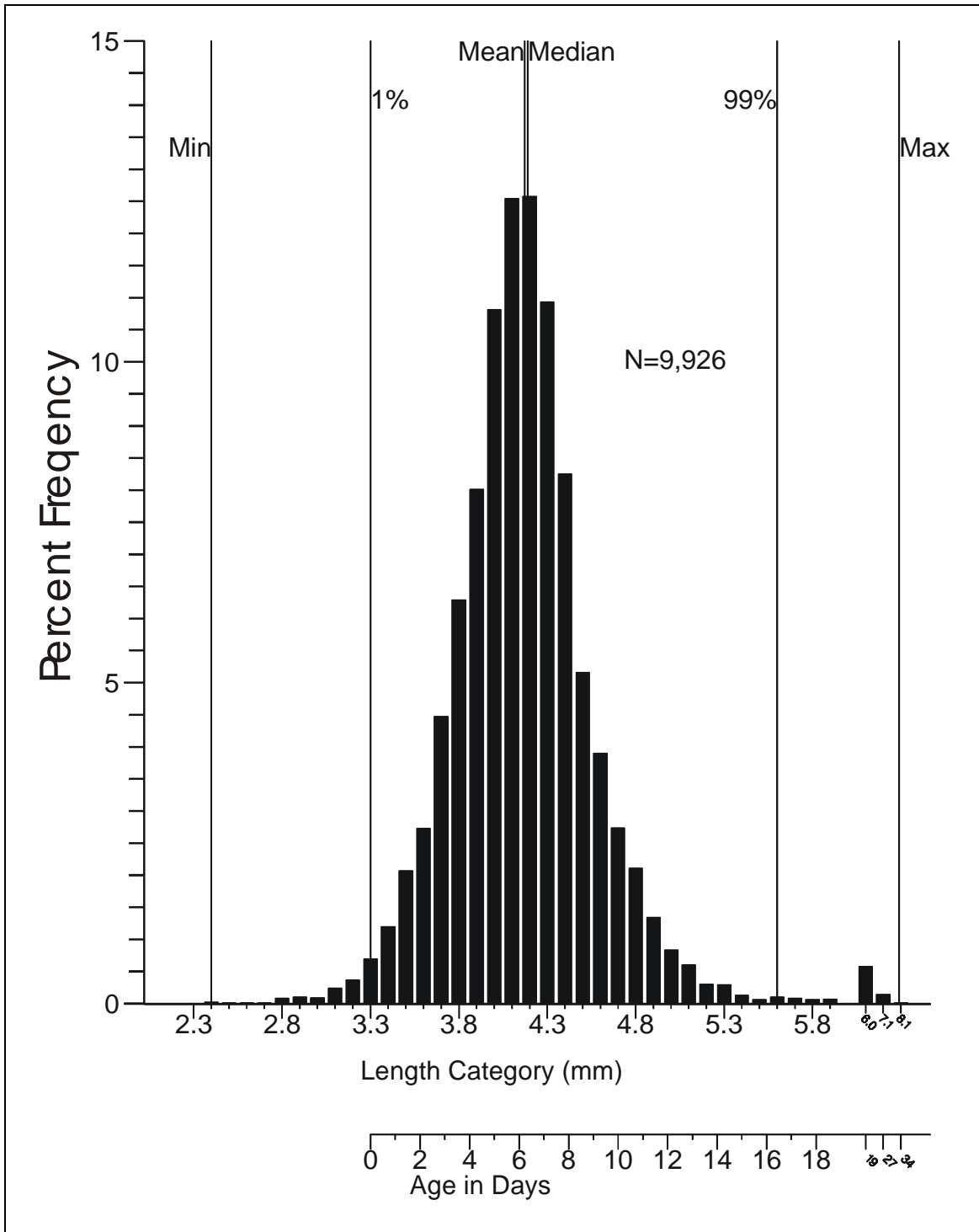


Figure 15. Length frequency distribution for kelp, gopher, and black-and-yellow (KGB) rockfish complex larvae measured from entrainment stations at Diablo Canyon Power Plant intake from October 1996 to June 1999. The x-scale is not continuous at larger lengths. Alternate x-scale shows age in days estimated using growth rate of $0.14 \text{ mm}^{-\text{d}}$.

Table 19. Diablo Canyon Power Plant fecundity hindcasting (FH) estimates for kelp, gopher, and black-and-yellow (KGB) rockfish complex for two year-long analysis periods. Upper and lower estimates represent the changes in the model estimates that result from varying the value of the corresponding parameter in the model.

Analysis Period	Adjusted Entrainment Estimate	Estimate Std. Error	Upper FH Estimate	Lower FH Estimate	FH Range
1) Oct 1996–Sept 1997					
FH Estimate	617	1,470	31,500	12	31,488
Adjusted Entrainment	275,000,000	24,700,000	708	526	182
2) Oct 1997–Sept 1998					
FH Estimate	497	1,190	25,400	10	25,390
Adjusted Entrainment	222,000,000	28,900,000	603	391	212

Adult Equivalent Loss

Similar to the FH calculations the same life history parameter values from blue rockfish used for the MBPP study (Table 13) were also used to calculate AEL estimates for KGB rockfish at DCP. The AEL estimates were extrapolated forward from the average age at entrainment of 6.2 d, the same value used in the FH hindcasting. Survivorship, to an assumed recruitment age of 3 years, was apportioned into these life stages, and AEL was calculated assuming the entrainment of a single age class having the average age of recruitment. Survival from the average age at entrainment (6.2 d) to the age at transformation (20 d) was estimated as 0.145 ($0.145 = e^{(-0.14)(20-6.2)}$). The other stages used the survival estimates from Table 19.

Paralleling the FH results, estimates of adult equivalents lost due to larval entrainment were fairly similar among survey periods (Table 20). The AEL estimate of 1,120 adults predicted from E_{T-Adj} at DCP during 1996–97 reflects the slightly higher abundance of KGB rockfish larvae present during this year when compared to the 1997–1998 period (AEL= 905). The relatively constant larval abundance and subsequent estimates of effects varied little among survey periods, indicating that recruitment for the species in this complex remained relatively constant over the two years.

Similar to the results for MBPP, the FH and AEL estimates for DCP were very close to the theoretical relationship of $2FH \equiv AEL$, the AEL was only extrapolated to age three. The estimate would decrease by extrapolating to five years, the age of maturity used in the FH calculations.

Table 20. Diablo Canyon Power Plant adult equivalent loss (AEL) estimates for kelp, gopher, and black-and-yellow (KGB) rockfish complex. Upper and lower estimates represent the changes in the model estimates that result from varying the value of the corresponding parameter in the model.

Analysis Period	Adjusted Entrainment Estimate	Estimate Std. Error	Upper AEL Estimate	Lower AEL Estimate	AEL Range
1) Oct 1996–Sept 1997					
AEL Estimate	1,120	3,410	166,000	8	165,992
Annual Entrainment	275,000,000	24,700,000	1,290	958	332
2) Oct 1997–Sept 1998					
AEL Estimate	905	2,750	134,000	6	133,994
Annual Entrainment	222,000,000	28,900,000	1,100	712	388

Empirical Transport Model

The data used in computing the ETM estimates of P_M for KGB rockfish for the two study periods are presented in Tables 21 and 22 and in more detail in Appendices E and F. Average PE estimates for the two periods were similar in value and the values of f_i showed that the largest weights were applied to the PE values for the April and May surveys in both periods (Table 21). The estimate of larval duration of 16.4 days was used in the ETM calculations for both study periods.

The ETM model used for DCPD included adjustments for P_s similar to the model used at MBPP. Unlike the MBPP study, P_s was calculated using two approaches. The first approach was similar to the MBPP study, but instead of using average current speed, alongshore current displacement was used to estimate the alongshore distance that could have been traveled by KGB rockfish larvae during the day of the survey and during the 16.4-day period before the survey that they were susceptible to entrainment (Table 22). The ratio of the alongshore length of the nearshore sampling area to the alongshore current displacement was used to calculate an estimate of P_s for each survey. The second approach used the alongshore current displacement to determine the alongshore length of the source water population, but also used onshore current movement over the same period to determine the offshore distance of the source water population. During the 1997 through 1998 period, when the pattern of abundances within the nearshore sampling area was slightly increasing with distance offshore (positive slope), the offshore extent of the extrapolated source water population was set using the onshore current displacement (Table 22A and Appendix F). When the pattern of abundances showed a decline with distance offshore during the 1998 through 1999 period, the estimated offshore extent was the distance offshore that the extrapolated density was equal to zero (x-intercept), or the offshore extent of the sampling area (3,008

m) if the x-intercept was inside the sampling area (Table 22B and Appendix F). This was typically less than the measured onshore displacement during the surveys. The P_s was calculated as the ratio of the estimated number of KGB rockfish larvae in the nearshore sampling area to the estimated number in the source water area. The average values of P_s were used in the ETM calculations.

The ETM estimates for KGB rockfish are presented with the results of the other taxa included in the assessment for the DCP (Table 23). ETM estimates of proportional mortality (P_M) were calculated using two methods to estimate the proportion of source water sampled (P_s). One method assumed that the source water only extended alongshore and did not extend outside the nearshore sampling area. Only this first estimate was calculated for three fishes that occur primarily as adults in the shallow nearshore. The other method assumed that the source water extended alongshore and could extend some distance outside the nearshore sampling area. Only this estimate was calculated for two fishes that occur as adults over large oceanic areas. Both estimates were calculated for the other nine fishes. No estimate was calculated for Pacific sardine in the Analysis Period 4 because of very low abundances that year.

Estimates of P_M were relatively similar in value between periods for the estimates calculated using the alongshore displacement estimate of P_s . There was a much greater difference between periods for the estimates calculated using the P_s based on extrapolating the source water population extending both alongshore and offshore. This was a result of the difference in the pattern of abundances in the nearshore sampling area between sampling periods (Figure 14). The source population was extrapolated further offshore during the 1997-1998 period resulting in a larger source water population estimate, which resulted in a smaller estimate of P_s and a smaller estimate of P_M .

Results for Other Taxa

Modeling results for the other taxa selected for detailed assessment showed that, similar to the results for MBPP, demographic models could only be used for half of the fishes analyzed (Table 23). There was a large variation in the demographic model results among taxa that was not necessarily reflective of the differences in entrainment estimates. This was the result of the large variation in life history among the fishes analyzed. For example, although the entrainment estimates for Pacific sardine and blue rockfish were similar, the demographic model results were different by greater than two orders of magnitude.

Table 21. Estimates used in calculating empirical transport model (ETM) estimates of proportional entrainment (PE) for kelp, gopher, and black-and-yellow (KGB) rockfish complex for Diablo Canyon Power Plant from monthly

surveys conducted for two periods A) July 1997 through June 1998, and B) July 1998 through June 1999. The larval duration used in the calculations was 16.4 days. More detailed data used in the calculations are presented in Appendices E and F.

A) July 1997 – June 1998

Survey Date	PE_i	PE_i Std. Error	f_i	f_i Std. Error
21-Jul-97	0.0107	0.0151	0.0004	0.0004
25-Aug-97	0	0	0	0
29-Sep-97	0	0	0	0
20-Oct-97	0	0	0	0
17-Nov-97	0	0	0	0
10-Dec-97	0	0	0.0003	0.0003
22-Jan-98	0.0008	0.0009	0.0121	0.0053
26-Feb-98	0.0021	0.0013	0.0180	0.0038
18-Mar-98	0.0587	0.0297	0.0279	0.0050
15-Apr-98	0.0076	0.0035	0.1732	0.0214
18-May-98	0.0036	0.0008	0.6384	0.0334
8-Jun-98	0.0353	0.0084	0.1297	0.0165
	0.0167	Sum =	1.00000	

B) July 1998 – June 1999

Survey Date	PE_i	PE_i Std. Error	f_i	f_i Std. Error
21-Jul-98	0.0033	0.0035	0.0035	0.0011
26-Aug-98	0	0	0	0
16-Sep-98	0	0	0	0
6-Oct-98	0	0	0	0
11-Nov-98	0	0	0	0
9-Dec-98	0	0	0	0
12-Jan-99	0	0	0.0240	0.0053
3-Feb-99	0.0005	0.0005	0.0243	0.0045
17-Mar-99	0.0327	0.0198	0.0809	0.0108
14-Apr-99	0.0137	0.0075	0.1906	0.0328
24-May-99	0.0115	0.0026	0.5926	0.0456
23-Jun-99	0.0170	0.0125	0.0841	0.0509
	0.0131	Sum =	1.00000	

Table 22. Onshore and alongshore current meter displacement used in estimating proportion of source water sampled (P_s) from monthly surveys conducted for two periods A) July 1997 through June 1998, and B) July 1998 through June 1999 for kelp, gopher, and black-and-yellow (KGB) rockfish complex at the Diablo Canyon Power Plant. More detailed data is included in Appendices E and F.

A) July 1997 – June 1998

Survey Date	Cumulative Alongshore Displacement (m)	Onshore Current Displacement (m)	Estimated Offshore Extent of Source Water (m)	Offshore P_s	Alongshore P_s
21-Jul-97	31,300	4,820	4,820	0.0153	0.5545
25-Aug-97	–	–	–	–	–
29-Sep-97	–	–	–	–	–
20-Oct-97	–	–	–	–	–
17-Nov-97	–	–	–	–	–
10-Dec-97	146,000	31,600	31,600	0.0000	0.1189
22-Jan-98	120,000	23,400	23,400	0.0020	0.1443
26-Feb-98	33,700	8,710	8,710	0.0693	0.5152
18-Mar-98	181,000	12,400	12,400	0.0090	0.0960
15-Apr-98	76,100	12,800	12,800	0.0404	0.2282
18-May-98	67,100	19,900	19,900	0.0334	0.2589
8-Jun-98	111,000	5,670	5,670	0.0761	0.1559
Average =				0.0307	0.2590

B) July 1998 - June 1998

Survey Date	Cumulative Alongshore Displacement (m)	Onshore Current Displacement (m)	Estimated Offshore Extent of Source Water (m)	Offshore P_s	Alongshore P_s
21-Jul-98	76,300	11,100	3,010	0.2278	0.2278
26-Aug-98	–	–	–	–	–
16-Sep-98	–	–	–	–	–
6-Oct-98	–	–	–	–	–
11-Nov-98	–	–	–	–	–
9-Dec-98	–	–	–	–	–
12-Jan-99	46,200	24,100	3,010	0.3755	0.3755
3-Feb-99	81,900	19,700	3,010	0.2122	0.2122
17-Mar-99	36,900	8,540	4,170	0.4334	0.4709
14-Apr-99	163,000	10,200	8,000	0.0636	0.1068
24-May-99	180,000	21,800	21,000	0.0251	0.0967
23-Jun-99	158,000	5,970	4,380	0.0986	0.1100
Average =				0.2052	0.2286

The fishes analyzed were separated into three groups based on their adult distributions: fishes that were widely distributed over large oceanic areas included northern anchovy and Pacific sardine, fishes that were primarily distributed in the shallow nearshore included smoothhead sculpin (*Orthonopias triacis*), monkeyface prickleback (*Cebidichthys violaceus*), and clinid kelpfishes (*Gibbonsia* spp.), and the rest of the fishes that were primarily nearshore, but could be found in deeper subtidal areas. The source water population used in calculating P_s was estimated using both alongshore currents and along- and off-shore extrapolation for the last group of fishes, resulting in two ETM estimates for each analysis period. Only one ETM estimate for each analysis period was made for the other two groups, depending on whether it was primarily nearshore or primarily offshore. The ETM estimates of P_M ranged from <0.001 (0.1 percent) to 0.310 (31.0 percent) with the estimated effects being greatest for the fishes that were distributed primarily as adults in shallow nearshore areas. These fishes such as sculpins (Cottidae), monkeyface pricklebacks, and kelpfishes all had proportional mortalities due to power plant entrainment of greater than 10 percent. The ETM calculations were calculated using both estimates of P_s for snubnose sculpin because they occur slightly deeper as adults than the other nearshore fishes. The results showed that the extrapolated ETM estimates were approximately equal to the estimates using only alongshore current displacement because the densities for this species did not increase with distance offshore. The results for DCPP are similar to the other two studies in showing that the greatest effects occur to fishes that primarily occupy habitats in close proximity to the intake and do not occur at the same level in other areas of the source water.

Table 23. Results of entrainment monitoring and FH, AEL, and ETM modeling for fourteen fishes at Diablo Canyon Power Plant. The four analysis periods correspond to 1) Oct. 1996 – Sept. 1997, 2) Oct. 1997 – Sept. 1998, 3) July 1997 – June 1998, and 4) July 1998 – June 1999. Adjusted entrainment (E_{Adj-T}), FH and AEL not calculated for Analysis Period 4. Nearshore sampling of source waters began in June 1998, so ETM estimates of proportional mortality (P_M) was only calculated for Analysis Periods 3 and 4.

Taxon	Analysis Period	E_{Adj-T}	FH	AEL	P_M Alongshore	P_M Offshore and Alongshore
Pacific sardine	1.	8,470,000	3,170	2,630	–	–
	2.	22,600,000	8,460	7,000	–	–
	3.	22,600,000	8,460	7,000	not calculated	<0.001
	4.				not calculated	not calculated
northern anchovy	1.	136,000,000	16,100	43,200	–	–
	2.	376,000,000	44,700	120,000	–	–
	3.	377,000,000	44,700	120,000	not calculated	<0.001
	4.				not calculated	<0.001
KGB rockfish complex	1.	275,000,000	617	1,120	–	–
	2.	222,000,000	497	905	–	–
	3.	222,000,000	497	905	0.039	0.005
	4.				0.048	0.043
blue rockfish complex	1.	84,040,000	43	353	–	–
	2.	33,800,000	18	164	–	–
	3.	33,900,000	20	142	0.004	<0.001
	4.				0.028	0.002
painted greenling	1.	24,200,000	–	–	–	–
	2.	9,610,000	–	–	–	–
	3.	12,100,000	–	–	0.063	0.051
	4.				0.056	0.043
smooth-head sculpin	1.	57,700,000	–	–	–	–
	2.	115,000,000	–	–	–	–
	3.	129,000,000	–	–	0.114	not calculated
	4.				0.226	not calculated
snubnose sculpin	1.	110,000,000	–	–	–	–
	2.	83,500,000	–	–	–	–
	3.	105,000,000	–	–	0.149	0.139
	4.				0.310	0.310
cabezon	1.	51,900,000	–	–	–	–
	2.	36,300,000	–	–	–	–
	3.	36,300,000	–	–	0.011	0.009
	4.				0.015	0.008
white croaker	1.	305,000,000	5,110	14,700	–	–
	2.	440,000,000	7,380	21,300	–	–
	3.	447,000,000	7,500	21,600	0.007	<0.001
	4.				0.035	0.004
Monkey-face prickleback	1.	83,100,000	–	–	–	–
	2.	61,500,000	–	–	–	–
	3.	60,200,000	–	–	0.138	not calculated
	4.				0.118	not calculated
clinid kelpfishes	1.	181,000,000	–	–	–	–
	2.	308,000,000	–	–	–	–
	3.	458,000,000	–	–	0.189	not calculated
	4.				0.250	not calculated
blackeye goby	1.	128,000,000	12,000	75,200	–	–
	2.	109,000,000	10,300	64,100	–	–
	3.	128,000,000	12,100	75,400	0.115	0.027
	4.				0.065	0.036
sanddabs	1.	7,160,000	426	2,370	–	–
	2.	1,540,000	92	511	–	–
	3.	6,610,000	393	2,190	0.010	0.001
	4.				0.008	0.001
California halibut	1.	8,260,000	–	–	–	–
	2.	15,700,000	–	–	–	–
	3.	15,500,000	–	–	0.005	0.001
	4.				0.071	0.006

CHAPTER 4: DISCUSSION

The results from these studies demonstrate the importance of a site-specific approach to assessing the effects of CWIS entrainment on marine organisms. Even though Morro Bay and San Diego Bay are both tidally influenced embayments, the resulting studies, sampling, and analytical approaches were very different. And both of these studies were dramatically different from Diablo Canyon. The source waters determined to be affected by entrainment were the primary factor responsible for the differences among studies. In San Diego Bay, in the area of SBPP, the turnover in water due to tidal exchange allowed the authors to treat the source water population as a closed system. A larger number of stations was sampled in San Diego compared to Morro Bay because of the potential for reduced exchange among the various habitats in the San Diego source water study area. Differences in fish composition among habitats in San Diego Bay shown by Allen (1999) were also reflected in some of the differences in larval composition among stations. This resulted in site-specific effects on species such as longjaw mudsuckers, which had a relatively high ETM estimate of P_M at SBPP. Mudsucker larvae were not particularly abundant in the source waters but were abundant in the SBPP intake canal, which provided excellent habitat for adults. Similarly, effects on combtooth blennies estimated using ETM were lower than other fishes because they were more abundant in areas of the bay that had extensive pier pilings and other structures that provide habitat for adult blennies. The high level of site fidelity in the community composition in south San Diego Bay was likely due to the lower tidal exchange rates relative to an area such as Morro Bay. The results supported the decision to sample an extensive range of habitats in south San Diego Bay.

The source water sampling in Morro Bay was less extensive than the SBPP study but included sampling at a nearshore station outside the bay that was representative of water transported into the bay on flood tides. The less intensive sampling was justified by the large tidal exchange that results in rapid turnover of the water in the bay relative to a large tidal embayment such as San Diego Bay. The shallow mudflats and tidal channels in Morro Bay are drained out through the deeper navigation channel where sampling occurred. Although this may have resulted in undersampling of larvae from certain fishes that could avoid strong tidal currents, as has been shown for longjaw mudsuckers and other species of gobies (Barlow 1963, Brothers 1975), it was probably representative of the larvae that would be transported on outgoing tides past the plant where they would be exposed to entrainment. The greatest CWIS effects using ETM were estimated for combtooth blennies that occur in the piers and other structures located near the plant. This was similar to the SBPP results for longjaw mudsuckers that occur in highest numbers at the entrainment station in the intake canal. These results showed the importance of sampling all habitats and the potential for increased impacts on species with habitats near plant intakes. This also indicates that potential for large

impacts exist when habitats are not uniformly distributed in the source water for a CWIS and the potential for larger effects on fishes associated with habitats that may not be abundant throughout the source water.

The nearshore sampling area for DCPP was very extensive to represent the range of habitats along the exposed rocky headland where the power plant is located. The size of the sampling area was also designed to be representative of the distance north and south that larvae could be transported by alongshore currents over a 24 hour period to correspond with the ETM model that uses daily estimates of conditional mortality resulting from entrainment to estimate CWIS-related mortality. This extensive sampling showed similar results to SBPP and MBPP by estimating that the greatest CWIS effects using ETM occurred on fishes with nearshore habitats that were disproportionately affected by entrainment. In the ETM model, species that have higher abundances in entrainment samples result in larger PE estimates of daily conditional mortality.

The authors examined the relative distribution of individual species in the sampling areas by comparing the average PE to the ratio of the cooling water to source water volumes. For example, in SBPP the average PE for CIQ gobies was 0.012, which was very close to the volumetric ratio of 0.015. In contrast, the average PE for longjaw mudsuckers was 0.19, which was much greater than the ratio of cooling water to source water. Although this is potentially useful for helping to determine the potential distribution of the larvae in the source water, it may not be a good indicator of impacts. When the PE is close to the volumetric ratio, the resulting impacts are directly dependent on the number of days that the larvae are exposed to entrainment. Therefore, even though the average PE was much greater for longjaw mudsuckers, the time (4 days) that they were exposed to entrainment was much less than CIQ gobies because they were in highest abundance in the areas directly around the CWS intake. In contrast, even though the average PE for CIQ goby was close to the volumetric ratio, the estimated effects of entrainment based on ETM were higher than the estimated effects on mudsuckers (0.215 vs. 0.171) because goby larvae were estimated to be exposed to entrainment for 23 days.

The final source water area used to adjust the PE estimates also affected the CWIS effects estimated using ETM. The MBPP results for KGB rockfish contrast with those for estuarine fishes such as gobies and blennies. Relative to fishes that are primarily estuarine inhabitants, adult KGB rockfishes are more widely distributed, resulting in larger source water body populations and reduced entrainment effects. As a result, the PE estimates were adjusted using P_s to account for the larger source water population beyond the area sampled for KGB rockfishes. All of the results for DCPP were adjusted to account for the onshore and alongshore currents that can transport larvae over

hundreds of kilometers, resulting in very low estimated effects for species, such as northern anchovy, that have widely distributed source populations.

The source water sampling for all three of these studies was done to satisfy the requirements of the ETM. Source water sampling would not have been required if the assessments were done using only more traditional demographic modeling approaches. The source water sampling was necessary because the ETM directly links mortality to a source population. As a consequence, the habitat occupied by that source population can be described, and ecosystem losses can be mitigated. The area of production foregone (APF) is one approach for estimating the amount of habitat that would need to be replaced to compensate for the larval production lost due to entrainment.

Area of Production Foregone (APF) models can be used to understand the scale of loss resulting from an impact and the extent of mitigation that could yield compensation for the loss. It is based on the idea that losses from environmental impacts can usually only be estimated from a group of species and that the true impact results from the sum of direct and indirect losses attributable to the impact. The use of APF allows for the estimation of both the direct and indirect consequences of an impact and provides a currency (that is, habitat acreage) that may be useful for understanding the extent of compensation required to offset an impact.

Probably the most controversial issue in APF assessment is how it treats the few taxa actually analyzed in the assessment. In most assessments, including “habitat replacement cost” (HRC) (Strange et al. 2002), estimates of loss of taxa are implicitly considered to be without error. In APF, each estimate is considered to be prone to (sometimes) massive error (indeed, estimates of confidence intervals in ETM calculations often cross through zero). In APF models the assumption is that each taxon represents a sample and that the mean of the samples is representative of the true loss rate. For example, assume 5 taxa and the ETM calculations indicate that for an estuarine system of 2000 acres the loss rates for the 5 taxa are 5, 10, 3, 22 and 15 percent. In APF the estimate of loss would be the average of the 5 values or 11 percent. Because APF considers taxa to be simply independent replicates useful for calculating the expected impact, the choice of taxa for analysis may differ from HRC assessments. In APF the concern is more that each taxon is representative of other taxa that are either unsampled (most invertebrates, plants and holoplankton) or not analyzed (the vast majority of fish). In APF, the average loss across taxa then represents the average loss across all entrained organisms. This is a fundamental difference between APF and economic based models like HRC. The underlying statistical-philosophic basis of APF addresses one of the most problematic issues in impact estimation: the typical inability to estimate impact for unevaluated taxa.

In APF, the next step is to take the average ETM loss rate and turn it into an ecological currency, which then can be used to understand the impact and form a basis for mitigation. This can be quite a simple step. Loss is turned into habitat from which production is foregone. This is calculated as the area of habitat that would need to be added to the system to make up the lost resources. In the example above, the estimate was that 11 percent of organisms at risk in a 2000-acre estuary were lost to entrainment. The estimate of APF then would simply be 2,000 acres x 11 percent or 220 acres. Therefore the creation of 220 acres of new estuarine habitat would compensate for the losses due to entrainment. This does not mean that all biological resources were lost from an area of 220 acres, which is a common misunderstanding. Instead it means that if 220 acres of new habitat were created, then all losses, calculated and not calculated, would likely be compensated. Here again is an important feature of APF. The currency of impact (acres needed to compensate) includes all impacts, even indirect ones. One common criticism of the approach of focusing more detailed analysis to only a limited number of taxa is that not only are other taxa directly affected by entrainment not assessed, but that there is also no provision for estimation of indirect impacts (often food web considerations). APF addresses this concern by expressing impact in terms of habitat and assuming that indirect impacts are addressed by the complete compensation of all directly lost resources.

In the given example, APF would predict that the creation of 220 acres of new habitat would compensate for all impacts due to entrainment. What sort of habitat should be created? Again the statistical-philosophic basis of APF contributes to the answer. Because taxa in APF are simply independent replicates that yield a mean loss rate, habitat is not directed by taxa. Instead, the approach assumes that habitat should be created that represents the habitat for the populations at risk. If the habitat in the estuary was 60 percent subtidal eelgrass beds, 15 percent mudflats, and 25 percent vegetated intertidal marsh, then these same percentages should be maintained in the created habitat. Doing so would ensure that impacts on all affected taxa would be addressed.

The logic of the example would seem to imply that this approach would only be useful if there were habitat creation opportunities. However, even if there are not local opportunities, the approach is useful for other reasons:

- 1) Opportunities may exist in other locations (such as another nearby estuary);
- 2) Area of Production Foregone can be useful in understanding the scale and relative importance of the impact, which helps with permitting decisions, and in establishing a cost-basis for the impact; and

- 3) Often there are alternative mitigation strategies that could be implemented whose scale would be determined by APF. An example would be the size of the creation of an artificial reef or the area of a marine reserve designated as mitigation for entrainment losses.

In the most general model, APF is estimated from the product of P_M and the source water area for each taxa analyzed. In the example above, the source water area was the same for all taxa as it was the area of the estuary. Clearly, the approach becomes more difficult on the open coast where the source water areas differ across taxa. The task is simplified by the proportional relationship between P_M and the size of the source water population used in calculating P_S . As the size of the source water area increases relative to the sampling area, P_S decreases resulting in a proportional decrease in P_M . If the habitat in the larger source water can be assumed to be distributed in the same relative proportions as the area sampled, then one only needs to use the areas of various habitats in the sampled area to estimate APF by using the uncorrected P_M . This greatly simplifies the application of APF and reduces the need to rely on limited current data information to extrapolate beyond the areas sampled. In practice, when many taxa are impacted, each having varying habitat requirements, APF estimation becomes a matter of restoration using an estimate such as

$$\frac{\sum_{i=1}^N \frac{1}{P_{S_i}} P_{M_i}}{N},$$

for $I = 1$ to N taxa.

One of the advantages of the ETM model over more traditional demographic approaches towards CWIS assessment is the reduced need for life history data. As the results show, the necessary life history information on reproduction and age-specific mortality for the FH and AEL models was only available for a limited number of fishes. The life history information was collected from data in the scientific literature, but the level of uncertainty surrounding published demographic parameters was rarely reported. The likelihood is that the uncertainty associated with the information was very large. This needs to be considered when interpreting results from FH and AEL models because the accuracy of estimated entrainment effects will depend on the accuracy of age-specific mortality and fecundity estimates. This limits the utility of these modeling approaches, especially on the Pacific Coast of California where fishes in highest abundance in entrainment samples are small, forage species with limited life history information. The authors were fortunate that the work of Brothers (1975) provided demographic information on CIQ gobies, the most abundant larvae collected in two of the studies.

Unlike demographic models the only life history information required by ETM, which it shares with FH and AEL, is an estimate of the duration of the period the larvae are vulnerable to entrainment, estimated in these studies by the age of the larvae entrained. This was estimated using larval lengths measured from the samples and larval growth rates obtained or derived from the scientific literature. The average length was used to estimate the average age at entrainment (average length – length at 1st percentile), and the maximum length based on the length at the 99th percentile was used to estimate the maximum number of days that the larvae were exposed to entrainment. It is possible that these estimates were biased. Other reported data (for example, Moser 1996) for various species suggested that hatching lengths could be either smaller or larger than the size estimated from the samples, and indicated that the smallest observed larvae represented either natural variation in hatch lengths within the population or shrinkage following preservation (Theilacker 1980). The possibility remains that all larvae from the observed minimum length to the greatest reported hatching length (or to some other size) could have just hatched, leading to overestimation of larval age.

The extensive weekly sampling at DCPD over more than two years resulted in measurements of almost 10,000 KGB rockfish larvae from entrainment samples. Despite this large data set, the authors did not have a high level of confidence that these data necessarily provided a more accurate estimate of size at extrusion. The reported size of KGB rockfish at extrusion is 4.0-5.5 mm (Moser 1996) indicating that the average size at entrainment, 4.2 mm, could be a more accurate minimum size for estimating age at entrainment than the much smaller value used in the calculations. Although the minimum and average sizes were different than reported in the literature, this shouldn't present a problem in estimating the number of days of exposure to entrainment as long as the growth rate used in the calculations is valid for that size of larvae. The uncertainty regarding the estimation of the period of exposure to entrainment has resulted in reporting of ETM results using larval durations based on the mean and maximum lengths at MBPP and DCPD. This uncertainty can easily be resolved by aging entrained larvae using otoliths. Removing the uncertainty associated with the age of the entrained larvae may justify the additional costs associated with this approach.

The duration that larvae may be subject to entrainment is affected not only by growth and behavior of the larvae, but also by the hydrodynamic characteristics of the source waters. In closed systems such as south San Diego Bay or freshwater lakes, biological factors are probably more important than hydrodynamic factors. In open systems, both biological and physical factors affect the length of time that larvae are subject to entrainment. For power plants located in coastal areas, such as DCPD, the effects of currents and larval growth both need to be considered in determining the size of the source population potentially affected by entrainment, but in estuarine areas such as Morro Bay, hydrodynamic forces have a much greater effect on exposure to

entrainment. The large tidal exchange ratio in Morro Bay results in huge exports of larvae out of the bay and into nearshore waters. Brothers (1975) showed that tidal exchange in Mission Bay, California resulted in much higher larval mortality rates than his calculated values for CIQ gobies. He hypothesized that larval behavior similar to that observed in longjaw mudsucker (Barlow 1963) resulted in the higher observed survival rates. Barlow described that longjaw mudsucker post-larvae are found close to the bottom. The location of MBPP near the harbor entrance of Morro Bay probably results in reduced effects on estuarine fish populations because the large majority of entrained larvae would be exported out to sea. The source water calculations for MBPP did not account for the strong effects of tidal exchange on entrainment exposure, which was used to argue that mean larval lengths should have been used in calculating larval exposure to entrainment instead of the length of the 99th percentile. More sophisticated models incorporating hydrodynamic factors should be considered for estuarine systems similar to Morro Bay where hydrodynamic forces strongly affect the period that larvae are exposed to entrainment. This could have been done by increasing the source water volume to account for tidal outflow that transports larvae out of the bay into the ocean over the same number of days that the larvae are exposed to entrainment. This would also require that the nearshore area be included in the calculation of the source water population estimate because the larvae transported out of the bay would still be subject to entrainment.

The sampling frequency may be another source of bias associated with the authors' estimate of the age of the larvae being entrained. The potential for biased sampling would be more prevalent in fishes that do not have prolonged spawning periods such as KGB rockfishes or on the East Coast where spawning occurs more seasonally. It would be less of a potential problem in fishes such as CIQ goby that have larvae that are present almost year-round. Entrainment sampling occurring monthly or less frequently could miss certain periods when certain age classes are present. Although more frequent sampling may not be required in the source water, this may argue for more frequent weekly or bi-weekly entrainment sampling.

The frequency for source water sampling also needs to be considered for species with limited spawning periods. This should be one of the considerations in selecting taxa for detailed assessment since species with limited spawning periods will have few estimates of PE decreasing the confidence in the ETM estimates for those taxa. Unfortunately, the current sampling approach may also result in the selection of taxa that have prolonged spawning durations. This can be avoided if the period of spawning for important taxa can be accounted for in the study design.

In an entrainment assessment being prepared for the Potrero Power Plant in San Francisco Bay, the source water sampling frequency was increased during the spawning

season for Pacific herring (*Clupea pallasii*), which was identified as an important species during the study design (Tenera Environmental, unpublished data). If this is not accounted for in the sampling and selection of species for analysis, it may result in biased estimates for certain species. This is especially problematical if a species is collected relatively infrequently and in low numbers but is included in the assessment because of its commercial or recreational value. Examples from these studies include Pacific herring at MBPP and California halibut (*Paralichthys californicus*) at DCP. Both of these fishes represented less than 1.0 percent of the total larvae collected during entrainment sampling but were included in the assessments (Tables 4, 11, and 17). In both cases, the results of the demographic modeling were important in placing the results for these species in context. In the case of Pacific herring at MBPP, the ETM estimate of entrainment mortality of 16 percent represented the estimated loss of 532 adults calculated using the FH method (Table 16). No demographic estimates were available for California halibut at DCP (Table 23). This problem did not occur at SBPP where the assessment was limited to the most abundant fishes regardless of their commercial or recreational value.

The approach used at SBPP for selecting taxa for analysis is acceptable if the taxa used in the assessment represent the range of habitats and fishes found in the source water potentially impacted by entrainment. If the list of taxa represents a reasonable sample from the fishes in the source water, then the P_M estimates for the fishes can be averaged to obtain an estimate of the expected entrainment impacts on other fish and invertebrate larvae, zooplankton, and phytoplankton not included in the assessment. As the examples in the previous paragraph demonstrate, no single estimate of P_M may be particularly reliable, and therefore the use of the average P_M may be more appropriate as a estimator of average losses to the population. As previously discussed, the average value can be also used in calculating APF estimates for scaling restoration projects that could be used to compensate for entrainment losses.

Using averages for APF does not imply that there is an average mortality within the area estimated by the APF, but rather that averages are useful for estimating the amount of habitat affected. In order to view mortality spatially, it may be useful to allocate the mortality estimate over the area of the source population. A first approximation would be to allocate mortality in a linear or Gaussian fashion across the range of the source population. This was the approach used to estimate the cumulative effects of CWIS at all of the power plants in Southern California (MBC and Tenera 2005). In this way mortality is equal to zero at the periphery of the source population, the furthest distances from the power plant intake. In addition, the source population is subject to stochastic and variable deterministic processes with a result of a changing source population area. Using current measurements, numerical or physical modeling can be used to make further refinements.

The simple volumetric approach for estimating cumulative effects (MBC and Tenera 2005) can be expanded using more accurate estimates of P_M for a range of species. This would involve combining source water population, oceanographic, and hydrographic data from individual power plants. Cumulative effects result when the source water populations for the various power plants overlap. The ETM is easily adjusted to calculate cumulative effects by expanding the estimates of the source water and entrainment populations (Eq. 18) to include all of the power plants being considered.

The period that larvae are exposed to entrainment needs to be adjusted for fishes with planktonic egg stages. This was not considered in these studies because the fishes analyzed for entrainment effects were mostly species that did not have a planktonic egg stage. Therefore, the durations used in the ETM modeling for anchovies, croakers, and flatfishes should have been increased by the average number of days that the eggs for these fishes were potentially exposed to entrainment. Since it would not be feasible to age eggs collected from entrainment samples, this adjustment would need to rely on estimates of egg duration from the scientific literature. This requires the assumption that the estimate of PE applies to both egg and larval stages and that mortality on passage through the cooling system is 100 percent for both egg and larval stages. If there is concern that egg stages are less abundant in the source waters than larval stages, separate PE estimates could be calculated for egg and larval stages using an approach similar to the original ETM concept presented by Boreman et al. (1978 and 1981), which conceptualized an ETM model incorporating separate PE estimates and durations for each life stage. This approach will be difficult to implement for most fishes because fish eggs can only be identified for a few species on the West Coast. Therefore, the most conservative approach would be to assume that fish eggs are entrained in the same relative proportions as fish larvae and account for the egg planktonic duration in the assessment models. For organisms with available life history information, estimates of larval and egg survival can be used to estimate the number of eggs that would have been entrained from abundances of larvae in the samples.

One often proposed method to estimate egg entrainment is to assume a 1:1 eggs to larvae entrainment ratio. However, egg mortality may be significantly different than larval mortality. For example, the estimates of instantaneous natural mortality (M) rates for northern anchovy were 0.191 d^{-1} for eggs and 0.114 d^{-1} for larvae. One million eggs would become 512,477 larvae at the end of 3.5 days, the estimated duration of entrainment for eggs. At the end of a larval duration of 70 days, there would be 175 fish assuming negative exponential survival. The assumption of exponential survival and stable age distribution of eggs and larvae over the 3.5- and 70-day periods can be used to estimate the numbers of all ages by integration as follows:

$$N = \int_0^t N_0 e^{-Mt} dt = \frac{N_0 e^{-Mt}}{-M} \Big|_0^t.$$

Separate integration of eggs and larvae results in a 0.568:1 estimated entrainment ratio of eggs to larvae, thus showing a higher risk to larvae due to the prolonged susceptibility.

The focus of the discussion on ETM results reflects the authors' belief that entrainment effects from CWIS are best assessed using this approach. Although these studies focus on ETM, the multiple modeling approaches used in these studies was valuable for several reasons. First of all, the demographic models provide valuable context for assessing effects on commercially and recreationally valuable species that also allows for comparison with ETM. For example, DCPD estimates of AEL for KGB rockfishes were compared to harvest data assuming 100 percent catchability of adult equivalents and assuming no compensatory mortality. These assumptions likely result in overestimating fishery values (for example, price per kilogram). Given these conditions, an estimated economic loss to the local fishery could be based on an average weight of 1.0 kg for a 3 year old KGB rockfish recruiting to the live-fish fishery. The annual average AEL estimate of 1,013 rockfishes translates to a potential direct economic loss of \$7,749 based on the average price of \$7.65/kg. This value represented approximately 2 percent of the ex-vessel revenue attributed to KGB complex rockfishes landed at ports in the Morro Bay area in 1999 (PSMFC PacFin Database). Similar conversions to fishery value can be performed using FH estimates.

This type of conversion also allows for indirect comparison of demographic model results with ETM by similar conversion of ETM losses into fishery value. To continue the example using the DCPD results for KGB rockfishes, the authors assumed that the probable effect of entrainment losses at DCPD on fisheries was likely localized to the ports within the Morro Bay area since most fishes in this complex demonstrate high site fidelity (Lea et al. 1999). In addition, extension of effects based on alongshore currents and larval duration indicate that the area potentially affected was only three to seven times the size of the nearshore sampling area, which was likely within the range of fishers from either Port San Luis or Morro Bay. The estimate of entrainment mortality (P_M) was between 4 and 5 percent for this area. Applying this range of proportional reduction to the local catch from the Morro Bay area in 1999 yielded estimated dollar losses to the Morro Bay area fishery of approximately \$20,000. In this example, the fishery value estimates using ETM and AEL are reasonably close. The same type of indirect comparison could be done for species without any fishery value by converting ETM estimates of P_M to APF. The estimate of APF could be used with data on abundances to obtain estimates of adult populations that could be compared with demographic model results.

The demographic modeling approaches and conversions to fishery value using either demographic or ETM model results ignore any potential effects of compensation. The authors took this approach because there remain conflicting opinions whether larval mortality is compensated in some fashion. One side of the argument is that if compensation occurs, the estimates of FH, AEL and P_M will overestimate the number of adults lost and ecosystem losses (Saila et al. 1997). The response is that it is difficult to determine if compensation occurs at all (Rose et al. 2001, Nisbet et al. 1996). Additionally, if population mortality is density independent or weakly dependent, then the recruited population size will fluctuate in response to either changes in larval abundances or mortality. In the case of large density dependent mortality, little change due to changes in recruitment might be observed in local population sizes (Cayley et al. 1996). Field experiments on West Coast species of fishes have been equivocal (for example, Stephens et al. 1986), and recent studies on bocaccio (*Sebastes paucispinis*) showed no evidence of compensation in the stock-recruitment relationship (Tolimieri and Levin 2005). Currently, the USEPA and the California Energy Commission consider that compensation does not reduce impacts from entrainment and impingement on adult populations.

Results from demographic models are also necessary for combining estimates from entrainment and impingement unless independent data on adult fish populations are available for comparison with impingement losses. Impingement studies are designed to collect data on juveniles and adult fishes that are used to develop estimates of annual impingement. An AEL model is then used to extrapolate the number of impinged fishes either backward or forward to the numbers of adults of a certain age. By using the average age of reproductively mature females in the extrapolation, these results can be combined with FH or AEL entrainment estimates to obtain estimates of the combined effects of impingement and entrainment. This approach assumes that the FH and AEL entrainment estimates are extrapolated to the same age used in the impingement estimates. Combined assessments can only be done on the few fishes with life history data available for estimating FH, AEL, or one of the other demographic models. Fortunately, the total impingement losses at these three plants were relatively low due to the CWIS designs, and species with the highest impingement estimates were not entrained in high abundances (Tenera Environmental 2000, 2001, 2004). This is not always the case, and combining impingement and entrainment estimates into comprehensive CWIS assessments remains problematic for most species due to incomplete life history data.

Another approach for combining results from impingement and entrainment would involve using the numbers of impinged individuals for a species to estimate the relative losses to the population. The impingement mortality and entrainment mortality rate estimated by ETM can be converted to survival and multiplied to estimate cumulative

CWIS effects. This approach involves the assumption that there are no compensatory mechanisms acting on the population between larval and adult stages such that entrainment losses estimated by ETM represent losses to the adult population. It also assumes that impingement and entrainment losses apply to the same stock. Although this is reasonable for a closed system such as south San Diego Bay, it would be much more difficult in an open system. In addition, there are few species with adequate data on adult stocks that could be used in this approach.

Finally, demographic model results provide a direct comparison with ETM results for both fishery and non-fishery species. It is obviously preferable to present data as both percentages relative to a source population using ETM and as absolute numbers of fishes using one or both demographic models. This helps ensure that P_M estimates are properly interpreted and instances where a large P_M that equates to only a few adults fishes are not misinterpreted. Ensuring the species included in the assessment were adequately sampled is the best way to avoid this type of problem. Unfortunately, these types of comparisons are only possible for the limited number of fishes on the West Coast with published life history data. This approach is also complicated by the uncertainty related to the levels of any compensatory, depensatory, or behavioral mechanisms that may have been operating on the subject populations when the life history data were collected. The availability and uncertainty associated with life history information continue to be the greatest limitations to the use of demographic models for CWIS assessment.

Despite these limitations, the USEPA made extensive use of demographic models in the assessments used in the rulemaking for 316(b). This was necessary because of the need to determine the economic costs associated with implementing certain technologies that could be used to help meet performance standards for impingement (80-95 percent) and entrainment (60-90 percent) reduction mandated in the new 316(b) rule. These methods will continue to be used due to the availability of an option for site-specific compliance. This option involves a cost-benefit analysis that compares the costs of technological or operational measures for achieving the performance standards against environmental benefits calculated using benefits valuation methods. As a result of these requirements, there is active research being done to increase the availability of life history data for Pacific Coast fishes.

Guidelines for Entrainment Impact Assessment

The three studies presented in this paper make it clear that it is not feasible to use a prescriptive approach to entrainment assessment design. Based on experiences with these and other studies, the authors provide some general considerations that might be helpful in the design, sampling, and analysis of entrainment impact assessments. These

comments are presented in the hopes that others may benefit from our experiences in conducting CWIS entrainment assessments.

Considerations for Study Design

1. Determine potential species that could be affected by entrainment using historical data on entrainment for the power plant, if available, and data from surrounding waters. Insure that sampling will account for any endangered, threatened, or other listed species that could potentially be affected by entrainment.
2. Determine the source water areas potentially affected by entrainment including the distribution of habitats that might be differentially affected by CWIS entrainment. Different habitats may require use of different sampling gear and methods.
3. The authors have used oblique tows with bongo and wheeled bongo frames that sample the entire water column for both entrainment and source water because the intake structures for these plants were assumed to withdraw water from the entire water column. Power plants with intakes that withdraw water from a discrete depth in the water column may require the use of pumps or closing nets for entrainment sampling at discrete water depths where water withdrawal occurs. Hydrodynamic studies should be done to verify the intake flow field for sampling at discrete depths. The authors have not used pumps to sample inside power plant cooling water systems because of potential bias due to predation by biofouling organisms.
4. Determine appropriate sampling frequency based on species composition and important species that might have short spawning seasons. This could include adjusting sampling frequency seasonally based on presence of certain species. Sampling of entrainment can be done more frequently than source water sampling to provide more accurate estimates of length frequencies of entrained larvae and may also be desirable to provide more accurate estimates for calculating baseline conditions for compliance with new 316(b) rules.
5. These studies were generally conducted over a one-year period except in the case of DCP where one of the strongest ENSO events of that century occurred during the first year of sampling. The relative effects of entrainment estimated by the ETM model should be much less subject to interannual variation than absolute estimates using FH, AEL or other demographic models. Therefore if source water sampling is done with entrainment sampling, one year is a reasonable period of sampling for these studies.
6. Use hydrodynamics of source waters to determine appropriate sampling area. In a closed system, this may be the entire source water. In an open system, ocean or tidal currents should be used to determine the appropriate sampling area for

estimating daily entrainment mortality (PE) for the larger source water population.

Ad hoc rule 1: Since PE is estimated as a daily mortality the sampling area should include the area potentially affected during a 24-hour period. This area is a pragmatic way to arrive at a first stage estimate of daily mortality and hence survival. The use of a current meter positioned near the intake but outside the influence of its flow allows the estimation of advection in the nearby source water. The current meter approach can be combined with estimates of larval dispersion (Largier 2003) for an understanding of the magnitude of source water population affected.

Ad hoc rule 2: The PE is applied to a larger source population that is potentially affected in the time period of a larval duration. (Another option would be to use the range of the stock.) In an open system, the estimation of P_M includes extrapolating the population of the sampling area to the larger source water population over a larval duration. It is difficult to say that the single current meter accurately reflects the advection of the source water population to the intake. In addition, a single current meter says very little about diffusion processes. Be sure that appropriate physical data are collected during the study to model hydrodynamics and determine size of source population.

7. The uncertainties associated with estimating larval durations and hydrodynamics used in estimating the size of the source water populations make estimating variance for ETM problematic. One approach the authors have used is to base the variance calculations solely on the sampling variances used in estimating the variance of PE. A similar approach would use the CV from the source water sampling (which includes both entrainment and source water data) to estimate the variance for ETM or use a Monte Carlo approach using the upper and lower confidence limit values for the PE values. These approaches have been considered because of the large unrealistic error terms derived using the Delta method that incorporates all of the multiple intercorrelated sources of error in the model.

Considerations for Sampling and Processing

1. The authors have used sample volumes of 30-60 m³ per sample for these and other studies, but this volume should be adjusted for the larval concentrations in the source waters. The appropriate sample volume is best determined by preliminary sampling using the gear proposed for the study.
2. Be sure that mesh size used for net sampling is appropriate for taxa that might be the focus of detailed analysis. The authors have used 335 μm mesh nets because we have observed fish larvae being extruded through 505 μm mesh nets. Much smaller sized mesh would be needed to sample invertebrate larvae effectively.

3. Although the authors generally combine the subsamples from the two bongo nets for analysis, preserving one of them directly in 70-80 percent ethanol allows for genetic analyses to be conducted and analysis of otoliths to determine age and growth rates. Larval fishes are generally easier to identify when initially preserved in 5-10 percent formalin.
4. If aging using larval otoliths is not done, be sure that length frequencies measured from entrainment samples are realistic based on available life history. The authors applied general rules for using the length data for determining mean, minimum, and maximum ages but would recommend developing criteria based on the length frequency distribution for each species.
5. Be sure to account for egg stages that would be subject to entrainment if fish eggs are not sorted and identified from the samples.

Considerations for Analysis

1. Use multiple modeling approaches to validate results and provide additional data for determining effects at the adult population level.
2. Similar to the approach of using multiple models to provide additional data for determining effects at the adult population level, the ETM results can be converted into another currency using APF. This approach is probably most appropriate for scaling restoration projects that could be used to help offset losses due to entrainment.
3. Although FH and AEL models can be hindcast or extrapolated to the same age, they will not necessarily provide the same estimate unless the data used in the two models are derived from a life table assuming a stable age distribution.
4. FH and AEL are estimates of the number of adults at a specific age. To estimate the number of adult females in the population, N_F , the average fecundity, can be used instead of TLF. The AEL analog is extrapolation to all adult fish ages - AEL' . A comparison can be made using the relation $AEL' = 2N_F$. This age of entry into the adult population may need to be adjusted to the average age of fishery catch if comparisons are being made with fishery data. The use of AEL and FH (Horst 1975 and Goodyear 1978), aligning at fishery age, is one method of estimating losses in terms of adult animals.
5. Another estimate would use production foregone or total biomass that would have been produced by entrained or impinged animals had they not been entrained or impinged (Rago 1984). Production foregone includes all biomass lost through all forms of mortality had the animals survived entrainment or impingement. This measure is most often used for forage species and represents ecosystem losses, for example, to other trophic levels. Age-1 equivalent loss is a measure similar to AEL and FH that is most commonly used for harvested species. The USEPA (2002) used age-1 equivalents to evaluate power plant losses

“because methods are unavailable for valuing fish eggs and larvae.” They conservatively estimated fish landings value using the number of age-1 individuals, as the average fishery age is older in most cases. However, the USEPA believed the method may underestimate the true value of reducing impingement and entrainment because life history data were not available for most species. If survival rates from the age of entrainment until adulthood are accurate, FH and AEL underestimate the numbers of lost adults because they are extrapolated to a single age, for example, age of maturity in the case of FH. An improved approach to FH will be to use the average annual fecundity to estimate the equivalent number of females N_F removed from the standing stock of adults. Similarly, AEL can be extrapolated to all adult ages and summed to estimate the number of adult equivalents AEL' and these measures can then be compared with fishery losses. However, the accuracy of these kinds of estimates is subject to the accuracy of the underlying survival and fecundity estimates.

6. Another estimate of the number of equivalent adults lost by larval entrainment is to use the mortality estimate from the ETM procedure and apply it to a survey of the standing stock. This accuracy of this estimate is subject to the accuracy of the estimate of the source population affected. This method may result in improvements when there is little confidence in survival estimates or when there is conjecture about compensatory processes that may negate the underlying models of AEL and FH.

Conclusion

As should be clear from this report, the authors feel that CWIS impacts are best evaluated using empirically based source water body information and the ETM model and not using demographic models based on life history information derived from various sources with varying, or unknown, levels of confidence. Although demographic models are useful for providing context for ETM estimates, there is no reason to base an assessment solely on demographic modeling results with the availability of approaches such as the ETM that provide estimates based on empirically derived estimates. In contrast to demographic models, uncertainty associated with ETM model estimates can be controlled through changes to the sampling design for the entrainment and source water sampling. The Energy Commission and CCC have all required the ETM approach in recent studies. Hopefully the information in this paper will assist others in the design and analysis of CWIS assessments that meet the requirements of both 316(b) and regulatory requirements of other agencies.

LITERATURE CITED

- Allen, L. G., R. E. Jensen, and J. R. Sears. 1990. "Open coast settlement and distribution of young-of-the-year California halibut (*Paralichthys californicus*) along the southern California coast between Point Conception and San Mateo Point," June-October, 1988. Calif. Dep. Fish Game, Fish. Bull. 174:145–152.
- Allen, L. G. 1999. *Fisheries Inventory and Utilization of San Diego Bay, San Diego, California. Final Report: Sampling Period July 1994 to April 1999*. Prepared for the U.S. Navy and the San Diego Unified Port District.
- Barlow, G.W. 1963. Species structure of the Gobiid fish *Gillichthys mirabilis* from coastal sloughs of the eastern Pacific. *Pacific Science*. XVII(1):47–72.
- Barnthouse, L. W. 2000. "Impacts of power-plant cooling systems on estuarine fish populations: The Hudson River after 25 years." In *Environmental Science & Policy, Power Plants & Aquatic Resources: Issues and Assessment* (Wisniewski, J., ed.), Vol. 3, Sup. 1. p. S341–S348. Elsevier Science Ltd., NY.
- Barnthouse, L. W., R. J. Klauda, D. S. Vaughan, and R. L. Kendall. 1988. "Science, Law, and Hudson River Power Plants: A case study in environmental impact assessment." *American Fisheries Society Monograph* 4, 346 p.
- Baruskov, V. V. 1981. "A brief review of the subfamily Sebastinae." *Journal of Ichthyology*. 21:1–26.
- Behrens, D. W., D. C. Sommerville. 1982. *Impingement studies at the Morro Bay Power Plant*. Report 026.22-80.1. Pacific Gas and Electric Company, Dept. Eng. Res., San Ramon, CA.
- Boreman, J., C. P. Goodyear, and S. W. Christensen. 1978. *An empirical transport model for evaluating entrainment of aquatic organism by power plants*. US Fish Wildl. Ser. FWS/OBS-78/90, Ann Arbor, MI.
- Boreman, J., C. P. Goodyear, and S. W. Christensen. 1981. "An empirical methodology for estimating entrainment losses at power plants sited on estuaries." *Transactions of the American Fisheries Society*. 110:253–260.
- Brothers, E. B. 1975. "The comparative ecology and behavior of three sympatric California gobies." Ph.D. Thesis, Univ. Calif., San Diego, CA.

- Bulleit, K. A. N. 2000. "Achieving sustainable development: A review of the environmental balancing act in two key clean water act regulatory programs." In *Environmental Science & Policy; Power Plants & Aquatic Resources: Issues and Assessment* (Wisniewski, J., ed.), Vol. 3, Supplement 1. Elsevier Science Ltd., NY, 512 p.
- Burge, R. T., and S. A. Schultz. 1973. "The marine environment in the vicinity of Diablo Cove, with special reference to abalones and bony fishes." *Marine Research Technical Report No. 19*.
- California Energy Commission. 2005. *Issues and Environmental Impacts Associated with Once-Through Cooling at California's Coastal Power Plants*. California Energy Commission Report CEC-700-2005-013.
- Cayley, M. J., M. H. Carr, M. A. Hixon, T. P. Hughes, G. P. Jones, and B. A. Menge. 1996. "Recruitment and the local dynamics of open marine populations." *Annual Review of Ecology and Systematics*. 27:477–500.
- DeLacy, A. C., C. R. Hitz, and R. L. Dryfoos. 1964. "Maturation, gestation, and birth of rockfish (*Sebastes*) from Washington and adjacent waters." Washington Department of Fisheries. *Fisheries Research Papers* 2(3):51–67.
- Dey, W. P. 2003. "Use of equivalent loss models under Section 316(b) of the Clean Water Act." In *Defining and Assessing Adverse Environmental Impact from Power Plant Impingement and Entrainment of Aquatic Organism* (D. A. Dixon, J. A. Veil, and J. Wisniewski, eds.), p. 247–263. A. A. Balkema Publishers, Netherlands.
- Ehrler, C. P., J. R. Steinbeck, E. A. Laman, J. B. Hedgepeth, J. R. Skalski, and D. L. Mayer. 2003. "A process for evaluating adverse environmental impacts by cooling-water system entrainment at a California power plant." In *Defining and Assessing Adverse Environmental Impact from Power Plant Impingement and Entrainment of Aquatic Organism* (D. A. Dixon, J. A. Veil, and J. Wisniewski, eds.). p. 79–102. A. A. Balkema Publishers, Netherlands.
- Englert, T. L., and J. Boreman. 1988. "Historical review of entrainment impact estimates and the factors influencing them." *American Fisheries Society Monograph* 4:143–151.
- Goodyear, C. P. 1978. "Entrainment impact estimates using the equivalent adult approach." United States Fish and Wildlife Service, FWS/OBS-78/65, Ann Arbor, MI.
- Horst, T. J. 1975. "The assessment of impact due to entrainment of ichthyoplankton." In *Fisheries and Energy Production: A symposium* (S. B. Saila, ed.). p. 107–118. Lexington Books, D.C. Heath and Company, Lexington, MA.

- Kendall, A. W. Jr., and W. H. Lenarz. 1987. "Status of early life history studies of northeast Pacific rockfishes." In *Proceedings of the International Rockfish Symposium*. p. 99–128. Univ. Alaska SeaGrant Rep. 87-2.
- Laidig, T. E., K. M. Sakuma, and M. M. Nishimoto. 1995. "Description of pelagic larval and juvenile stripetail rockfish, *Sebastes saxicola* (family Scorpaenidae), with an examination of larval growth." *Fishery Bulletin* 94:289–299.
- Largier, J. L. 1995. *San Diego Bay circulation: a study of the circulation of water in San Diego Bay for the purpose of assessing, monitoring and managing the transport and potential accumulation of pollutants and sediment in San Diego Bay*. Scripps Institute of Oceanography. Technical Report #1-188-190-0. Final Report prepared for California State Water Resources Control Board and the California Regional Water Quality Control Board, San Diego Region.
- Largier, J. L., C. J. Hearn, and D. B. Chadwick. 1996. "Density structures in low inflow estuaries." In *Buoyancy Effects on Coastal Estuarine Dynamics Coastal Estuarine Studies* (D. G. Aubrey and C. T. Friedrichs, eds.). p. 227-242. American Geophysical Union, Vol. 53, Washington, D.C.
- Largier, J. L. 2003. "Considerations in estimating larval dispersal distances from oceanographic data." *Ecological Applications* 13(1) Sup 71–89.
- Lea, R. N., R. D. McAllister, and D. A. VenTresca. 1999. "Biological aspects of nearshore rockfishes of the genus *Sebastes* from central California." California Department of Fish Game. *Fish Bulletin* 177, 107 p.
- Love, M. S., and K. Johnson. 1999. "Aspects of the life histories of grass rockfish, *Sebastes rastrelliger*, and brown rockfish, *S. auriculatus*, from southern California." *Fishery Bulletin* 97(1):100–109.
- Lynn, R. J., T. Baumgartner, J. Garcia, C. A. Collins, T. L. Hayward, K. D. Hyrenbach, A. W. Mantyla, T. Murphree, A. Shankle, F. B. Schwing, K. M. Sakuma, and M. J. Tegner. 1998. "The state of the California Current, 1997–1998: Transition to El Niño conditions." *California Cooperative Oceanic Fisheries Investigations Reports* 39:25–51.
- MacCall, A. D., K. R. Parker, R. Leithiser, and B. Jessee. 1983. "Power plant impact assessment: A simple fishery production model approach." *Fishery Bulletin* 81(3): 613–619.

- MacGregor, J. S. 1970. "Fecundity, multiple spawning and description of gonads in *Sebastes*." U.S. Fish and Wildlife Service. *Special Scientific Report: Fisheries*, No. 596, 12 p.
- MBC Applied Environmental Sciences and Tenera Environmental. 2005. *AES Huntington Beach L.L.C. Generating Station entrainment and impingement study: final report*. Prepared for AES Huntington Beach L.L.C. and the California Energy Commission. April 2005, 224 p.
- Mayhew, D. A., L. D. Jensen, D. F. Hanson, and P. H. Muessig. 2000. "A comparative review of entrainment survival studies at power plants in estuarine environments." In *Environmental Science & Policy; Power Plants & Aquatic Resources: Issues and Assessment* (J. Wisniewski ed.), Vol. 3, Supplement 1, p. S295–S302. Elsevier Science Ltd., NY.
- Miller, D. J., and R. N. Lea. 1972. "Guide to the Coastal Marine Fishes of California." California Department of Fish and Game. *Fish Bulletin*. 157. Sacramento, CA, 249 p.
- Moreno, G. 1993. "Description of early larvae of four northern California species of rockfishes (Scorpaenidae: *Sebastes*) from rearing studies." *NOAA Technical Report NMFS 116*, 18 p.
- Moser, H. G. 1996. "The early stages of fishes in the California current region." *California Cooperative Oceanic Fisheries Investigations*, Atlas No. 33; 1214–1226. Allen Press Inc., Lawrence, KS.
- Moser, H. G., E. H. Ahlstrom, and E. M. Sandknop. 1977. "Guide to the identification of scorpionfish larvae (family Scorpaenidae) in the eastern Pacific with comparative notes on species of *Sebastes* and *Helicolenus* from other oceans." *NOAA Technical Report NMFS CIRC 402*, 71 p.
- Moser, H. G. and E. H. Ahlstrom. 1978. "Larvae and pelagic juveniles of blackgill rockfish, *Sebastes melanostomus*, taken in midwater trawls off southern California and Baja California." *Journal of the Fisheries Research Board of Canada*. 35(7):981–996.
- Nagle, D. G., and J. T. Morgan, Jr. 2000. "A draft regulatory framework for analyzing potential adverse environmental impact from cooling water intake structures." In *Environmental Science & Policy; Power Plants & Aquatic Resources: Issues and Assessment* (J. Wisniewski, ed.), p. IX–XIV. Vol. 3, Sup. 1. Elsevier Science Ltd., NY.
- Nisbet, R. M., W. Murdoch and A. Stewart-Oaten. 1996. "Consequences for adult fish stocks of human-induced mortality on immatures." In: *Detecting Ecological Impacts:*

Concepts and Applications in Coastal Habitats (R. J Schmitt and C. W. Osenberg, eds.), p. 257–277. Academic Press, San Diego, CA.

Nishimoto, M. M. In prep. "Identification of *Sebastes* larvae."

NOAA. 1999. "El Niño-Southern Oscillation (ENSO)" (<http://www.ogp.noaa.gov/enso/>).

Pacific Gas and Electric Co. 1983. *Moss Landing Power Plant Cooling Water Intake Structures 316(b) Demonstration*. Prepared by Ecological Analysts, Inc., Lafayette, CA. 1983 for Pacific Gas and Electric Co., San Francisco, CA.

Parker, K. R. 1980. "A direct method for estimating northern anchovy, *Engraulis mordax*, spawning biomass." *Fishery Bulletin* 78:541–544.

Parker, K. R. 1985. "Biomass model for the egg production method." In *An Egg Production Method for Estimating Spawning Biomass of Pelagic Fish: Application to the Northern Anchovy, Engraulis mordax*, (R. Lasker, ed.), p. 5-6. U.S. Department of Commerce, NOAA Technical Report NMFS 36.

Parker, K. R., and E. E. DeMartini. 1989. *Chapter D: Adult-Equivalent Loss*. Technical Report to the California Coastal Commission. Prepared by Marine Review Committee, Inc., 56 p.

Parrish, R. H., Serra, R. and W. S. Grant 1989. "The monotypic sardine, *Sardina* and *Sardinops*: their taxonomy, distribution, stock structure, and zoogeography." *Canadian Journal of Fisheries and Aquatic Sciences*. 2019–2036.

Public Service Electric and Gas Company (PSE&G). 1993. "Appendix I—Modeling." Permit No. NJ0005622. Prepared by Lawler, Matusky, and Skelly Engineers, Pearl River, NY. Comments on NJPDES Draft, 82 p.

Rago, P. J. 1984. "Production forgone: An alternative method for assessing the consequences of fish entrainment and impingement losses at power plants and other water intakes." *Ecological Modelling* 24:789–111

Rose, K. A., J. H. Cowan, K. O. Winemiller, R. A. Myers, and R. Hilborn. 2001. "Compensatory density dependence in fish populations: importance, controversy, understanding, and prognosis." *Fish and Fisheries* 2:293–327.

Ricker, W. E. 1975. "Computation and interpretation of biological statistics of fish populations." *Bulletin of the Fisheries Research Board of Canada* 91, 382 p.

- Saila, S. B., X. Chen, K. Erzini, and B. Martin. 1987. *Compensatory Mechanisms in Fish Populations: Literature Reviews. Vol. 1: Critical Evaluation of Case Histories of Fish Populations Experiencing Chronic Exploitation or Impact*. EA-5200. Report prepared for the Electric Power Research Institute.
- Seber, G. A. F. 1982. *The Estimation of Animal Abundance and Related Parameters*. McMillan, London. 654 p.
- Smith, P. E., and S. L. Richardson. 1977. "Standard techniques for pelagic fish egg and larva surveys." *FAO Fisheries Technical Paper* 175:1–100.
- Strange, E., H. Galbraith, S. Bickel, D. Mills, D. Beltman, and J. Lipton. 2002. "Determining ecological equivalence in service-to-service scaling of salt marsh restoration." *Environmental Management* 29:290–300.
- Tenera Environmental. 1997. *Diablo Canyon Power Plant 316(b) demonstration study: Phase 1: Entrainment study design, Part II: Selection of target organisms, sampling methods, and gear testing*. Prepared for Pacific Gas & Electric Co., San Francisco, CA.
- Tenera Environmental. 2000. *Diablo Canyon Power Plant: 316(b) demonstration report*. Prepared for Pacific Gas and Electric Co., San Francisco, CA.
- Tenera Environmental. 2001. *Morro Bay Power Plant modernization project 316(b) resource assessment*. Prepared for Duke Energy Morro Bay, LLC, Morro Bay, CA.
- Tenera Environmental. 2004. *South Bay Power Plant cooling water system effects on San Diego Bay; Volume II: Compliance with Section 316(b) of the Clean Water Act for the South Bay Power Plant*. Prepared for Duke Energy South Bay, Chula Vista, CA.
- Theilacker, G. H. 1980. "Changes in body measurements of larval northern anchovy, *Engraulis mordax*, and other fishes due to handling and preservation." *Fishery Bulletin* 78:685–692.
- Tolimieri, N., and P. S. Levin. 2005. "The roles of fishing and climate in the population dynamics of bocaccio rockfish." *Ecological Applications* 15:458–468.
- U.S. Environmental Protection Agency (USEPA). 1977. *Guidance for evaluating the adverse impact of cooling water intake structures on the aquatic environment: Section 316(b) P.L. 92-500*, 58 p.
- USEPA. 2002. *Case study analysis for the proposed Section 316(b) Phase II existing facilities rule*. EPA-821-R-02-002.

- USEPA. 2004. "National Pollutant Discharge Elimination System: Final regulations to establish requirements for cooling water intake structures at Phase II existing facilities; Final Rule, 40 CFR Parts 9, 122 et al." Published in *Federal Register*, Vol. 69:41575–41693, July 9, 2004.
- Veil, J. A. 2000. "Potential impacts of 316(b) regulatory controls on economics, electricity reliability, and the environment." In *Environmental Science & Policy. Power Plants & Aquatic Resources: Issues and Assessment*, (J. Wisniewski, ed.). Vol. 3, Sup. 1 pp S1–S6. Elsevier Science Ltd., NY, 512 p.
- Veil, J. A., M. G. Puder, D. J. Littleton, and N. Johnson. 2003. "A holistic look at minimizing adverse environmental impact under Section 316(b) of the Clean Water Act." In *Defining and assessing adverse environmental impact from power plant impingement and entrainment of aquatic organism* (D. A. Dixon, J. A. Veil, and J. Wisniewski, eds.). p. 40–55. A.A. Balkema Publishers, Netherlands, 291 pp.
- Wang, J. C. S. 1986. "Fishes of the Sacramento-San Joaquin estuary and adjacent waters, California: A guide to the early life stages.: *Technical Report 9*, January 1986.
- Wilson, C. D., and G. W. Boehlert. 1990. "The effects of different otolith ageing techniques on estimates of growth and mortality for the splitnose rockfish, *Sebastes diploproa*, and canary rockfish, *S. pinniger*." *California Fish and Game* 76(3):146–160.
- Wyllie Echeverria, T. 1987. "Thirty-four species of California rockfishes: maturity and seasonality of reproduction." *Fishery Bulletin* 85(2):229–250.
- Yoklavich, M. M., V. J. Loeb, M. Nishimoto, and B. Daly. 1996. "Nearshore assemblages of larval rockfishes and their physical environment off central California during an extended El Niño event, 1991–1993." *Fishery Bulletin* 94:766–782.

APPENDIX A

VARIANCE EQUATIONS FOR IMPACT ASSESSMENT MODELS

A1. Fecundity Hindcasting (*FH*)

The variance of *FH* was approximated by the Delta method (Appendix E2) (Seber 1982):

$$\text{Var}(FH) = (FH)^2 \left[CV^2(E_T) + \sum_{j=1}^n CV^2(S_j) + CV^2(\bar{F}) + \left(\frac{\text{Var}(A_L) + \text{Var}(A_M)}{(A_L - A_M)^2} \right) \right]$$

where

$CV(E_T)$ = CV of estimated entrainment,

$CV(S_j)$ = CV of estimated survival of eggs and larvae up to entrainment,

$CV(\bar{F})$ = CV of estimated average annual fecundity,

A_M = age at maturation, and

A_L = age at maturity.

The behavior of the estimator for *FH* appears log-linear, suggesting that an approximate confidence interval can be based on the assumptions that $\ln(FH)$ is normally distributed and uses the pivotal quantity

$$Z = \frac{\ln FH - \ln \bar{FH}}{\sqrt{\frac{\text{Var}(FH)}{FH^2}}}$$

A 90% confidence interval for *FH* was estimated by solving for *FH* and setting Z equal to

+/-1.645, i.e.

$$FH \cdot e^{-1.645 \sqrt{\frac{\text{Var}(FH)}{FH^2}}} \text{ to } FH \cdot e^{+1.645 \sqrt{\frac{\text{Var}(FH)}{FH^2}}}$$

A2. Adult Equivalent Loss (*AEL*)

The *AEL* approach uses estimates of the abundance of entrained or impinged organisms to forecast the loss of equivalent numbers of adults. Starting with the number of age class j larvae entrained (E_j), it is conceptually easy to convert these numbers to an equivalent number of adults lost (*AEL*) at some specified age class from the formula:

$$AEL = \sum_{j=1}^n E_j S_j,$$

where

n = number of age classes,

E_j = estimated number of larvae lost in age class j , and

S_j = survival rate for the j th age class to adulthood (Goodyear 1978).

Age-specific survival rates from larval stage to recruitment into the fishery (through juvenile and early adult stages) must be included in this assessment method. For some commercial species, survival rates are known for adults in the fishery; but for most species, age-specific larval survivorship has not been well described.

Survivorship to recruitment, to an adult age, was apportioned into several age stages, and *AEL* was calculated using the total entrainment as

$$AEL = E_r \prod_{j=1}^n S_j,$$

where

n = number of age classes from entrainment to recruitment and

S_j = survival rate from the beginning to end of the j th age class.

The variance of *AEL* can be estimated using a Taylor series approximation (Delta method of Seber 1982) as

$$\text{Var}(AEL) = AEL^2 \left(CV^2(E_r) + \sum_{j=1}^n CV^2(S_j) \right).$$

A3. Proportional Entrainment and *ETM*

The Empirical Transport Model (*ETM*) calculations provide an estimate of the probability of mortality due to power plant entrainment. The values used in calculating proportional entrainment (*PE*) are population estimates based on the respective larval densities and volumes of the cooling water system flow and source water areas. On any one sampling day, the conditional entrainment mortality can be expressed as

$$PE_i = \frac{\text{abundance of entrained larvae}_i}{\text{abundance of larvae in source population}_i}$$

= probability of entrainment in *i*th time period ($i = 1, \dots, N$).

In turn, the daily probability can be estimated and expressed as

$$PE_i = \frac{E_i}{R_i}$$

where

E_i = estimated abundance of larvae entrained in the *i*th time period ($i = 1, \dots, N$);

R_i = estimated abundance of larvae at risk of entrainment from the source population in the *i*th time period ($i = 1, \dots, N$).

The variance for the period estimate of *PE* can be expressed as

$$Var(PE_i) = Var\left(\frac{E_i}{R_i} \mid E_i, R_i\right).$$

Assuming zero covariance between the entrainment and source and using the delta method (Seber 1982), the variance of an estimator formed from a quotient (like PE_i) can be effectively approximated by

$$Var\left(\frac{A}{B}\right) \approx Var(A) \left(\frac{\partial \left[\frac{A}{B}\right]}{\partial A}\right)^2 + Var(B) \left(\frac{\partial \left[\frac{A}{B}\right]}{\partial B}\right)^2.$$

The delta method approximation of $\text{Var}(PE_i)$ is shown as

$$\text{Var}(PE_i) = \text{Var}\left(\frac{E_i}{V_s \cdot \rho_{Si}}\right)$$

which by the Delta method can be approximated by

$$\text{Var}(PE_i) \approx \text{Var}(E_i) \left(\frac{1}{V_s \cdot \rho_{Si}}\right)^2 + \text{Var}(V_s \cdot \bar{\rho}_{Si}) \left(\frac{-E_i}{V_s \cdot (\bar{\rho}_{Si})^2}\right)^2$$

and is equivalent to

$$= PE_i^2 \left[CV(E_i)^2 + CV(V_s \cdot \bar{\rho}_{Si})^2 \right]$$

where

$$R_i = V_s \cdot \bar{\rho}_{Si} \text{ and}$$

$$CV(\theta) = \frac{\text{Var}(\theta)}{\theta^2}.$$

APPENDIX B. Mean larval fish concentrations (larvae per 1000 m³) by station for monthly surveys from February 2001 through January 2002 in San Diego Bay.

Taxon	Common Name	Stations									Mean
		SB1	SB2	SB3	SB4	SB5	SB6	SB7	SB8	SB9	
CIQ goby complex	gobies	2,095.9	1,549.6	2,391.7	2,914.0	3,003.0	4,109.9	3,995.8	2,743.1	2,400.4	2,800.4
<i>Anchoa</i> spp.	bay anchovies	556.5	476.4	231.4	159.6	938.9	1,327.7	1,042.7	520.4	73.3	591.9
<i>Hypsoblennius</i> spp.	cometooth blennies	27.2	45.7	140.8	81.6	210.8	84.6	575.7	94.4	453.6	190.5
Atherinopsidae	silversides	18.2	57.1	6.0	42.2	11.4	22.4	5.3	58.5	18.2	26.6
<i>Syngnathus</i> spp.	pipefishes	12.5	13.7	8.3	4.5	16.0	8.1	12.8	6.9	9.2	10.2
<i>Gillichthys mirabilis</i>	longjaw mudsucker	27.1	4.3	11.5	3.1	15.9	1.5	12.2	0.7	1.2	8.6
<i>Engraulis mordax</i>	northern anchovy	0.4	0.8	0.9	-	6.9	0.8	18.6	15.1	11.1	6.1
<i>Hypsopsetta guttulata</i>	diamond turbot	0.4	0.8	1.9	2.1	5.9	2.6	10.7	11.8	18.4	6.1
<i>Acanthogobius flavimanus</i>	yellowfin goby	2.4	3.5	0.6	12.0	2.9	15.1	1.0	1.9	2.0	4.6
<i>Paralabrax</i> spp.	sand basses	-	0.2	0.6	-	12.2	1.1	17.6	1.7	6.9	4.5
Labrisomidae	labrisomid kelpfishes	-	1.4	2.5	4.8	2.0	1.1	10.1	9.0	5.5	4.0
<i>Genyonemus lineatus</i>	white croaker	0.5	1.0	1.8	2.3	6.3	5.3	6.7	4.3	4.8	3.7
Sciaenidae	croakers	0.7	0.4	1.0	0.2	5.1	0.3	10.1	0.2	4.2	2.5
<i>Cheilotrema saturnum</i>	black croaker	0.2	0.3	0.5	0.8	4.1	3.0	3.9	0.8	3.8	1.9
<i>Paralichthys californicus</i>	California halibut	0.1	0.5	0.2	0.2	0.5	0.7	2.0	0.4	2.4	0.8
<i>Gibbonsia</i> spp.	clinid kelpfishes	-	-	0.2	1.8	0.8	0.5	-	0.7	0.8	0.5
<i>Trachurus symmetricus</i>	jack mackerel	-	-	-	-	-	-	-	-	3.5	0.4
Serranidae	sea basses	-	-	-	-	-	-	-	0.9	1.5	0.3
<i>Lepidogobius lepidus</i>	bay goby	0.1	-	0.3	0.4	0.2	-	0.5	0.2	0.4	0.2
<i>Roncador stearnsi</i>	spotfin croaker	-	-	0.4	-	0.6	-	0.4	0.4	0.2	0.2
<i>Menticirrhus undulatus</i>	California corbina	-	-	-	-	0.9	-	0.5	-	0.1	0.2
<i>Citharichthys stigmaeus</i>	speckled sanddab	-	-	-	0.4	-	-	-	0.2	1.0	0.2
Clupeiformes	herrings and anchovies	-	-	-	-	-	1.2	-	-	0.2	0.2
<i>Odontopyxis trispinosa</i>	pygmy poacher	0.3	-	-	0.6	-	0.3	-	-	0.2	0.2
<i>Gobiesox</i> spp.	clingfishes	0.2	-	-	0.3	-	-	-	0.6	-	0.1
<i>Hippocampus ingens</i>	Pacific seahorse	-	-	0.3	-	-	0.3	-	0.4	-	0.1
<i>Clinocottus analis</i>	wooly sculpin	-	-	-	-	-	-	0.7	-	0.2	0.1
<i>Typhlogobius californiensis</i>	blind goby	0.1	-	-	-	0.3	-	0.3	-	0.2	0.1
<i>Strongylura exilis</i>	California needlefish	0.9	-	-	-	-	-	-	-	-	0.1
<i>Ruscarius creaseri</i>	roughcheek sculpin	0.3	-	0.3	-	-	-	-	-	0.2	0.1
<i>Leptocottus armatus</i>	Pacific staghorn sculpin	-	-	-	0.2	-	-	0.3	0.3	-	0.1
<i>Arteidius</i> spp.	sculpins	-	-	-	-	0.3	-	-	-	0.2	0.1
<i>Hyporhamphus rosae</i>	California halfbeak	0.4	0.2	-	-	-	-	-	-	-	0.1
Paralichthyidae	lefteye flounders & sanddabs	-	-	-	-	-	0.3	-	0.2	-	0.1
Cottidae	sculpins	-	-	-	-	0.2	-	-	0.2	-	0.1
<i>Oligocottus</i> spp.	sculpins	-	-	-	-	-	-	0.2	0.2	-	0.1
<i>Pleuronichthys ritteri</i>	spotted turbot	-	-	-	-	-	-	-	0.4	-	0.1
<i>Atractoscion nobilis</i>	white seabass	-	-	-	-	0.2	-	-	0.2	-	<0.1
<i>Porichthys myriaster</i>	specklefin midshipman	-	-	-	-	-	0.3	-	-	-	<0.1
Clupeidae	herrings	-	-	-	-	-	-	0.3	-	-	<0.1
<i>Nannobranchium</i> spp.	lanternfishes	-	-	-	-	-	-	0.2	-	-	<0.1
<i>Gobiesox rhesodon</i>	California clingfish	-	-	-	-	-	0.2	-	-	-	<0.1
<i>Sebastes</i> spp.	rockfishes	-	-	-	-	-	-	0.2	-	-	<0.1
<i>Citharichthys</i> spp.	sanddabs	-	-	-	-	-	-	-	-	0.2	<0.1
Station Total		2,744.3	2,155.7	2,801.3	3,231.0	4,245.4	5,587.0	5,728.8	3,474.2	3,024.3	

APPENDIX C. Estimates of CIQ goby larvae at South Bay Power Plant entrainment and source water stations from monthly surveys conducted from February 2001 through January 2002 used in calculating empirical transport model (*ETM*) estimates of proportional entrainment (*PE*) and annual estimate of proportional mortality (P_M). The daily cooling water intake volume used in calculating the entrainment estimates was 2,275,244 m³, and the volume of the source water used in calculating the source water population estimates was 149,612,092 m³. The number of days that the larvae were exposed to entrainment was estimated at 22.86 days.

Survey Date	Entrainment Concentration (#/m ³)	Estimated Number Entrained	Source Water Concentration (#/m ³)	Estimated Number in the Source Water	<i>PE</i> Estimate	Days in Survey Period	Estimate of Source Water Population for Period	Proportion of Source Population for Period (f)	$=f_i(1-PE_i)^d$
28-Feb-01	2.143	4,877,000	5.712	8.546E+08	0.0057	41	3.504E+10	0.2165	0.1900
29-Mar-01	1.069	2,433,000	3.643	5.451E+08	0.0045	29	1.581E+10	0.0977	0.0882
17-Apr-01	1.997	4,544,000	2.794	4.180E+08	0.0109	19	7.942E+09	0.0491	0.0382
16-May-01	2.036	4,633,000	1.770	2.649E+08	0.0175	29	7.682E+09	0.0475	0.0317
14-Jun-01	3.747	8,525,000	2.311	3.458E+08	0.0247	29	1.003E+10	0.0620	0.0350
26-Jul-01	4.047	9,208,000	2.740	4.100E+08	0.0225	42	1.722E+10	0.1064	0.0633
23-Aug-01	0.648	1,475,000	2.609	3.904E+08	0.0038	28	1.093E+10	0.0675	0.0619
25-Sep-01	1.057	2,406,000	2.307	3.452E+08	0.0070	33	1.139E+10	0.0704	0.0600
23-Oct-01	1.254	2,852,000	2.553	3.820E+08	0.0075	28	1.070E+10	0.0661	0.0557
27-Nov-01	1.655	3,764,000	2.390	3.576E+08	0.0105	35	1.252E+10	0.0773	0.0607
20-Dec-01	1.861	4,233,000	2.745	4.107E+08	0.0103	23	9.446E+09	0.0584	0.0461
17-Jan-02	3.554	8,087,000	3.132	4.686E+08	0.0173	28	1.312E+10	0.0811	0.0545
Average =					0.0118			$P_M =$	0.2147

APPENDIX D. Estimates of KGB rockfish larvae at MBPP entrainment and source water stations from monthly surveys conducted from January 2000 through December 2000 used in calculating empirical transport model (*ETM*) estimates of proportional entrainment (*PE*) and annual estimate of proportional mortality (P_M). The daily cooling water intake volume used in calculating the entrainment estimates was 1,619,190 m³, and the volume of the source water used in calculating the source water population estimates was 15,686,663 m³. Bay volume = 20,915,551 m³. The larval duration used in the calculations was 11.28 days.

Survey Date	Estimated Number Entrained	Estimated Number in the Bay	Bay <i>PE</i>	Estimated Number in the Offshore Area	Offshore <i>PE</i>	Total <i>PE</i>	Source Water Population for Period	Proportion of Source Population for Period (<i>f</i>)	$=f_i(1-PE_iP_S)^d$	
17-Jan-00	5,500	17,800	0.3097	0	–	0.3097	17,800	0.0099	0.0073	
28-Feb-00	2,180	20,700	0.1052	22,100	0.0988	0.0509	42,800	0.0239	0.0227	
27-Mar-00	0	6,550	–	186,000	–	–	192,000	0.1076	0.1076	
24-Apr-00	38,100	715,000	0.0533	576,000	0.0661	0.0295	1,291,000	0.7218	0.7010	
15-May-00	4,460	11,800	0.3785	202,000	0.0220	0.0208	214,000	0.1197	0.1173	
12-Jun-00	0	14,900	–	15,000	–	–	30,300	0.0169	0.0169	
10-Jul-00	0	0	–	0	–	–	0	–	–	
8-Aug-00	0	0	–	0	–	–	0	–	–	
5-Sep-00	0	0	–	0	–	–	0	–	–	
2-Oct-00	0	0	–	0	–	–	0	–	–	
27-Nov-00	0	0	–	0	–	–	0	–	–	
18-Dec-00	0	0	–	0	–	–	0	–	–	
			$\bar{x} = 0.0705$			$\bar{x} = 0.0156$			$\bar{x} = 0.0342$	$P_M = 0.0271$

APPENDIX E. Estimates used in calculating empirical transport model (ETM) estimates of proportional entrainment (PE) for kelp, gopher, and black-and-yellow (KGB) rockfish complex for Diablo Canyon Power Plant. Entrainment estimates and estimates from the nearshore sampling area from monthly surveys conducted for two periods A) July 1997 through June 1998, and B) July 1998 through June 1999. The daily cooling water intake volume used in calculating the entrainment estimates was 9,312,114 m³, and the volume of the sampled source water used in calculating the nearshore population estimates was 1,738,817,356 m³. The larval duration used in the calculations was 16.4 days.

A) July 1997 – June 1998

Survey Date	Start Date Based on Larval Duration	Estimated Number Entrained	Entrainment Std. Error	Estimated Population in Nearshore Sampling Area	Nearshore Population Std. Error	PE _i	PE _i Std. Error	f _i	f _i Std. Error
21-Jul-97	5-Jul-97	2,770	2,770	258,000	255,000	0.0107	0.0151	0.0004	0.0004
25-Aug-97	9-Aug-97	0	–	0	–	–	–	–	–
29-Sep-97	13-Sep-97	0	–	0	–	–	–	–	–
20-Oct-97	4-Oct-97	0	–	0	–	–	–	–	–
17-Nov-97	1-Nov-97	0	–	0	–	–	–	–	–
10-Dec-97	24-Nov-97	0	–	216,000	216,000	–	–	0.0003	0.0003
22-Jan-98	6-Jan-98	6,280	6,280	7,775,000	3,345,000	0.0008	0.0009	0.0121	0.0053
26-Feb-98	10-Feb-98	23,900	13,900	11,534,000	2,267,000	0.0021	0.0013	0.0180	0.0038
18-Mar-98	2-Mar-98	1,051,000	503,000	17,903,000	2,903,000	0.0587	0.0297	0.0279	0.0050
15-Apr-98	30-Mar-98	847,000	376,000	111,247,000	12,360,000	0.0076	0.0035	0.1732	0.0214
18-May-98	2-May-98	1,468,000	288,000	409,996,000	51,937,000	0.0036	0.0008	0.6384	0.0334
8-Jun-98	23-May-98	2,940,000	622,000	83,336,000	9,213,000	0.0353	0.0084	0.1297	0.0165
Mean =						0.0167	Sum =	1.0000	

B) July 1998 – June 1999

Survey Date	Start Date Based on Larval Duration	Estimated Number Entrained	Entrainment Std. Error	Estimated Population in Nearshore Sampling Area	Nearshore Population Std. Error	PE_i	PE_i Std. Error	f_i	f_i Std. Error
21-Jul-98	5-Jul-98	7,000	7,000	2,118,000	636,000	0.0033	0.0035	0.0035	0.0011
26-Aug-98	10-Aug-98	0	–	0	–	–	–	–	–
16-Sep-98	31-Aug-98	0	–	0	–	–	–	–	–
6-Oct-98	20-Sep-98	0	–	0	–	–	–	–	–
11-Nov-98	26-Oct-98	0	–	0	–	–	–	–	–
9-Dec-98	23-Nov-98	0	–	0	–	–	–	–	–
12-Jan-99	27-Dec-98	0	–	14,709,000	3,038,000	–	–	0.0240	0.0053
3-Feb-99	18-Jan-99	6,830	6,830	14,905,000	2,462,000	0.0005	0.0005	0.0243	0.0045
17-Mar-99	1-Mar-99	1,621,000	967,000	49,607,000	5,491,000	0.0327	0.0198	0.0809	0.0108
14-Apr-99	29-Mar-99	1,601,000	825,000	116,783,000	22,089,000	0.0137	0.0075	0.1906	0.0328
24-May-99	8-May-99	4,168,000	868,000	363,131,000	33,925,000	0.0115	0.0026	0.5926	0.0456
23-Jun-99	7-Jun-99	877,000	287,000	51,558,000	33,815,000	0.0170	0.0125	0.0841	0.0509
Mean =						0.0131	Sum =	1.0000	

APPENDIX F. Regression estimates, onshore and alongshore current meter displacement, source water estimates, and estimates of the proportion of source water sampled (P_S) from monthly surveys conducted for two periods A) July 1997 through June 1998, and B) July 1998 through June 1999 for kelp, gopher, and black-and-yellow (KGB) rockfish complex at the Diablo Canyon Power Plant. The common slope used in calculating source water estimates was 0.000117 for the 1997-1998 period and -0.000367 for the 1998-1999 period. The ratio of the length of the nearshore sampling area (17,373 m) to the alongshore current displacement was used to calculate P_S for each survey (alongshore P_S). The regression coefficients and onshore and alongshore current displacement were used to calculate an estimate of the population in the source water for each survey. The ratio of the estimated population in the nearshore sampling area to the estimated population in the source water was used to calculate an estimate of P_S for each survey (offshore P_S).

A) July 1997 - June 1998

Survey Date	Y-Intercept	X-Intercept	Cumulative Alongshore Displacement (m)	Onshore Current Displacement (m)	Estimated Offshore Extent of Source Water (m)	Extrapolated Number Beyond Nearshore Sampling Area	Total Extrapolated Offshore Source Population	Total Extrapolated Alongshore Source Population	Offshore P_S	Alongshore P_S
21-Jul-97	-0.171	1,460	31,300	4,820	4,820	16,382,000	16,848,234	466,000	0.0153	0.5545
25-Aug-97	-	-	-	-	-	-	0	0	-	-
29-Sep-97	-	-	-	-	-	-	0	0	-	-
20-Oct-97	-	-	-	-	-	-	0	0	-	-
17-Nov-97	-	-	-	-	-	-	0	0	-	-
10-Dec-97	-0.172	1,470	146,000	31,600	31,600	7,772,826,000	7,774,642,009	1,816,000	<0.0001	0.1189
22-Jan-98	-0.015	125	120,000	23,400	23,400	3,753,412,000	3,807,288,976	53,877,000	0.0020	0.1443
26-Feb-98	0.064	-545	33,700	8,710	8,710	144,140,000	166,528,437	22,388,000	0.0693	0.5152
18-Mar-98	0.165	-1,410	181,000	12,400	12,400	1,801,789,000	1,988,251,728	186,463,000	0.0090	0.0960
15-Apr-98	2.115	-18,000	76,100	12,800	12,800	2,264,580,000	2,752,044,506	487,464,000	0.0404	0.2282
18-May-98	8.127	-69,400	67,100	19,900	19,900	10,706,927,000	12,290,666,879	1,583,740,000	0.0334	0.2589
8-Jun-98	1.376	-11,700	111,000	5,670	5,670	559,792,000	1,094,442,999	534,651,000	0.0761	0.1559
Mean =									0.0307	0.2590

B) July 1998 - June 1999

Survey Date	Y-Intercept	X-Intercept	Cumulative Alongshore Displacement (m)	Onshore Current Displacement (m)	Estimated Offshore Extent of Source Water (m)	Extrapolated Number Beyond Nearshore Sampling Area	Total Extrapolated Offshore Source Population	Total Extrapolated Alongshore Source Population	Offshore P_s	Alongshore P_s
21-Jul-98	0.596	1,620	76,300	11,100	3,010	0	9,299,000	9,299,000	0.2278	0.2278
26-Aug-98	-	-	-	-	-	-	0	0	-	-
16-Sep-98	-	-	-	-	-	-	0	0	-	-
6-Oct-98	-	-	-	-	-	-	0	0	-	-
11-Nov-98	-	-	-	-	-	-	0	0	-	-
9-Dec-98	-	-	-	-	-	-	0	0	-	-
12-Jan-99	0.859	2,340	46,200	24,100	3,010	0	39,166,000	39,166,000	0.3755	0.3755
3-Feb-99	0.859	2,340	81,900	19,700	3,010	0	70,254,000	70,254,000	0.2122	0.2122
17-Mar-99	1.529	4,169	36,900	8,540	4,170	9,113,397	114,452,000	105,339,000	0.4334	0.4709
14-Apr-99	2.936	8,003	163,000	10,200	8,000	744,108,728	1,837,168,000	1,093,059,000	0.0636	0.1068
24-May-99	7.716	21,036	180,000	21,800	21,000	10,709,111,477	14,464,376,000	3,755,264,000	0.0251	0.0967
23-Jun-99	1.605	4,376	158,000	5,970	4,380	54,169,916	522,822,000	468,652,000	0.0986	0.1100
Mean =									0.2052	0.2286

M

**AGUA HEDIONDA LAGOON
HYDRODYNAMIC STUDIES**

by

Hany Elwany, Ph.D.
Reinhard Flick, Ph.D.
Martha White, M.S.
Kevin Goodell

Prepared for

Tenera Environmental
141 Suburban Road, Suite A-2
San Luis Obispo, California 93401

Prepared by

Coastal Environments
2166 Avenida de la Playa, Suite E
La Jolla, CA 92037

25 October 2005
CE Reference No. 05-10

TABLE OF CONTENTS

1.0 INTRODUCTION 1

2.0 DESCRIPTION OF AGUA HEDIONDA LAGOON 6

 2.1 OCEAN TIDES 13

 2.2 POWER PLANT INTAKE FLOW RATES 13

3.0 WATER LEVEL, VELOCITY, SALINITY, AND TEMPERATURE MEASUREMENTS 16

 3.1 WATER LEVEL 16

 3.2 WATER VELOCITY 16

 3.3 SALINITY AND TEMPERATURE 26

4.0 RESIDENCE TIME OF WATER IN THE LAGOON 27

5.0 SUMMARY AND CONCLUSIONS 36

 5.1 LAGOON DESCRIPTION 36

 5.2 FIELD MEASUREMENTS 36

 5.3 RESIDENCE TIME 37

6.0 REFERENCES 38

LIST OF APPENDICES

Appendix A Water Level Measurements at Outer, Inner, and Middle Basins

Appendix B Water Velocity Measurements at Outer and Inner Basins

Appendix C Lagoon Tidal Prism with Contributions of Outer, Inner, and Middle Basins to Tidal Prism

Appendix D Temperature and Salinity Measurements at Outer and Inner Basins

LIST OF FIGURES

Figure 1-1 Map showing the location of Agua Hedionda Lagoon 2

Figure 1-2 Map of Agua Hedionda Lagoon showing the locations of its three basins, the Outer, Inner, and Middle Basins 3

Figure 1-3 Configurations of intake and discharge channels of Agua Hedionda Lagoon 4

Figure 2-1 Bathymetry map of Agua Hedionda Lagoon 7

Figure 2-2 Bathymetry map of Outer Basin 8

Figure 2-3 Bathymetry map of Middle Basin 9

Figure 2-4 Bathymetry map of Inner Basin 10

Figure 2-5 Agua Hedionda Lagoon surface area and water volume 11

Figure 2-6 Potential tidal prism for the Outer, Middle, and Inner Basins and the lagoon (total) 12

Figure 2-7 Hourly Encina Power Station intake flow 15

Figure 3-1	Measurement locations for stations S0 (water level, water velocity, temperature, salinity), S2A (water level, water velocity, temperature, salinity), S2B (water level), and S2C (water level)	17
Figure 3-2	Locations of benchmarks used in this study	18
Figure 3-3	Comparison of water level at sites S0, S2A, S2B, and S3 during neap tide .	19
Figure 3-4	Comparison of water level at sites S0, S2A, S2B, and S3 during spring tide	20
Figure 3-5	Comparison of water level at sites S0, S2A, S2B, and S3 during mean tide .	21
Figure 3-6	Water level and velocity measurements during neap tide	22
Figure 3-7	Water level and velocity measurements during spring tide	23
Figure 3-8	Water level and velocity measurements during mean tide	24
Figure 3-9	Tidal prism of the lagoon between June 1, 2005 and July 6, 2005	25
Figure 4-1	Percentage of old water in the lagoon vs. tidal cycle	28
Figure 4-2	Percentage of old water in the lagoon vs. day, with solid line showing best-fit curve	29
Figure 4-3	Lagoon inflow and outflow through the inlet per tidal cycle during 1 June 05 through 7 July 05	32
Figure 4-4	Lagoon inflow and outflow through the inlet per day during 1 June 05 through 7 July 05	33
Figure 4-5	Ratio between inflowing water and water taken in by power plant cooling system by tidal cycle. The solid line represents the mean ratio measurement time period	34
Figure 4-6	Ratio between inflowing water and water taken in by power plant cooling system by day. The solid line represents the mean ratio over the measurement time period	35

APPENDIX FIGURES

Figure A-1	Comparison between water level measurements at Station S0 and ocean tide	A-1
Figure A-2	Comparison between water level measurements at Station S2A & ocean tide	A-2
Figure A-3	Comparison between water level measurements at Station S2B & ocean tide	A-3
Figure A-4	Comparison between water level measurements at Station S3 and ocean tide	A-4
Figure B-1	East component of water velocity at Station S0	B-1
Figure B-2	North component of water velocity at Station S0	B-2
Figure B-3	East component of water velocity at Station S2B	B-3
Figure B-4	North component of water velocity at Station S2B	B-4
Figure C-1	Tidal prism of Outer Basin as computed from water level measurements at Station S0	C-1
Figure C-2	Tidal prism of Middle Basin as computed from water level measurements at Station S2A	C-2
Figure C-3	Tidal prism of Middle Basin as computed from water level measurements at Station S2B	C-3
Figure C-4	Tidal prism of Inner Basin as computed from water level measurements at Station S3	C-4
Figure C-5	Agua Hedionda Lagoon tidal prism	C-5
Figure D-1	Water temperature measurements at Station S0	D-1
Figure D-2	Water temperature measurements at Station S2B	D-2
Figure D-3	Water salinity measurements at Station S2B	D-3

LIST OF TABLES

Table 2-1	Tidal levels with respect to MLLW and NGVD (1960-1978)	14
Table 4-1	Curve-fitting parameters for “old water” percentage per tidal cycle	31
Table 4-2	Curve-fitting parameters for “old water” percentage per day	31
Table 4-3	Residence time of water in Agua Hedionda Lagoon	31

AGUA HEDIONDA LAGOON HYDRODYNAMIC STUDIES

1.0 INTRODUCTION

The purpose of this report is to evaluate the hydrodynamics of Agua Hedionda Lagoon, which is located in Carlsbad, California (Figure 1-1). The lagoon consists of three basins, the Outer, Middle, and Inner Basins (Figure 1-2). The lagoon is connected to the Pacific Ocean through an inlet channel protected by two jetties.

The results of this study will be used to estimate entrainment mortality on a bay or lagoon population caused by the operation of the Encina Power Station (EPS). The EPS is located adjacent to Agua Hedionda Lagoon. The five power-generating units withdraw about 635 to 670 million gallons of water per day (mgd) from the lagoon to the power plant condenser systems for cooling purposes. The heated water is discharged through a channel across the beach. Figure 1-3 shows the configurations of the inlet and discharge channels.

The main questions for this study are:

1. What are the general hydrodynamics of Agua Hedionda Lagoon?
2. What are the volumes of the three lagoon basins at various elevations?
3. What is the tidal prism, defined in this study as the volume of water in the lagoon between maximum and minimum water level per tidal cycle?
4. What is the residence time of water in the lagoon and its basins?

Chapter 1 describes the purpose of the study and outlines the required tasks. Chapter 2 describes the lagoon and the tidal cycles that control the water level in the lagoon. Chapter 3 provides information about the water level, velocity, salinity, and temperature measurements in the lagoon that were conducted between 1 June 2005 and 7 July 2005. Chapter 4 describes the method used to estimate the residence time of water in the lagoon and provides the results. Chapter 5 gives a brief summary of the results; a list of the references used in this study is given in Chapter 6. The appendices provide a summary of the results obtained from the fieldwork conducted during the study.

Our efforts during this study included:

1. Site visits to Agua Hedionda Lagoon;
2. A review of the existing oceanographic data and literature;
3. Installation of instruments at four temporary data collection stations;
4. Collection of data for a one-month period, including water level, water velocity, salinity, and temperature measurements;
5. Computation of the tidal prism; and
6. Presentation of our findings in this report.

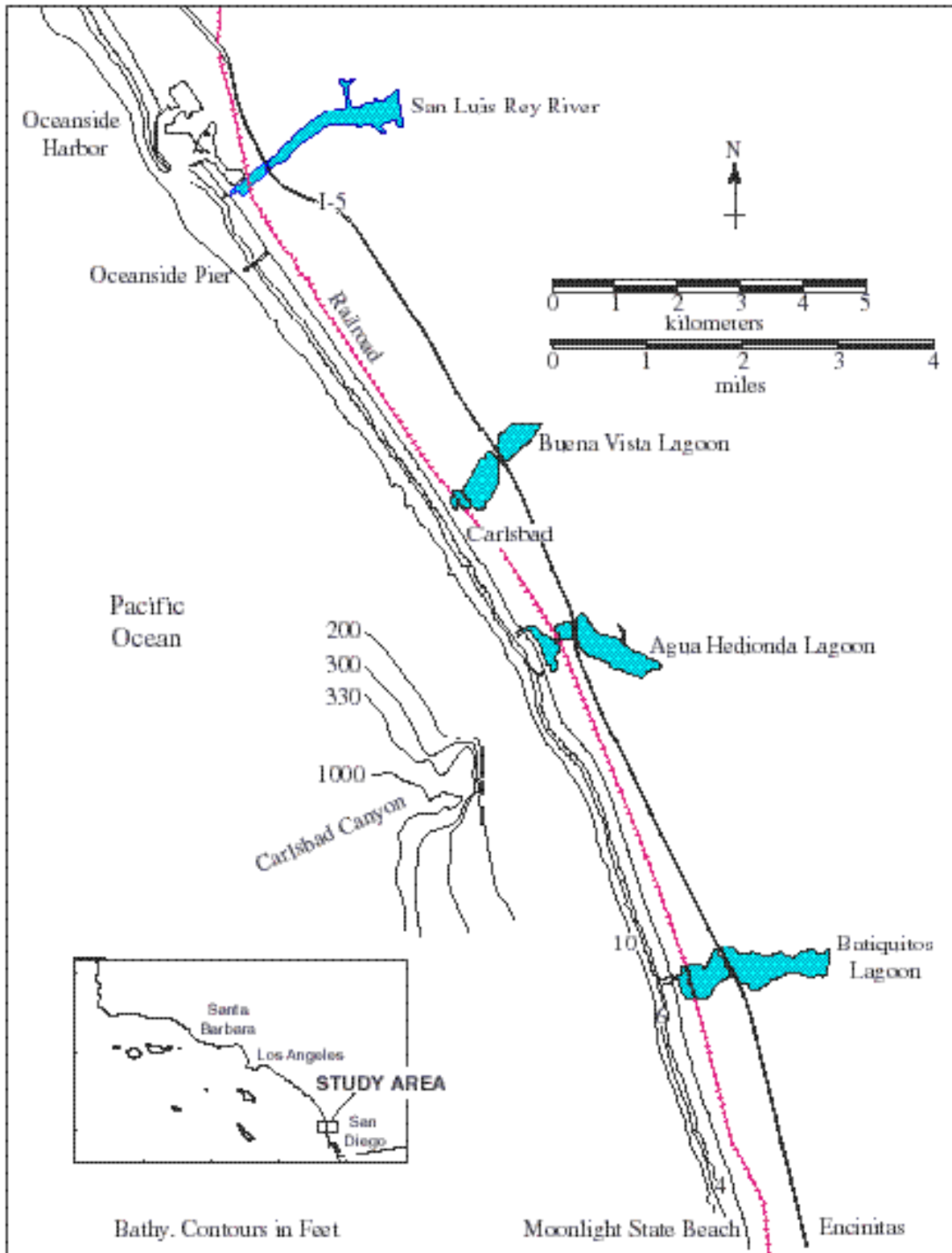


Figure 1-1. Map showing the location of Agua Hedionda Lagoon

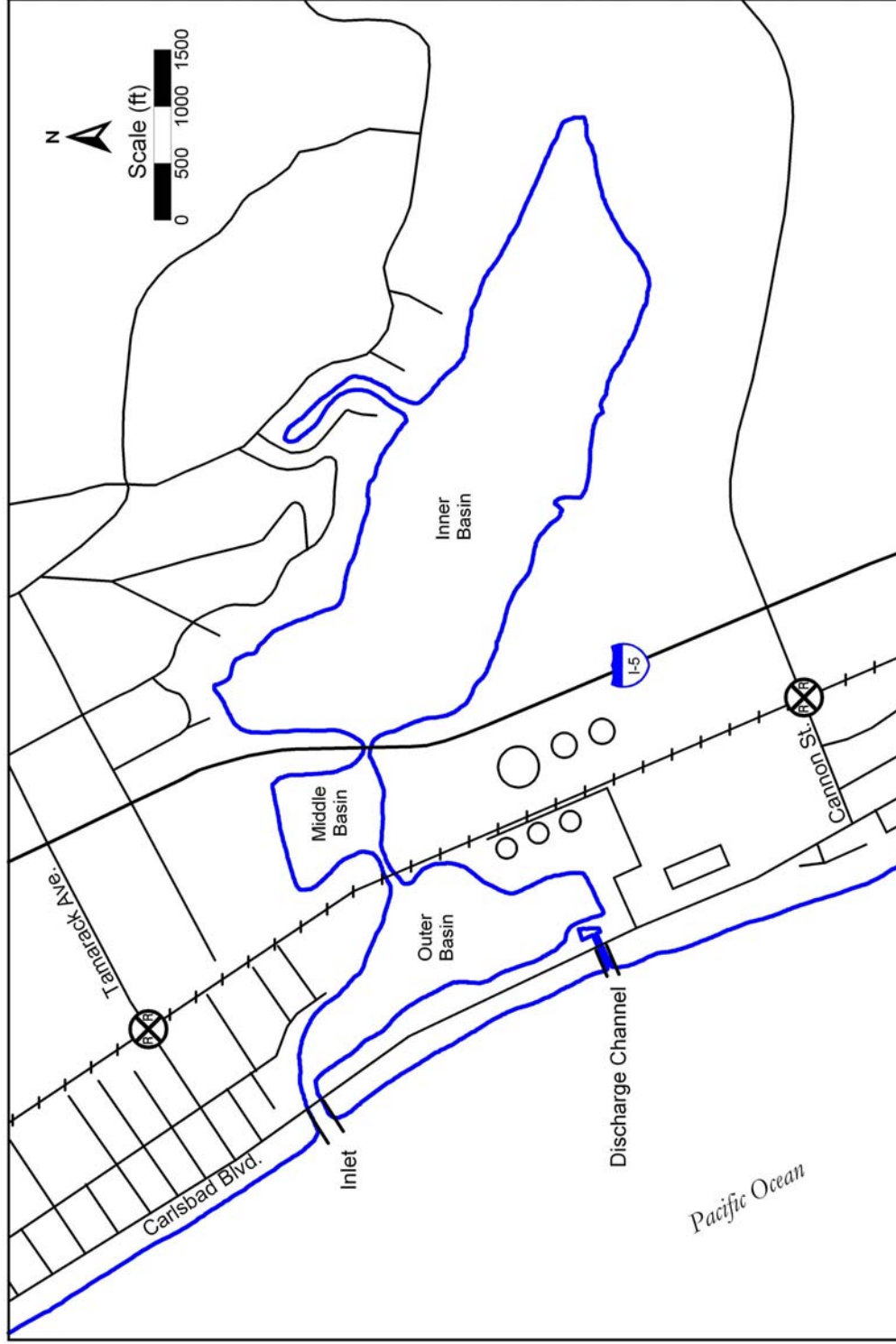


Figure 1-2. Map of Agua Hedionda Lagoon showing the locations of its three basins: the Outer, Inner, and Middle Basins.

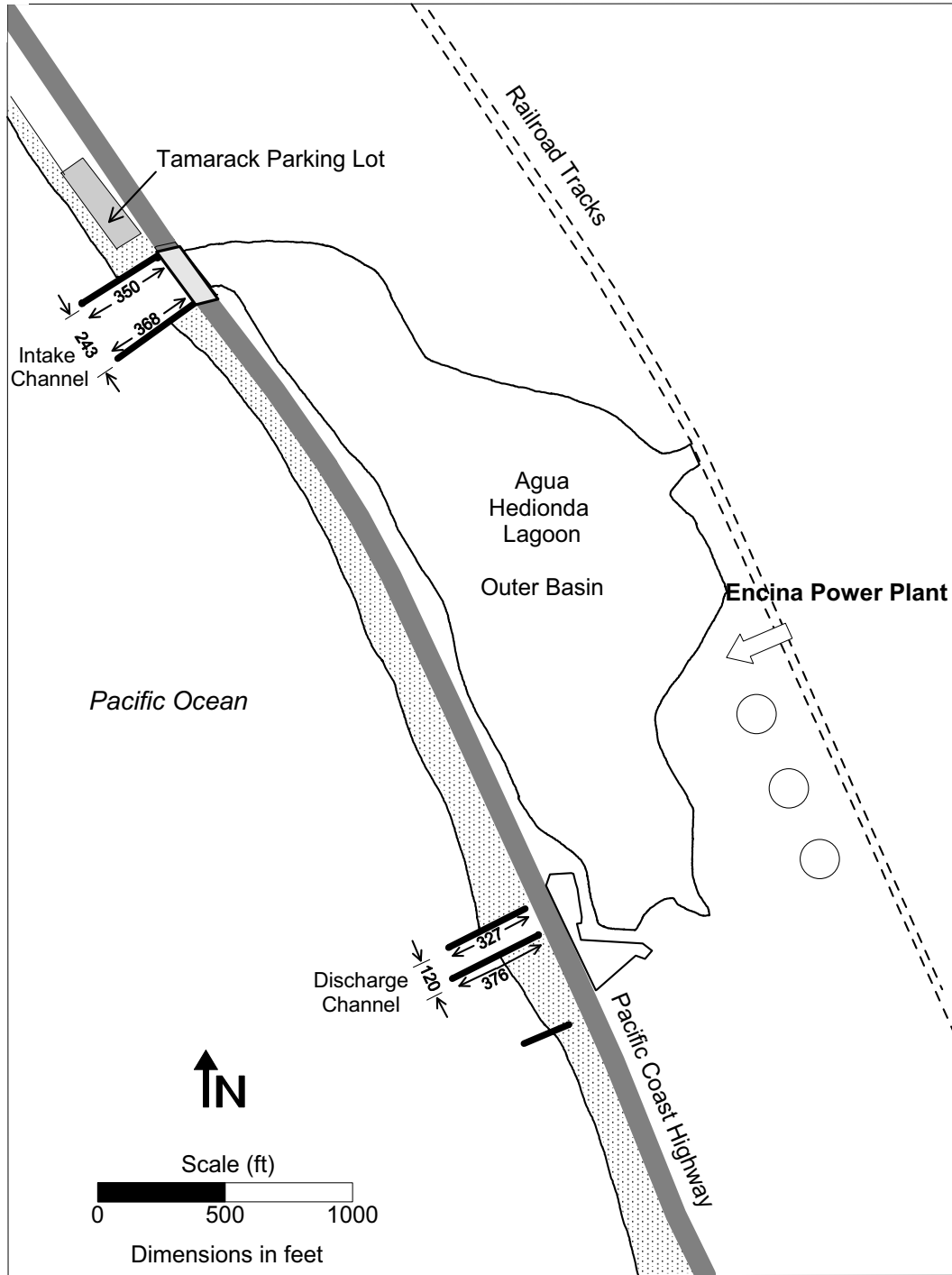


Figure 1-3. Configurations of intake and discharge channels of Agua Hedionda Lagoon.

Several studies have previously been conducted to determine the effect of the operation of the cooling system of Encina Power Station on lagoon sedimentation (Ellis, 1954; Bhogal et al., 1989; EA Engineering Science and Technology, 1997; Jenkins and Wasyl, 2001). Studies to determine the impact on marine environments have been presented by Jenkins and Skelly (1998) and Jenkins et al. (1989). Elwany et al. (1999) described the oceanographic conditions (waves and tides) at Agua Hedionda Lagoon in detail. A bibliography of pertinent research on existing conditions and monitoring studies in the vicinity of Agua Hedionda lagoon is given in Coastal Environments (1998).

2.0 DESCRIPTION OF AGUA HEDIONDA LAGOON

Agua Hedionda Lagoon is located within the City of Carlsbad, California. The lagoon is bounded on the west by the Pacific Coast Highway (called “Carlsbad Boulevard” in this area), on the north by the City of Carlsbad residential community, and on the east and south by undeveloped hill slopes and bluffs. On the south side above the bluffs lie cultivated fields and the EPS.

The Santa Fe Railroad and Interstate 5 freeway (“I-5”) divide Agua Hedionda Lagoon into three sections, the Inner, Middle and Outer Basins, which have areas of 186, 22, and 50 acres, respectively. The natural resources of Agua Hedionda Lagoon have been described in Bradshaw et al. (1976).

In 2004 and 2005, the Encina Power Station conducted topographic surveys in the lagoon. Surveys of the Outer, Middle, and Inner Basins were conducted in March 2005, November 2004, and May 2005, respectively. Figure 2-1 is a bathymetric map of the lagoon. There is a cooling water intake channel and an effluent discharge channel offshore from the lagoon. The intake jetties are located west of the Coast Highway bridge and have lengths of about 350 ft (north) and 368 ft (south). The distance between the centerline of the two jetties is about 243 ft. The jetties at the discharge channel are about 327 and 376 ft long, with the south jetty extending longer than the north jetty. The distance that the intake and discharge jetties extend varies with the changing location of the shoreline.

Figures 2-2 through 2-4 show the bathymetry of the Outer, Middle and Inner Basins. The bottom elevations in the basins range from about -42 ft (NGVD 29), in the deepest portion of the Outer and Middle Basins, to about 10 ft NGVD along the shoreline of the Inner Basin. The Outer Basin and the channel leading to the Inner Basin are the deepest areas of the lagoon. The Middle and Inner Basins are shallower at -16 ft, NGVD, in comparison to the majority of the Outer Basin, which is at a depth of -20 to -32 ft, NGVD. From these maps, cumulative surface area (in acres) and cumulative water volume (in acre-ft) were obtained. The potential tidal prism (in acre-ft) versus elevation (ft, NGVD) was computed.

The surface area of the lagoon at 6 ft, NGVD is about 350 acres. The surface area of the lagoon is reduced to about 225 acres at mean low lower water (MLLW). At MLLW, the volume of water in the lagoon is about 1750 acre-ft. The majority of the area and volume come from the large Inner Basin (Figure 2-5).

The potential tidal prism, as a function of lagoon water level elevation, is shown for the Outer, Middle, and Inner Basins and for the total lagoon (Figure 2-6). The tidal prism of the lagoon is defined as the volume of water in the lagoon between the maximum and minimum water levels. Here we assume the minimum water level to be -1 ft, NGVD, for the purpose of computation. Tidal prism is referred to as “potential tidal prism,” because we assume that the water level in the entire lagoon is the same, with no friction losses (i.e., no tidal muting). Figure 2-6 shows that the tidal prism of the Inner Basin constitutes the largest portion of the lagoon tidal prism.

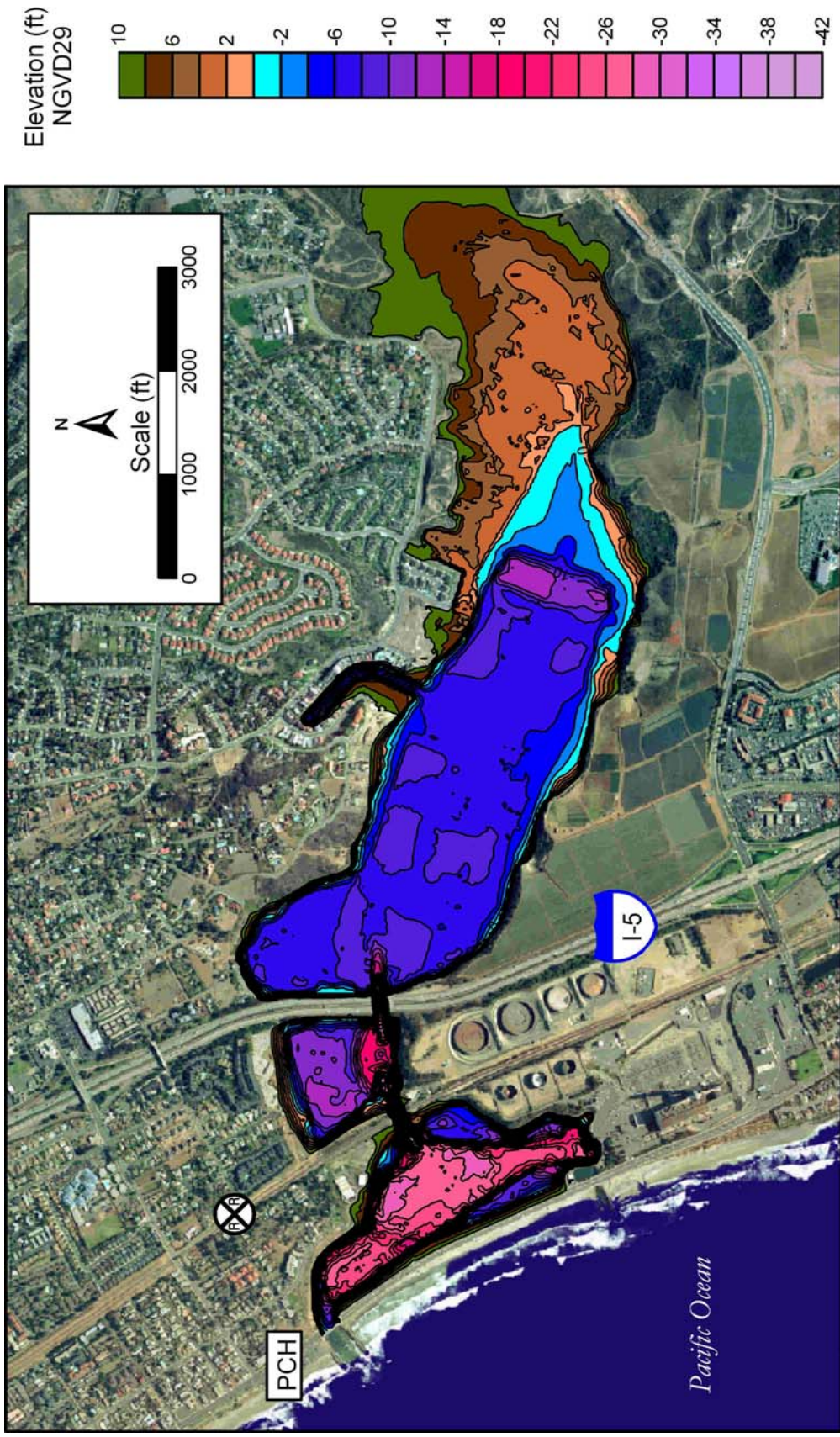


Figure 2-1. Bathymetry map of Agua Hedionda Lagoon.

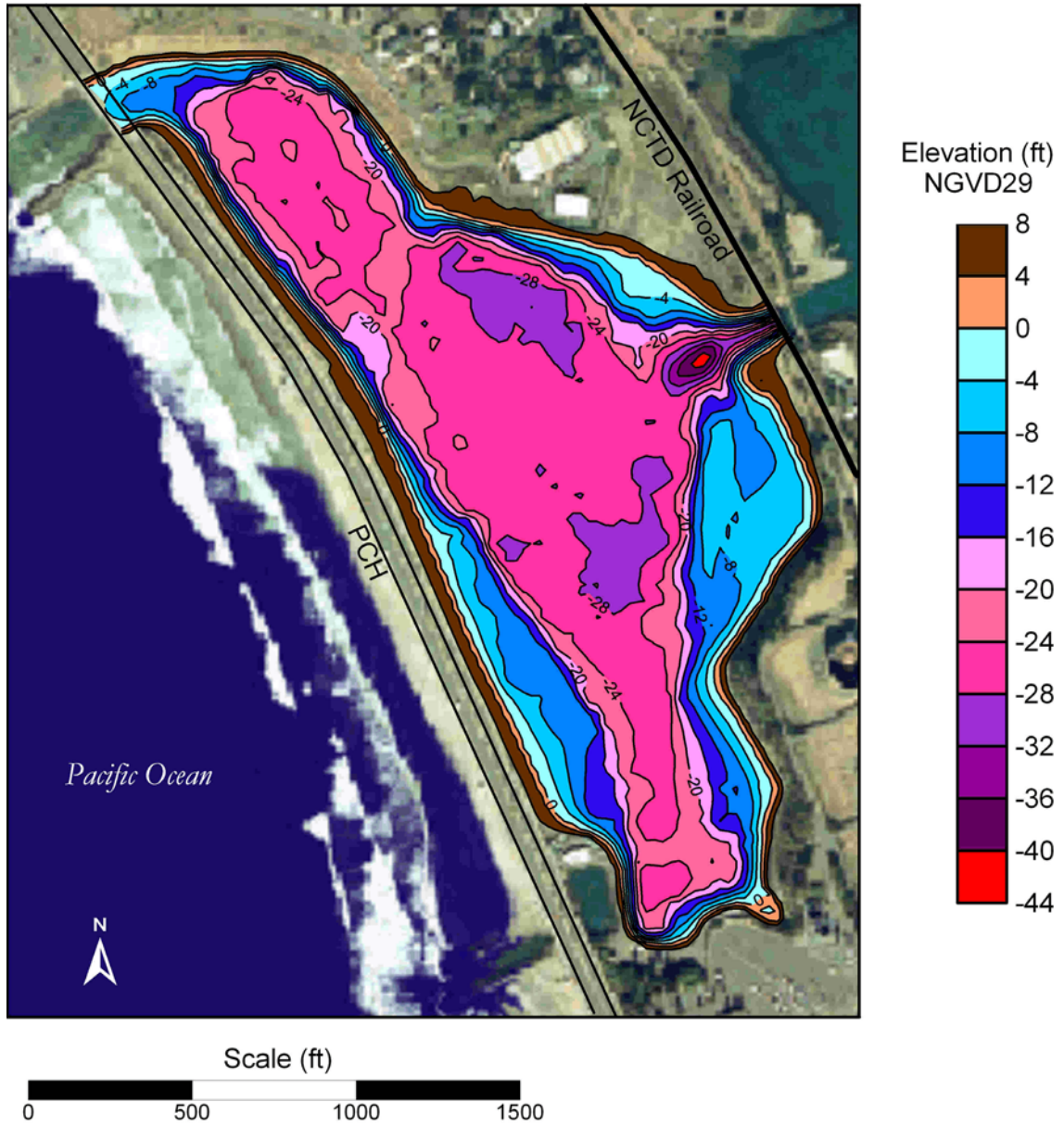


Figure 2-2. Bathymetry map of Outer Basin.

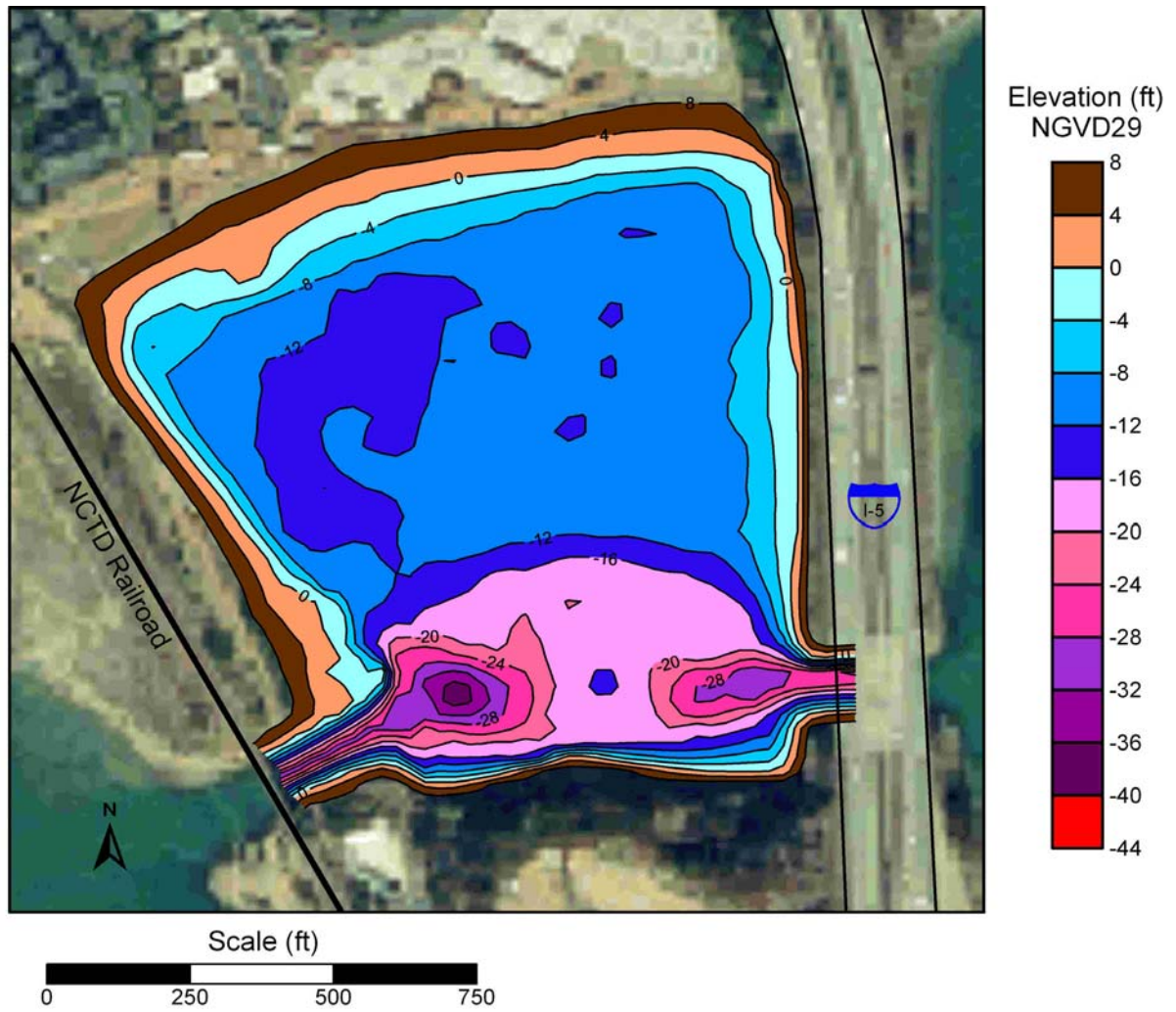


Figure 2-3. Bathymetry map of Middle Basin.

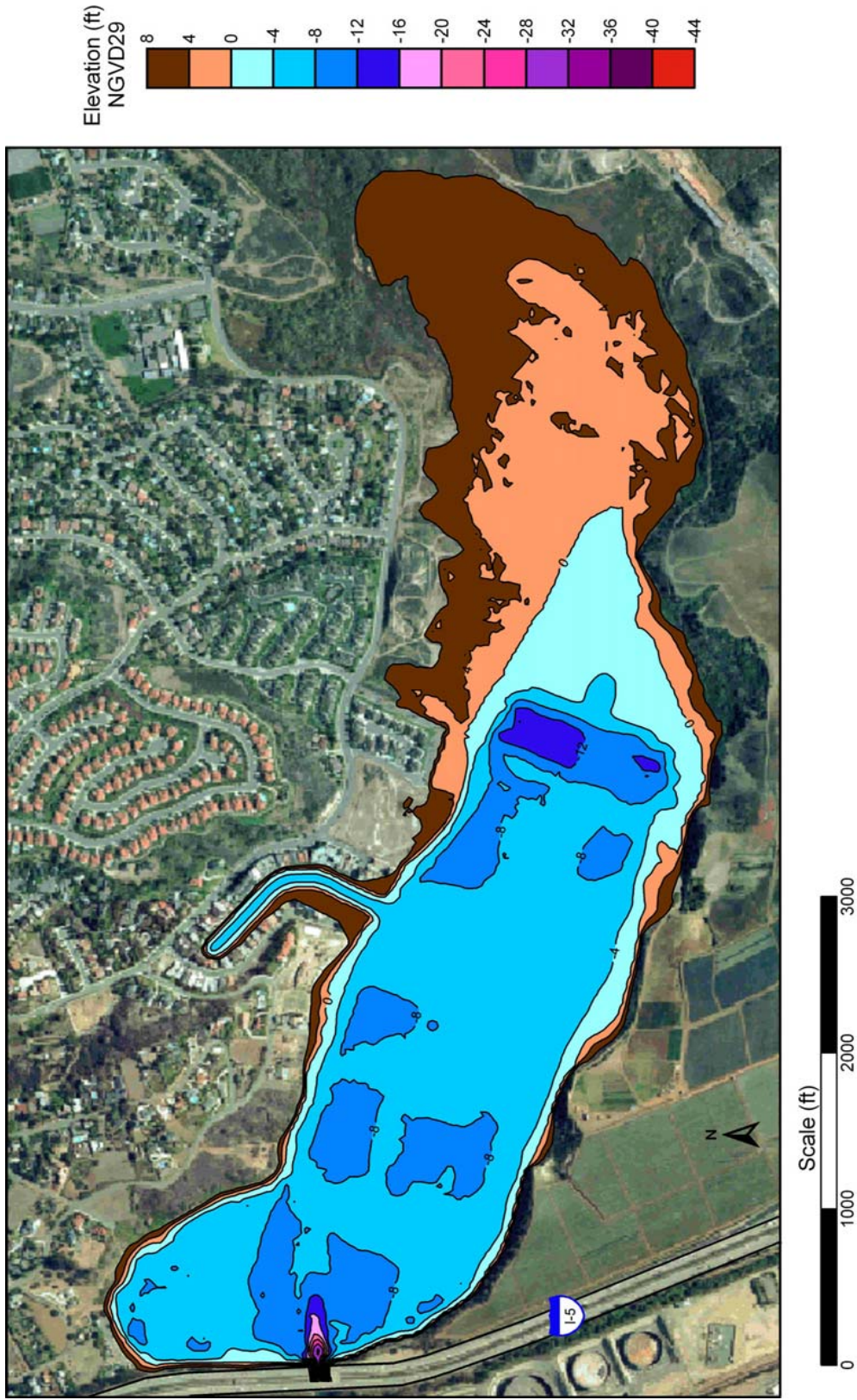


Figure 2-4. Bathymetry map of Inner Basin.

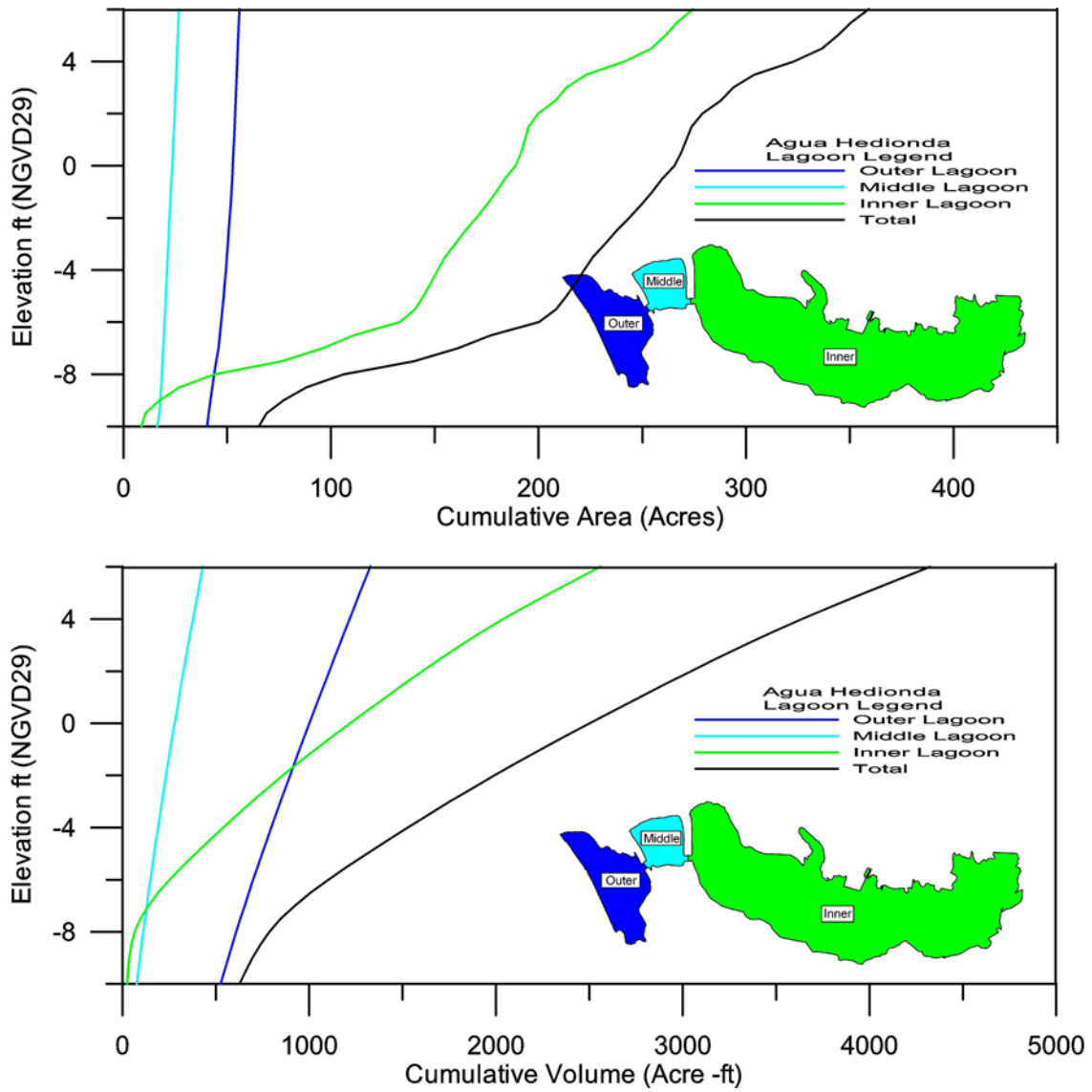


Figure 2-5. Agua Hedionda Lagoon surface area (top) and water volume (bottom).

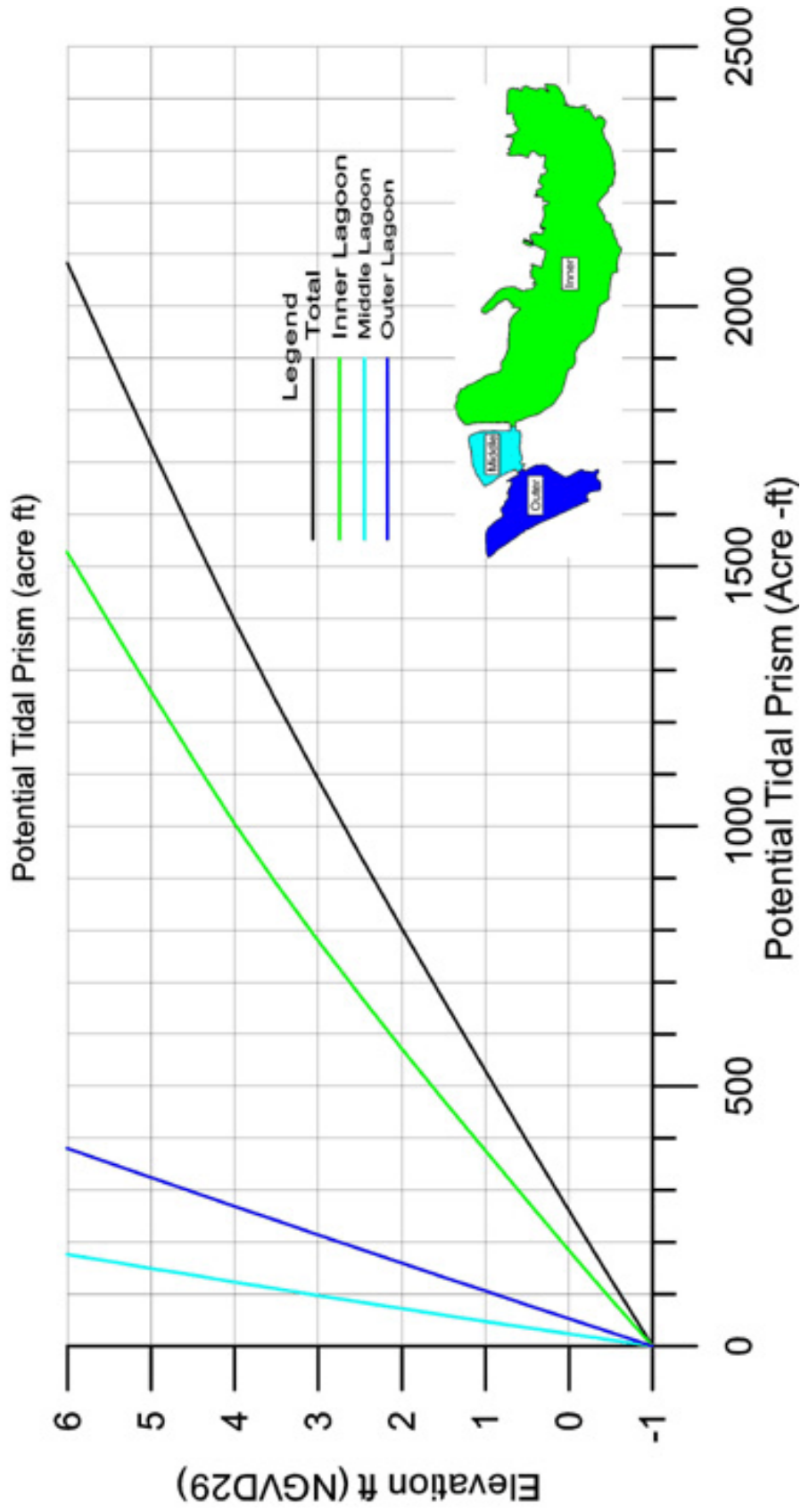


Figure 2-6. Potential tidal prism for the Outer, Middle, and Inner Basins and for the lagoon (total).

2.1 OCEAN TIDES

Ocean tides force water fluctuations in the lagoon. The tide is the change of ocean water level caused by the astronomical forces of the moon and sun. Tides are predictable and can be decomposed into a set of constituent frequencies near one and two cycles per day, each having a given amplitude and phase at any location. Longer period fluctuations in amplitude occur at two cycles per month and two cycles per year, every 4.4 and 18.6 years.

On the San Diego coast, the tide is mixed and has nearly equal semi-daily and daily components (Zetler and Flick, 1985). The highest monthly tides in the winter and summer are higher than the highest monthly tides in the spring and fall as a result of lunar and solar declination effects. Also, the extreme monthly higher-high tide in the winter tends to occur in the morning.

The tidal fluctuations are superimposed at sea level. Seasonal sea level in the San Diego area tends to be highest in the fall and lowest in the spring, with differences of about 0.5 ft. Local warming or cooling resulting from offshore shifts in water masses can alter the average sea level by several tenths of a foot over periods lasting several months (e.g., El Niño years) (Reid and Mantyla, 1976).

Tidal elevations are usually referenced to Mean Lower Low Water (MLLW), which is defined as the average elevation of the lowest water level readings of each day over a specified 19-year interval. In the study area, the maximum tidal range is about 9 ft (7.2 ft above MLLW to 1.8 ft below MLLW). Tidal elevations can be converted to other vertical datum using the appropriate conversion values. Table 2-1 gives some of these datum with respect to MLLW and NGVD.

2.2 POWER PLANT INTAKE FLOW RATES

Figure 2-7 shows the hourly flow rates of the power plant intake between 1 June 2005 and 7 July 2005. Plant diversion of lagoon waters reduces the outflow water from the lagoon to the ocean. Actual plant inflow rates during high-use periods are typically 635 to 670 million gallon per day (mgd). This is about 26 to 28 million gallons per hour.

Table 2-1. Tidal levels with respect to MLLW and NGVD (1960-1978).

Parameters	Mean Lower Low Water (MLLW) ft	National Geodetic Vertical Datum (NGVD) ft
Mean Higher High Water (MHHW)	5.37	2.81
Mean High Water (MHW)	4.62	2.06
Mean Sea Level (MSL)	2.75	0.19
NGVD	2.56	0
Mean Lower Low Water (MLLW)	0	2.56

Agua Hedionda Lagoon

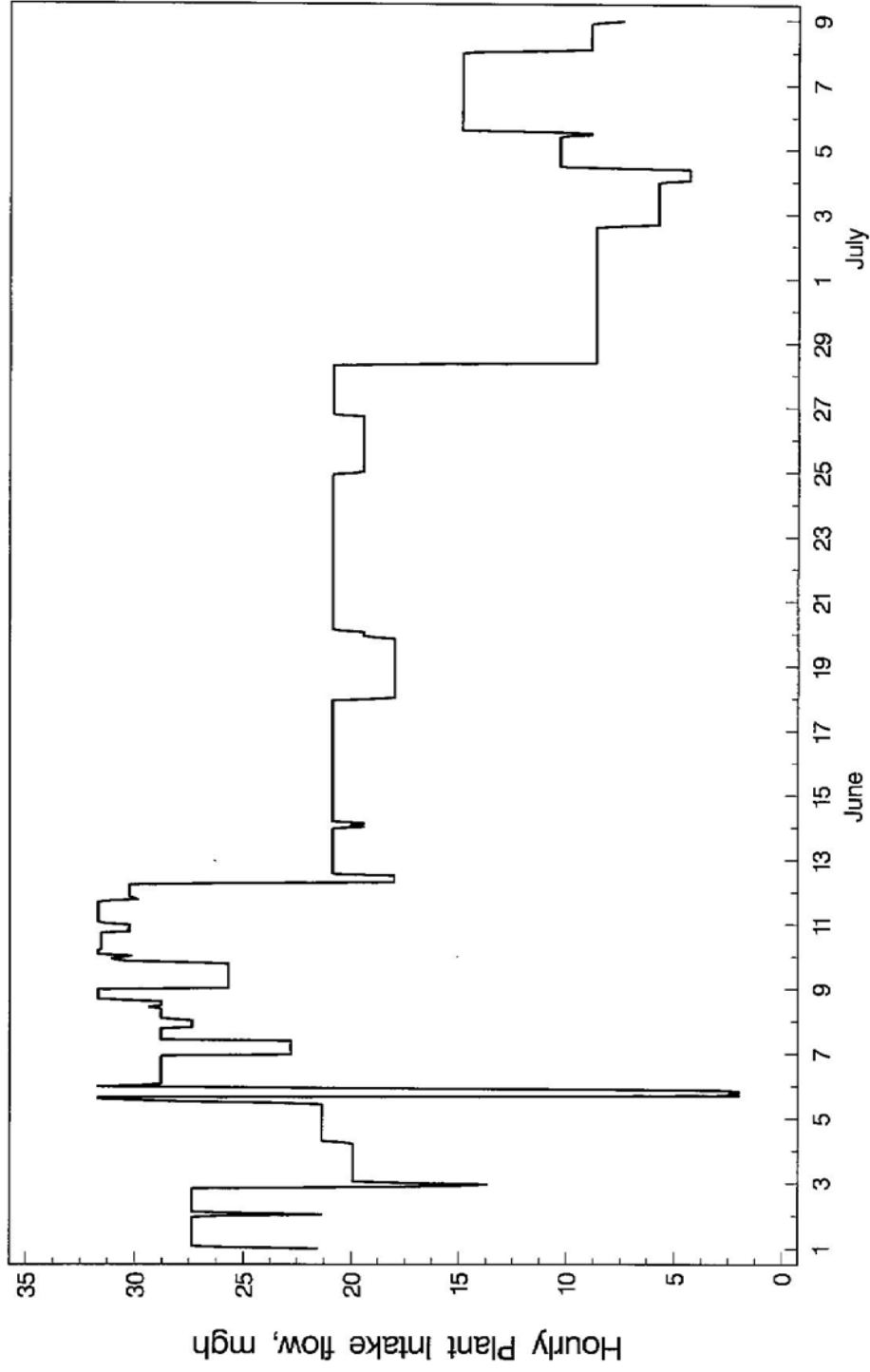


Figure 2-7. Hourly Encina Power Station intake flow.

3.0 WATER LEVEL, VELOCITY, SALINITY, AND TEMPERATURE MEASUREMENTS

3.1 WATER LEVEL

Water level measurements were acquired at four locations throughout the study area (Stations S0, S2A, S2B, and S3) for a period of approximately one month from 1 June 2005 to 7 July 2005. Measurements were taken using self-contained pressure sensors recording water surface elevations at five-minute intervals. Complete results for all locations are shown in Appendix A.

Station S0 is located at the inlet to the Outer Basin; station S2A is located in the northern portion of the Inner Basin; station S2B is located at the inlet to the Inner Basin; and station S3 is located in the southeastern portion of the Inner Basin. The station locations are shown in Figure 3-1, and the benchmarks are shown in Figure 3-2.

Three benchmarks were used during this study to calibrate the pressure data (from the sensors) into water elevations. The process required installing manual tide staffs and taking manual water level elevations for a few hours.

Figures 3-3 through 3-5 show water levels at the four stations during neap, spring, and mean tides, respectively. The measurements presented show that there are only small variations between water level elevations at the four stations during neap tide. There was a time lag between water level at the inlet and water level at the Inner Basin (< 1 hour). During neap tide, water elevation at the entrance to the Outer Basin and water elevation at the interior of the Inner Basin fill to approximately equivalent levels. During spring and mean tides, there is a short time lag and a variation in water elevation (~ 0.25 ft) between the inlet to the lagoon (Station S0) and the interior stations (Figures 3-4 and 3-5).

3.2 WATER VELOCITY

Water velocities were measured at Station S0 during neap, spring, and mean tides (Figures 3-6 through 3-8). Water velocities were high during spring tide (approximately + 4.5 ft to -3.5 ft). The highest water velocity measurements at Station S0 were +5 ft/sec and -3 ft/sec (during spring tide). See Appendix B for further data and figures.

Tidal prism was computed (Figure 3-9) from data collected in the basins during the approximate one-month study period between 1 June and 6 July 2005. During this time period, the cumulative tidal prism for the lagoon ranged from 175 acre-ft to 2075 acre-ft. Water in the Middle and Outer Basins had fewer fluctuations and a much smaller tidal prism (about 50 to 300 acre-ft) than water in the large Inner Basin. The Inner Basin contains the majority of the water in the lagoon (see Appendix C).

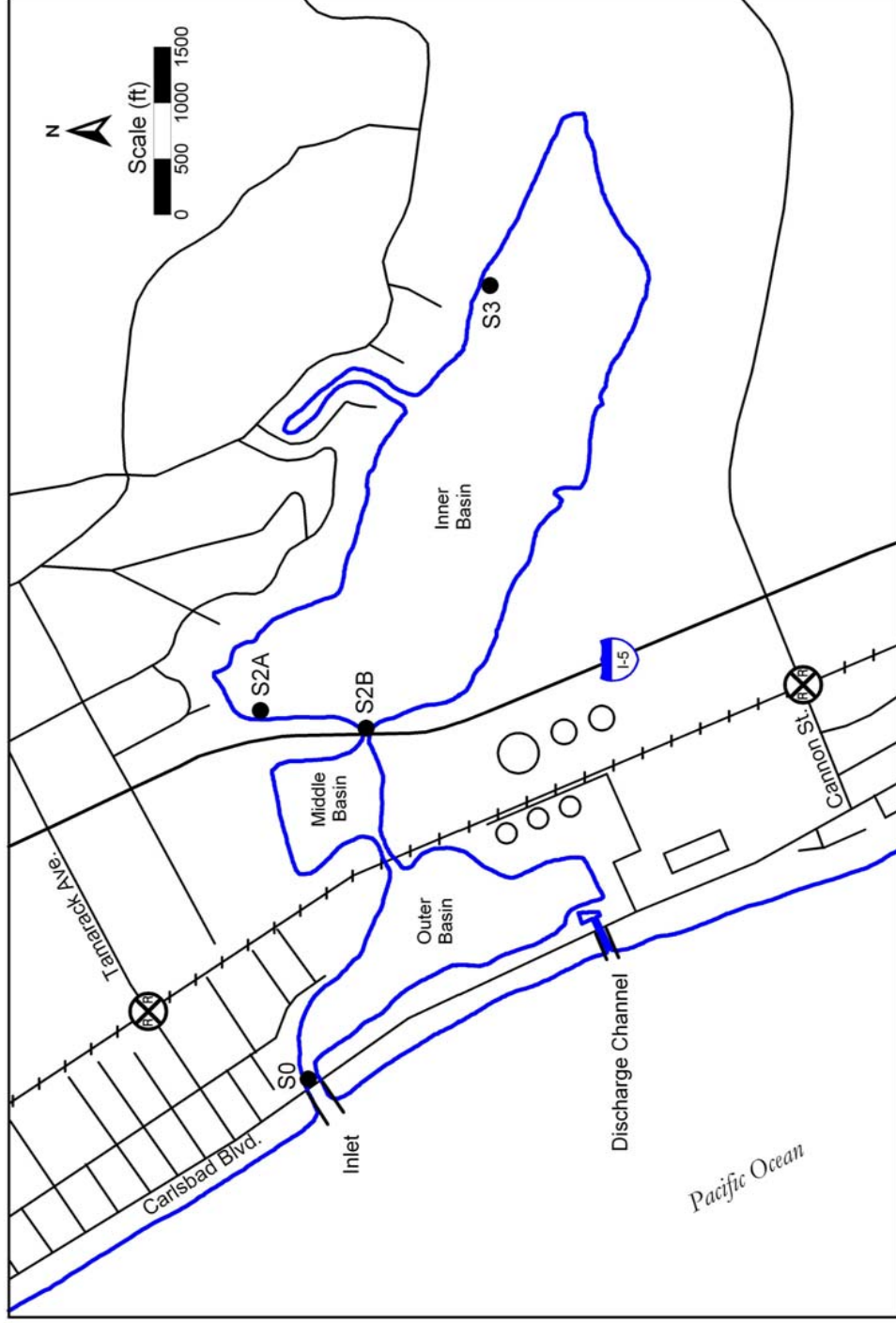


Figure 3-1. Measurement locations for Stations S0 (water level, water velocity, temperature, salinity), S2A (water level), S2B (water level, water velocity, temperature, salinity), and S3 (water level).



Figure 3-2. Locations of benchmarks used in this study.

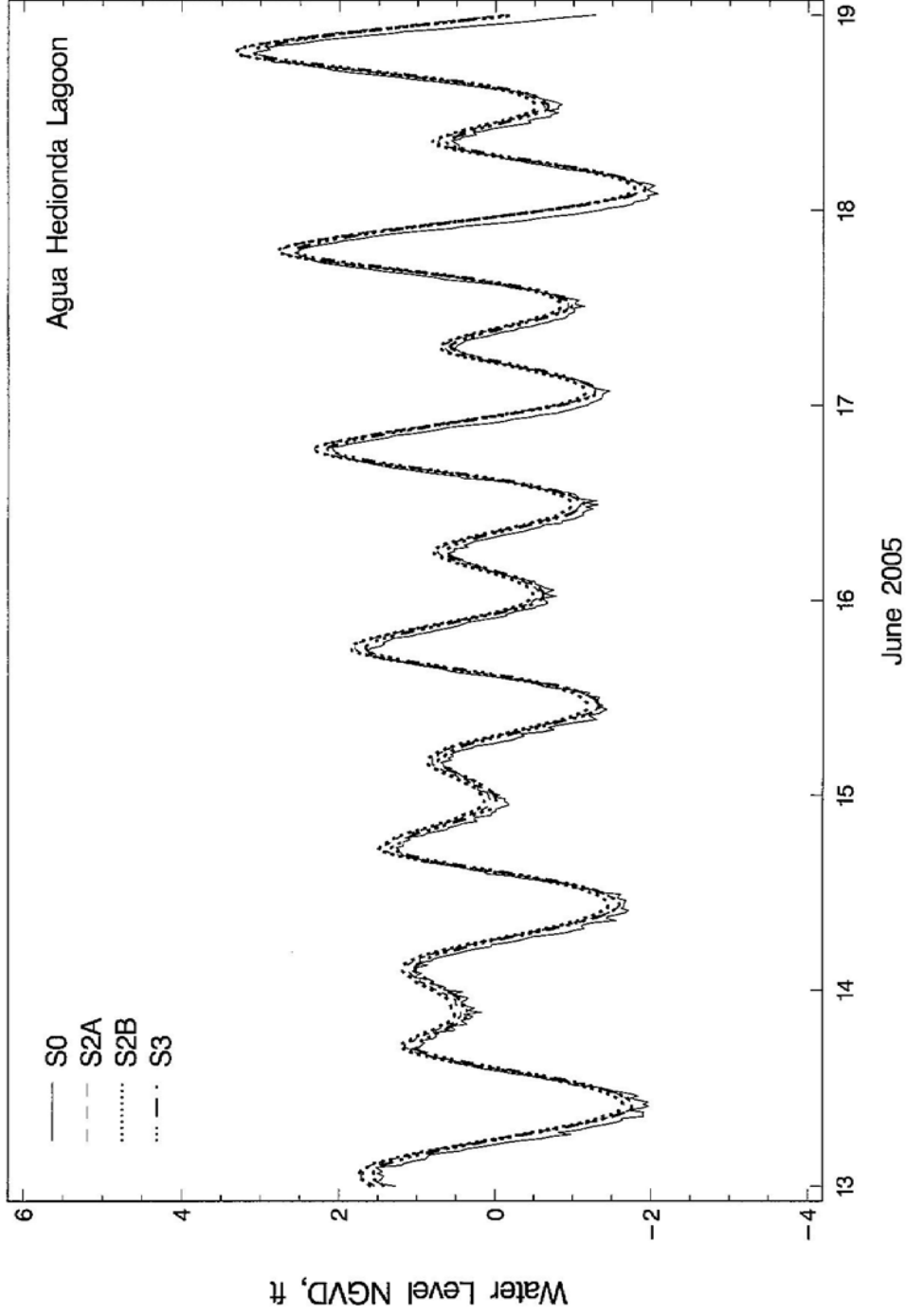


Figure 3-3. Comparison of water level at Stations S0, S2A, S2B, and S3 during neap tide.

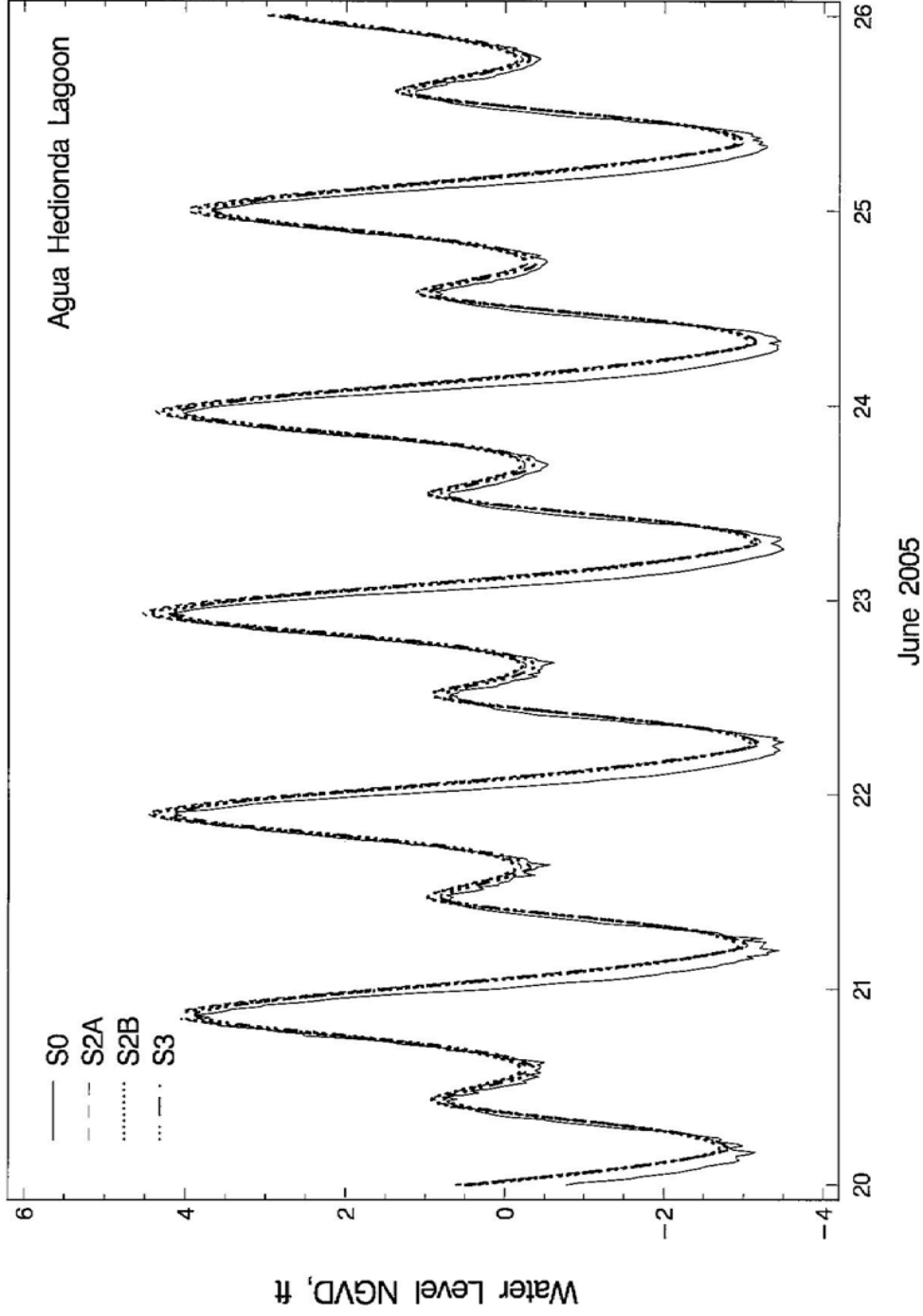


Figure 3-4. Comparison of water level at Stations S0, S2A, S2B, and S3 during spring tide.

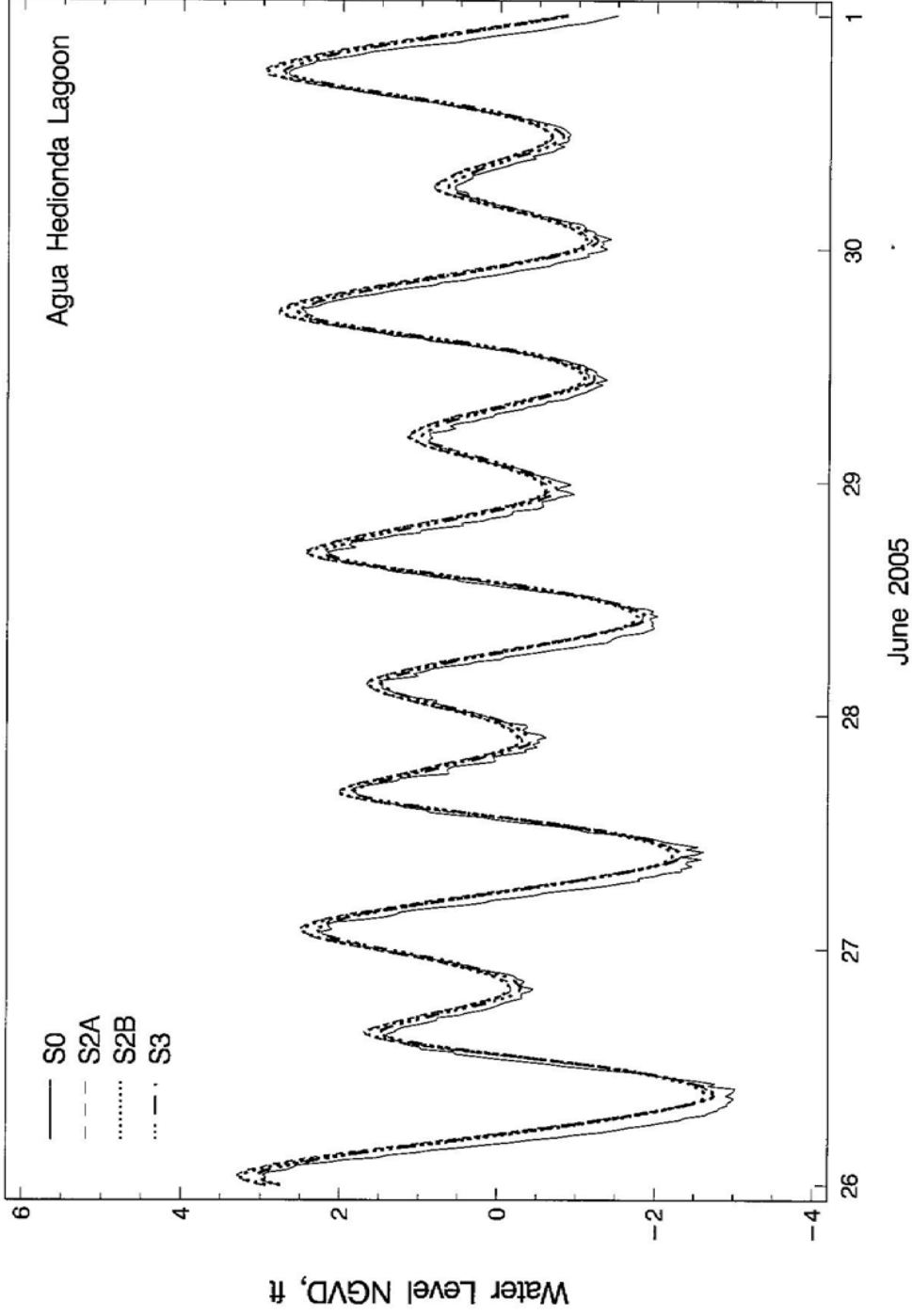


Figure 3-5. Comparison of water level at Stations S0, S2A, S2B, and S3 during mean tide.

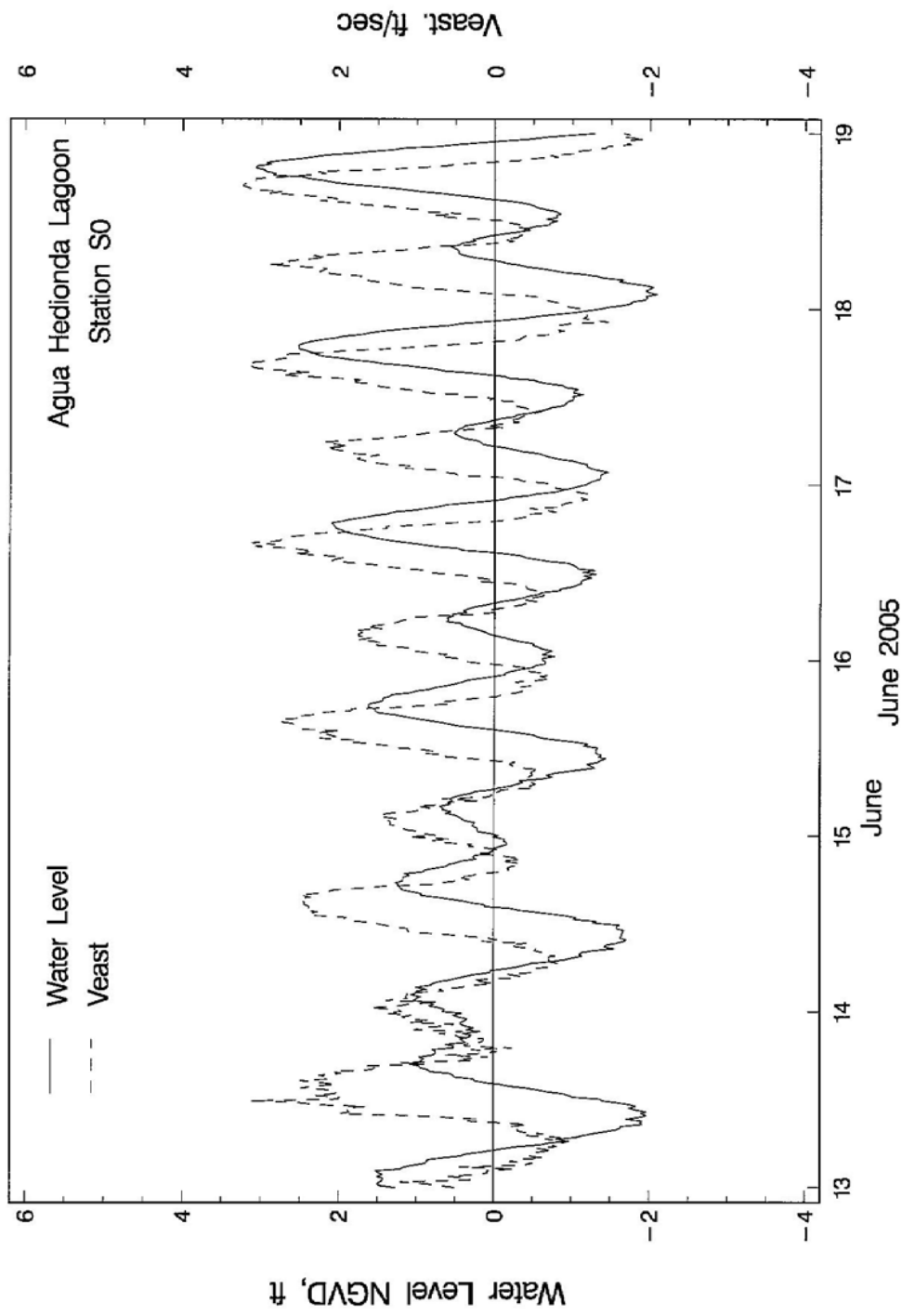


Figure 3-6. Water level and velocity measurements during neap tide.

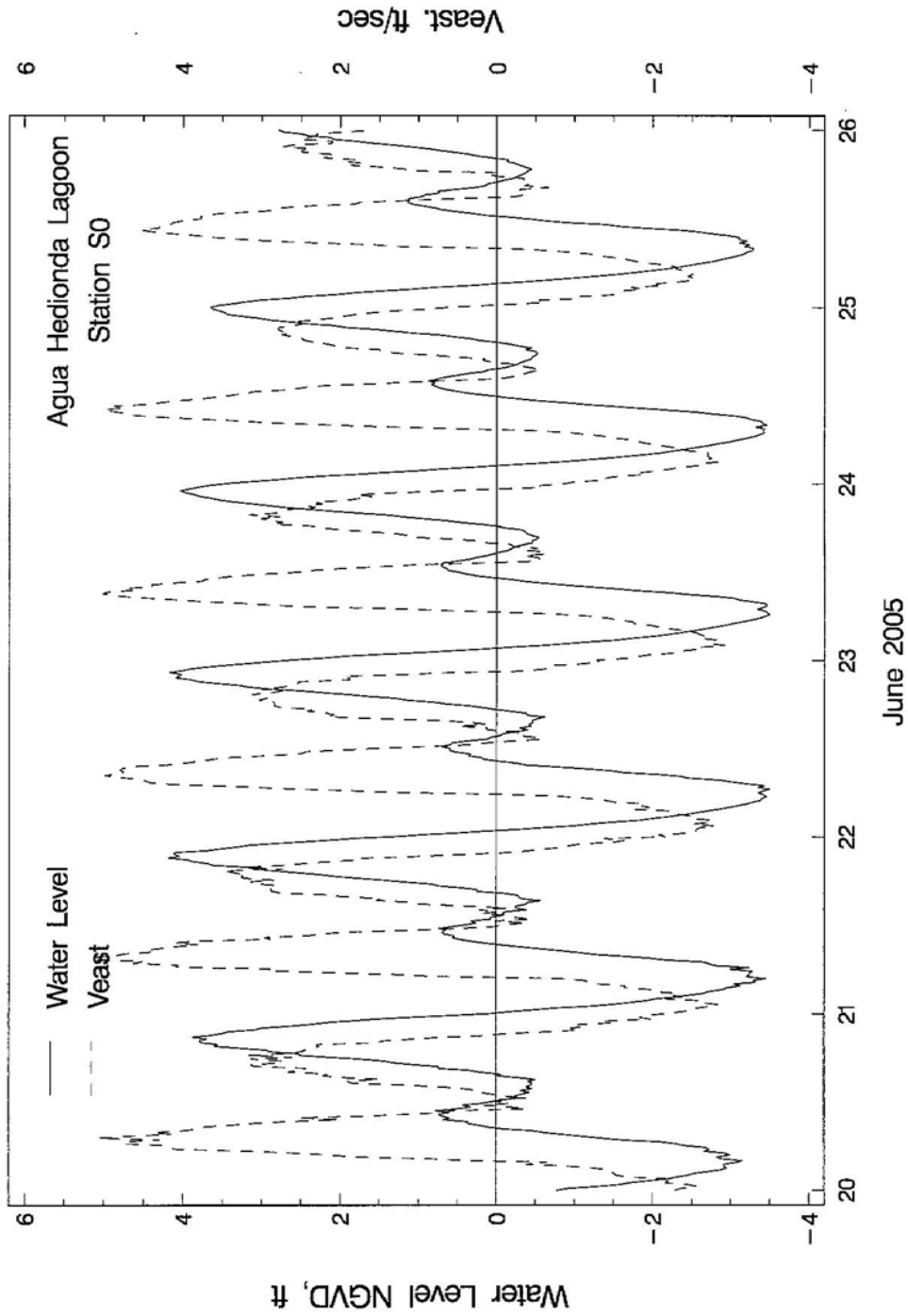


Figure 3-7. Water level and velocity measurements during spring tide.

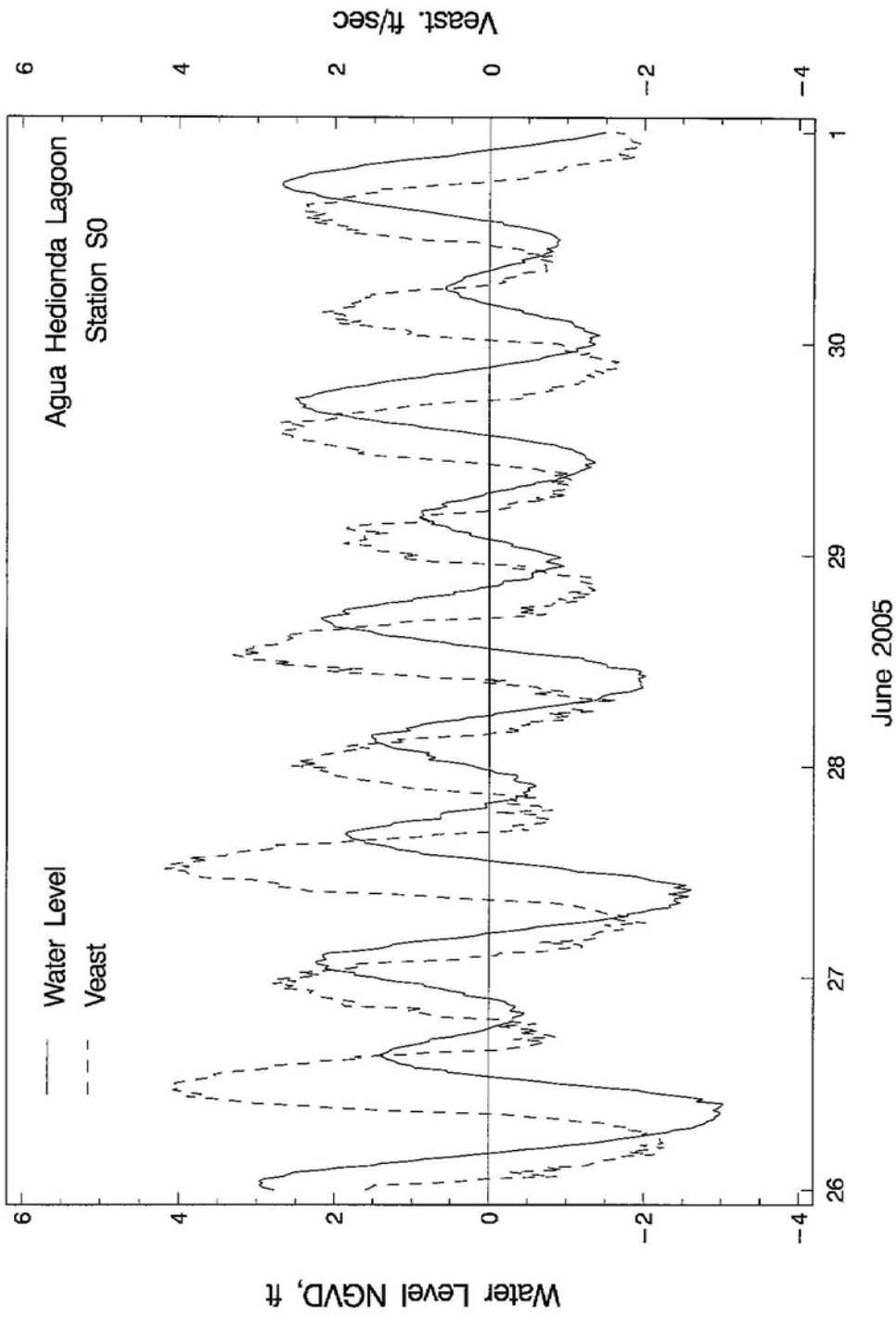


Figure 3-8. Water level and velocity measurements during mean tide.

Agua Hedionda Lagoon

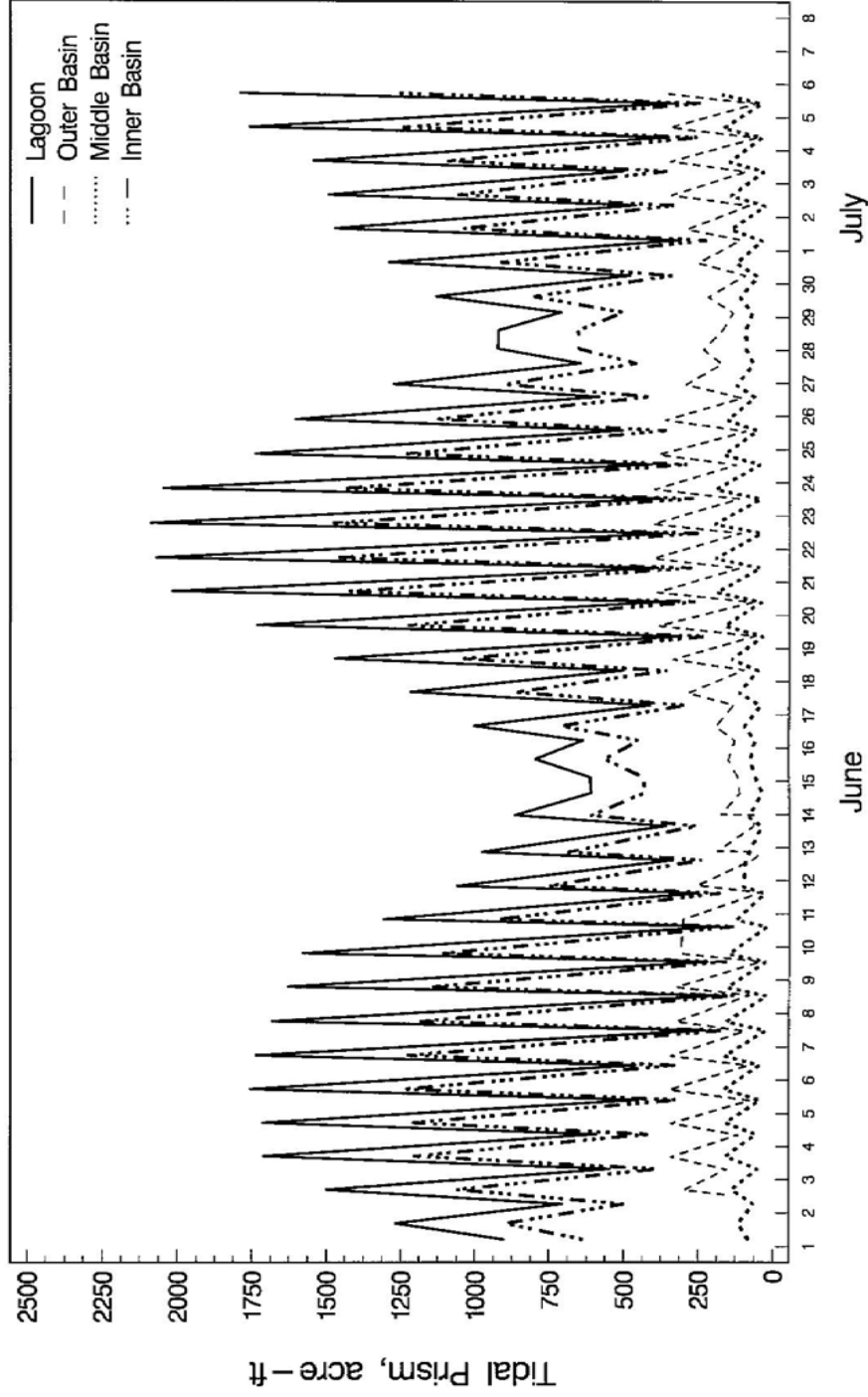


Figure 3-9. Tidal prism of the lagoon between June 1, 2005 and July 6, 2005.

3.3 SALINITY AND TEMPERATURE

Conductivity and temperature measurements were taken at Station S2B over a one-month period in order to compute water salinity. Salinity fluctuated between about 31.5 and 34 PSU (see Appendix D).

Temperature data were collected over a one-month period at Stations S0 and S2B. During the first two weeks of June, the temperature was about 20 to 22° C, while during late June to early July, the temperature decreased and fluctuated significantly, ranging between 14 and 20° C (see Appendix D).

4.0 RESIDENCE TIME OF WATER IN THE LAGOON

The term “old water” is defined here as water that remains in the lagoon system after the water outflow during ebb tide. It is water that has not yet been flushed out of the lagoon. As new water comes into the lagoon during flood tides, the “old water” becomes more diluted with each tidal cycle until all of it is eventually replaced by new water.

A computer program has been written to compute the percentage of remaining old water in the lagoon from the time immediately after the tidal cycle until the time when the remaining old water in the lagoon is less than 2%. The procedure is as follows.

If Q_{\min} is the volume of water in the lagoon after the ebb tide, then Q_{\min} will be diluted after the first tidal cycle by

$$D_i = (V_{\max}(i+1) - V_{\min}(i) + I_{p\max}(i+1)) / V_{\max}(i+1) \quad (1)$$

where D = dilution,
 i = the number of the tidal cycle and takes the values 1, 2, 3, ... , n,
 V_{\max} = the volume of water in the lagoon corresponding to the maximum water level,
 V_{\min} = the volume of water in the lagoon corresponding to the minimum water level, and
 $I_{p\max}$ = the volume of water taken from the lagoon by the power plant intake between the minimum and maximum water levels.

A tidal cycle is defined as the tidal period between two successive upcrossings of water level above the mean water elevation of the lagoon. The computed values of D_i (< 1) are multiplied after each tidal cycle, until the value of $D_i < 0.02$.

$$D_n = D_1 \times D_2 \times D_3 \times \dots \times D_n \quad (2)$$

The incoming water to the lagoon during a tidal cycle is calculated from the equation:

$$Q_{\text{in}} = V_{\max} - V_{\min} + I_{p\max} \quad (3)$$

while the outgoing water from the lagoon is given by:

$$Q_{\text{out}} = V_{\max} - V_{\min} - I_{p\min} \quad (4)$$

where $I_{p\min}$ is the volume of water taken from the lagoon by the power plant intake between the maximum and minimum water levels.

In performing the computations for the individual basins, we apportioned the power plant intake flows by the volume of the basins at the minimum water level per tidal cycle. Figures 4-1 and 4-2 present the percentage of “old water” in the lagoon vs. the tidal cycles and daily tidal flushing, respectively. The solid lines show the best-fit curve for the data.

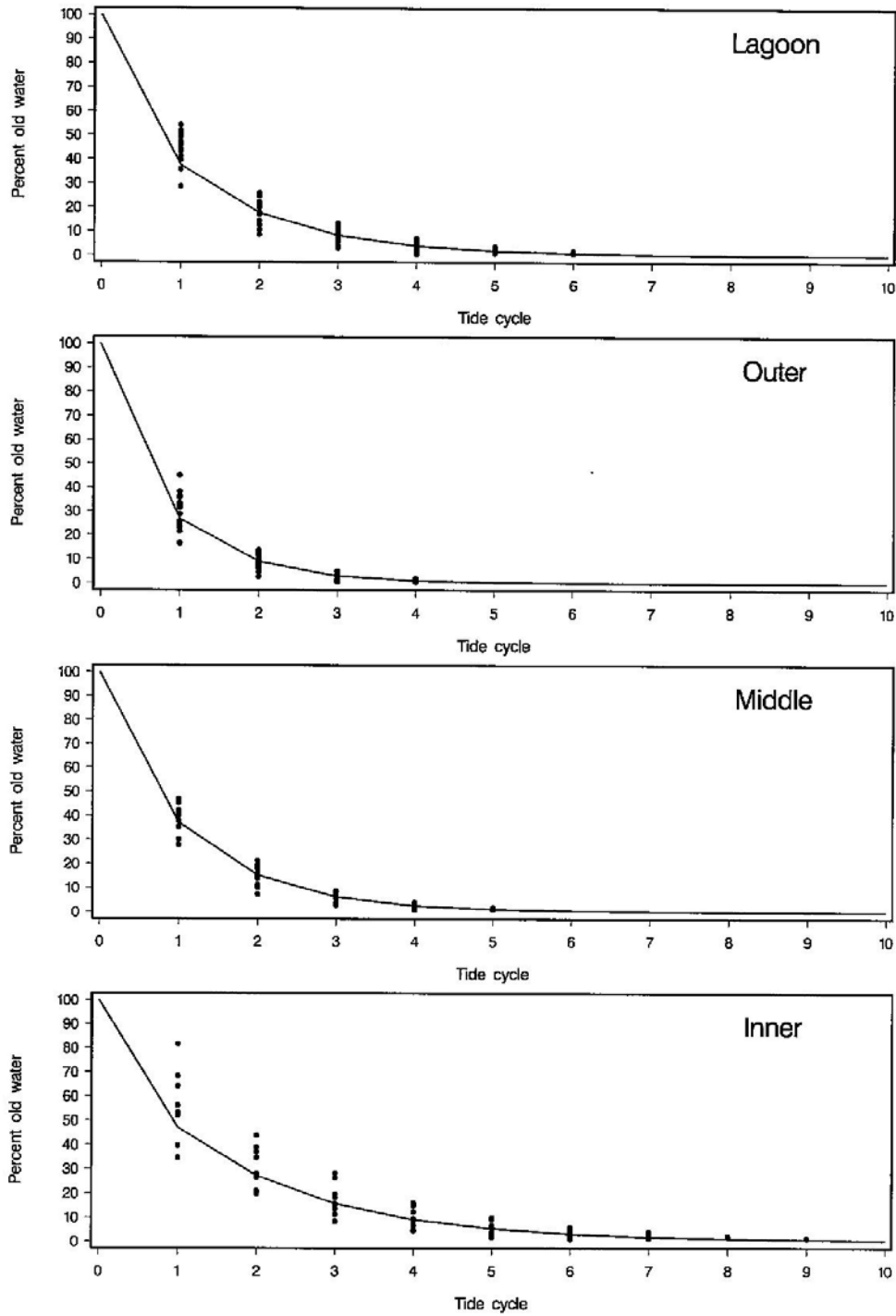


Figure 4-1. Percentage of old water in the lagoon vs. tidal cycles.

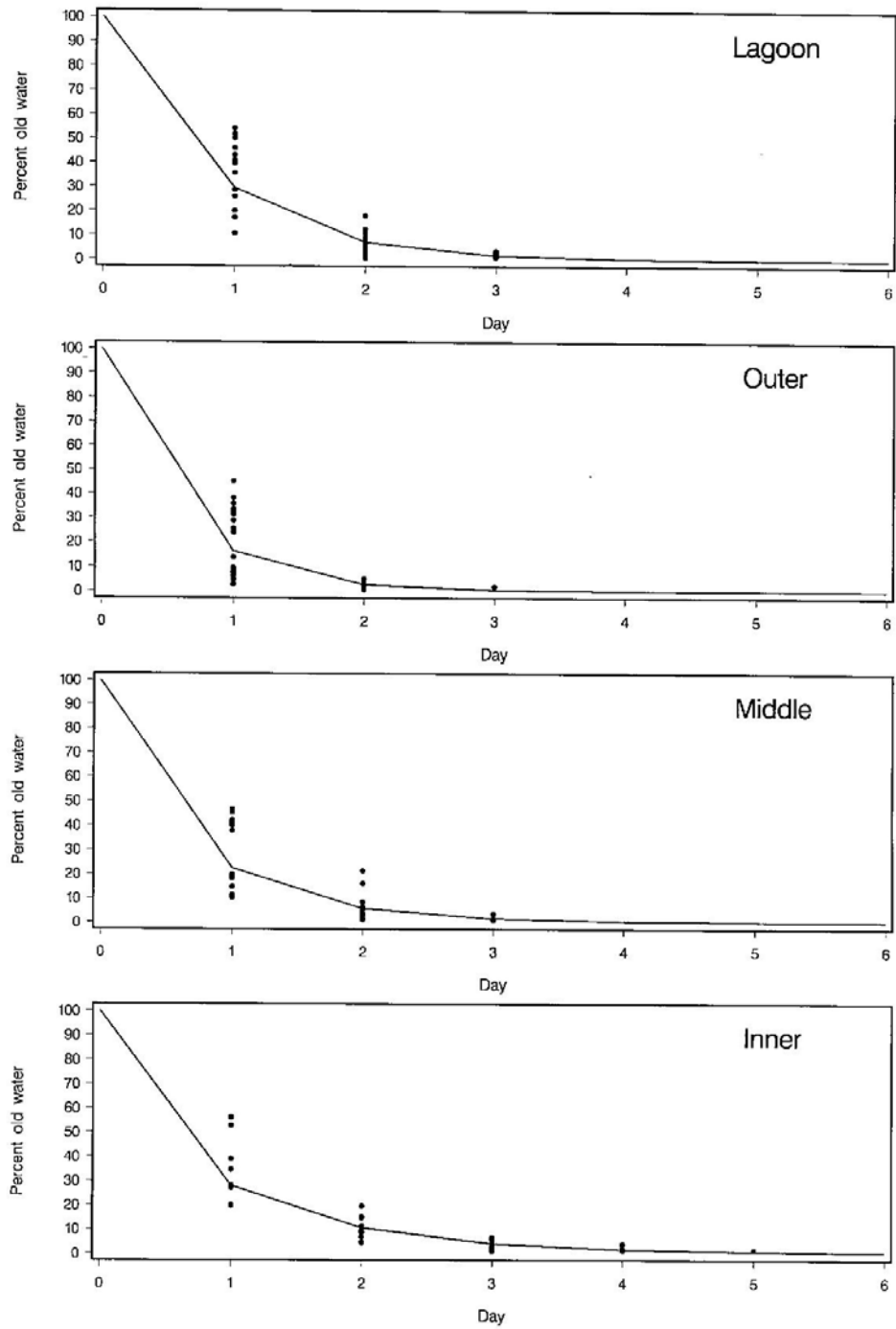


Figure 4-2. Percentage of old water in the lagoon vs. day, with solid line showing best-fit curve.

The best-fit curve is given by the equation:

$$y(x) = A e^{-Bx} \quad (5)$$

where A and B are equation parameters, and x is the number of tidal cycles or days.

Tables 4-1 and 4-2 give the curve-fitting parameters from equation (5), that is A and B , for the percentage of old water in the lagoon and lagoon basins per tidal cycle and per day, respectively.

Table 4-3 gives the residence time of water in Agua Hedionda Lagoon. This table provides the mean, standard deviation, and range for both tidal cycles and days for the lagoon (total) and for the three basins, Outer, Middle, and Inner. Water remains in the lagoon (total) for a mean period of about 5.0 tidal cycles or 2.6 days. In the Inner Basin, water remains for a mean period of 6.27 tidal cycles or 3.2 days.

The lagoon inflow and outflow through the inlet during the period 1 June 05 through 7 July 05 is shown in Figures 4-3 and Figure 4-4 per tidal cycle and day, respectively. These figures are based on the water level and velocity measurements carried out in this study (Chapter 3).

The ratio between the inflowing water and the water taken in by the power plant cooling system is plotted in Figures 4-5 and 4-6 per tidal cycle and day, respectively. The solid lines in these two figures represent the mean ratio over the measurement time period. On average, the power plant cooling system takes in 51% of the inflowing water per tidal cycle and 46% per day.

Table 4-1. Curve-fitting parameters for “old water” percentage per tidal cycle.

Location	A	B
Lagoon	79.6766	-0.75256
Outer Basin	80.2683	-1.09736
Middle Basin	90.1073	-0.88907
Inner Basin	81.4989	-0.55056

Table 4-2. Curve-fitting parameters for “old water” percentage per day.

Location	A	B
Lagoon	122.360	-1.42331
Outer Basin	100.384	-1.82958
Middle Basin	87.945	-1.36858
Inner Basin	73.958	-0.97584

Table 4-3. Residence time of water in Agua Hedionda Lagoon.

Location	Tidal Cycles			Days		
	Mean	Std^a	Range	Mean	Std^a	Range
Lagoon	5.0	1.2	2 - 6	2.6	1.0	1 - 4
Outer Basin	3.6	0.5	2 - 4	1.9	0.5	1 - 3
Middle Basin	4.47	0.8	2 - 5	2.3	0.6	1 - 3
Inner Basin	6.27	1.8	2 - 9	3.2	1.0	1 - 5

^a Std = Standard Deviation

Agua Hedionda Lagoon

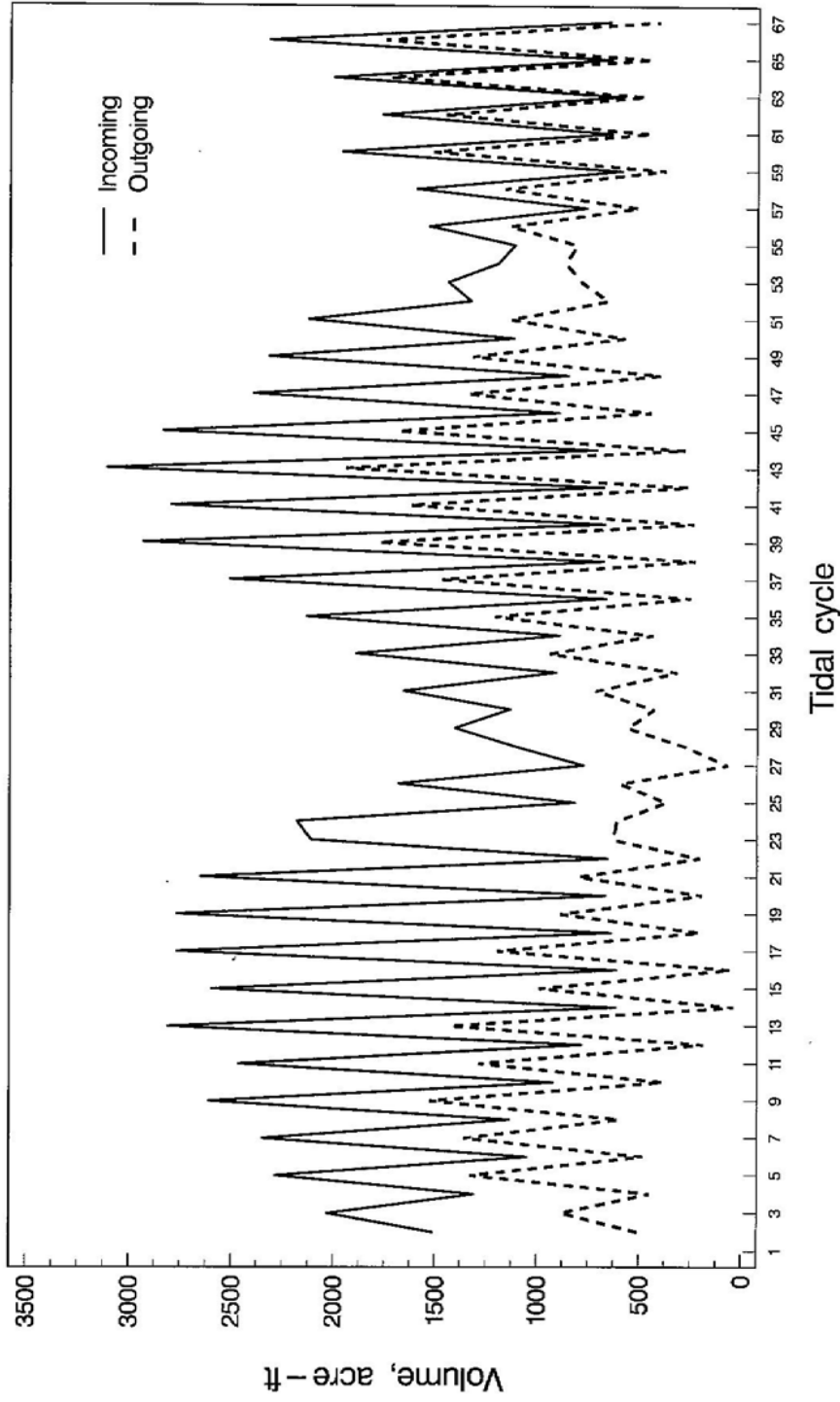


Figure 4-3. Lagoon inflow and outflow through the inlet per tidal cycle during 1 June 05 through 7 July 05.

Agua Hedionda Lagoon

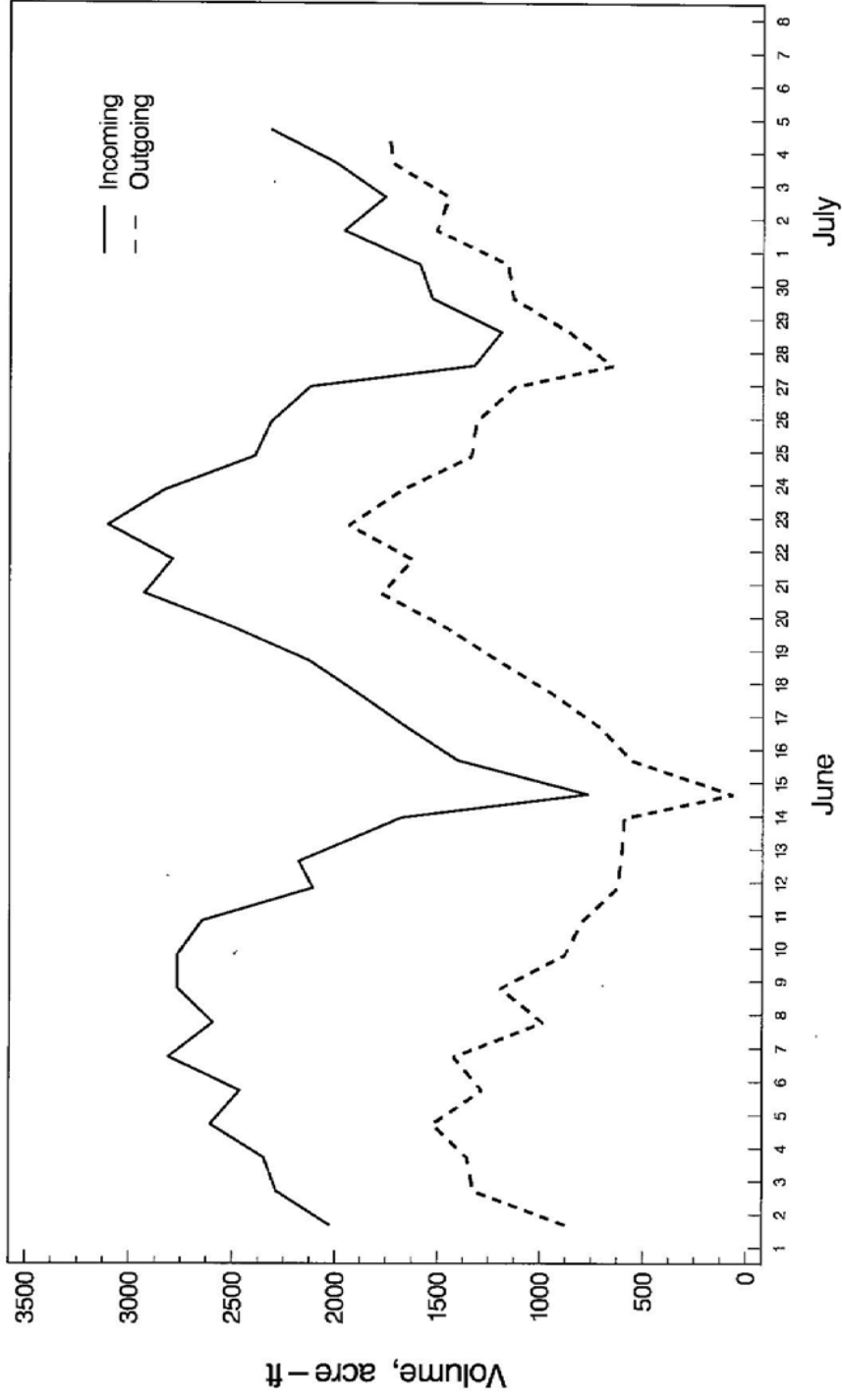


Figure 4-4. Lagoon inflow and outflow through the inlet per day during 1 June 05 through 7 July 05.

Agua Hedionda Lagoon

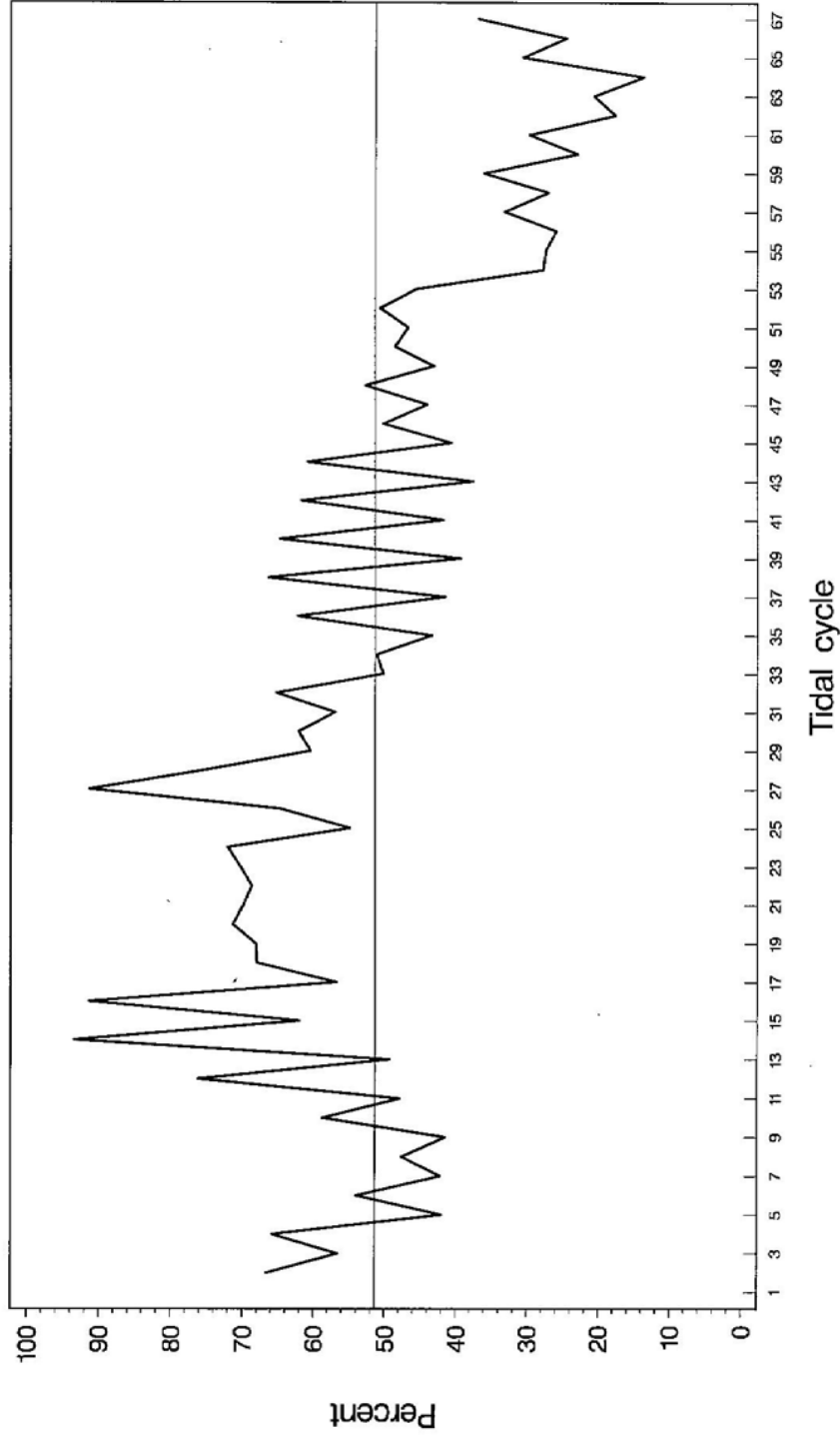


Figure 4-5. Ratio between inflowing water and water taken in by power plant cooling system by tidal cycle. The solid line represents the mean ratio over the measurement time period.

Agua Hedionda Lagoon

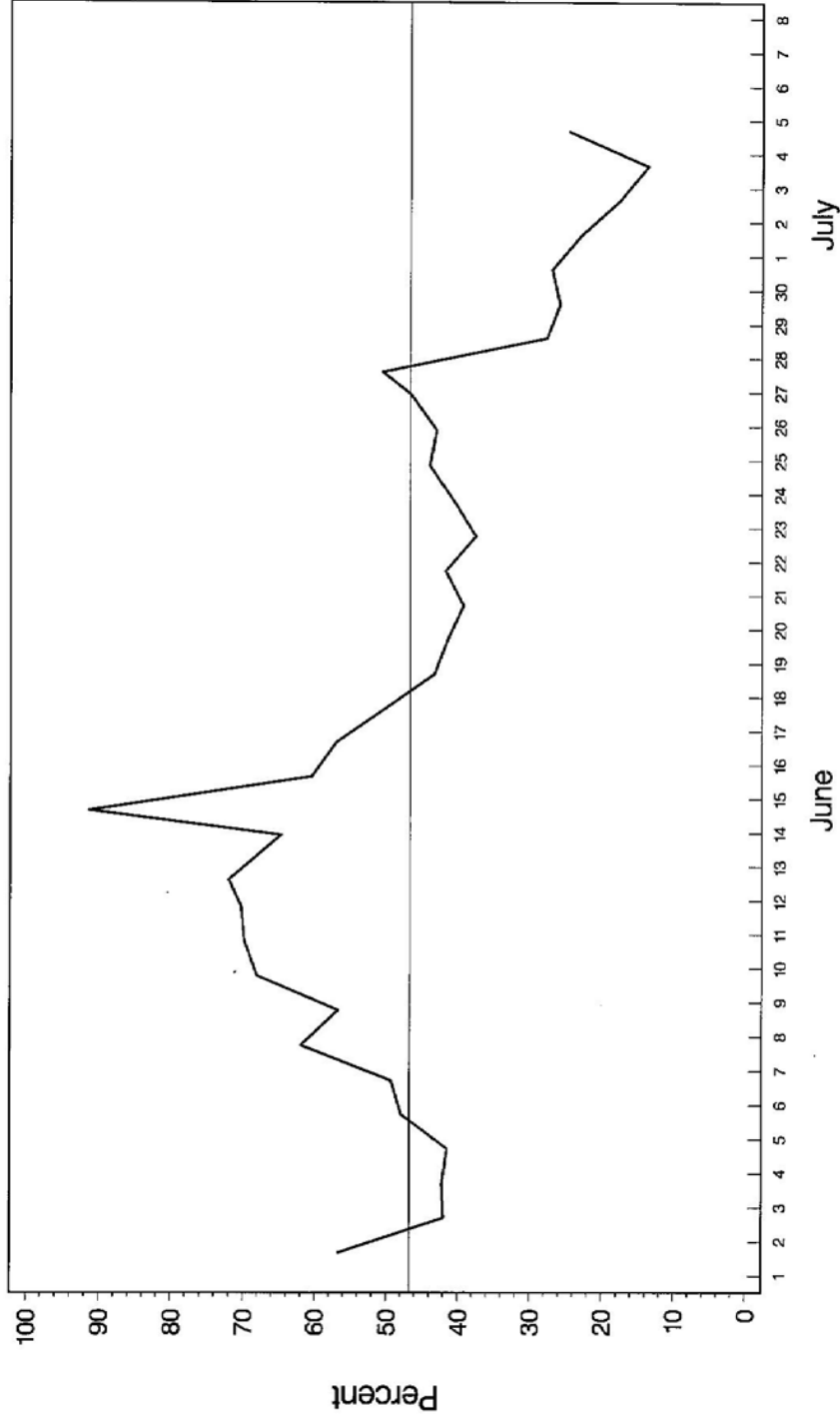


Figure 4-6. Ratio between inflowing water and water taken in by power plant cooling system by day. The solid line represents the mean ratio over the measurement time period.

5.0 SUMMARY AND CONCLUSIONS

In this study, we have provided a description of the Agua Hedionda Lagoon and the general lagoon hydrodynamics. Agua Hedionda Lagoon differs from other southern California lagoons in the respect that the volume of inflowing water is vastly larger than the volume of outflowing water. The operation of the cooling system at the Encina Power Station alters these hydrodynamics. The power generating units take about 625-670 mgd of water from the lagoon to the power plant condenser system for cooling purposes. This process reduces the volume of the outflow water from the lagoon by about 40-50%. The heated water is discharged directly to the ocean through the discharge channel (Figure 1-2).

5.1 LAGOON DESCRIPTION

Data from a bathymetry survey conducted in 2005 were used in this study (Figure 2-1). Surface area and water volume in the lagoon were computed from this survey. The results are shown in Figure 2-5. The surface area of the lagoon was about 360 acres at 6 ft NGVD and 225 acres at MLLW. At MLLW, the volume of the lagoon was about 1750 acre-ft. The majority of the area and water volume come from the large Inner Basin.

5.2 FIELD MEASUREMENTS

Data were collected during a one-month survey at four stations (Figure 3-1) in the lagoon from 1 June 2005 to 7 July 2005. The four stations are S0, S2A, S2B, and S3. Water level measurements were taken at all four stations, and water velocity measurements were taken at two of the stations, S0 and S2B. Water levels generally followed the tides (Figures 3-3 to 3-5). Water velocity was predominately in an east-west direction, with a small component in a north-south direction (Appendix B). Tidal conditions during three time periods were identified for neap, spring and mean tides (Figures 3-3, 3-4, and 3-5). Figures overlaying flow velocity over water level measurements are shown in Figures 3-6, 3-7, and 3-8. Water level and velocity measurements were used to estimate tidal prism, determine the volume of inflow and outflow water, and estimate the residence time of water in the lagoon.

Water elevation, velocity, salinity, and temperature measurements were taken. These data were used to describe lagoon dynamics and compute water exchange between the lagoon and ocean. The tidal prism of the lagoon during the time period of the measurements is shown in Figure 3-9. It varied from approximately 1000 acre-ft during neap tide to 2125 acre-ft during spring tide to 1700 acre-ft during mean tide.

Salinity measurements were made primarily to find out whether there was a difference between the salinity of the water coming into the lagoon and the outgoing water. It was found that the difference was so small that the approach used by Largier (1996) in San Francisco Bay and Jay (2001) at Morro Bay to estimate the residence time of water in the lagoon was not appropriate.

5.3 RESIDENCE TIME

A mathematical model designed to compute the residence time of water in the lagoon and its three basins is described in Chapter 4. Based on this model, we determined the amount of “old water” in the lagoon during a tidal cycle. In the lagoon (total) after 5.0 tidal cycles or 2.6 days, the “old water” is essentially flushed out of the lagoon. In the Inner Basin, 6.27 tidal cycles, or 3.2 days, are required to flush out the “old water.” Due to water intake by the cooling system of the EPS, the outgoing flow through the inlet is less than the incoming flow through the inlet . Figures 4-3 and 4-4 show the lagoon inflow and outflow during the period of 1 June through 7 July 2005, per tidal cycle and per day, respectively. The mean reduction of the outflow water from the lagoon with respect to incoming water was about 51% per tidal cycle and 48% per day during the time period of the measurements.

6.0 REFERENCES

- Bhogal, V., and S. Costa, 1989. Modeling Flood Tidal Deposits in Tidal Inlets. In *Oceans '89: An International Conference Addressing Methods for Understanding the Global Ocean*, Seattle, Washington, September 18-21, 1989, IEEE Publication Number 89CH2780-5, p. 90-95.
- Bradshaw, J., B. Browning, K. Smith, J. Speth, and E. Fullerton, 1976. The Natural Resources of Agua Hedionda Lagoon. Coastal Wetlands Series #16. Prepared for U.S. Fish and Wildlife Service, June 1976. 110 pp. + 9 appendices.
- Coastal Environments, 1998. Bibliography of Pertinent Research on Existing Conditions and Monitoring Studies in the Vicinity of Agua Hedionda Lagoon. Prepared for the California Coastal Commission, City of Carlsbad, and San Diego Gas and Electric Company, 2 January 1988, CE Ref. No. P98-1. 2 pp. + 3 appendices.
- EA Engineering, Science, and Technology, 1997. Final Encina Power Plant Supplemental 316(a) Assessment Report, Volume 2 of 2, Appendices. Prepared for San Diego Gas & Electric Co., July 1997. 2 appendices.
- Ellis, J., 1954. Dredging Final Report, October 29, 1954, Agua Hedionda Slough Encina Generating Station. San Diego Gas & Electric Co., Carlsbad, CA, 43 pp.
- Elwany, M. H. S., A-L. Lindquist, R. Flick, W. O'Reilly, J. Reitzel, and W. Boyd, 1999. Study of Sediment Transport Conditions in the Vicinity of Agua Hedionda Lagoon, Volume 1: Technical Report. SIO Reference No. 00-07, Scripps Institution of Oceanography, Center for Coastal Studies, La Jolla, CA, 8 January 1999. 10 chapters + 3 appendices.
- Jay, D., 2001. The Morro Bay Power Plant and Circulation Processes in Morro Bay. Prepared for Duke Energy North American, Oakland, CA, 15 March 2001. 106 pp.
- Jenkins, S., and D. Skelly, 1988. An Evaluation of the Coastal Database Pertaining to Seawater Diversion at Encina Power Plant, Carlsbad, CA. Prepared for San Diego Gas & Electric Co., July 1988. 56 pp.
- Jenkins, S., D. Skelly, and J. Wasyl, 1989. Dispersion and Momentum Flux Study of the Cooling Water Outfall at Agua Hedionda. Scripps Institution of Oceanography, Center for Coastal Studies, La Jolla, CA. Prepared for San Diego Gas & Electric Co., September 1989. 36 pp. + 3 appendices.
- Jenkins, S., and J. Wasyl, 2001. Agua Hedionda Lagoon North Jetty Restoration Project: Sand Influx Study. Submitted to Cabrillo Power LLC, Carlsbad, CA on 14 September 2001. 178 pp. + 8 appendices.

- Largier, J. L., 1996. Hydrodynamic Exchange Between San Francisco Bay and the Ocean: The Role of Ocean Circulation and Stratification. In *San Francisco Bay, The Ecosystem: Further Investigations*. Proceedings of the 75th Annual Meeting, Pacific Division, American Association for the Advancement of Science, held in San Francisco, CA, June 19-24, 1994, pp. 69-104.
- Reid, J., and A. Mantyla, 1976a. The Effect of the Geostrophic Flow Upon Coastal Sea Elevations in the Northern North Pacific Ocean. *Jour. Geophysical Research*, v.81, n.18, 3100-3110.
- Zetler, B., and R. Flick, 1985. Predicted Extreme High Tides for California, 1983–2000. *Jour. Waterway, Port, Coastal, and Ocean Engineering*, ASCE, v. 111 (4), 758–765.

APPENDIX A

WATER LEVEL MEASUREMENTS AT OUTER, MIDDLE, AND INNER BASINS

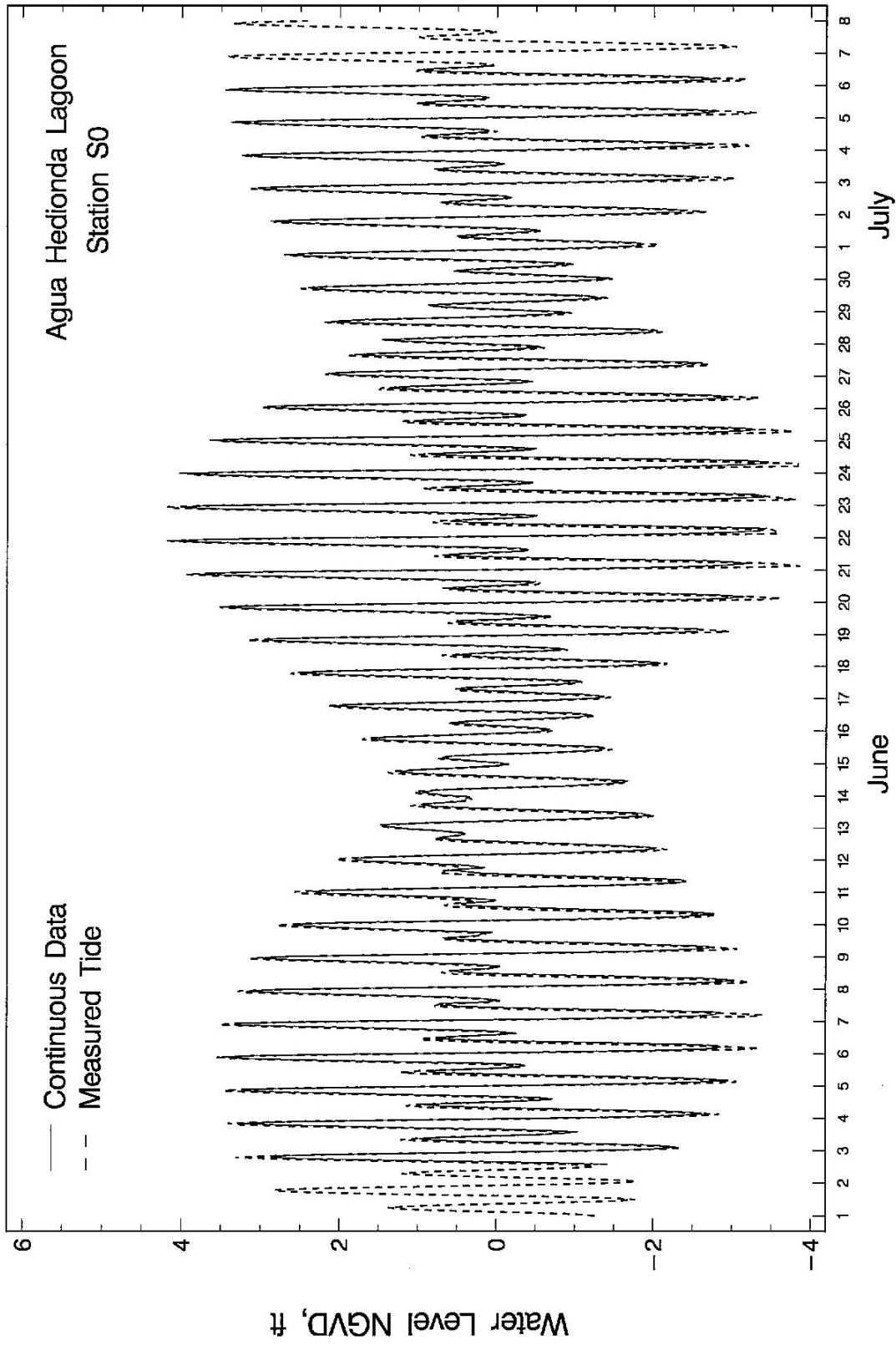


Figure A-1. Comparison between water level measurements at Station S0 and ocean tide.

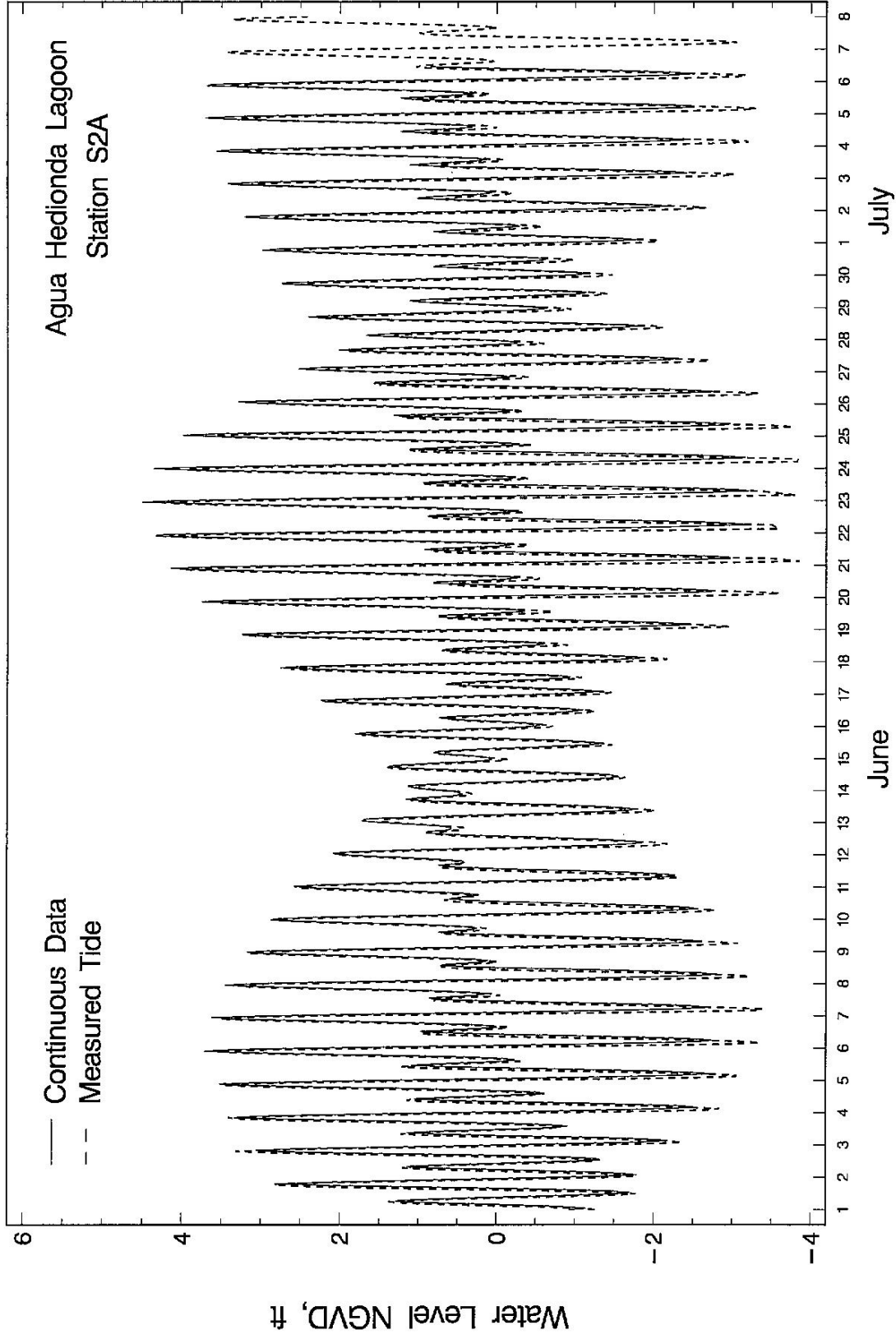


Figure A-2. Comparison between water level measurements at Station S2A and ocean tide.

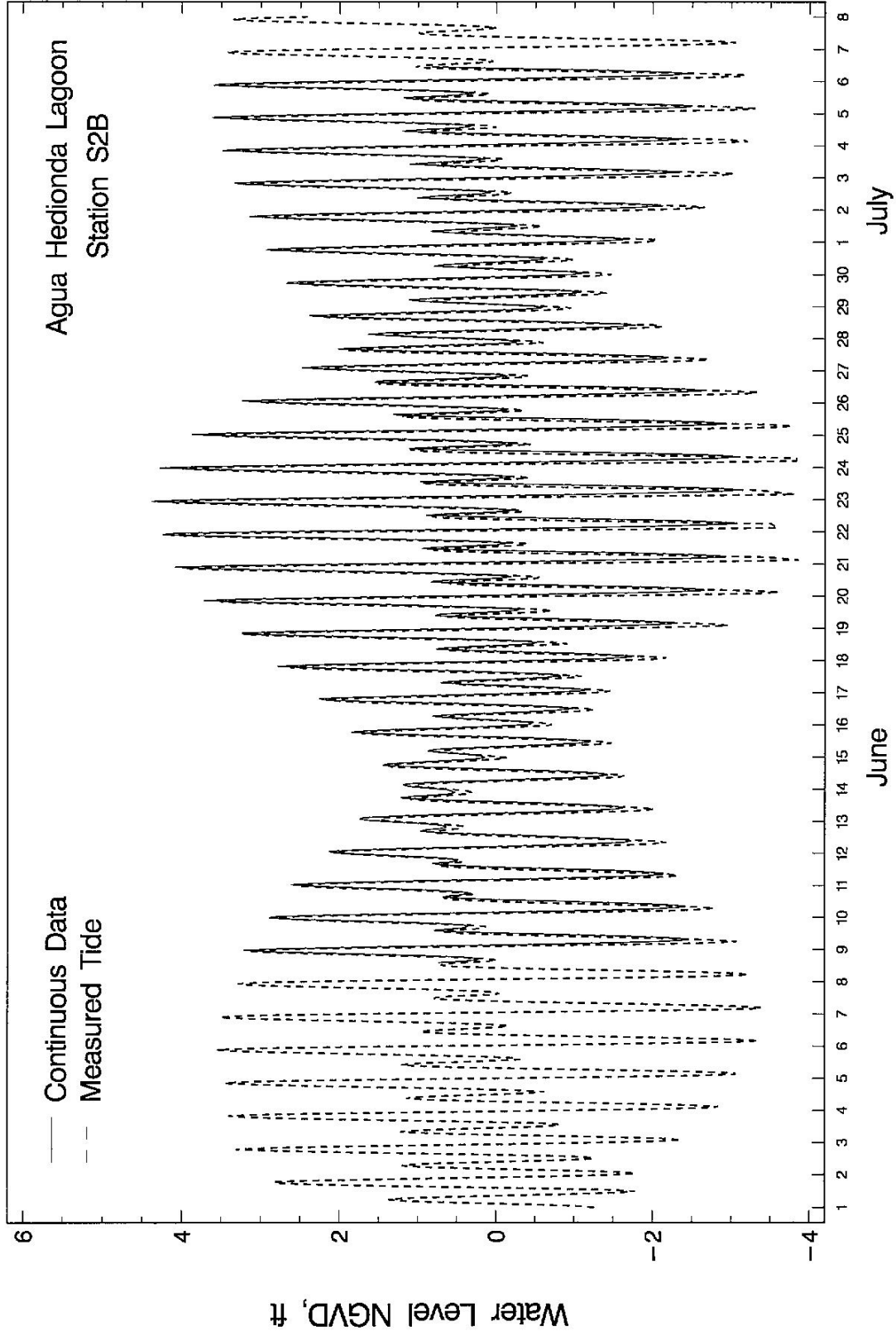


Figure A-3. Comparison between water level measurements at Station S2B and ocean tide.

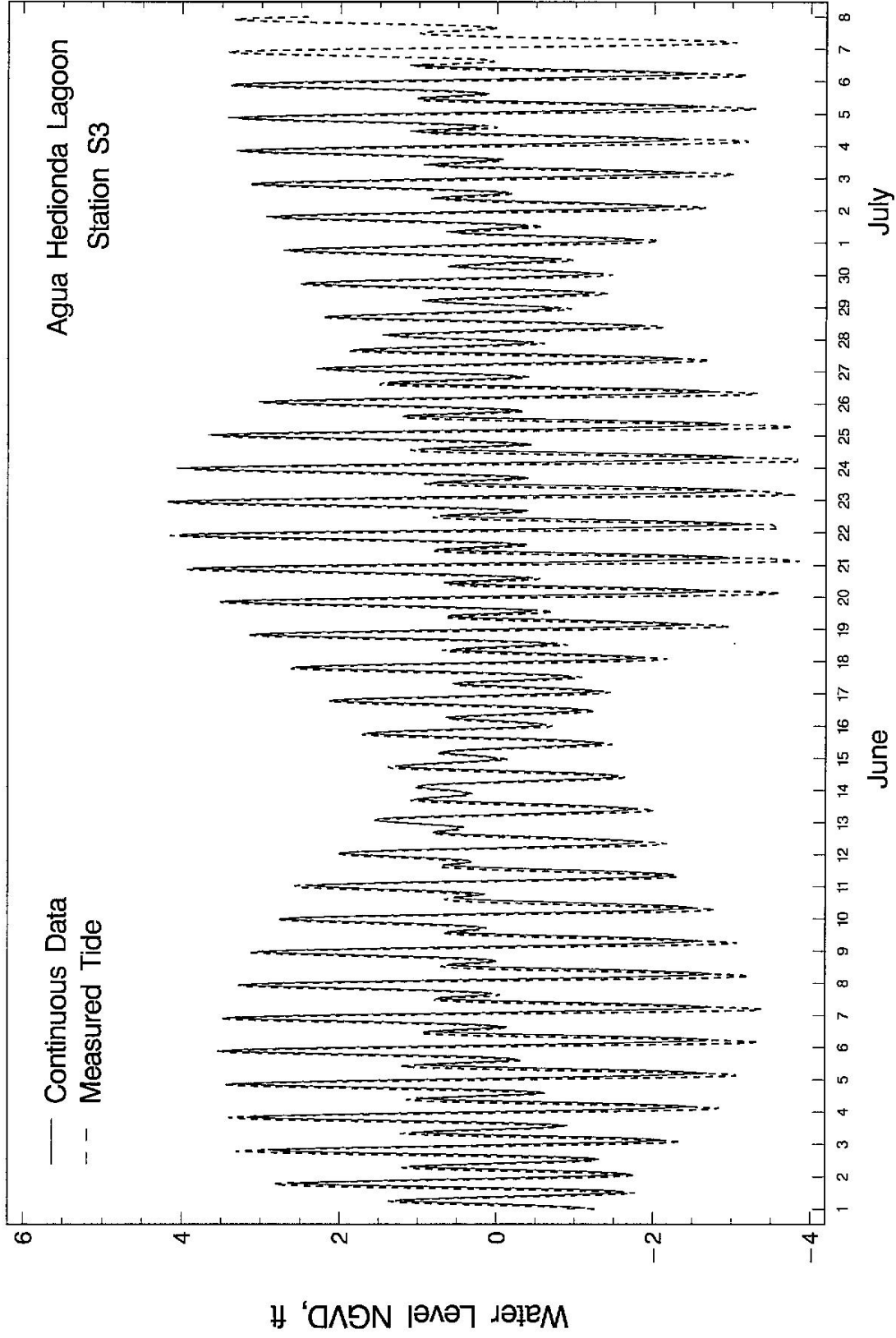


Figure A-4. Comparison between water level measurements at Station S3 and ocean tide.

APPENDIX B

WATER VELOCITY MEASUREMENTS AT OUTER AND INNER BASINS

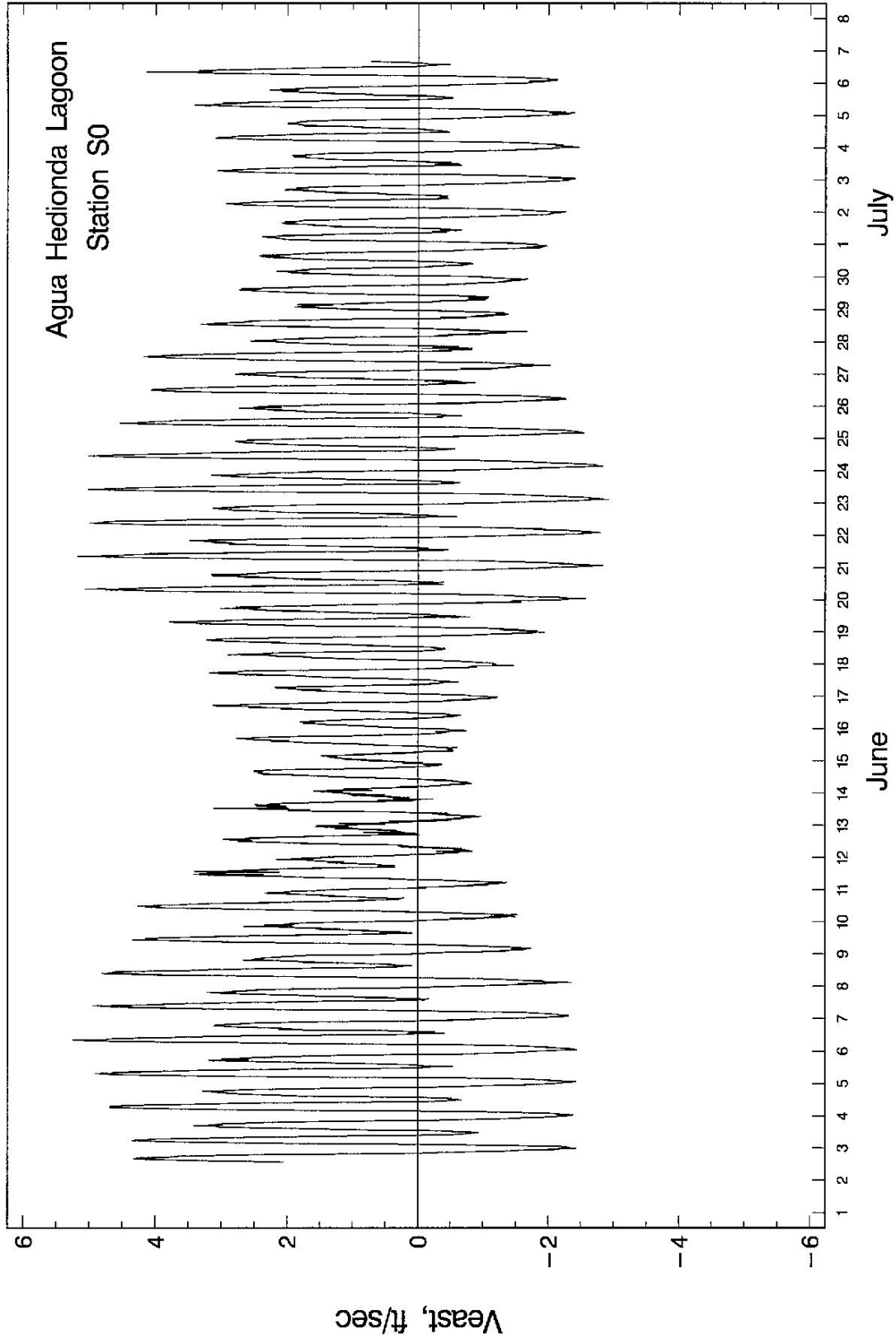


Figure B-1. East component of water velocity at Station S0.

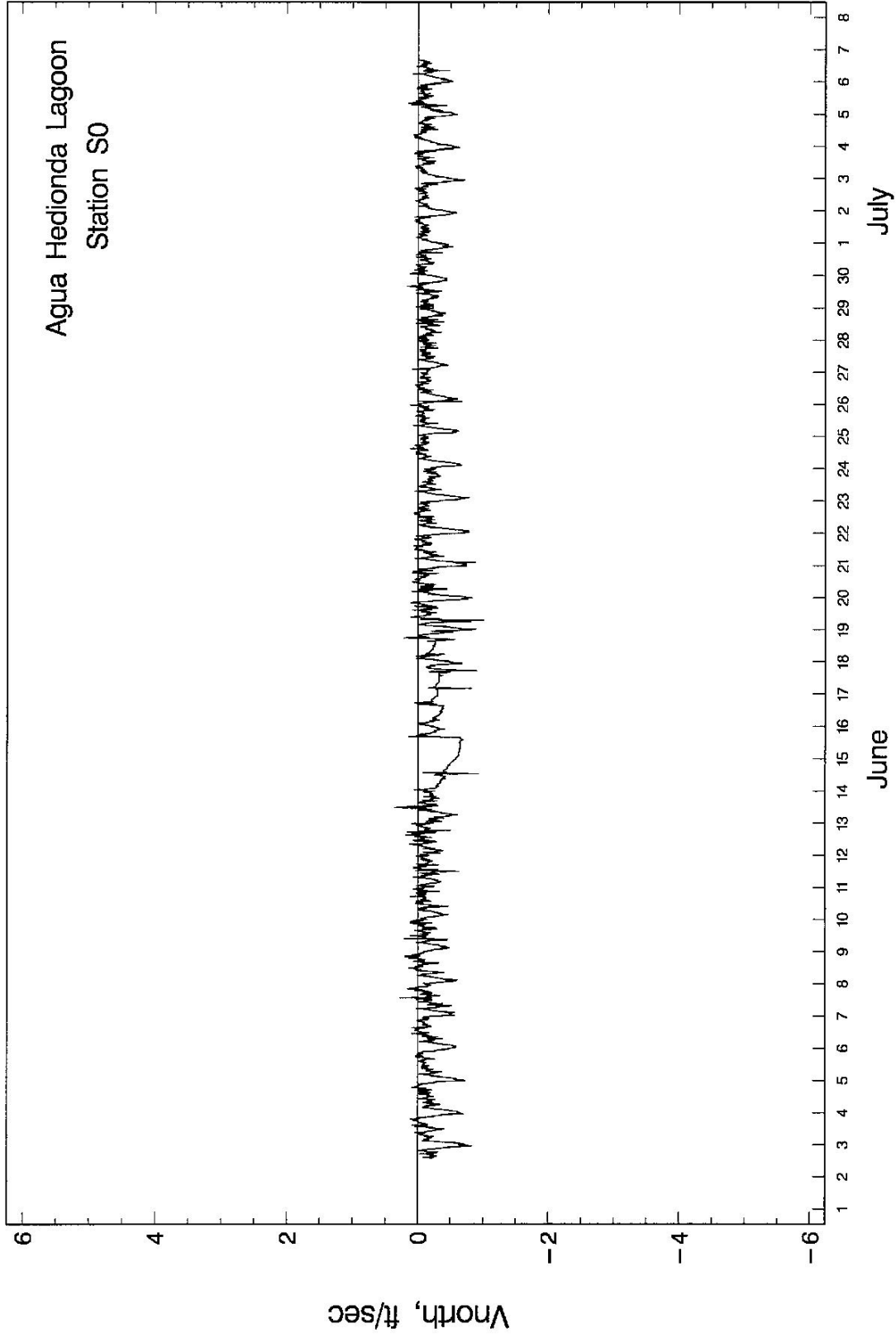


Figure B-2. North component of water velocity at Station S0.

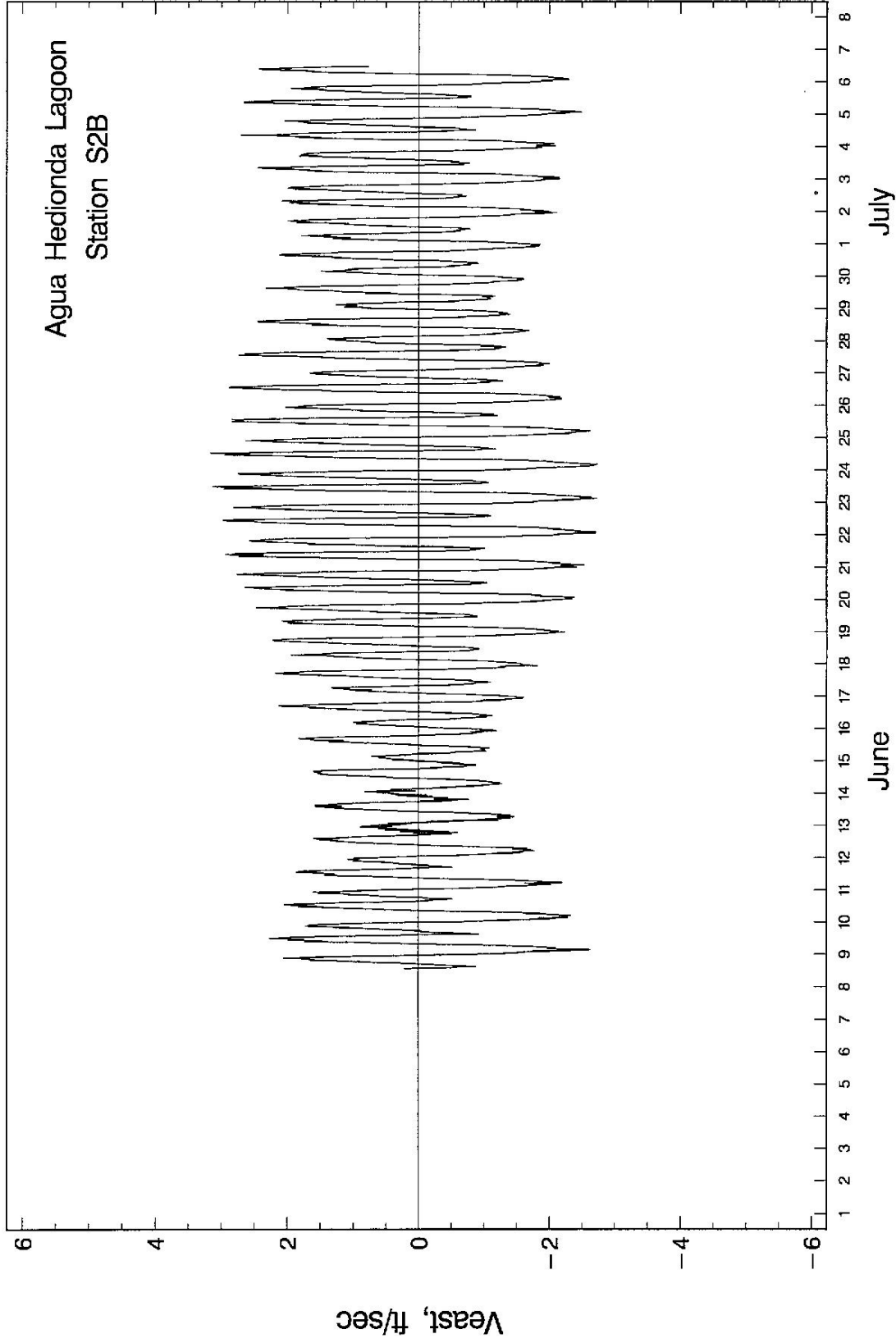


Figure B-3. East component of water velocity at Station S2B.

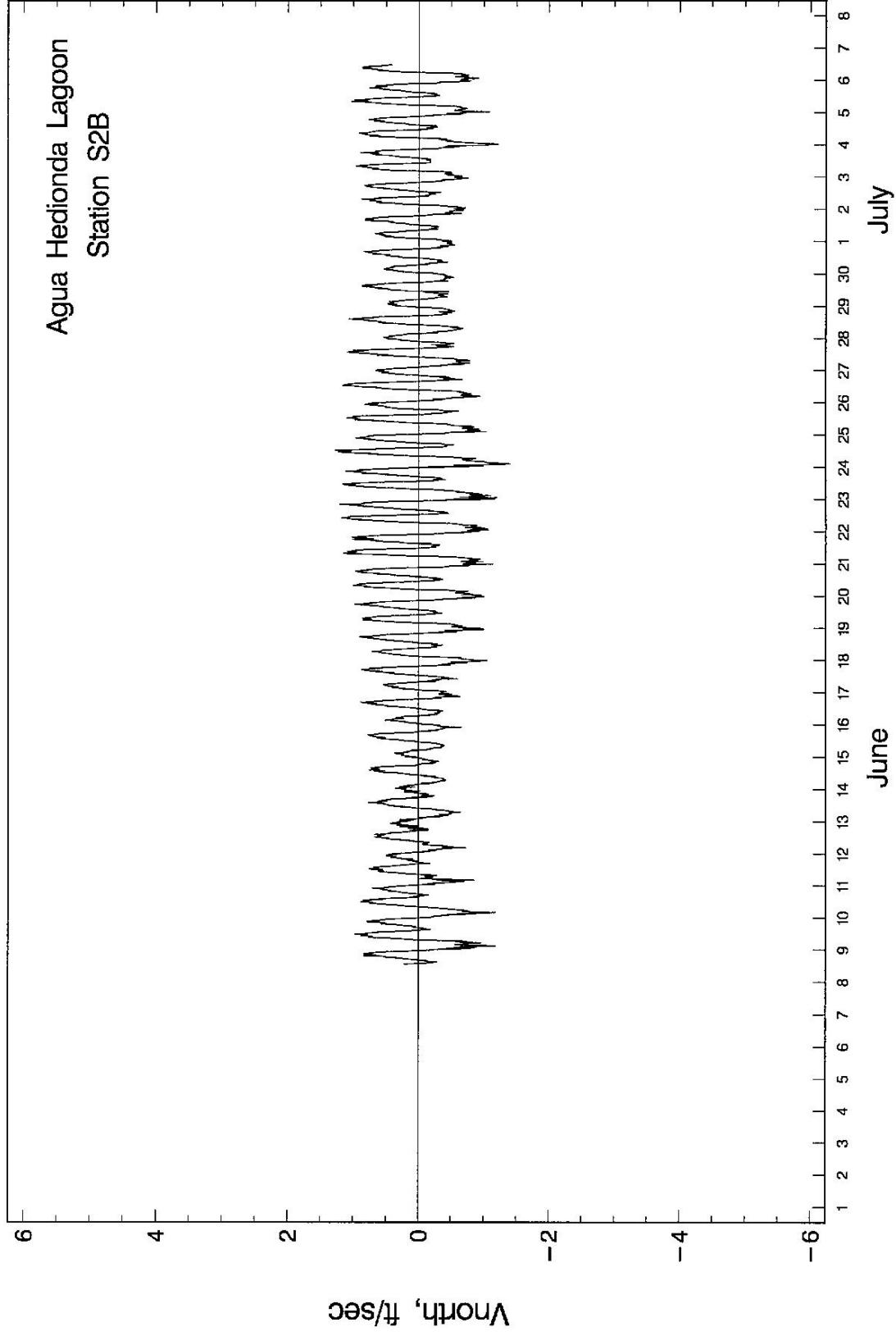


Figure B-4. North component of water velocity at Station S2B.

APPENDIX C

**LAGOON TIDAL PRISM ALONG WITH CONTRIBUTIONS OF
OUTER, INNER, AND MIDDLE BASINS TO THE TIDAL PRISM**

Agua Hedionda Lagoon

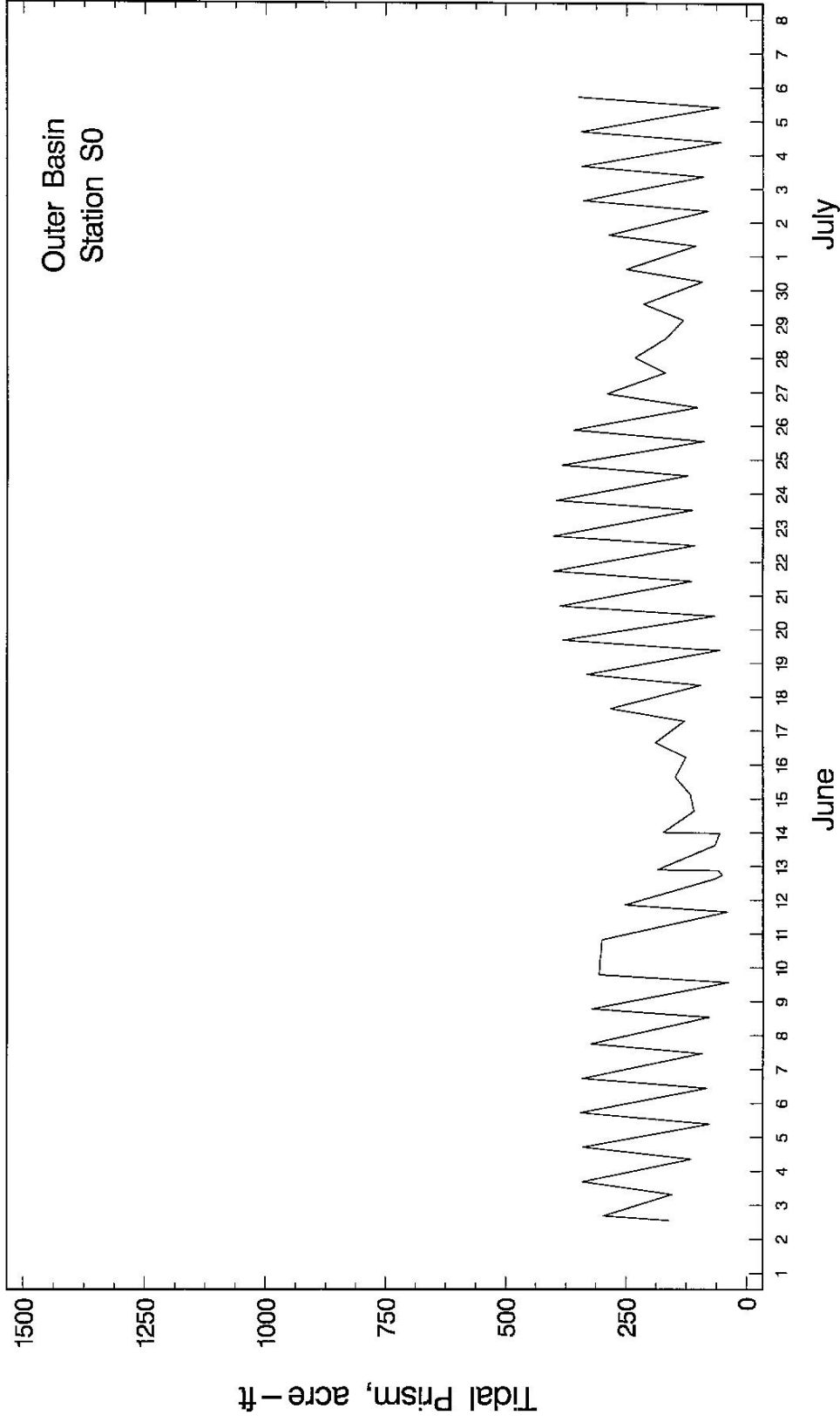


Figure C-1. Tidal prism of Outer Basin as computed from water level measurements at Station S0.

Agua Hedionda Lagoon

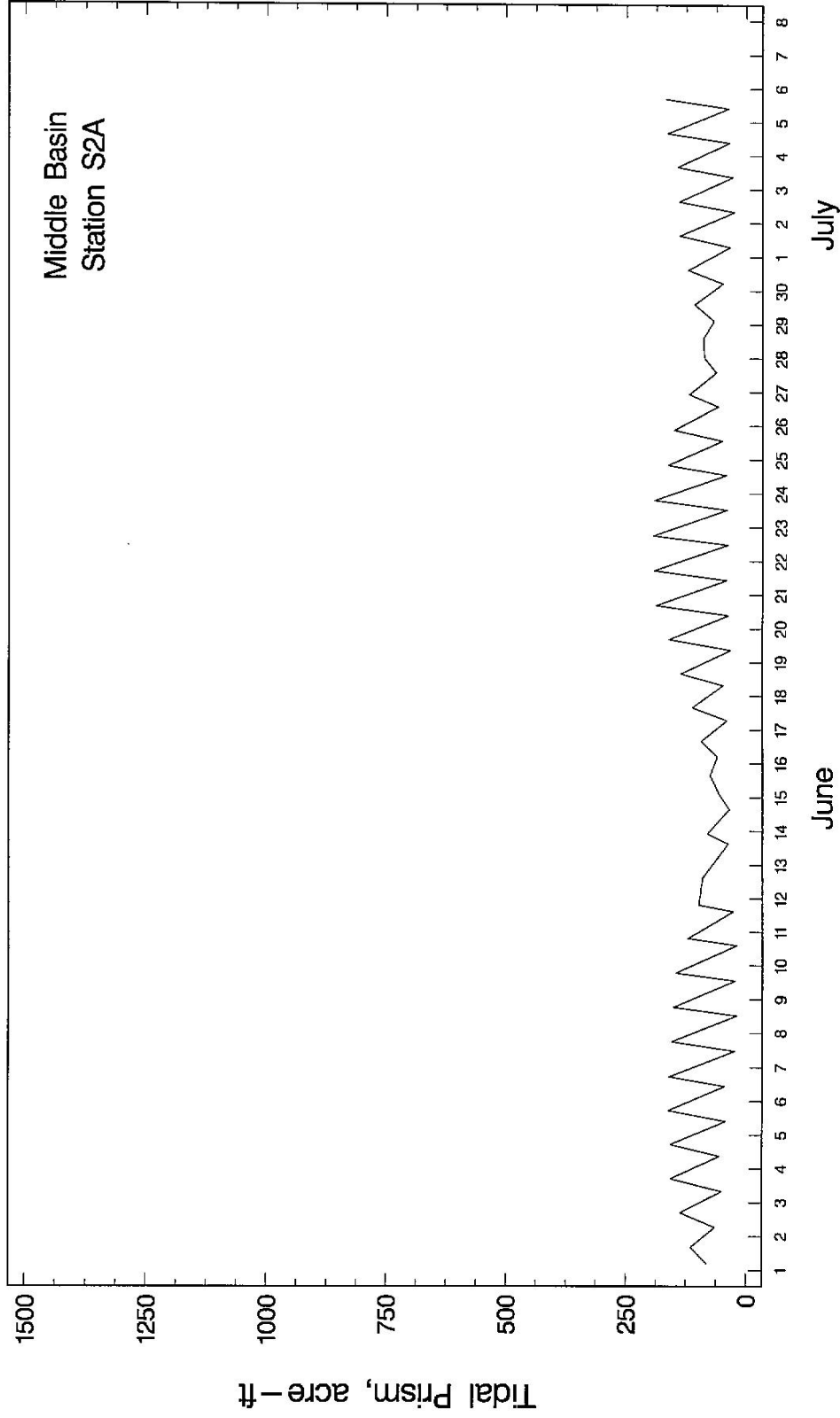


Figure C-2. Tidal prism of Middle Basin as computed from water level measurements at Station S2A.

Agua Hedionda Lagoon

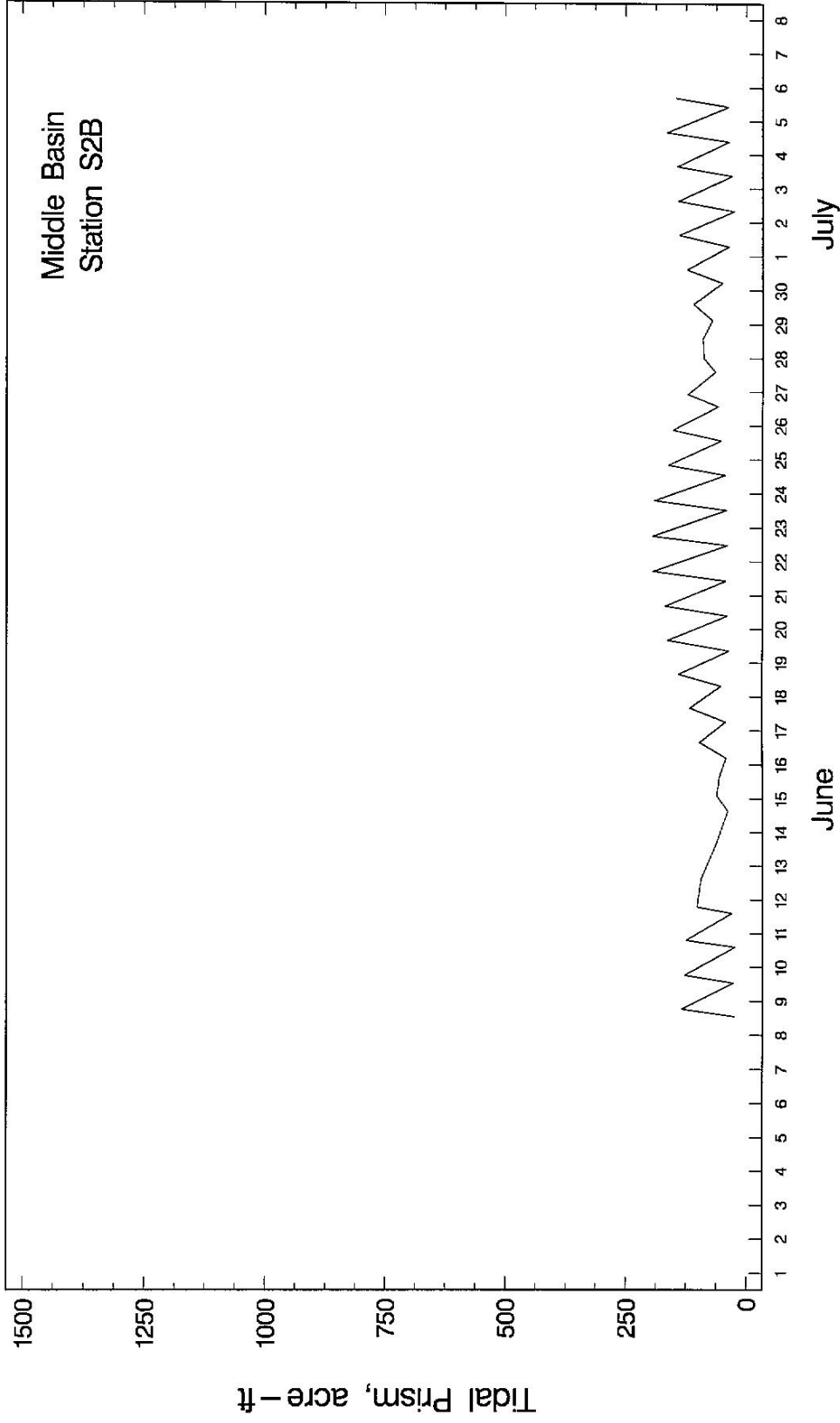


Figure C-3. Tidal prism of Middle Basin as computed from water level measurements at Station S2B.

Agua Hedionda Lagoon

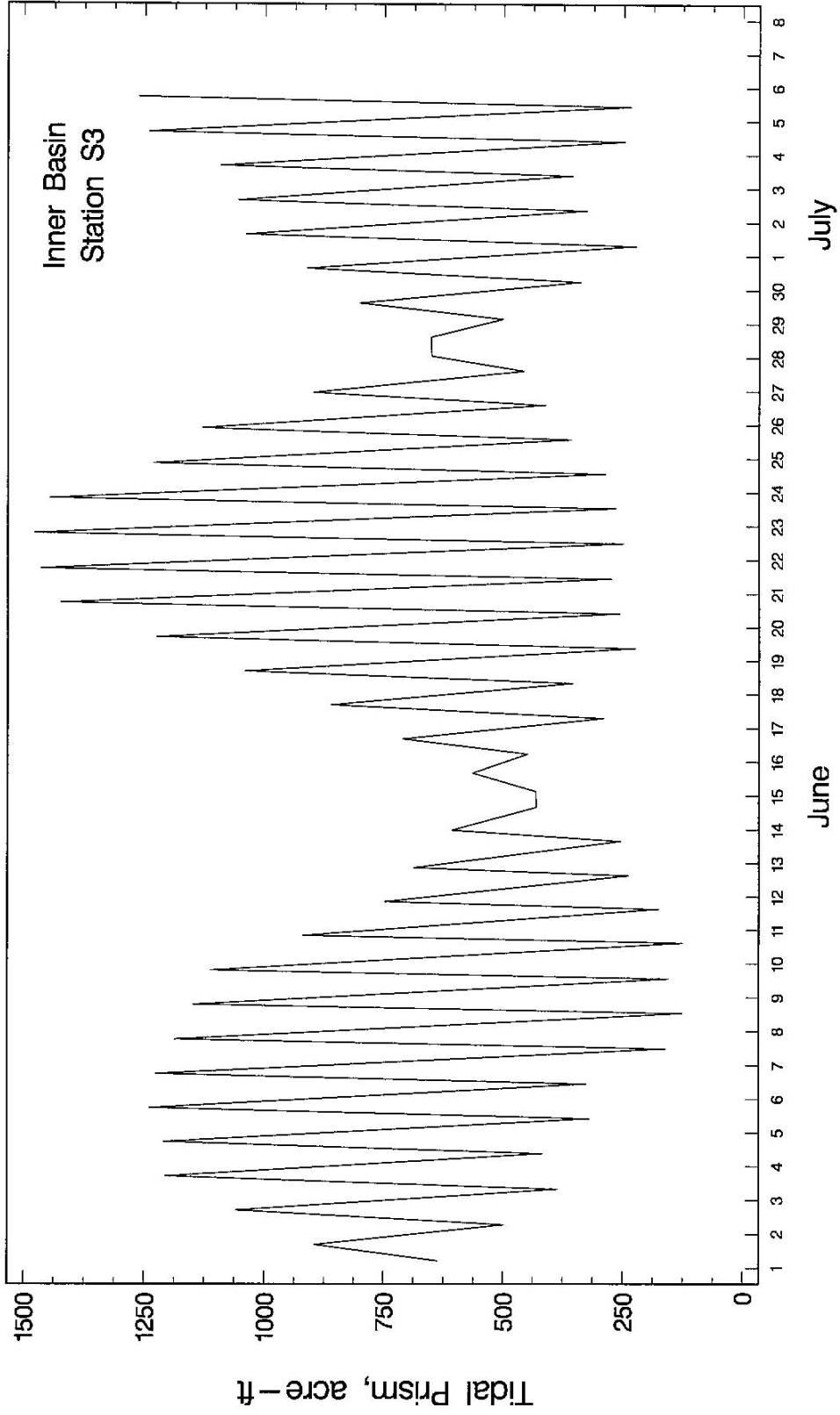


Figure C-4. Tidal prism of Inner Basin as computed from water level measurements at Station S3.

Agua Hedionda Lagoon

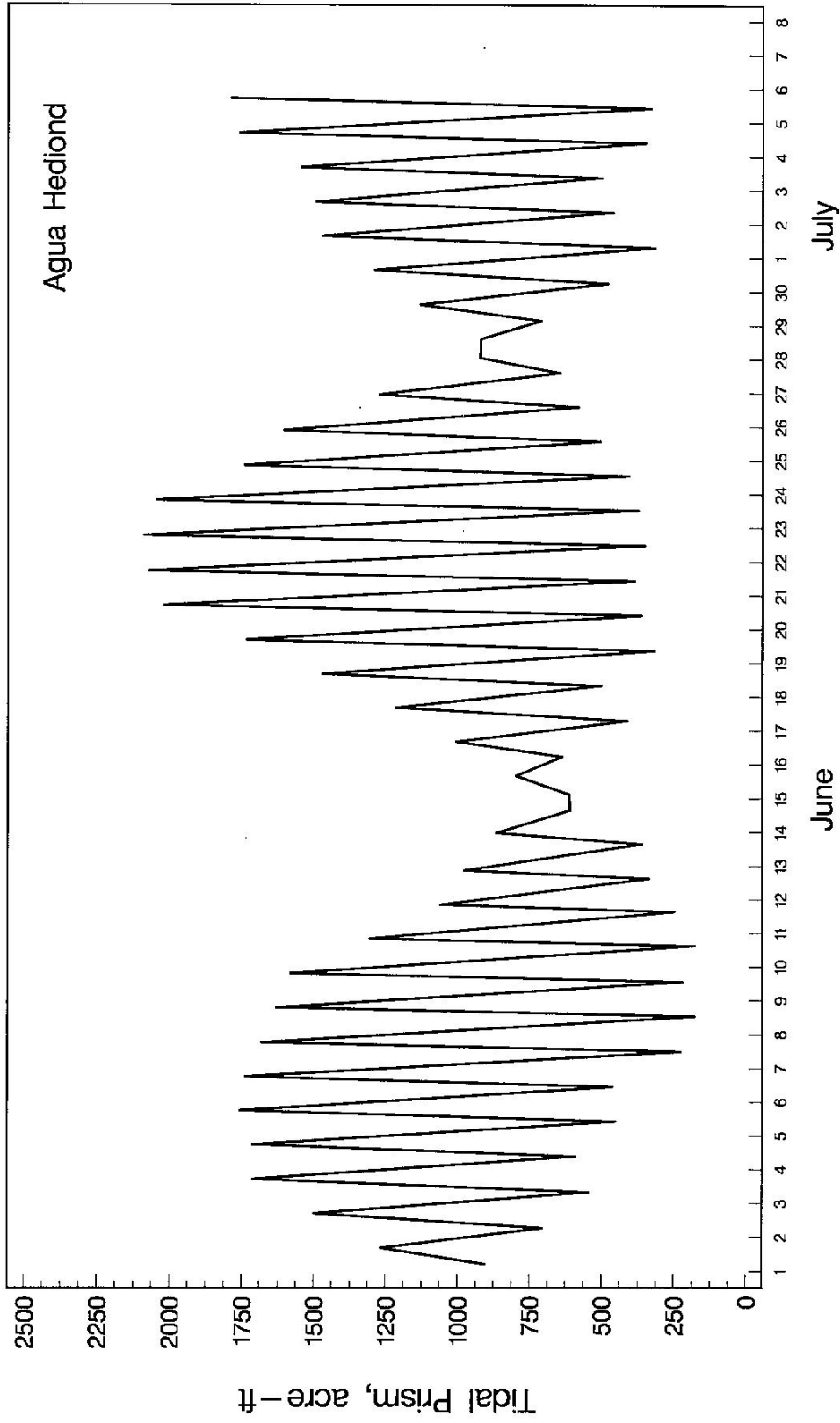


Figure C-5. Agua Hedionda Lagoon tidal prism.

APPENDIX D
TEMPERATURE AND SALINITY MEASUREMENTS
AT OUTER AND INNER BASINS

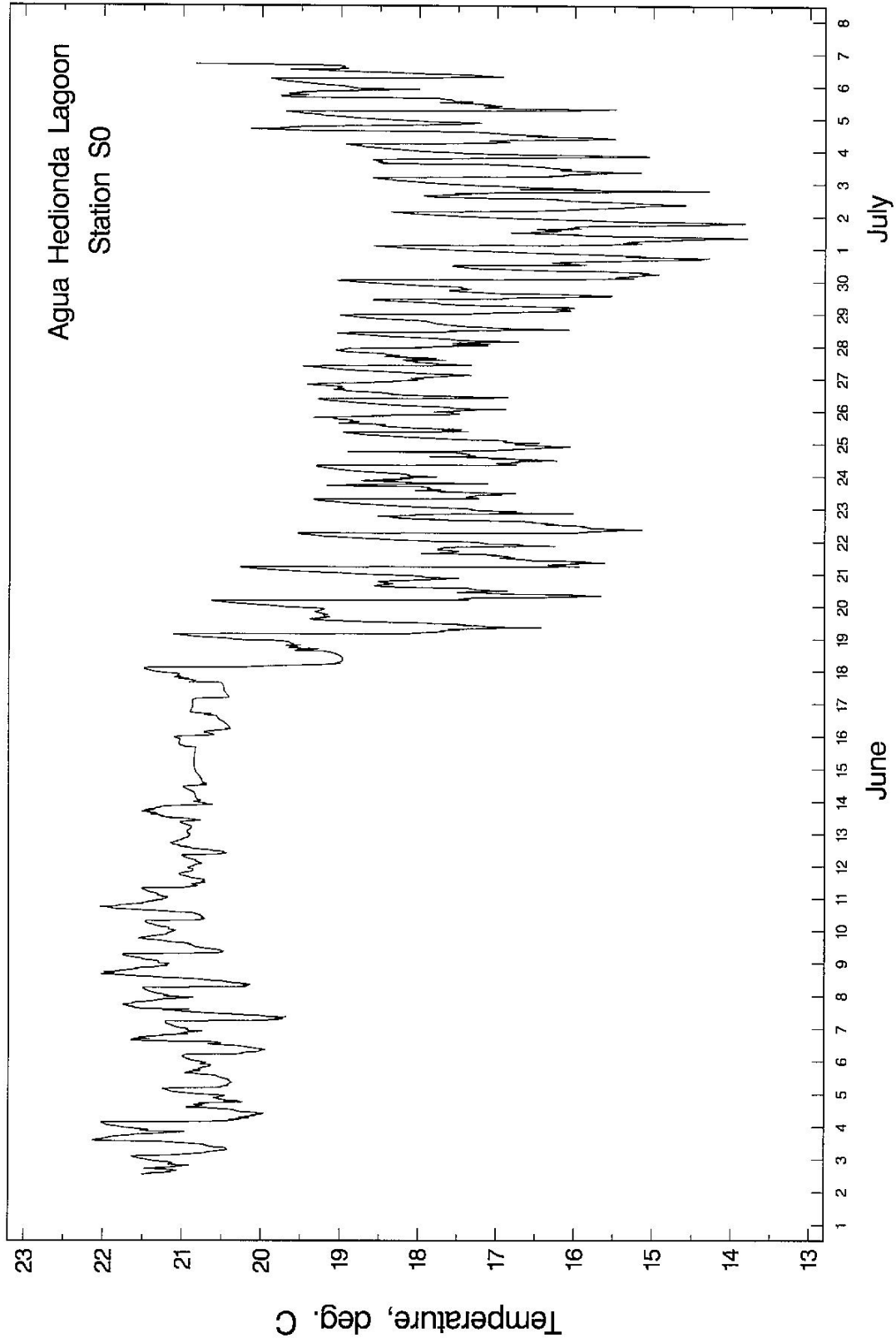


Figure D-1. Water temperature measurements at Station S0.

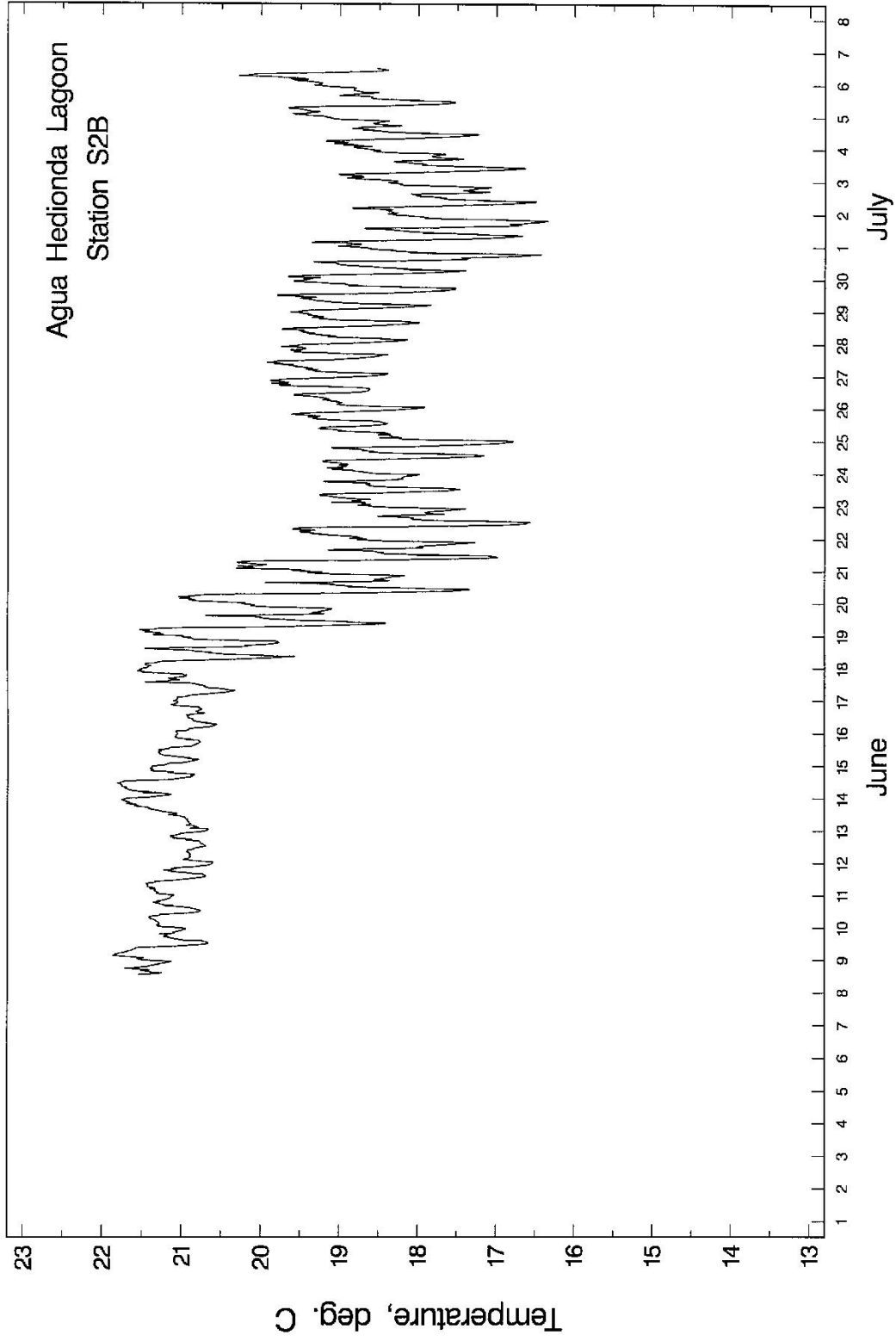


Figure D-2. Water temperature measurements at Station S2B.

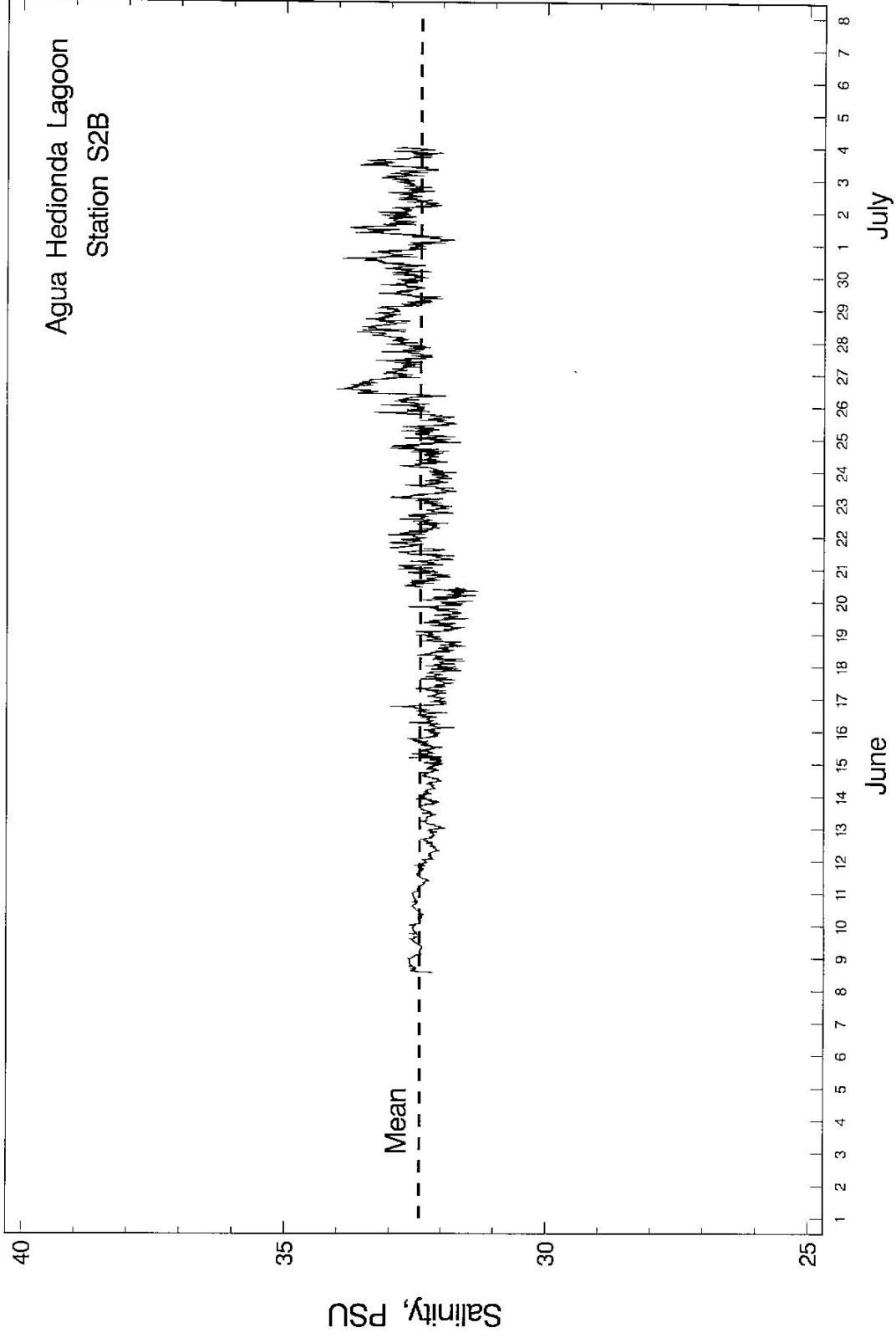


Figure D-3. Water salinity measurements at Station S2B.

N

Coastal Processes Effects of Reduced Intake Flows at Agua Hedionda
Lagoon

Submitted by:

Scott A. Jenkins, Ph. D. and Joseph Wasyl
Dr. Scott A. Jenkins Consulting
14765 Kalapana Street, Poway, CA 92064

Submitted to:

Tenera Environmental
141 Suburban Rd., Suite A2
San Luis Obispo, CA 93401

and

Poseidon Resources, Suite 840
501 West Broadway
San Diego, CA 92101

13 December 2006

Abstract:

This study evaluates the coastal processes effects associated with reduced flow rate operations of a stand alone desalination plant co-located at Encina Generating Station. The generating station presently consumes lagoon water at an average rate of about 530 mgd. If this consumption rate were reduced to 304 mgd to maintain end-of-pipe salinity below 40 ppt, we find that the capture rates of littoral sediment would be reduced by 42.5%, thereby reducing the environmental impacts associated with maintenance dredging. Reduced flow rate operations will not increase the magnitude of cyclical variations in habitat or residence time that presently occur throughout each maintenance dredge cycle, but will increase the length of time over which those variations occur. Low flow rate operations will result in reductions of 8% to 10% in the fluxes of dissolved nutrients and oxygen into the lagoon through the ocean inlet, but this effect is relatively minor in comparison to the 17.4% decline in nutrient and D.O. flux

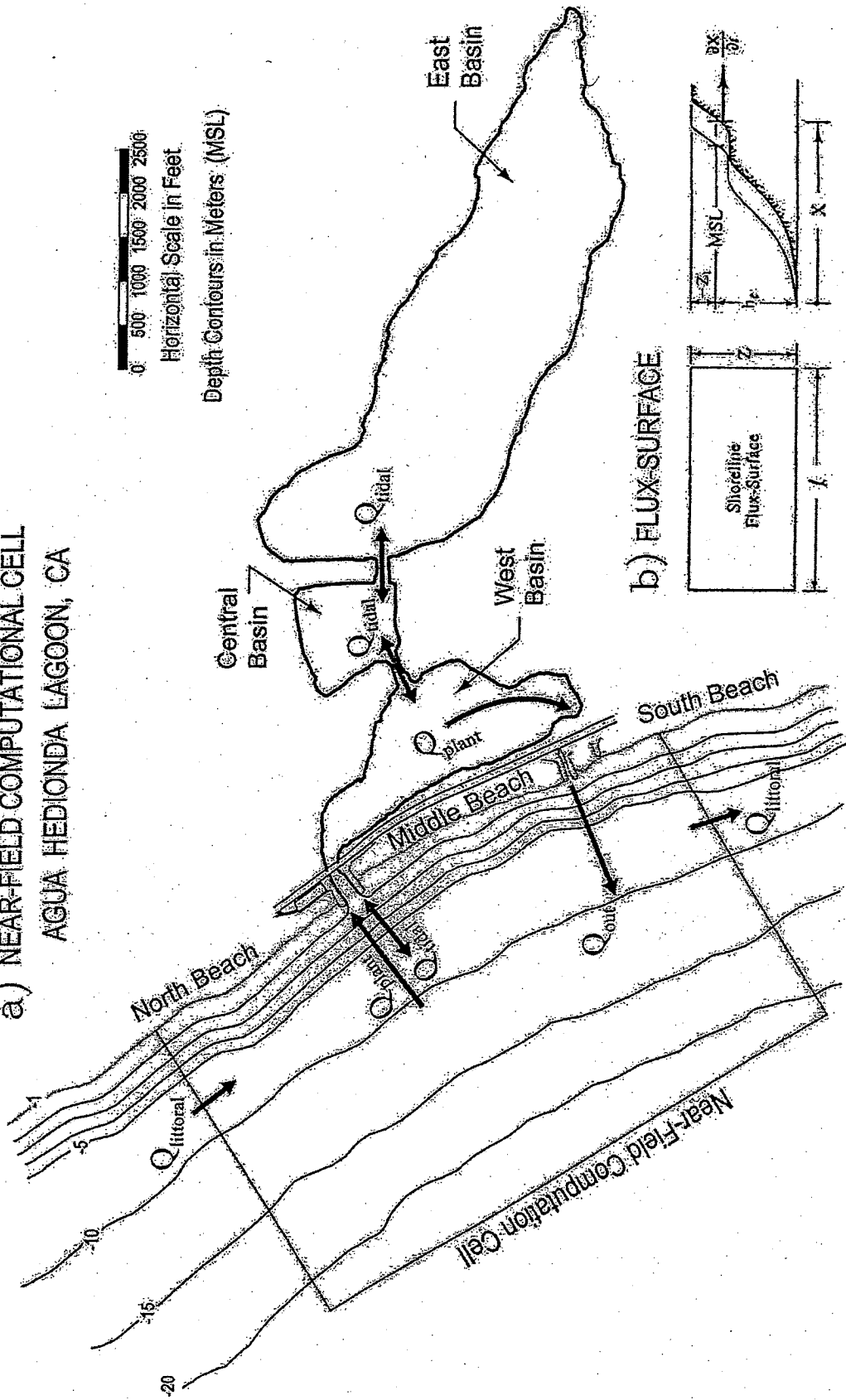
that occurs in the latter stages of each dredge cycle. On balance, low flow operations do not appear to create any significant adverse impacts on either the lagoon environment or the local beaches; and it could be argued that the reduction in capture rates of littoral sediment is a project benefit.

1.0) Introduction:

The present day Agua Hedionda Lagoon is not a natural geomorphic structure, rather it is a construct of modern dredging. Its west tidal basin (Figure 1) is unnaturally deep (-20 to -32 ft NGVD) and the utilization of lagoon water for once-through cooling by the Encina Generating Station renders Agua Hedionda's hydraulics distinctly different from any other natural tidal lagoon. Power plant cooling water uptake (Q_{plant}) acts as a kind of "negative river." Whereas natural lagoons have a river or stream adding water to the lagoon, causing a net outflow at the ocean inlet, the power plant in-fall removes water from Agua Hedionda Lagoon, resulting in a net inflow of water (Q_{plant}) through the ocean inlet. This net inflow has several consequences for particulate transport into and out of the lagoon: 1) it draws nutritive particulate and suspended sediment from the surf zone into the lagoon, the latter forming bars and shoals (Figure 2) that subsequently restrict the tidal circulation, and 2) the net inflow of water diminishes or at times cancels the ebb flow velocities out of the inlet, thereby providing insufficient transport energy to flush sediments (essentially uphill) out of the deep west basin of the lagoon. Therefore, the plant demand for lagoon water strongly controls the rate at which Agua Hedionda traps sediment and other solid particulate.

This is a technical note on the potential coastal processes effects arising from reduced once-through flow rates at the Encina Generating Station, Carlsbad, CA. Specifically, we evaluate long-term, stand-alone operation of a proposed desalination plant at this site using the minimum once-through flow rate available with the existing hydraulic infrastructure that will allow the production of 50 mgd of potable water by reverse osmosis (R.O.) without exceeding 40 ppt salinity at end-of-pipe. When taken in combination with worst-case mixing conditions in the receiving water, this minimum flow rate configuration is referred to in the certified project EIR as the "unheated

a) NEAR-FIELD COMPUTATIONAL CELL
 AGUA HEDIONDA LAGOON, CA



0 500 1000 1500 2000 2500
 Horizontal Scale in Feet

Depth Contours in Meters (MSL)

b) FLUX SURFACE

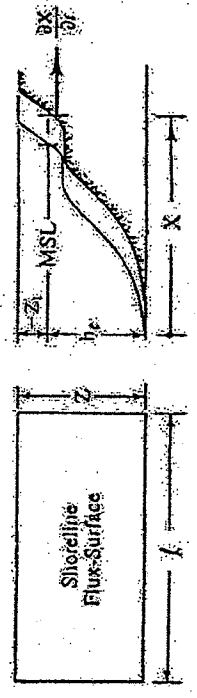


Figure 1. Near-field computational cell for calculating sediment transport at Agua Hedionda Lagoon, CA;
 a) Lagoon Plan View, b) Beach Cross-section.

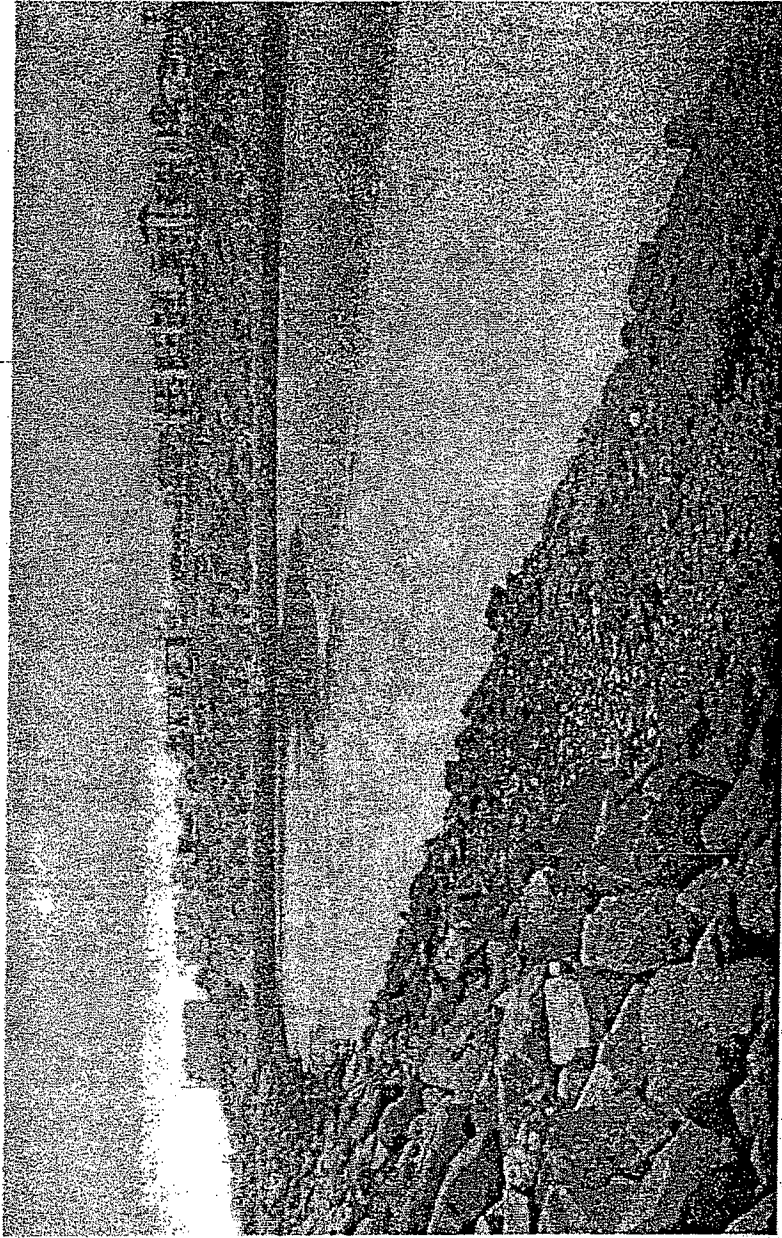
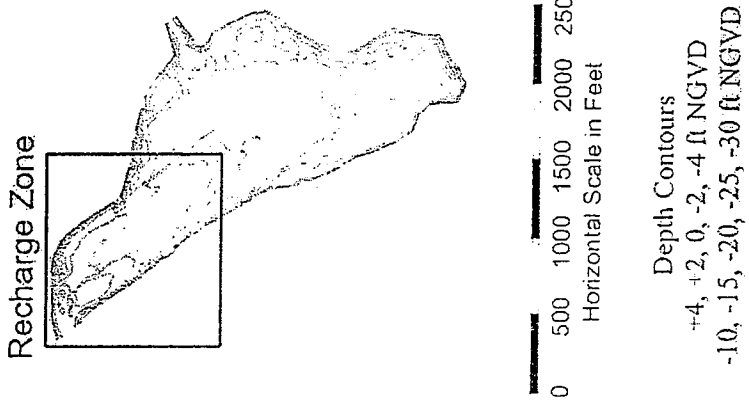


Figure 2. West Basin of Agua Hedionda Lagoon showing inlet (flood) bar formation at low tide. Insert shows the recharge area of the lagoon where this bar forms and the preponderance of maintenance dredging is performed.

historical extreme" and involves a once through flow rate of 304 mgd at the intake structure located at the southern end of the west basin of Agua Hedionda Lagoon. Table 1 below gives various operational combinations of existing circulation and service water pumps that can provide this minimum flow rate within 5%.

The existing cascade of circulation and service water pumps available at Encina Generating Station can provide a maximum once-through flow rate of 808 mgd, but has averaged about 530 over the long term (Jenkins and Wasyl, 2001). During peak user demand months for power (summer), plant flow rates are typically between 635 and 670 mgd (Elwany, et al, 2005). Thus the flow rates passing through the Encina facility during stand-alone desalination operations would be about 43% less than the present average when power generation is occurring, and 62% less than the peak flow rate capability. In this technical note, we utilize data from the existing literature to deduce probable impacts that this flow rate reduction would have on sand and nutrient flux into Agua Hedionda Lagoon and implications for the neighboring beaches and nearshore morphology.

2.0) Reduced Flow Effects on Sediment Flux

The most profound and far-reaching consequence of long-term operation of the Encina facility at reduced flow rate will be on the flux of sand into the lagoon through the ocean inlet. The sand influx controls the tidal exchange in the lagoon by regulating the depth of an inlet sill associated with inlet bars that form in the West Basin of the lagoon (see Figure 2). These sand bars restrict the effective tidal range in the lagoon and ultimately threaten closure of the inlet, thereby requiring periodic maintenance dredging to mitigate that threat. The bars are formed by sands that are suspended in the surfzone and entrained by the inflowing stream of water through the inlet. During peak demand months for power, typically 46% of the daily inflow volume is due the power plant flow rate, causing the daily outflow through the inlet to be 48% less than the inflow (Elwany, et al, 2005). As a result, the transport of sand into the lagoon through the ocean inlet has a strong inflow bias (flood dominance) that scales in direct proportion to the power plant flow rate. In the review of lagoon sedimentation that follows, we will show a correlation between sand influx rates and plant flow rates, indicating that reduction of plant flow rates will reduce the influx rate of sand into the lagoon. While this is an apparent benefit

Table 1. COMBINATIONS OF PUMPS OF TOTAL CAPACITY WITHIN 5 % OF 304 MGD

<u>Operational Condition 1 – 304.7 MGD</u>		
Unit 1 (Both Pumps)	=	68.3 MGD
		Subtotal = 104.3 MGD (Desal Intake)
Unit 2 (2 S Pump)	=	36.0 MGD
Unit 3 (Both Pumps)	=	63.9 MGD
		Subtotal = 200.4 MGD (Dilution)
Unit 4 (4 W Pump)	=	136.5 MGD
Total	=	304.7 MGD (0.2 % above 304 MGD)
<u>Operational Condition 2 – 306.3 MGD</u>		
Unit 4 (Both Pumps)	=	270.4 MGD
Unit 1 (1 S Pump)	=	35.9 MGD
Total	=	306.3 MGD (1 % above 304 MGD)
<u>Operational Condition 3 – 306.4 MGD</u>		
Unit 4 (Both Pumps)	=	270.4 MGD
Unit 2 (2 S Pump)	=	36.0 MGD
Total	=	306.4 MGD (1 % above 304 MGD)
<u>Operational Condition 4 – 315.4 MGD</u>		
Unit 4 (4 E Pump)	=	133.9 MGD
Unit 5 (5 W Pump)	=	157.0 MGD
Unit 2 (2 N Pump)	=	24.5 MGD
Total	=	315.4 MGD (3.8 % above 304 MGD)
<u>Operational Condition 5 – 315.4 MGD</u>		
Unit 5 (Both Pumps)	=	315.4 MGD
Total	=	315.4 MGD (3.8 % above 304 MGD)
<u>Operational Condition 6 – 302.1 MGD</u>		
Unit 1 (Both Pumps)	=	68.3 MGD
		Total = 104.3 MGD (Desal Intake)
Unit 2 (2 S Pump)	=	36.0 MGD
Unit 3 (Both Pumps)	=	63.9 MGD
		Total = 197.8 MGD (Dilution)
Unit 4 (4 E Pump)	=	133.9 MGD
Total	=	302.1 MGD (0.6 % below 304 MGD)

of stand alone operations of a desalination plant, it raises a number of cost trade-off and regulatory issues that would ultimately need to be decided.

2.1) Lagoon Sedimentation History: Prior to the 1950's, Agua Hedionda was a slough comprised of shallow marsh channels filled with anaerobic hyper-saline water and flushed only briefly during winter months when high tides and rain runoff from Agua Hedionda Creek would broach the barrier berm across the lagoon inlet. A Southern

Pacific Railroad survey of the track across Agua Hedionda in 1889 (Figure 3) shows no extensive open water areas where the present day lagoon is situated. Instead, only winding marsh channels and marsh vegetation is apparent. Also apparent in this survey map is the closed state of the inlet on the south side of the marsh plain, and a narrow barrier beach with cobble ridge system across the entire extent of Middle Beach and portions of North Beach and South Beach. (ref. Figure 1 for beach nomenclature). Thus these were historically narrow beaches that did not retain large volumes of sand given the presence of the surveyed cobble ridges.

Over a period of 247 days beginning June 1953, a total of 4,279,000 cubic yards of mostly beach grade sediment was dredged from the Agua Hedionda Lagoon system. Referring to Figure 1, the total dredge volume was 1,025,000 cubic yards from the outer or western basin, and 3,254,000 cubic yards from the middle and east basins, see Ellis (1954). This dredged material was deposited primarily on Middle Beach with residual amounts on North and South Beach, forming a large deltaic shoreline form which had the effect of widening the beach by an additional 500 ft. In order to allow the intake and discharge flows to cross this man-made delta, the intake and discharge channels were armored with rubble mound jetty structures approximately 700-750 ft. in length as measured from the center line of the Pacific Coast Highway (Jenkins and Wasyl, 2001).

The dredge delta caused wave energy to converge on this section of shoreline inducing erosion progressively over time until the original beach width at Agua Hedionda was re-established by 1956 (Jenkins and Wasyl, 2001). As the delta eroded, the un-engineered rock structures were exposed to large breaking wave forces and the intake and discharge jetties were reduced by this storm damage to their present nominal lengths circa 1960 to 1963. Meanwhile, the 4.3 million cubic yards of sand that had made up the dredged delta formation was transported southward by the net littoral drift that predominates throughout the Oceanside Littoral Cell as shown in Figure 4. In the Oceanside Littoral Cell, the prevailing wave direction is from the northwest due to the combined effects of coastline orientation, island sheltering and the most prevalent storm track which is associated with extra tropical cyclones and cold fronts from the Gulf of

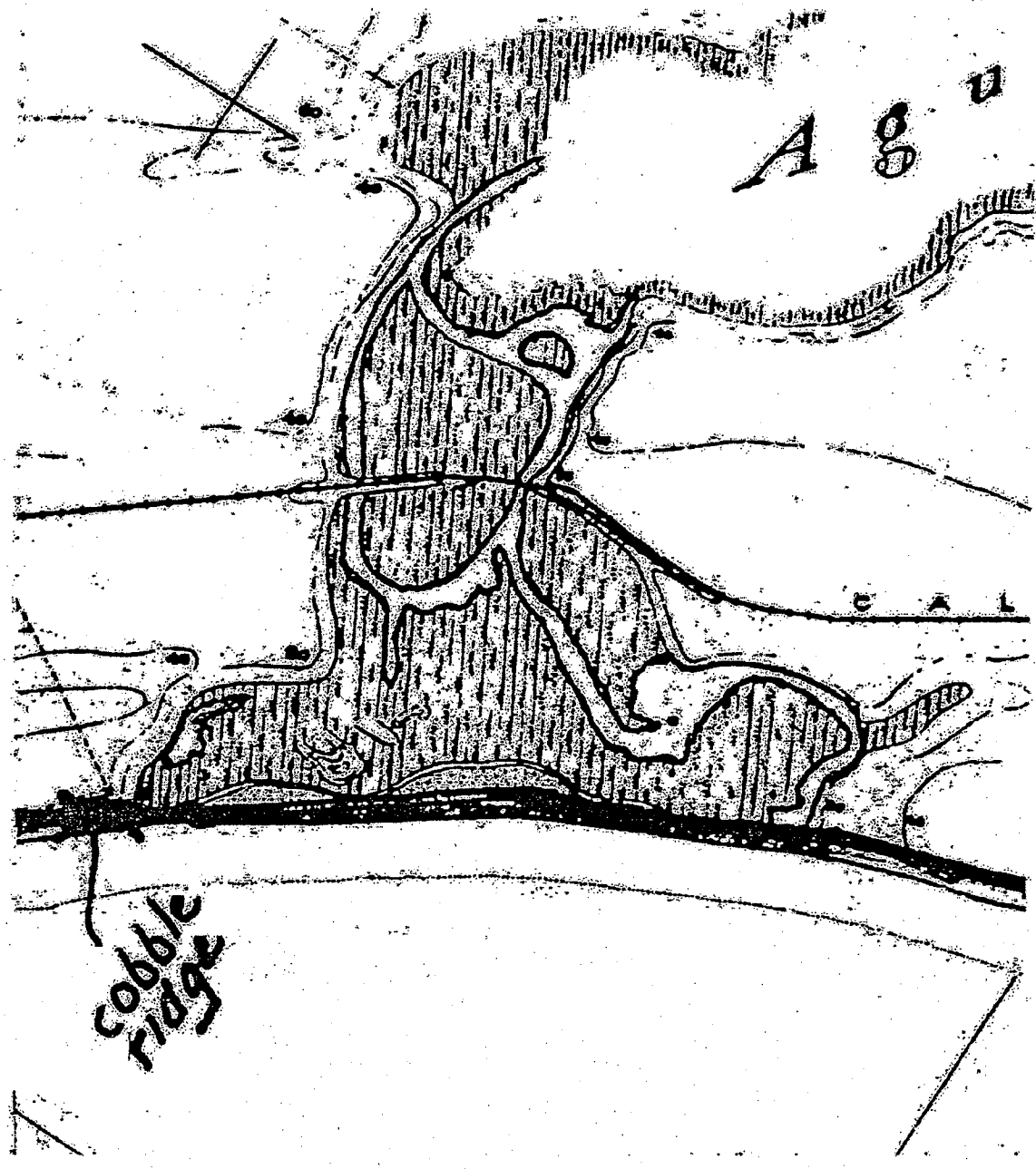


Figure 3 Railroad Survey of Agua Hedionda Lagoon, 1884.

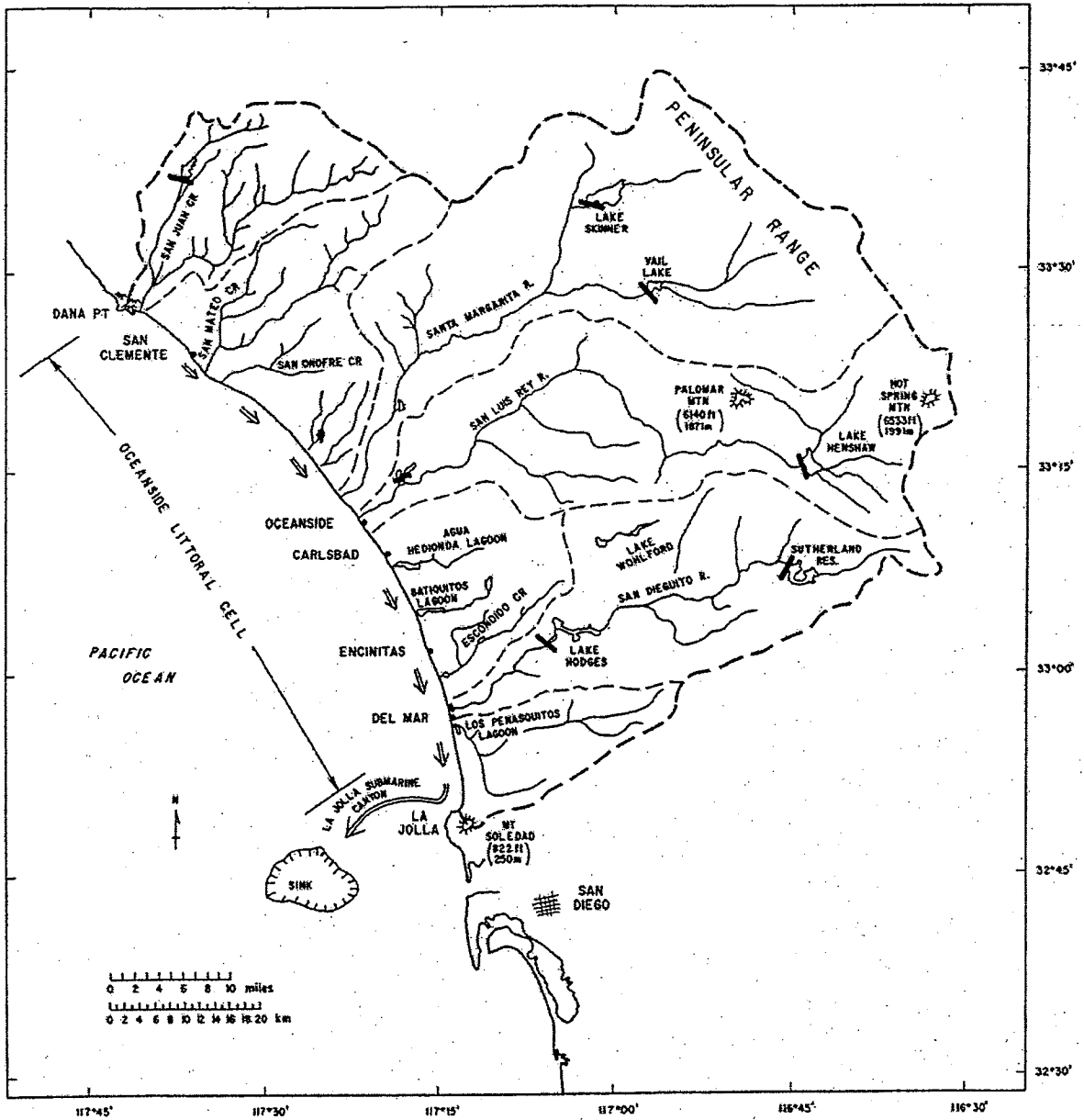


Figure 4. Oceanside Littoral Cell [Inman and Brush, 1973].

Alaska. Consequently, the long-term average littoral drift is from north to south as shown in Figure 4. This southward directed littoral drift is intercepted by submarine canyons (the La Jolla and Scripps Submarine Canyons) at the extreme southern (down-drift) end of the littoral cell where it is lost in turbidity currents that flow down the shelf rise, making the Oceanside Littoral Cell is a constant loss system. The only way the beaches can remain stable in this constant loss system is by continual replacement of these sand losses. When the inflowing stream of water into Agua Hedionda entrains sand from the littoral drift and deposits it in the west basin, the beaches down-drift of the lagoon suffer a loss of sand supply unless maintenance dredging returns those sands to the beaches. Since the inflow rates increase with the rate of consumption of cooling water, it is logical to look for a relationship between dredge quantities and cooling water consumption. To quantify this relationship we examine the historic dredge and flow rate data.

Table 2 gives a listing of the complete dredging history at Agua Hedionda Lagoon. The dredging events listed as "maintenance" in Table 2 occurred within the recharge zone of the west basin (Figure 2) and give estimates of sediment influx rates when the volumes for these events are factored against the time intervals between them. Annual sand influx rates calculated in this way are compared against the annual consumption of cooling water in Figure 5. Annual consumption of cooling water is plotted against the left hand axis in Figure 5 (black) in units of millions of gallons of seawater; while the annual sand influx volume is plotted against the right hand axis (red) in units of thousands of cubic yards. The individual data appear for each year as black diamonds for flow rate and red crosses for sand influx rates. Over-laid on these data are linear best fits to each. There is a clear trend showing that the consumption of cooling water by the power plant has increased over time (in response to expansion of generating capacity and increased user demand for power); and that the sand influx rates have followed that increase. From the best fit lines derived from the 48 year period of record in Figure 5, annual consumption of cooling water by the power plant has increased nearly 5 fold (growing on average by 3.3 billion gallons per year), while the annual influx of sand has doubled (increasing by 2 thousand cubic yards per year). Although the

Table 2. Dredging and Disposal History at Agua Hedionda Lagoon (from Jenkins and Wasyl, 2001)

Dredging And Disposal History							
Year	Dredging		Disposal		Comments		
	Date		Volume (yds ³)	Basin Dredged	Volume (yds ³)	Location Placed 1	
	Start	Finish					
1954	Feb-54	Oct-54	4,279,319	Outer, Middle, & Inner	4,279,319	N, M, S	Initial construction dredging
1955	Aug-55	Sep-55	90,000	Outer	90,000	S	Maintenance
1957	Sep-57	Dec-57	183,000	Outer	183,000	S	Maintenance
1959-60	Oct-59	Mar-60	370,000	Outer	370,000	S	Maintenance
1961	Jan-61	Apr-61	227,000	Outer	227,000	S	Maintenance
1962-63	Sep-62	Mar-63	307,000	Outer	307,000	S	Maintenance
1964-65	Sep-64	Feb-65	222,000	Outer	222,000	S	Maintenance
1966-67	Nov-66	Apr-67	159,108	Outer	159,108	S	Maintenance
1968-69	Jan-68	Mar-69	96,740	Outer	96,740	S	Maintenance
1972	Jan-72	Feb-72	259,000	Outer	259,000	S	Maintenance
1974	Oct-74	Dec-74	341,110	Outer	341,110	M	Maintenance
1976	Oct-76	Dec-76	360,981	Outer	360,981	M	Maintenance
1979	Feb-79	Apr-79	397,555	Outer	397,555	M	Maintenance
1981	Feb-81	Apr-81	292,380	Outer	292,380	M	Maintenance
1983	Feb-83	Mar-83	278,506	Outer	278,506	M	Maintenance
1985	Oct-85	Dec-85	403,793	Outer	403,793	M	Maintenance
1988	Feb-88	Apr-88	333,930	Outer	103,000	N	Maintenance
					137,860	M	Maintenance
					93,070	S	Maintenance
1990-91	Dec-90	Apr-91	458,793	Outer	24,749	N	Maintenance
					262,852	M	Maintenance
					171,192	S	Maintenance
1992	Feb-92	Apr-92	125,976	Outer	125,976	M	Maintenance
1993	Feb-93	Apr-93	115,395	Outer	115,395	M	Maintenance
1993-94	Dec-93	Apr-94	158,996	Outer	74,825	N	Maintenance
					37,761	M	Maintenance
					46,410	S	
1995-96	Sep-95	Apr-96	443,130	Outer	106,416	N	Maintenance
					294,312	M	
					42,402	S	
1997	Sep-97	Nov-97	197,342	Outer	197,342	M	Maintenance

Table 1. Continued

Dredging And Disposal History							
Year	Dredging				Disposal	Comments	
	Date		Volume (yds ³)	Basin Dredged	Volume (yd ³)	Location Placed 1	
	Start	Finish					
1998	Dec-97	Feb-98	60,962	Middle	60,962	M	Modification dredging
	Feb-98	Feb-99	498,736	Inncr	370,297	M	Modification dredging
					128,439	S	
1999	Feb-99	May-99	202,530	Outer	202,530	N	Maintenance
2000-01	Nov-00	Apr-01	429,084	Outer	142,000	N	Maintenance
					202,084	M	
					85,000	S	
2002	Sept02	Dec 02	190,600		190,600	M	Maintenance
Total			11,482,966		11,482,966		

N = North

Beach

M = Middle

S = South

Beach

coefficient of determination (R-squared) is 0.68 for the cooling water relation and 0.60 for the sand influx relation, the scatter in the data about the best fit lines is due to several transient external factors. The cooling water relationship is effected by weather events and variations in climate patterns, especially the occurrence of warm humid El Niño (ENSO) events that result in protracted heat waves, increasing user demand for power to cool homes and work places. The sand influx relationship is similarly impacted since these same ENSO events also correlate with intensification of wave climate, accelerated beach erosion and transport; and consequently more suspended sediment in the neighborhood of the lagoon inlet to be entrained by the net inflowing stream. However, the sand influx rates are further impacted by beach nourishment activities up-drift of the

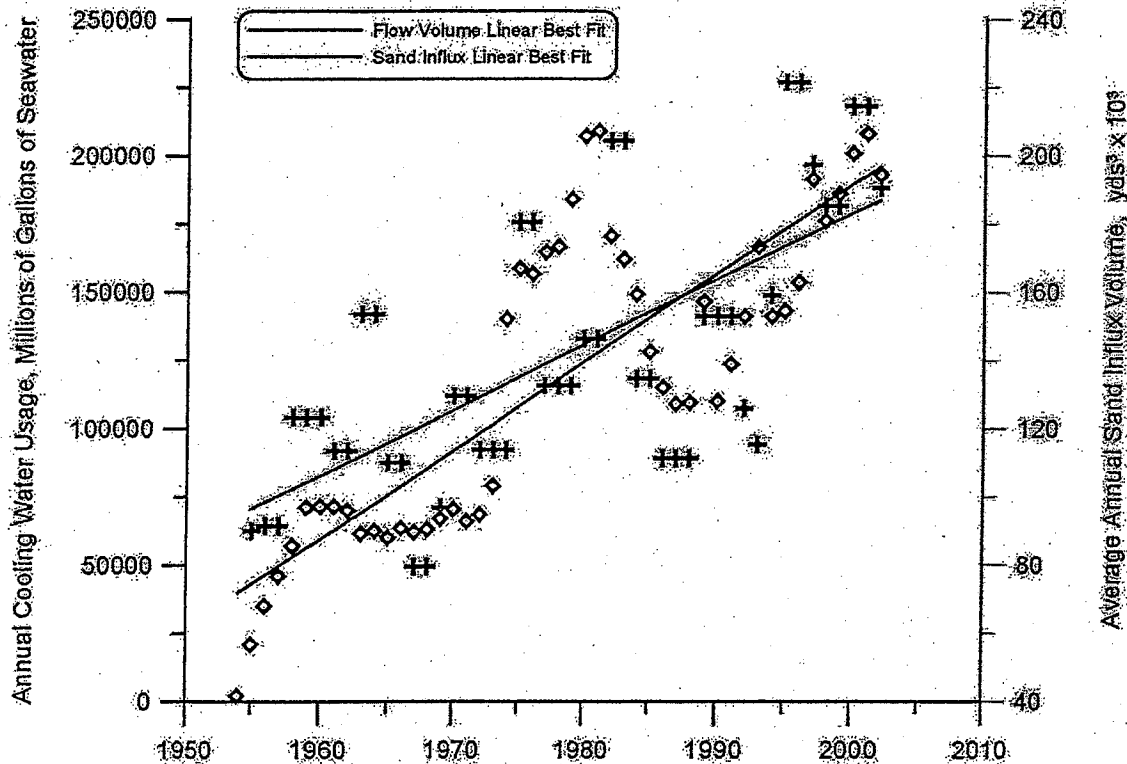


Figure 5. Time history of annual Encina cooling water usage and average annual sand influx from dredged volume for the years 1954-2002, [data from Jenkins and Wasyl, 1998 and 2003].

lagoon. Beach nourishment activities up-drift of Agua Hedionda are seen to have roughly doubled the daily influx rates to 400-600 cubic yards per day, as occurred following beach building projects in 1963, 1973, 1982, 1994 and 2001. Because of the transient impacts of beach restoration on sand influx rates, the coefficient of determination for the sand influx relation in Figure 5 is less than that for the cooling water flow rate relation. For a more detailed account of the effects of regional beach nourishment projects on sand influx rates at Agua Hedionda, see Appendix A.

2.2) Effects of Reduced Flow Operations on Sedimentation: From the flow rate and influx rate relations in Figure 5, we conclude that, on average, the lagoon presently traps $184,724 \text{ yds}^3$ of sand per year in response to an average daily once-through plant flow rate of 528.69 mgd. Probability analysis of inlet closure in Jenkins and Wasyl (1997,

2001) finds that the accumulated risk of inlet closure grows at 11% per year for sand influx rates of this magnitude, making inlet closure more probable than not within 4.5 years if no maintenance dredging is performed. In view of this risk, the historic dredge record in Table 2 shows that the longest interval between dredge events has been 3 years, and the predominant dredge interval has been 2 years. With in-house dredge assets home ported inside the lagoon, mobilization costs have been held to a minimum and marginal dredge costs have been running about \$2.70 per cubic yard (Dyson, 2006). Thus, the costs of maintaining an open inlet (and hence, a healthy lagoon) under the present power generation operating scenario is about \$499,000 per year.

If the flow rate is reduced to 304 mgd under the scenario of a stand-alone desalination plant, then the linear best fits in Figure 5 indicate that the average sand influx rates into the lagoon would be reduced to 106,218 yds³ per year. This represents a 42.5% reduction in sand influx rates into the lagoon relative to the present power generation operating scenario. The reduction in sand influx rates reduces the accumulation of closure risk to only 6.3% per year, extending the safe interval for no dredge maintenance to 7.9 years before inlet closure would become more likely than not. Assuming the present marginal dredge cost of \$2.70 per cubic yard, the annual cost of maintaining an open inlet under the reduced flow scenario would be \$287,000 per year. Not factored into these cost comparisons are the costs of obtaining dredge permits and providing the pre- and post-dredging surveys and documentation necessary to obtain those permits. Dredge permits must be obtained from the City of Carlsbad, the California Coastal Commission, and the US Army Corps of Engineers on a year-to-year basis, as no blanket permits are currently issued.

Although the reduced flow rate scenario will reduce the rate of sand influx into the lagoon, it is clear that some degree of maintenance dredging must be continued for the indefinite future by whatever enterprise continues to use the lagoon for source water. While inlet closure becomes more probable than not after 7.9 years under the low flow rate scenario, it is a virtual certainty within 15 years in the absence of any form of maintenance dredging. Closure would be the consequence of about 840,000 cubic yards of sand being trapped in the west basin of the lagoon (Jenkins and Wasy1,1997, 2001), representing a permanent loss to the beaches down-drift of the lagoon. The magnitude of

this loss (representing about 50% of the sand yield from the Bataquitos Lagoon Restoration) is quite significant to the down-drift beaches in Leucadia and Encinitas where chronic beach erosion has been the focus of public concern for many years. In addition to the beach impacts, inlet closure at Agua Hedionda would cause a precipitous drop in dissolved oxygen in lagoon waters (possibly even anaerobic) and a progressive transformation to hyper-saline conditions that would devastate the existing food web and related aqua culture. In time, the interior portions of the lagoon would in-fill with up-land sediments and be transformed back into the ephemeral system of marsh channels depicted in Figure 3. Hence, continued maintenance dredging of the west basin of the lagoon is vital for the continued health of the lagoon, as well as for the stability of the down-drift beaches and shoreline. The decisive question in the context of the reduced flow rate scenario is how frequently dredging should be performed.

If the presently practiced bi-annual/tri-annual dredge cycle is continued under the reduced flow rate scenario, the dredge volume will be on average 42.5 % smaller. This is a significant benefit to local beach stability (since less sand will be scavenged by the inflow from the local beach volume for any given 2 or 3 year period). However a bi-annual/tri-annual dredge cycle under reduced flow rate operations will raise the costs of maintaining an open inlet because mobilization/demobilization costs per cubic yard of dredged material will increase, and these are a major component of the total marginal dredge costs. A reasonable alternative is to base dredge scheduling on an equivalent dredge volume (~ 300 to 400 thousand cubic yards) as practiced under the existing bi-annual/tri-annual cycle, since these quantities when held and released from the lagoon appear to have an acceptable degree of impact on local beaches under present dredge permit conditions. Given these parameters, the dredge interval under the reduced flow rate scenario could be extended to once every 4 to 5 years, where rounding to nearest year gives:

$$\frac{(2 \text{ yr to } 3 \text{ yr})(184,724 \text{ yds}^3 / \text{yr})}{106,218 \text{ yds}^3 / \text{yr}} \cong 4 \text{ yr to } 5 \text{ yr} \quad (1)$$

By extending the dredge cycle for low flow operations, the west basin of the lagoon will exist in a partially shoaled condition for a longer period of time. In this condition, the inlet sill depth is reduced and the inlet flow stream must proceed through

constricted equilibrium tidal channels around the inlet bar. The flood flow channel forms along the north-west bank of the west basin immediately east of the HWY 101 bridge, while the ebb channel forms along the opposite bank with the inlet bar bedform lying in between. Typical morphology for this shoaled condition is shown in Figure 6 (taken from the pre-dredge survey of the west basin on 12 October 2002, prior to the 2002 maintenance dredging event). The constricted channels and reduced sill depth prevent the lagoon from fully draining during lower-low tide levels and induce hydraulic losses to friction and turbulence. These effects are referred to as *tidal muting* and reduce the tidal range throughout the interior of the lagoon system. With reduced tidal range, there is typically a reduction in inter-tidal habitat and a shift in the mix of habitat types.

3.0) Effects of Low Flow and Inlet Sedimentation on Tidal Hydraulics

To quantify potential effects associated with protracted periods of operations with a partially shoaled inlet, we perform tidal hydraulic simulations using the west bathymetry from Figure 6. The TIDE_FEM tidal hydraulics model presented in Jenkins and Inman (1999) was gridded for a computational mesh of Agua Hedionda Lagoon as shown in Figure 7, using pre- and post dredging bathymetry from the 2002 dredge event from Jenkins and Wasyl (2003). The pre-dredging bathymetry featured the inlet bar in the west basin that was mapped during the October 2002 sounding shown in Figure 6. The post-dredging survey performed in April 2003 indicated uniform deep water throughout the west basin with depths ranging from -20 ft NGVD to -30ft NGVD, similar to that found in Figure 2-2 of Elwany, et al (2005). The lagoon model was excited at the ocean inlet by the 4.5 year maximum spring tides derived from tidal harmonic constituents for the Scripps Pier tide gage (NOAA Station #941-0230). These tides provide an assessment of the maximum tidal range effects of the pre- and post-dredging bathymetry.

Figure 8 shows how the inlet bar formation in the pre-dredging bathymetry (green) reduces the tidal range in the east basin of the lagoon relative to the tidal response for the post-dredging bathymetry (red) when that bar formation has been removed. The primary effect of the inlet bar on tidal range is to limit the degree to which the lagoon can drain during low tide. In the pre-dredge condition the lower-low water level only drops to -2.7 ft NGVD, as compared to a LLW of -4.0 ft NGVD in the post-dredge condition

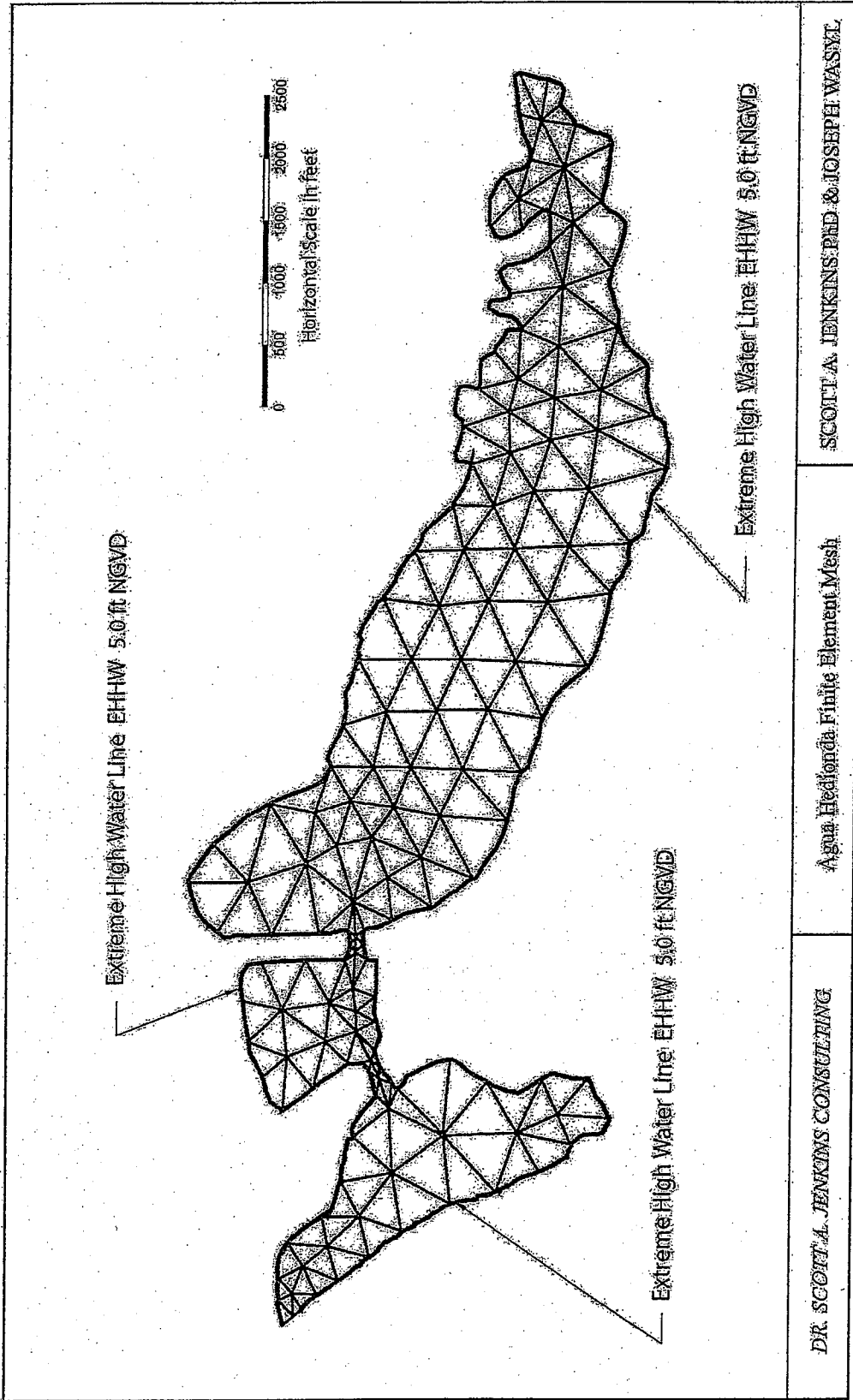


Figure 7. Computational mesh for TIDE_FEM tidal hydraulics model of Agua Hedionda Lagoon.

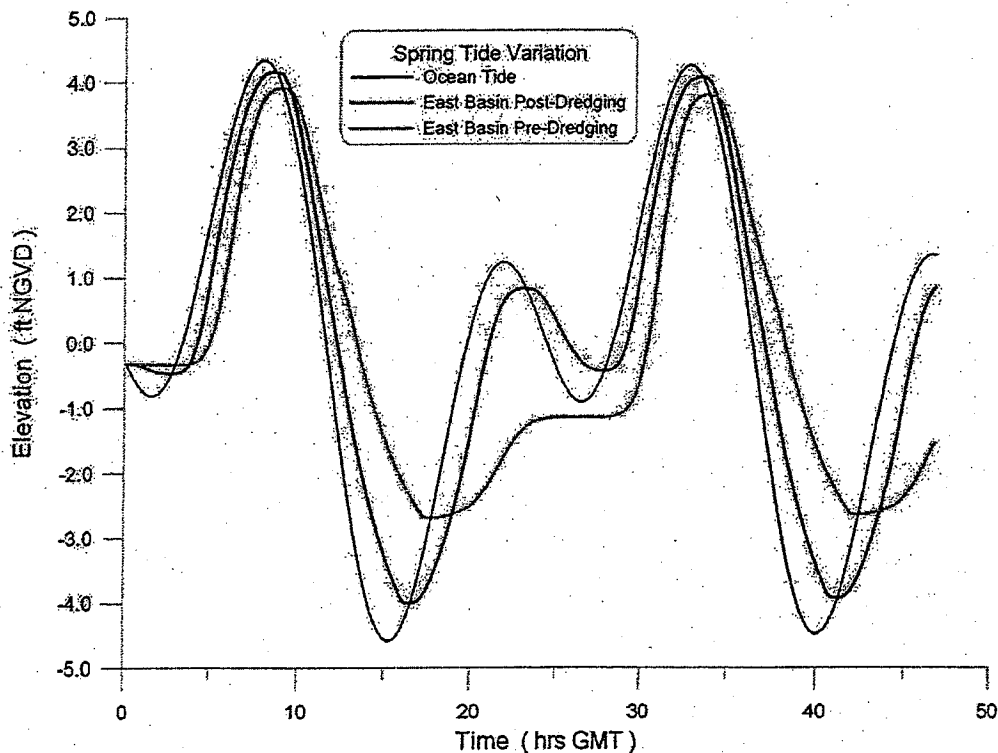


Figure 8. Effect of sedimentation on lagoon tidal range. Pre-dredging tide variation in East Basin (green); Post-dredging tides (red). Pre- and post- dredging tidal variations from TIDE_FEM simulation using ocean tides. Pre-dredging bathymetry from Jenkins & Wasyl 2003.

when the sill caused by the inlet bar is removed. The constricted inlet channels around the inlet bar also cause some muting of the higher-high water levels due to frictional losses and phase lags, with HHW for the pre-dredge condition reaching +3.9 ft NGVD as compared with +4.1 ft NGVD for HHW in the post-dredge condition. Altogether the inlet bar formation reduces the maximum diurnal tidal range by as much as 1.5 ft in the latter stages of west basin sedimentation prior to routine maintenance dredging.

To determine what effect the inlet bar exerts on lagoon habitat, we superimpose the diurnal tidal ranges obtained from hydraulic modeling on the area and volume rating functions of the lagoon derived from recent lagoon surveys by Elwany, et al (2005). Figure 9a shows that the maximum inter-tidal acreage of Agua Hedionda Lagoon is 107.9 acres due to spring tides acting on post-dredge bathymetry with no inlet bar formation. Sub-tidal acreage is 221.4 acres, giving a total lagoon habitat acreage of 329.3 acres post-

maintenance dredging. Later, when shoaling develops in the west basin and a pronounced inlet bar forms, the tidal range is reduced throughout the lagoon and the maximum inter-tidal habitat is reduced by 32.9 acres to 75 acres, as indicated by the pre-dredging assessment in Figure 10a. Sub-tidal acreage is increased by 14.6 acres to 236 acres, because the reduced sill depth over the inlet bar restricts the ability of the lagoon to drain on a falling tide (Figure 8). Tidal muting of the higher-high water levels reduces the total lagoon habitat by 18.8 acres to 311 acres.

Consequently, a cyclical variation in the amount and proportions of lagoon habitat occurs throughout each dredge cycle, with the total lagoon habitat gradually declining by 5.7% following a post-dredging maximum, and reaching a minimum immediately before the mobilization of the next maintenance dredge event. This cyclical variation manifests itself most strongly in the inter-tidal habitat regime, where the habitat acreage declines by 30.5% following a post-dredging maximum. On the other hand, the sub-tidal habitat that supports the lagoon's fisheries varies inversely, with a post-dredging minimum followed by a gradual increase of as much as 6.5% prior to mobilization of the next maintenance dredge event. These variations are already built into the ecology of the present day lagoon and occur gradually enough over the existing bi-annual/tri-annual dredge cycle that significant impacts to that ecology have not been observed. What the reduced flow rate operations of a stand-alone desalination plant would do is extend the period of these variations by another 1 or 2 years (assuming the equivalent dredge volume policy of the previous section is adopted). The magnitude of the cyclical habitat variations would be the same, but those variations would evolve more slowly in time, thereby reducing the rate of cyclical decline of inter-tidal habitat and the rate of growth of sub-tidal habitat. This would give the lagoon ecology a longer response time to adapt to those cyclical changes, and presumably reduce the potential for any adverse consequences that have not yet been identified in the literature.

The other important effect of the inlet bar formation and attendant dredge cycle is on the volume exchange that occurs between the ocean and the lagoon and the residence time of water in the lagoon. Figure 9b finds that the maximum diurnal tidal prism for the post-dredge bathymetry (no inlet bar) is 2,286 acre ft. This result obtained by hydraulic simulation for the 4.5 yr spring tide maximums agrees closely with the result of 2125

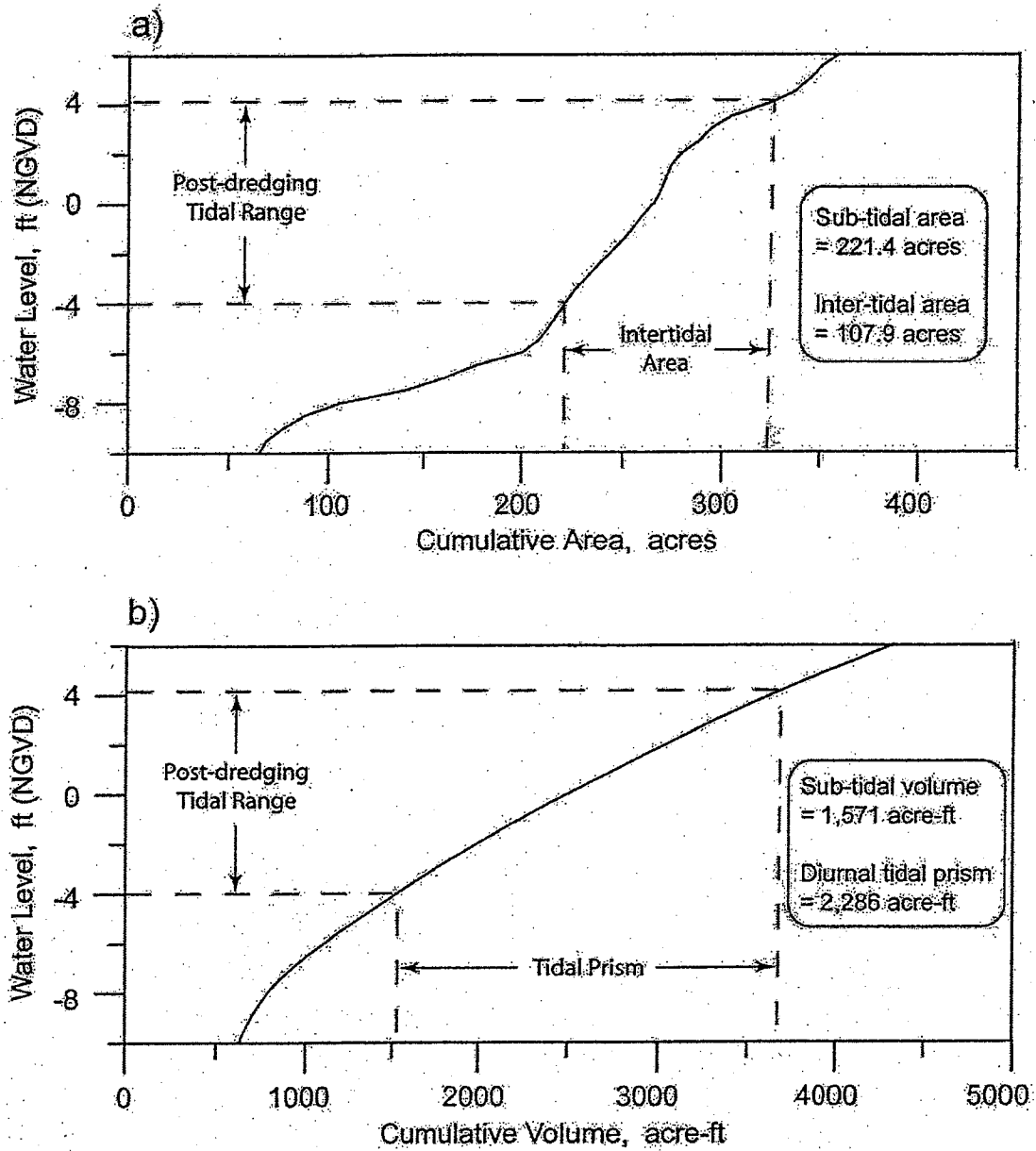


Figure 9. Post-dredging tidal hydraulics with West Basin inlet bar removed: a) Sub-tidal area and intertidal area during spring tide; b) Sub-tidal volume and diurnal tidal prism. Wetted area and volume function from Elwany et al., (2005).

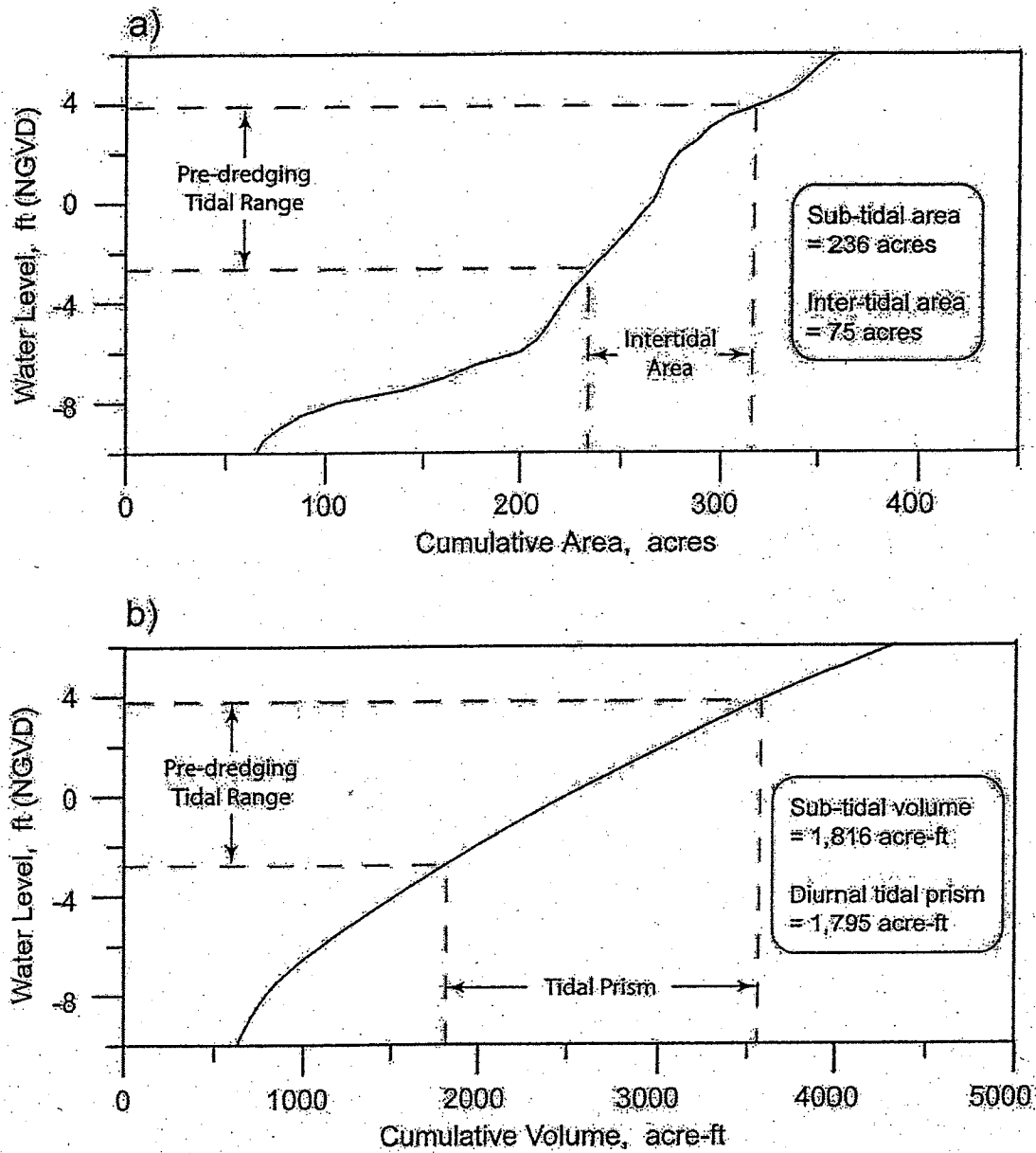


Figure 10. Pre-dredging tidal hydraulics with West Basin inlet bar per Figure 6: a) Sub-tidal area and intertidal area during spring tide; b) Sub-tidal volume and diurnal tidal prism. Wetted area and volume function from Elwany et al., (2005).

acre-ft obtained by water level measurements during spring tides in June 2005, as reported in Elwany (2005). This small discrepancy can be attributed to the larger tidal range of the ocean tides used in the hydraulic simulation in Figure 8. The hydraulic simulation in Figure 10b for the pre-dredge conditions (with well developed inlet bar) finds that the maximum diurnal tidal prism is reduced by 491 acre-ft to 1,795 acre-ft.

Thus, the west basin sedimentation diminishes the maximum diurnal prism of the lagoon by 21.5% over the course of a dredge cycle, and nearly 70% of this loss occurs in the east basin of the lagoon. Because the mass exchange between the east basin and the remainder of the lagoon is purely tidal in nature, the loss of tidal prism due to west basin sedimentation will impact the residence time of water in the highly productive east basin habitat zones. Figure 11 presents the water mass exchange rating functions of the east basin for pre- and post-dredging bathymetry. The hydraulic simulation (black) for the post-dredge bathymetry (with no inlet bar formation) gives a residence time of 3.7 days for water in the east basin. Here, residence time is taken as that point on the exchange rating curve when the percentage of old water declines to 2%. This compares with a mean value of 3.2 days reported in Elwany et al (2005) based on water level and velocity measurements over a one month period in June 2005. This is regarded as an insignificant difference that could easily be explained by differences between the 2003 bathymetry used in the hydraulic simulation versus the 2005 bathymetry that prevailed in the 2005 field measurements of Elwany et al (2005). With the reduction of tidal prism caused by the inlet bar formation, the residence time in the east basin is increased by 1 day to 4.7 days for pre-dredge bathymetry. Hence, the residence time in the largest basin of the lagoon experiences a cyclical increase of 27% of the course of the presently practiced bi-annual/tri-annual dredge cycle. This variation is not viewed to be significant as the residence time remains relatively short and oxygen deficiency or anoxic conditions have never been reported under present dredge practices. The effect of the of reduced flow operations of a stand alone desalination plant will not change the magnitude of this cyclical variation since mass exchange between the east and west basins is purely tidal. However, increasing the length of dredge cycle by 1 or 2 years under the reduced flow rate will increase the period of the residence time cycle by an equivalent duration.

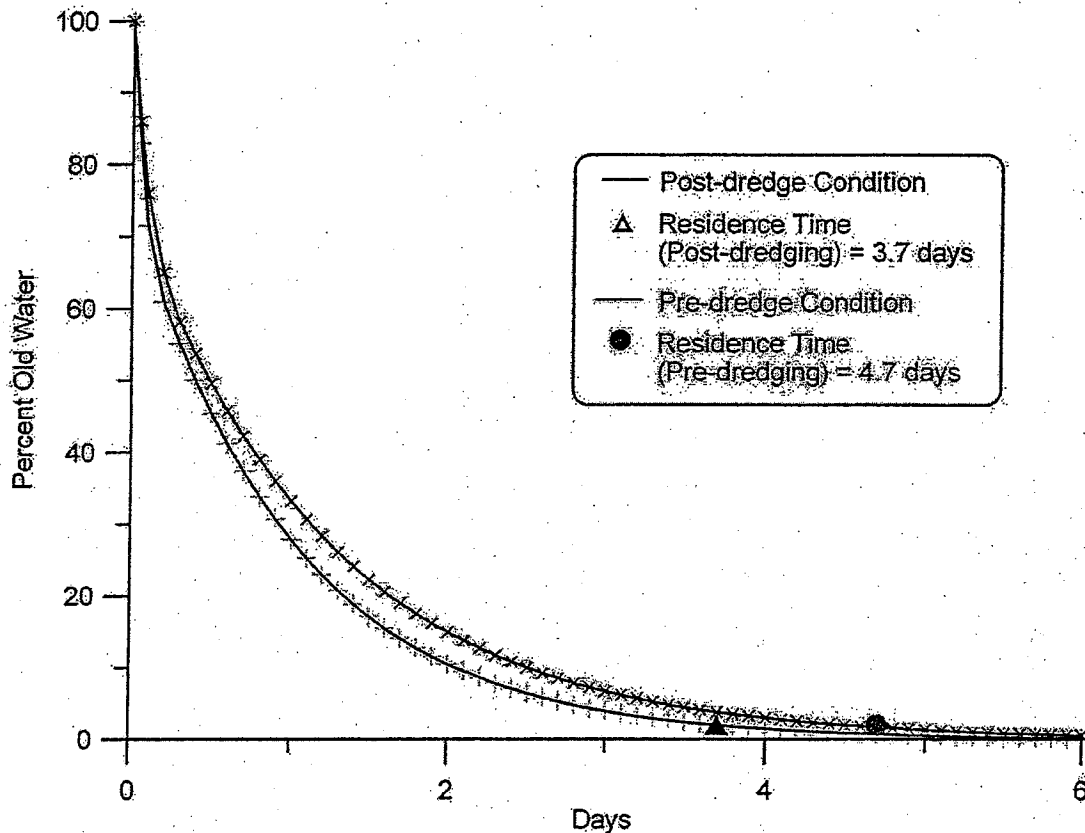


Figure 11. Water mass exchange rating function and residence time in the East Basin of Agua Hedionda Lagoon for pre-dredge (red) and post-dredge (black) bathymetry.

The effect of this longer cycle period, again, slows the rate at which biology must adapt to the cyclical increases residence time.

Reduced flow operations will affect the fluxes of nutrients and oxygen into the west basin. As commented in Section 2.2, fluxes of nutrients adsorbed to the surfaces of suspended sediment that enter the lagoon through the ocean inlet will be reduced by 42.5% under the low flow rate scenario. However, most of these sediments are sand sized and carry little if any nutrient load. The predominant nutrient load entering the lagoon through the ocean inlet is in the form of neutrally buoyant organisms and organic particles, colloids, and dissolved organic matter and oxygen. These constituents are fluxed with the inflow stream, and will be reduced by lower once-through flow rates

through the plant, or by diminished tidal prism through the tidal muting effects of the inlet bar.

Elwany et al (2005) determined that on average, 46% of the daily inflow stream through the inlet was due to the power plant cooling water consumption based on water level and velocity measurements during the 5 week period between 1 June 2005 and 7 July 2005. Taking an average power plant flow rate during that period of 529 mgd and an average tidal prism of 1,700 acre ft, the flux balance obtained from this finding indicates that only 29% of the daily inflow volume would be due to the plant's circulation pumps under a low flow rate assumption of 304 mgd. This flow rate reduction would reduce the daily volume flux of new water and dissolved nutrients into the lagoon by 10.1%. However, the plants impact on dissolved nutrient influx becomes less during spring tides when a larger fraction of the inflow stream is due to pure tidal exchange (see Figure 1). The hydraulic model simulations for tidal exchange during spring tides with the post-dredge bathymetry (red line, Figure 8) indicate that only 36.4% of the daily inflow of new water is due to the power plant operating at its average annual flow rate of 529 mgd. If the plant flow rate is dropped to 304 mgd under the low flow rate scenario, then 22.7% of the daily inflow during spring tides (post-dredging) is due to the action of circulation pumps, and the nutrient flux will be reduced by 8% relative to present average pumping rates during power generation. When the west basin is in a pre-dredge configuration with a well developed inlet bar, the spring tide daily nutrient flux into the lagoon is reduced by 17.4% under present average flow rates of 529 mgd, and by 18.9% under the low flow scenario (304 mgd). Hence, inlet sedimentation and cyclical dredging causes a greater reduction on nutrient flux than would the reduction in plant flow rate under the low flow scenario of a stand alone desalination plant.

Summary and Conclusions:

Coastal processes and tidal hydraulic effects arising from reduced once-through flow rates at the Encina Generating Station, Carlsbad, CA are evaluated in the context of stand-alone operations of a co-located desalination plant. Stand alone desalination involves a once through flow rate of 304 mgd at the intake structure located at the southern end of the west basin of Agua Hedionda Lagoon. This flow rate would limit

end-of-pipe salinity to no more than 40 ppt. The existing cascade of circulation and service water pumps available at Encina Generating Station can provide a maximum once-through flow rate of 808 mgd, but averages about 530 over the long term. Thus the flow rates passing through the Encina facility during stand-alone desalination operations would be about 43% less than the present average when power generation is occurring, and 62% less than the peak flow rate capability.

If the flow rate is reduced to 304 mgd under the scenario of a stand-alone desalination plant, then dredge records indicate that the average sand influx rates into the lagoon through the ocean inlet would be reduced to 106,218 yds³/yr from a present rate of 184,724 yds³/yr. This represents a 42.5% reduction in sand influx rates into the lagoon relative to the present power generation operating scenario. The reduction in sand influx rates reduces the accumulation of inlet closure risk to only 6.3% per year, extending the safe interval for no dredge maintenance to 7.9 years before inlet closure would become more likely than not. Assuming the present marginal dredge cost of \$2.70 per cubic yard, the annual cost of maintaining an open inlet under the reduced flow scenario would be \$287,000 per year as compared to present maintenance costs of \$499,000 per year. If dredge scheduling is based on an equivalent dredge volume (to minimize beach impacts) as practiced under the existing bi-annual/tri-annual cycle, the dredge interval under the reduced flow rate scenario could be extended to once every 4 to 5 years.

Under existing conditions with high flow rate power generation activity, a cyclical variation in the amount and proportions of lagoon habitat occurs throughout each dredge cycle, with the total lagoon habitat gradually declining by 5.7% following a post-dredging maximum, and reaching a minimum immediately before the mobilization of the next maintenance dredge event. This cyclical variation manifests itself most strongly in the inter-tidal habitat regime, where the habitat acreage declines by 30.5% following a post-dredging maximum. On the other hand, the sub-tidal habitat that supports the lagoon's fisheries varies inversely, with a post-dredging minimum followed by a gradual increase of as much as 6.5% prior to mobilization of the next maintenance dredge event. These variations are already built into the ecology of the present day lagoon and occur gradually enough over the existing bi-annual/tri-annual dredge cycle that significant impacts to that ecology have not been observed. What the reduced flow rate operations of

a stand-alone desalination plant would do is extend the period of these variations by another 1 or 2 years (assuming the equivalent dredge volume policy as stated above). The magnitude of the cyclical habitat variations would be the same, but those variations would evolve more slowly in time, thereby reducing the rate of cyclical decline of inter-tidal habitat and the rate of growth of sub-tidal habitat. This would give the lagoon ecology a longer response time to adapt to those cyclical changes.

The dredge cycle under existing high flow rate operations also impacts the volume exchange that occurs between the ocean and the lagoon, causing a cyclical variation in the residence time of water in the lagoon. West basin sedimentation diminishes the maximum diurnal prism of the lagoon by 21.5% over the course of a dredge cycle, and nearly 70% of this loss occurs in the east basin of the lagoon. With the reduction of tidal prism caused by the inlet bar formation, the residence time in the east basin is increased by 1 day to 4.7 days. Hence, the residence time in the largest basin of the lagoon experiences a cyclical increase of 27% over the course of the presently practiced bi-annual/tri-annual dredge cycle. This variation is not viewed to be significant as the residence time remains relatively short and oxygen deficiency or anoxic conditions have never been reported under present dredge practices. The effect of the of reduced flow operations of a stand alone desalination plant will not change the magnitude of this cyclical variation since mass exchange between the east and west basins is purely tidal. However, increasing the length of dredge cycle by 1 or 2 years under the reduced flow rate scenario will increase the period of the residence time cycle by an equivalent duration. The effect of this longer cycle period, again, slows the rate at which biology must adapt to the cyclical increases residence time.

Reduced flow operations will affect the fluxes of nutrients and oxygen into the west basin. Flow rate reductions to 304 mgd would reduce the average daily volume flux of new water and dissolved nutrients into the lagoon by 10.1%, (assuming a mean tidal range). However, the plant's impact on dissolved nutrient influx becomes less during spring tides when a larger fraction of the inflow stream is due to pure tidal exchange. Under the low flow rate scenario, nutrient flux will be reduced by 8% relative to present average pumping rates during power generation. When the west basin is in a pre-dredge configuration with a well developed inlet bar, the spring tide daily nutrient flux into the

lagoon is reduced by 17.4% under present average flow rates of 529 mgd, and by 18.9% under the low flow scenario (304 mgd). Hence, inlet sedimentation and cyclical dredging causes a greater reduction on nutrient flux than would the reduction in plant flow rate under the low flow scenario of a stand alone desalination plant.

In conclusion, the reduced flow rate operations of a stand alone desalination plant co-located at Encina Generating Station will reduce the capture rates of littoral sediment that presently occur under higher flow rates associated with power generation, thereby reducing the environmental impacts associated with maintenance dredging. Reduced flow rate operations will not increase the magnitude of cyclical variations in habitat or residence time that presently occur throughout each maintenance dredge cycle, but will increase the length of time over which those variations occur. Low flow rate operations will result in reductions of 8% to 10% in the fluxes dissolved nutrients and oxygen into the lagoon through the ocean inlet, but this effect is relatively minor in comparison to the 17.4% decline in nutrient flux that occurs in the latter stages of each dredge cycle. On balance, low flow operations do not appear to create any significant adverse impacts on either the lagoon environment or the local beaches; and it could be argued that the reduction in capture rates of littoral sediment is a project benefit.

Bibliography

- Abbott, M. B., A. Damsgaard and G. S. Rodenhuis, 1973, A System 21, Jupiter, @ *Jour. Hydraulic Res.*, v. 11, n. 1.
- Connor, J. J. and J. D. Wang, 1973, A finite element modeling of two-dimensional hydrodynamic circulation, @ *MIT Tech. Rpt.*, #MITSG 74-4, p. 1-57.
- Elwany, M. H. S., A. L. Lindquist, R. E. Flick, W. C. O'Reilly, J. Reitzel and W. A. Boyd, 1999, "Study of Sediment Transport Conditions in the Vicinity of Agua Hedionda Lagoon," submitted to California Coastal Commission, San Diego Gas & Electric, City of Carlsbad.
- Elwany, M. H. S., R. E. Flick, M. White, and K. Goodell, 2005, "Agua Hedionda Lagoon Hydrodynamic Studies," prepared for Tenera Environmental, 39 pp. + appens.
- Ellis, J.D., 1954, "Dredging Final Report, Agua Hedionda Slough Encina Generating Station," San Diego Gas and Electric Co., 44pp.
- Gallagher, R. H., 1981, *Finite Elements in Fluids*, John Wiley & Sons, New York, 290 pp.
- Inman, D. L., M. H. S. Elwany and S. A. Jenkins, 1993, "Shorerise and bar-berm profiles on ocean beaches," *Jour. Geophys. Res.*, v. 98, n. C10, p. 18,181-199.
- Inman, D. L. & S. A. Jenkins, 1999, "Climate change and the episodicity of sediment flux of small California rivers," *Jour. Geology*, v. 107, p. 251-270.

- Inman, D. L. & S. A. Jenkins, 2004, "Scour and burial of objects in shallow water," p. 1020-1026 in M. Schwartz, ed., *Encyclopedia of Coastal Science*, Kluwer Academic Publishers, Dordrecht, Netherlands.
- Jenkins, S. A. and D. W. Skelly, 1988, "An Evaluation of the Coastal Data Base Pertaining to Seawater Diversion at Encina Power Plant Carlsbad, CA," submitted to San Diego Gas and Electric, Co., 56 pp.
- Jenkins, S. A., D. W. Skelly, and J. Wasyl, 1989, "Dispersion and Momentum Flux Study of the Cooling Water Outfall at Agua Hedionda," submitted to San Diego Gas and Electric, Co., 36 pp. + appens.
- Jenkins, S. A. and J. Wasyl, 1993, "Numerical Modeling of Tidal Hydraulics and Inlet Closures at Agua Hedionda Lagoon," submitted to San Diego Gas and Electric, Co., 91 pp.
- Jenkins, S. A. and J. Wasyl, 1994, "Numerical Modeling of Tidal Hydraulics and Inlet Closures at Agua Hedionda Lagoon Part II: Risk Analysis," submitted to San Diego Gas and Electric, Co., 46 pp. + appens.
- Jenkins, S. A. and J. Wasyl, 1995, "Optimization of Choke Point Channels at Agua Hedionda Lagoon using Stratford Turbulent Pressure Recovery," submitted to San Diego Gas and Electric, Co., 59 pp.
- Jenkins, S. A. and J. Wasyl, 1997, "Analysis of inlet closure risks at Agua Hedionda Lagoon, CA and potential remedial measures, Part II," submitted to San Diego Gas and Electric, Co., 152 pp. + appens.
- Jenkins, S. A. and J. Wasyl, 1998a, Analysis of Coastal Processes Effects Due to the San Dieguito Lagoon Restoration Project: Final Report, submitted to Southern California Edison Co., 333 pp.
- Jenkins, S. A. and J. Wasyl, 1998b, Coastal Processes Analysis of Maintenance Dredging Requirements for Agua Hedionda Lagoon, submitted to San Diego Gas and Electric Co., 176 pp. + appens.
- Jenkins, S. A. and D. L. Inman, 1999, A Sand transport mechanics for equilibrium in tidal inlets, *Shore and Beach*, vol. 67, no. 1, pp. 53-58.
- Jenkins, S. A. and J. Wasyl, 2001, Agua Hedionda Lagoon North Jetty Resoration Project: Sand Influx Study, submitted to Cabrillo Power LLC., 178 pp. + appens.
- Jenkins, S. A. and J. Wasyl, 2003, Sand Influx at Agua Hedionda Lagoon in the Aftermath of the San Diego Regional Beach Sand Project, submitted to Cabrillo Power LLC., 95 pp. + appens
- Jenkins, S. A. and J. Wasyl, 2005, Hydrodynamic Modeling of Dispersion and Dilution of Concentrated Sea Water Produced by the Ocean Desalination Project at the Encina Power Plant, Carlsbad, CA. Part II: Saline Anomalies due to Theoretical Extreme Case Hydraulic Scenarios, submitted to Poseidon Resources, 97 pp.
- Jenkins, S. A. and D. L. Inman, 2006, "Thermodynamic solutions for equilibrium beach profiles", *Jour. Geophys. Res.*, v.3, C02003, doi:10.1029, 21pp.
- Leendertse, J. J., 1970, AA water quality model for well-mixed estuaries and coastal seas, @ vol. I, *Principles of Computation*, Memorandum RM-6230-RC, The Rand Corporation, Santa Monica, California, Feb.
- Liebeck, R. H., 1976, "On the design of subsonic airfoils of high lift," paper no. 6463, McDonnell Douglas Tech. Report, 25 pp.
- Liebeck, R.H., and Ormsbee, A.I., "Optimization of Airfoils for Maximum Lift," *AIAA*

- Journal of Aircraft*, v. 7, n. 5, Sept-Oct 1970.
- McCormick, B., 1979, *Aerodynamics, Aeronautics and Flight Mechanics*, John Wiley & Sons, New York, 652 pp.
- NOAA, 1998, A Verified/Historical Water Level Data@
http://www.opsd.nos.noaa.gov/data_res.html
- Stratford, B.S., 1959, The Prediction of Separation of the Turbulent Boundary Layer, *Jour. Fluid Mech.*, v. 5.
- Stratford, B.S., 1959, An Experimental Flow with Zero Skin Friction Throughout its Region of Pressure Rise, *Jour. Fluid Mech.*, v. 5.
- Weiyan, T., 1992, *Shallow Water Hydrodynamics*, Water & Power Press, Hong Kong, 434 pp.

APPENDIX-A: Beach Nourishment Projects Near Agua Hedionda Lagoon

The lagoon prior to the late 1980's typically ingested 200-300 cubic yards per day unless major up-drift nourishment occurred along Oceanside and Carlsbad beaches.

Table 3 gives a listing of all dredge disposal and beach nourishment activities occurring in the neighborhood of Agua Hedionda due to activities outside the lagoon's operation. Major beach building projects at Oceanside and Carlsbad were undertaken in 1963, 1973, 1982, 1994 and 2001. The most dramatic example of this updrift nourishment impact resulted from the massive beach nourishment projects in 1982 when 923,000 cubic yards of new sand was truck hauled from the San Luis Rey River and placed on Oceanside beaches. Coincidentally, the 1983-85 biannual maintenance dredging cycle of the west basin of Agua Hedionda yielded 447,464 cubic yards. This corresponded to an average daily influx rate of 613 cubic yards per day during that two year period. Such high daily influx rates had not been seen since 1960 when 841,200 cubic yards of beach nourishment was placed on Oceanside beaches following new construction dredging and enlargement of Oceanside Harbor facilities.

After the late 1980's there was only one minor new beach nourishment project in Oceanside, involving 40,000 cubic yards in 1994. However beginning in 1988, the City of Carlsbad imposed conditions requiring back-passing defined fractions of the Agua Hedionda dredge volume north of the inlet. In 1988, 103,000 cubic yards were back-passed from Agua Hedionda to North Beach (Figure 1), resulting in an influx of 458,793 cubic yards into Agua Hedionda Lagoon by 1990, for an influx rate of about 630 cubic yards per day. During 89 days of dredging operations between December 20, 1993 and April 26, 1994, there were 74,825 cubic yards placed immediately north (updrift) of the Agua Hedionda Lagoon and inlet jetty at the North Beach disposal site. The daily influx rate during this 89 day period rose to an average of 782 cubic yards per day. In 1996 there was 106,416 cubic yards of back-passing dredged sands from Agua Hedionda to North Beach and influx rates increased to 540 cubic yards per day in the year that followed. Although the volume of back-passing has been small relative to prior nourishment efforts in Oceanside, its effect on influx was large due to the close proximity of North Beach to the inlet of Agua Hedionda and the low retention of sand on this beach in the presence of rocky substrate immediately offshore, Elwany et al. (1999) .

Table 3: Dredge Disposal and Beach Nourishment Occurring Outside of Agua Hedionda Lagoon Operations

Year	Amt. Dredged (yd ³)	Material Source	Disposal Location	Comments
1942	500000	Del Mar Boat Basin	Increase grade around Boat Basin	Material was not placed on the beach
1944	200000	Entrance Channel	Upland	Material was not placed on the beach
1955	800,000	Harbor Construction	Oceanside Beach	Dredged Material
1960	41,000	Entrance Channel	Oceanside Beach	Dredged Material
1961	481,000	Channel	Oceanside Beach	Dredged Material
1963	3,800,000	Harbor	Oceanside Beach	1.4myd3 was new
1965	111,000	Entrance Channel	Oceanside Beach	Dredged Material
1966	684,000	Entrance Channel	2 nd St.-Wisconsin St.	Dredged Material
1967	178,000	Entrance Channel	3 rd St.-Tyson St.	Dredged Material
1968	434,000	Entrance Channel	River-Wilconsin St.	Dredged Material
1969	353,000	Entrance Channel	River-3rd	Dredged Material
1971	552,000	Entrance Channel	3 rd -Wisconsin St.	Dredged Material
1973	434,000	Santa Margarita R.	Tyson-Wisconsin St.	New Material-Beach
1974	560,000	Entrance Channel	Tyson-Whitterby	Dredged Material
1976	550,000	Entrance Channel	Tyson-Whitterby	Dredged Material
1977	318,000	Entrance Channel	Tyson-Whitterby	Dredged Material
1981	403,000	Entrance Channel	6 th St.-Buccaneer	Dredged Material
1981	403,000	Offshore Borrow Site	Oceanside Beach	Dredged Material
1982	923,000	San Luis Rey R.	Oceanside Beach	New Material-Beach
1983	475,000	Entrance Channel	Tyson Street	Dredged Material
1986	450,000	Entrance Channel	Tyson Street	Dredged Material
1988	220,000	Entrance Channel	Tyson Street	Dredged Material
1990	250,000	Entrance Channel	Tyson Street	Dredged Material
1992	106,700	Bypass System	Tyson Street	Dredged Material
1993	483,000	Modified Entrance	Tyson Street	Dredged Material
1994	40,000	Santa Margarita R.	Wisconsin St.	New Material-Beach
1994	161,000	Entrance Channel	Nearshore Wisconsin	Dredged Material
1994	150,000	Bataquitos Lagoon	Inlet South Side	New Material-Beach

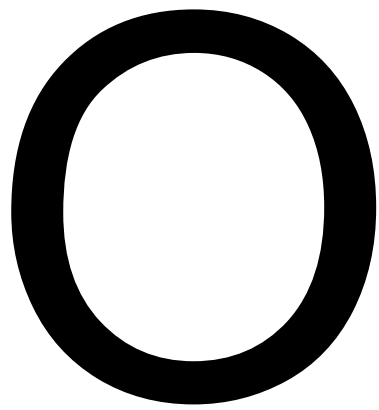
Table 3: (continued)

Year	Amt. Dredged (yd ³)	Material Source	Disposal Location	Comments
1995	1,600,000	Bataquitos Lagoon	Ponto Beach	New Material-Beach
1996	162,000	Entrance Channel	Nearshore Wisconsin	Dredged Material
1997a	150,000	Entrance Channel	Nearshore Oceanside	
1997b	100,000	Entrance Channel	Wisconsin St.	Dredged Material
	17,316,700	Total		
	178,017	Average (only including maintenance dredging)		

Following the east basin dredge project, 202,530 cubic yards were back-passed to North Beach in April 1999. A dredge survey in July 2000 determined that 360,800 cubic yards had influxed into the lagoon, increasing the daily rate to an average of 846 cubic yards per day. Altogether the percentage of lagoon dredging that has been back-passed to North Beach averages 14.7% of the total dredge volume during the 1981-2000 model period. The remaining fraction of dredge volume that was not back-passed was divided between the Middle and South Beach disposal sites. This fraction was historically split in an 85% to 15% ratio between Middle and South Beach.

In 1994-95 a major beach building effort was conducted at Ponto Beach immediately to the south of Agua Hedionda, where 1,750,000 cubic yards of beach fill was placed using dredged material from the construction of the Bataquitos Lagoon Restoration. The most recent beach building project to impact Agua Hedionda was the San Diego Regional Beach Sand Project completed in September 2001. This project placed 1.83 million cubic yards of on beaches between Oceanside and Torrey Pines, of which 921,000 cubic yards were placed in the nearfield of Agua Hedionda. Within one year following completion of the 2001 maintenance dredging of the lagoon, it was necessary to dredge the lagoon again to remove an additional 196,000 cubic yards from the west basin of the lagoon, despite an extremely dry year with below normal wave climate. During this one year period, the average wave height was only 0.8 m, which in the absence of the San Diego Regional Beach Sand Project, should have produced a sand influx volume of only 103,500 cubic yards (Jenkins and Wasyl, 2003).

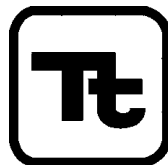
Table 3 indicates that, historically, sand influx rates rise dramatically in years during and immediately following beach nourishment activities in Oceanside or back-passing in Carlsbad. This is additional evidence to validate conclusions of Inman & Jenkins (1983) that longshore transport rate in this region is sand supply limited. In other words, there is more potential transport than the available sand supply can sustain. Any artificial intervention to increase up-drift sand supply will apparently increase longshore transport rates, and thereby increase the rate of sand influx into the lagoon.



Agua Hedionda Watershed Water Quality Analysis and Recommendations Report

Prepared for:
**City of Vista
California**

Prepared by:



TETRA TECH, INC.
1230 Columbia Street
Suite 1000
San Diego, CA 92101

December 2007

Table of Contents

- 1 Introduction 1
- 2 Description of Watershed 3
 - 2.1 Physical Features 4
 - 2.1.1 Geology, Soils, Topography 4
 - 2.1.2 Hydrology 7
 - 2.1.3 Beneficial Uses 9
 - 2.1.4 Land Use and Land Cover 12
 - 2.2 Human Environment 20
 - 2.2.1 Point Sources 20
 - 2.2.2 Sewered/Unsewered Areas 21
 - 2.2.3 Agriculture 23
- 3 Water Quality Assessment 25
 - 3.1 Impaired Waters 25
 - 3.2 Lagoon Monitoring 25
 - 3.2.1 Lagoon Sediment Monitoring 25
 - 3.2.2 Co-permittees’ Coastal Storm Drain Monitoring 26
 - 3.3 Existing Watershed Monitoring Data 26
 - 3.3.1 Data Sources 27
 - 3.3.2 Water Quality Parameter Summaries 29
 - 3.3.3 Metals 39
 - 3.3.4 Bacteria 40
 - 3.3.5 Pesticides 44
 - 3.3.6 Toxicity 45
 - 3.3.7 Benthic Macroinvertebrates 45
 - 3.4 Summary of Water Quality Data 46
- 4 Future Monitoring Recommendations 49
- 5 References 51
- Appendix A. Physicochemical Data 53
- Appendix B. Nutrient Data 61
- Appendix C. Bacterial Data 67
- Appendix D. Pesticide Data 75
- Appendix E. Metals Data 83

List of Tables

Table 1.	Key to Geology within the Agua Hedionda Watershed.....	5
Table 2.	Most Abundant Soils Series within the Agua Hedionda Watershed.....	5
Table 3.	Average Daily Discharge (cfs) Summary Statistics at Agua Hedionda Creek and El Camino Real	9
Table 4.	Agua Hedionda Watershed Existing Beneficial Uses for Inland Surface Waters.....	10
Table 5.	Agua Hedionda Watershed Existing Beneficial Uses for Coastal Waters	11
Table 6.	Agua Hedionda Watershed Beneficial uses for Groundwaters	12
Table 7.	Percent of Watershed for Each Land Use Class in 1986, 2007, and 2030.....	13
Table 8.	Vegetation Community Types in Agua Hedionda Watershed	18
Table 9.	Acreage of Invasive Plant Species Present in the Agua Hedionda Watershed (SELIC).....	18
Table 10.	San Diego Regional Board 2006 Clean Water Act Section 303d List of Water Quality Limited Segments for the Agua Hedionda Watershed.....	25
Table 11.	Summary of Existing Watershed Monitoring	29
Table 12.	Wet Weather Water Quality Summary Statistics.....	30
Table 13.	Ambient Dry Weather Water Quality Summary Statistics	31
Table 14.	Storm Drain Dry Weather Water Quality Summary Statistics	32
Table 15.	Turbidity Measurements (in NTU) Taken at Wet Weather, Ambient, and Storm Drain Sites.....	34
Table 16.	Wet Weather Nitrogen Summary Statistics	37
Table 17.	Wet Weather Phosphorus Summary Statistics.....	38
Table 18.	Criteria Exceedances for Co-Permittee Wet Weather Metals.....	40
Table 19.	Total Coliform (MPN/100ml) Summary Statistics for Wet Weather, Ambient, and Storm Drain Data.....	40
Table 20.	Fecal Coliform (MPN/100ml) Summary Statistics for Wet Weather, Ambient, and Storm Drain Data.....	40
Table 21.	Enterococcus (MPN/100ml) Summary Statistics for Wet Weather, Ambient, and Storm Drain Data.....	41
Table 22.	Co-permittee Wet Weather Pesticide Summary Statistics	44
Table 23.	Ambient Dry Weather Pesticide Summary Statistics.....	44
Table 24.	Storm Drain Dry Weather Pesticide Summary Statistics.....	44
Table 25.	Co-permittee Wet Weather Toxicity Summary Statistics	45
Table 26.	Index of Biotic Integrity Scores for Agua Hedionda Monitoring Sites (table taken from Foundation report).....	46

List of Figures

Figure 1.	Agua Hedionda Watershed	3
Figure 2.	Geology of the Agua Hedionda Watershed.....	4
Figure 3.	Soils in the Agua Hedionda Watershed	6
Figure 4.	Slopes in the Agua Hedionda Watershed.....	6
Figure 5.	Erosion Risk in the Agua Hedionda Watershed.....	7
Figure 6.	Federal Emergency Management Agency’s (FEMA) Flood Plain Classifications for the Watershed.....	8
Figure 7.	Average Daily Discharge at the Agua Hedionda Creek and El Camino Real Flow Gage (2005-2007).....	9
Figure 8.	Past Land Use (1986) within the Agua Hedionda Watershed.....	14
Figure 9.	Current Land Use within the Agua Hedionda Watershed.....	14
Figure 10.	Planned Land Use within the Agua Hedionda Watershed (Final 2030 City/County Forecast)	15
Figure 11.	Percent Impervious Surface Cover by Subbasins	16
Figure 12.	Cumulative Upstream Percent Impervious Surface Cover by Subbasin.....	17
Figure 13.	Vegetation Communities Available in the Watershed	17
Figure 14.	Invasive Plant Species Present in the Watershed.....	19
Figure 15.	Public and Private Open Space Distribution, 2007	20
Figure 16.	Potential Sources of Water Quality Impairment	21
Figure 17.	Stormwater and Sewer Line Distribution in the Agua Hedionda Watershed.....	22
Figure 18.	Non-Sewered Development in the Agua Hedionda Watershed	22
Figure 19.	Classification of Agricultural Land Use Intensity in the Agua Hedionda Watershed (SANDAG)	23
Figure 20.	Monitoring Stations in the Agua Hedionda Watershed	28
Figure 21.	Distribution of pH Measurement Collected as Part of the Co-permittee Dry Weather Storm Drain Monitoring	33
Figure 22.	Turbidity Measurements Taken at the Co-permittee Wet Weather Site Between 1999 and 2007 (Line Represents WQO of 20 NTU)	34
Figure 23.	Total Suspended Solids at the Co-permittee Wet Weather Site between 1998 and 2007.....	35
Figure 24.	Distribution of Salinity Measurements (ppt) Collected As Part of the Co-permittee Dry Weather Storm Drain Monitoring	36
Figure 25.	Total Dissolved Solids at the Co-permittee Wet Weather Site between 1998 and 2007 (Line Represents a WQO of 500mg/L).....	36
Figure 26.	Total Nitrogen Data Collected at the Co-permittee Wet Weather Site (1999-2007)	38
Figure 27.	Total Phosphorus Data from the Co-permittee Wet Weather Site Collected Between 1998 and 2007 (Line Represents WQO 0.1 mg/L)	39

Figure 28. Fecal Coliform Wet (Dark Blue) and Dry (Light Green) Data Collected from Agua Hedionda Creek at the Co-permittee Wet Weather Site (Line Represents WQO)..... 42

Figure 29. Enterococcus Wet (Dark Blue) and Dry (Light Green) Data Collected from the Agua Hedionda Creek at the Co-permittee Wet Weather Site 42

Figure 30. Fecal Coliform Spatial Distribution of Ambient Dry Weather Data from the Co-permittee Dry Weather and San Elijo Lagoon Conservancy Data..... 43

Figure 31. Enterococcus Spatial Distribution of Co-permittee Dry Weather Storm Drain Data (mean values)..... 43

1 Introduction

The following review of watershed and water quality data represents one of the initial components of a comprehensive effort to prepare a Watershed Management Plan (WMP) in the Agua Hedionda Watershed. This report satisfies Work Item No. 2.3.5, Water Quality and Recommendations Report per State Water Board Agreement No. 06-139-559-0. The report provides a general watershed characterization and a summary of past and current water quality conditions in the Agua Hedionda watershed. Using various regional and local datasets and previous assessment reports, this review describes both spatial and temporal trends in the watershed to evaluate current water quality conditions and provide recommendations to best meet existing and future regulatory and planning needs.

The health of the Agua Hedionda Watershed is subject to many stressors that can best be addressed through a comprehensive and strategically focused WMP. In response to the Clean Water Act Section 303(d), the San Diego Regional Water Quality Control Board (SDRWQCB) has identified waters that do not meet applicable water quality objectives including the Agua Hedionda Lagoon, Agua Hedionda Creek, and Buena Creek (SDRWQCB, 2007). The SDRWQCB is in the process of developing Total Maximum Daily Loads (TMDLs) for Agua Hedionda Creek and Agua Hedionda Lagoon. Other important considerations for the WMP are municipal separate storm sewer systems (MS4) permit requirements for management of increases in runoff from new development and preparation of a Hydromodification Management Plan. Monitoring is required to evaluate program effectiveness under this permit. Both the stormwater permit and TMDLs play heavily in this water quality evaluation and future planning.

(This page left intentionally blank.)

2 Description of Watershed

The Agua Hedionda watershed is located in San Diego County and within the Carlsbad Hydrologic Unit. It is approximately 18,837 acres (29.4 mi²) and is divided into two subareas: the Buena hydrologic subarea (904.32) in the upper watershed and Los Monos hydrologic subarea (904.31) in the lower watershed (Figure 1)¹. The watershed includes portions of four municipalities, Carlsbad, Vista, Oceanside, and San Marcos, as well as area in the unincorporated portions of the County of San Diego.

The watershed contains approximately 37 linear miles of stream including Agua Hedionda, Roman, Little Encinas, La Mirada, Calavera, and Buena Creeks. It also includes three significant standing bodies of water: the Agua Hedionda Lagoon, Lake Calavera, and Squires Reservoir. Major transportation corridors include Interstate 5, State Route 78, Pacific Coast Highway, and the Santa Fe Railroad.

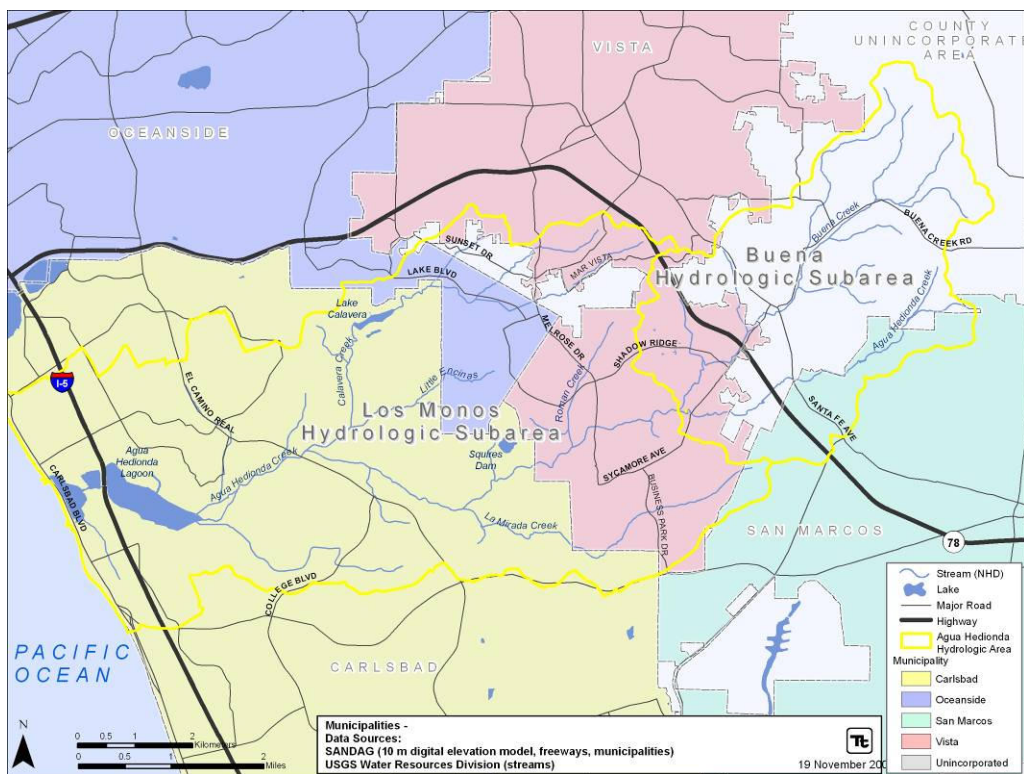


Figure 1. Agua Hedionda Watershed

¹ The watershed was delineated using a 10-m digital elevation model from the National Elevation Dataset. Boundaries were modified using the municipal storm sewer and 2-foot contour topography layers.

2.1 PHYSICAL FEATURES

2.1.1 Geology, Soils, Topography

The watershed is comprised primarily of Mesozoic granitic rock (grMz), Eocene marine rock (E), Mesozoic volcanic rock (Mzv), and Quaternary alluvium and marine deposits (Q) (Figure 2). Table 1 provides descriptions for geological classes represented in the watershed.

Table 2 and Figure 3 present Natural Resources Conservation Service (NRCS) SSURGO soils found in the watershed. According to this dataset, there are 53 distinct soil series in the watershed. The most abundant series are Las Flores loamy fine sand, Marina loamy coarse sand, and Altamont clay.

The lowest elevation in the watershed is along shore adjacent to the Lagoon, which is at sea level (Figure 4). The highest elevation is in the San Marcos Mountains (1,500 ft) (KTU+A, 2002). The coastal flat area adjacent to the lagoon is dominated by Marina loamy coarse sand with 2 to 9 percent slopes (Table 2; Figure 4). Although much of the watershed is only moderately sloped, areas adjacent to Squires Dam, Lake Calavera, and the upper watershed have nearly 40 percent slopes.

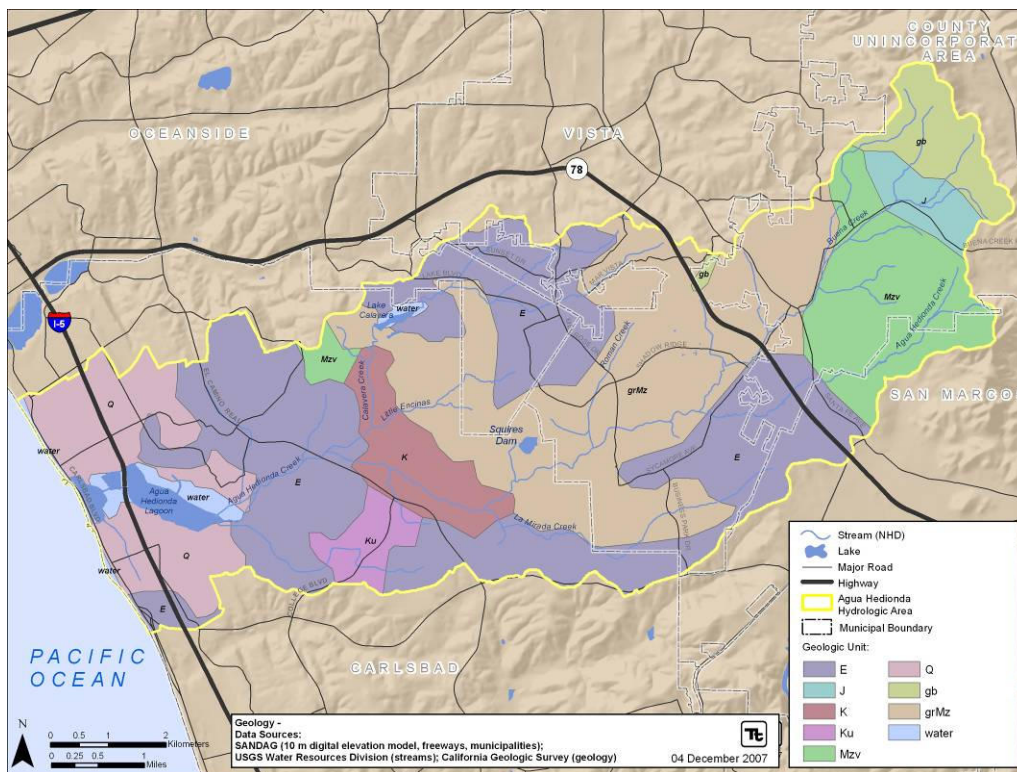


Figure 2. Geology of the Agua Hedionda Watershed

Table 1. Key to Geology within the Agua Hedionda Watershed

Label	Name	Description
E	Eocene marine rocks	Shale, sandstone, conglomerate, and minor limestone; in part Oligocene and Paleocene.
gb	Mesozoic gabbroic rocks, unit 2 (undivided)	Gabbro and dark dioritic rocks; chiefly Mesozoic
grMz	Mesozoic granitic rocks, unit 2 (Peninsular Ranges)	Mesozoic granite, quartz monzonite, granodiorite, and quartz diorite
J	Jurassic marine rocks, unit 4 (Peninsular Ranges and Western Transverse Ranges)	Shale, sandstone, minor conglomerate, chert, slate, limestone; minor pyroclastic rocks
K	Cretaceous marine rocks (in part nonmarine), unit 1 (Coast Ranges)	Undivided Cretaceous sandstone, shale, and conglomerate; minor nonmarine rocks in Peninsular Ranges
Ku	Upper Cretaceous marine rocks, unit 1 (Upper Great Valley Sequence)	Upper Cretaceous sandstone, shale, and conglomerate
Mzv	Mesozoic volcanic rocks, unit 4 (Peninsular Ranges)	Undivided Mesozoic volcanic and metavolcanic rocks. Andesite and rhyolite flow rocks, greenstone, volcanic breccia and other pyroclastic rocks; in part strongly metamorphosed. Includes volcanic rocks of Franciscan Complex: basaltic pillow lava, diabase,
Q	Quaternary alluvium and marine deposits	Alluvium, lake, playa, and terrace deposits; unconsolidated and semi-consolidated. Mostly nonmarine, but includes marine deposits near the coast.

Table 2. Most Abundant Soils Series within the Agua Hedionda Watershed

Symbol	Acreage	Description
Le	2,748	Las Flores loamy fine sand
MI	2,000	Marina loamy coarse sand
At	1,324	Altamont clay
Cl	1,181	Cieneba coarse sandy loam
Hr	1,154	Huerhuero loam
Da	1,107	Diablo clay

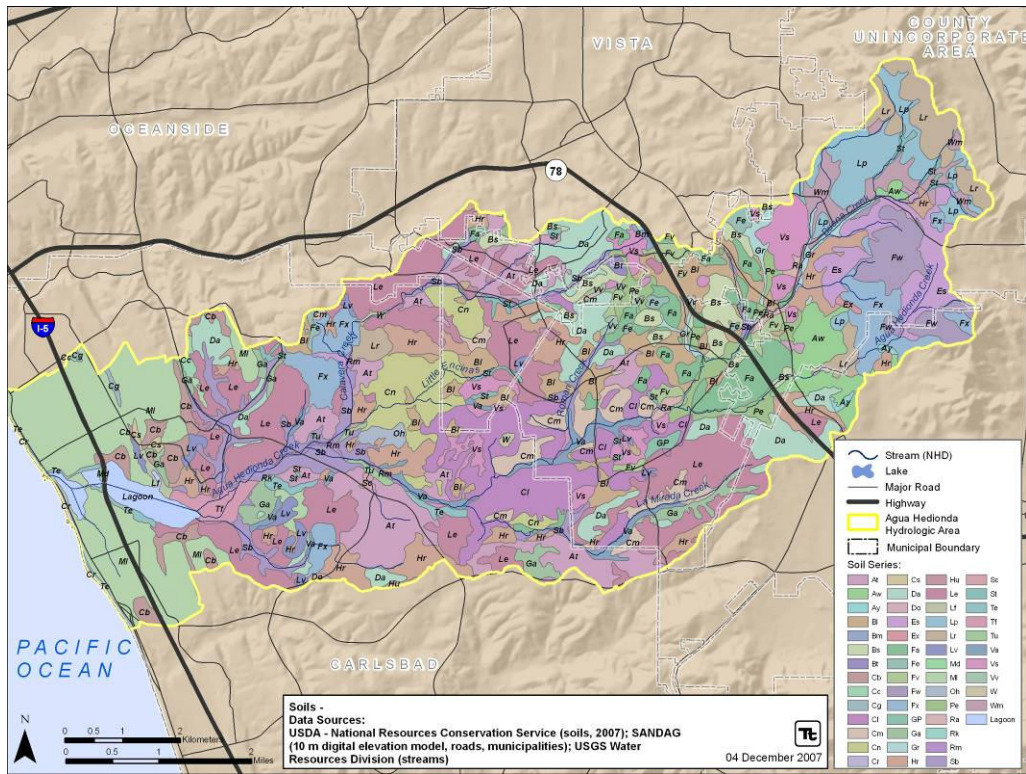


Figure 3. Soils in the Agua Hedionda Watershed

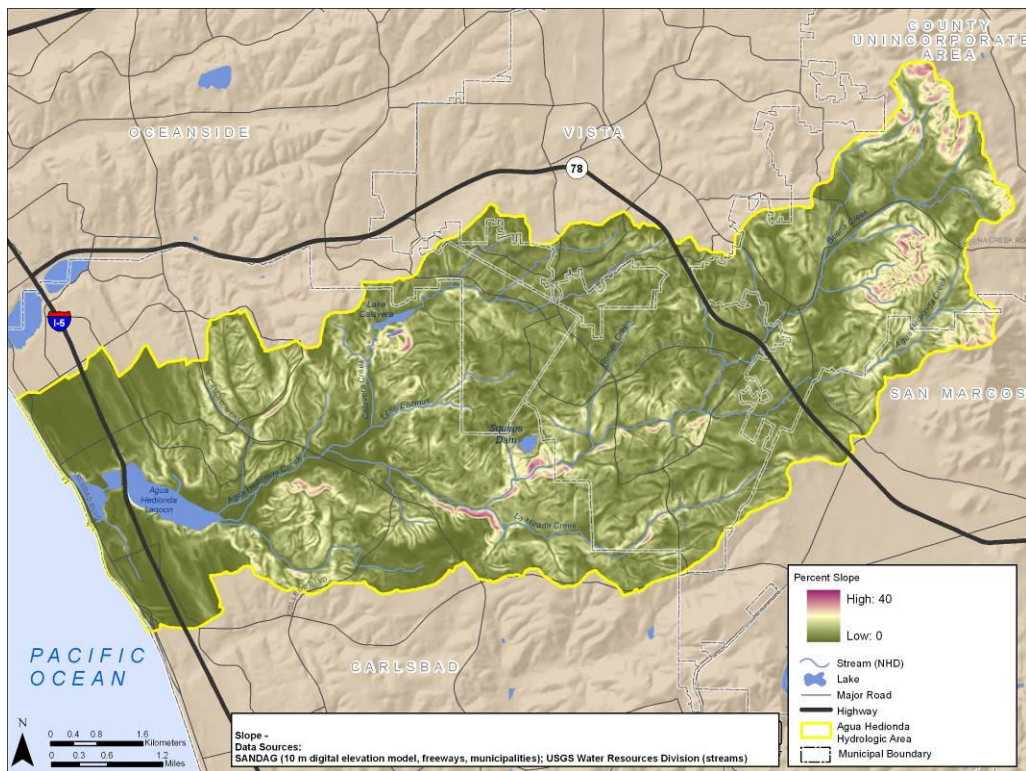


Figure 4. Slopes in the Agua Hedionda Watershed

Figure 5 presents potential erosion hazard or risk in the watershed derived by using the NRCS Soil Data Viewer based on slope and soil erosion factor from SSURGO soils data. Soil loss is caused by sheet and rill erosion where 50 to 75 percent of the surface has been exposed by disturbance. Risk is described as “slight,” “moderate,” “severe,” or “very severe.” A rating of “slight” indicates that erosion is unlikely under ordinary climatic conditions; “moderate” indicates that some erosion is likely and that erosion-control measures may be needed; “severe” indicates that erosion is very likely and that erosion-control measures, including revegetation of bare areas, are advised; and “very severe” indicates that significant erosion is expected, loss of soil productivity and offsite damage are likely, and erosion-control measures are costly and generally impractical. The majority of the watershed has a slight to moderate erosion risk if disturbed; however, there are a few areas of very severe erosion risk.

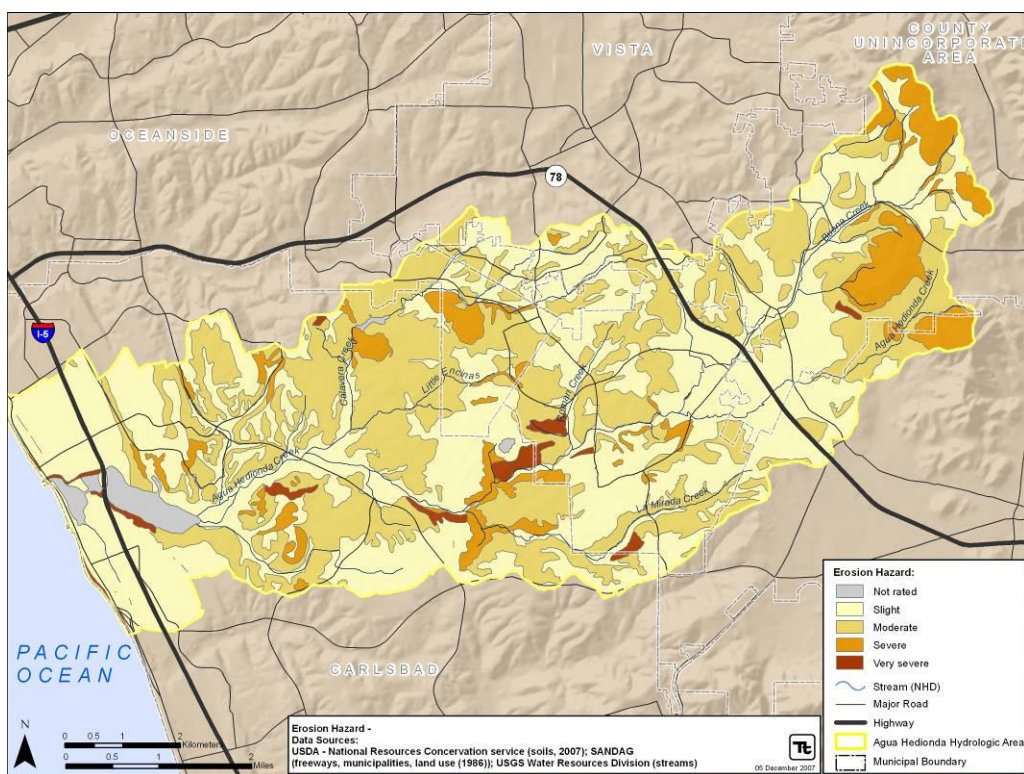


Figure 5. Erosion Risk in the Agua Hedionda Watershed

2.1.2 Hydrology

The watershed is located in a Mediterranean climate region with seasonally influenced precipitation. The vast majority of annual precipitation occurs between November and April. The average annual precipitation for the area is 15.6 inches per year and shows significant variation between years based on data from the Western Regional Climate Center.

Stormwater contributes the majority of runoff in the watershed. During non-storm periods urban runoff, agricultural runoff, and surfacing groundwater provide major sources of surface flow (IRWMP, 2007). There are limited quantities of groundwater in the regions and salinity limits its use as a potable water supply. Water for human use is predominately imported by the Water Authority from outside of the watershed (IRWMP, 2007).

Figure 6 displays the Federal Emergency Management Agency’s (FEMA) Flood Zones. According to the effective FEMA Flood Insurance Study (June 19th, 1997), the current condition 100-year peak flow rate in Agua Hedionda Creek at El Camino Real is 9,850 cfs (Vol. 1, 4, Summary of Discharge). Although most of the watershed is considered outside of the 100- and 500-year floodplain, large tracts adjacent to the lagoon and along Agua Hedionda Creek are within the 100-year flood zone. Furthermore, throughout the watershed, several miles of creeks are within 100-year and 500-year flood zones.

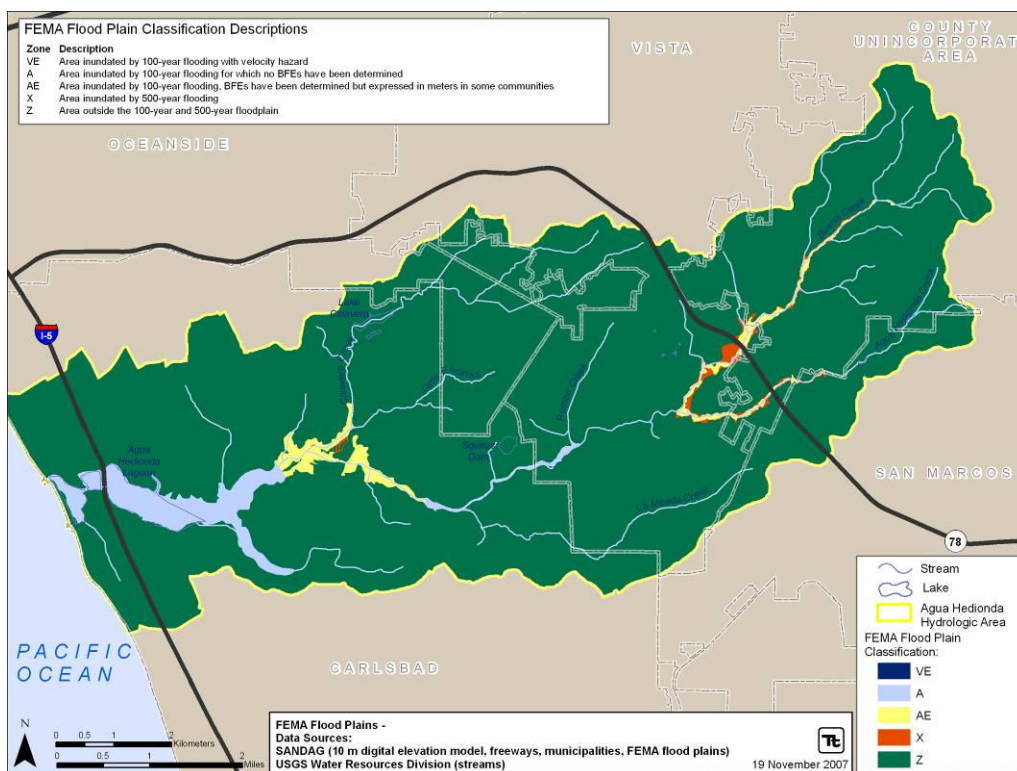


Figure 6. Federal Emergency Management Agency’s (FEMA) Flood Plain Classifications for the Watershed

Flow gaging is available from one site in the watershed at the intersection of Agua Hedionda Creek and the El Camino Real. These data were provided by the San Elijo Lagoon Conservancy (SELCO). Daily average discharge data are available from March of 2005 through April of 2007 (Figure 7). However, the gage was not operational between 3/6/2006 – 6/24/2006 due to city dredging operations.

There was an average daily discharge of 8.17 cubic feet per second (cfs) and median of 3.56 cfs at this gage over the monitoring period (Table 3). The minimum discharge (0.07 cfs) was measured in April 2007 while the maximum (314.21 cfs) was measured in January 2007.

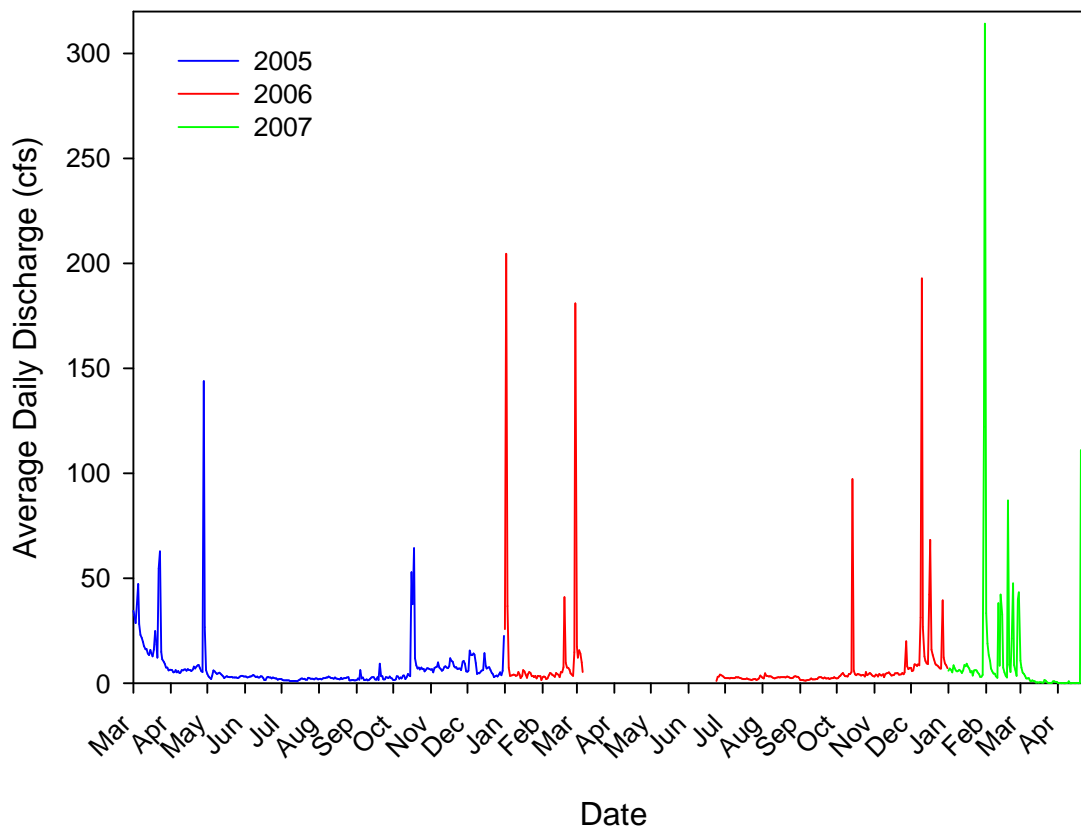


Figure 7. Average Daily Discharge at the Agua Hedionda Creek and El Camino Real Flow Gage (2005-2007)

Table 3. Average Daily Discharge (cfs) Summary Statistics at Agua Hedionda Creek and El Camino Real

Year	Number Measurements	Mean	Median	Minimum	Maximum	10th Percentile	90th Percentile
2005	306	7.08	3.54	0.91	143.91	1.65	13.80
2006	256	8.03	3.56	1.04	204.60	1.97	9.83
2007	120	11.20	3.62	0.07	314.21	0.10	23.67
Total	682	8.17	3.56	0.07	314.21	1.43	13.28

2.1.3 Beneficial Uses

Beneficial uses are defined as those uses of a waterbody necessary for the survival or well being of humans, plants and wildlife that promote economic, social, and environmental goals. Beneficial uses are defined for inland surface waters, coastal waters, reservoirs and lakes, and groundwater. The San Diego Basin Plan lists the beneficial uses of waters within the Agua Hedionda watershed, which determines the applicable water quality standards (SDRWQCB, 1994).

The Agua Hedionda Watershed includes several designated beneficial uses (Table 4 through Table 6). Inland surface waters, including Agua Hedionda Creek, Buena Creek, and Letterbox Canyon, are designated to provide municipal, domestic, agricultural and industrial service supplies, water recreation, and ecological habitat uses. The Agua Hedionda Lagoon is also designated for industrial service supply, recreation, and several ecological habitat uses, as well several other functions including aquaculture, fishing, shellfish and harvesting.

Table 4. Agua Hedionda Watershed Existing Beneficial Uses for Inland Surface Waters

Waterbody	Agua Hedionda Creek	Buena Creek	Agua Hedionda Creek	Letterbox Canyon
	Hydrologic Unit Basin Number	4.32	4.32	4.31
Municipal and Domestic Supply (MUN)	●	●	●	●
Agricultural Supply (AGR)	●	●	●	●
Industrial Process Supply (PROC)				
Industrial Service Supply (IND)	●	●	●	●
Groundwater Recharge (GWR)				
Freshwater Replenishment (FRSH)				
Hydropower Generation (POW)				
Contact Water Recreation (REC1)	●	●	●	●
Non-contact Water Recreation (REC2)	●	●	●	●
Warm Freshwater Habitat (WARM)	●	●	●	●
Cold Freshwater Habitat (COLD)				
Wildlife Habitat (WILD)	●	●	●	●
Preservation of Biological Habitats of Special Significance (BIOL)			●	
Rare, Threatened, or Endangered Species (RARE)				
Spawning, Reproduction, and/or Early Development (SPWN)				

Table 5. Agua Hedionda Watershed Existing Beneficial Uses for Coastal Waters

Waterbody	Agua Hedionda Lagoon
Hydrologic Unit Basin Number	4.32
Industrial Service Supply (IND)	●
Navigation (NAV)	
Contact Water Recreation (REC1)	●
Non-contact Water Recreation (REC2)	●
Commercial and Sport Fishing (COMM)	●
Aquaculture (AQUA)	●
Warm Freshwater Habitat (WARM)	
Estuarine Habitat (EST)	●
Marine Habitat (MAR)	●
Wildlife Habitat (WILD)	●
Preservation of Biological Habitats of Special Significance (BIOL)	●
Rare, Threatened, or Endangered Species (RARE)	●
Migration of Aquatic Organisms (MIGR)	●
Spawning, Reproduction, and/or Early Development (SPWN)	●
Shellfish Harvesting (SHELL)	●

Table 6 reports the beneficial uses for groundwater in the Agua Hedionda Watershed. There is limited groundwater available within the Carlsbad Hydrologic Unit and salinity poses additional limitations to its use as a potable supply (IRWMP, 2007). The Basin Plan reports that only a small portion of the basin supplies appreciable quantities of groundwater due to the lack of permeable geologic formations. Most groundwater in the region is designated as municipal and domestic or agricultural supply, however, groundwater in the watershed does not provide industrial process supply, groundwater recharge, or freshwater replenishment.

Table 6. Agua Hedionda Watershed Beneficial uses for Groundwaters

Hydrologic Unit, Area, or Subarea	Los Monos (HSA) ¹	Los Monos (HSA) ²	Los Monos (HSA) ³	Buena (HSA)
Hydrologic Unit Basin Number	4.31	4.31	4.31	4.32
Municipal and Domestic Supply (MUN)	●	○	○	●
Agricultural Supply (AGR)	●	○	●	●
Industrial Process Supply (PROC)				
Industrial Service Supply (IND)	●	○	○	●
Groundwater Recharge (GWR)				
Freshwater Replenishment (FRSH)				

Note: Solid circles indicate existing uses; empty circles indicate potential uses.

¹ These beneficial uses do not apply westerly of the easterly boundary of the right-of-way of Interstate 5 and this area is excepted from the sources of drinking water policy. Other beneficial uses for the remainder of the hydrologic area are as shown.

² These beneficial uses designations apply to the portion of HSA 4.31 bounded on the west by the easterly boundary of Interstate Highway 5 right-of-way, on the east by the easterly boundary of El Camino Real; and on the north by a line extending along the southerly edge of Agua Hedionda Lagoon to the easterly end of the lagoon, thence in an easterly direction to Evans Point, thence easterly to El Camino Real along the ridge lines separating Letterbox Canyon and the area draining to the Marcario Canyon.

³ These beneficial uses apply to the portion of HSA 4.31 tributary to Agua Hedionda Creek downstream from the El Camino Real crossing, except lands draining to Marcario Canyon (located directly southerly of Evans Point, land directly south of Agua Hedionda Lagoon, and areas west of Interstate Highway 5).

2.1.4 Land Use and Land Cover

Land Use

Historical (1986), current (2007), and planned land use (2030) information was obtained from SANDAG. The land use layers have been updated continuously since 2000 using aerial photography, the County Assessor Master Property Records file, and other ancillary information. The planned land use data were derived from the Series 11 Regional Growth Forecast using each municipality’s master development plans. Since each jurisdiction has their own individualized way of categorizing their future land use designations, an aggregate planned land use code was devised.

In 1986 the watershed was dominated by open space (37 percent), agriculture (19 percent) and single family residential (19 percent) areas (Table 7). Residential developments were centered along Highway 78 and in the northwest corner of the watershed, adjacent to Interstate 5 (Figure 8). The center and uppermost portions of the watershed were dominated by open space and agriculture.

By 2007 single family residential acreage increased to a quarter of the watershed area, while agricultural and open spaces decreased (Table 7). Residential developments spread into the central and upper watershed, bringing anthropogenic influence into closer contact with streams and displacing agriculture and open spaces (Figure 9). In fact, agricultural lands decreased 55 percent since 1986 levels. Most of

the transitional areas were developed into residential and industrial spaces. Industrial and transportation lands sharply increased, especially along the southern watershed boundary. However, some of the increase in industrial and transportation acreage appears to be due to the lack of road classifications in the 1986 land use data set.

The 2030 Regional Growth Forecast for the San Diego Region was derived from local, city, and county General & Community Planning documents (SANDAG, 2005). According to this forecast, the watershed is intended to become primarily single family residential (33 percent), industrial and transportation (23 percent), and open space (18 percent) (Table 7). Nearly all current agricultural land is planned for development, while open space will be reduced 39 percent from 2007 levels (Figure 10). Although the land use plans have provided for open space buffers along much of the streams in the lower portion of the watershed, the vast majority of the upper watershed shows development adjacent to stream corridors.

Table 7. Percent of Watershed for Each Land Use Class in 1986, 2007, and 2030

Land Use Classes	Past (1986)	Current (2007)	Planned (2030)
Rural Residential	6.5	5.1	9.5
Single Family Residential	18.5	24.8	33.3
Multifamily Residential	3.5	3.9	5.7
Commercial & Institutional	2.2	4.1	5.4
Industrial & Transportation	4.2	19.6	23.1
Parks - Recreation	0.6	1.7	1.8
Open - Recreation	1.0	1.1	1.5
Agriculture	19.2	8.5	0.2
Open	36.5	29.7	18.0
Water	1.5	1.5	1.5
Transitional	6.2	0.1	0.0

Notes: The current and planned land use information was obtained from the SANDAG websites. It has been updated continuously since 2000 using aerial photography, the County Assessor Master Property Records file, and other ancillary information. The land use information was reviewed by each of the local jurisdictions and the County of San Diego to ensure its accuracy.

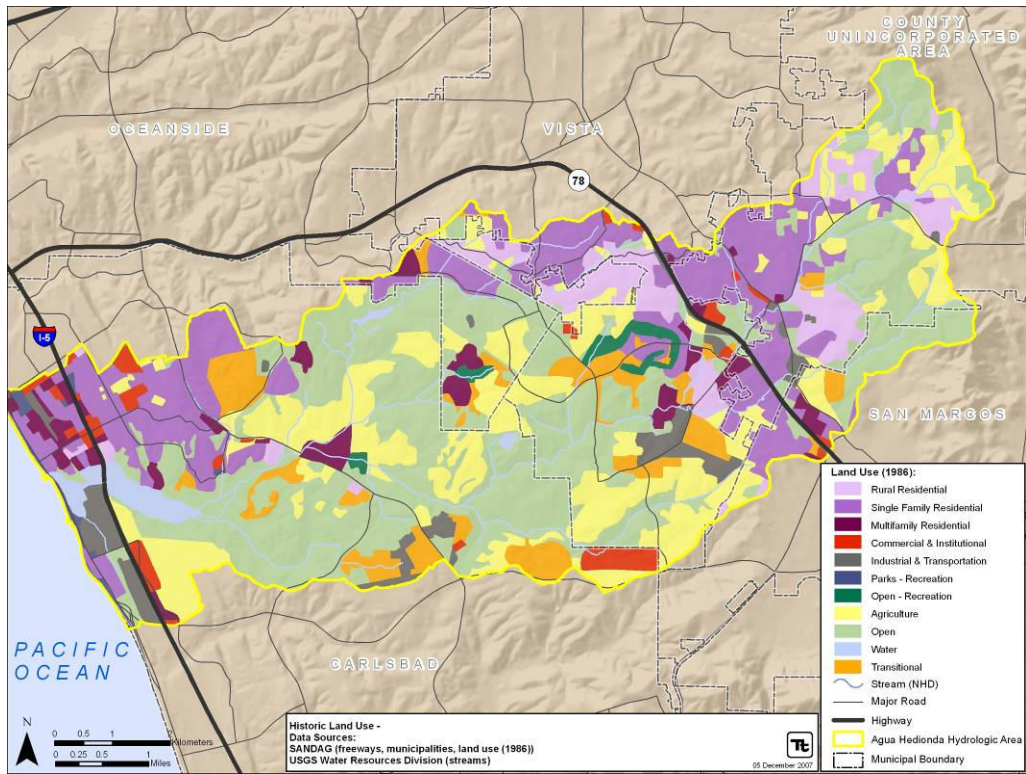


Figure 8. Past Land Use (1986) within the Agua Hedionda Watershed

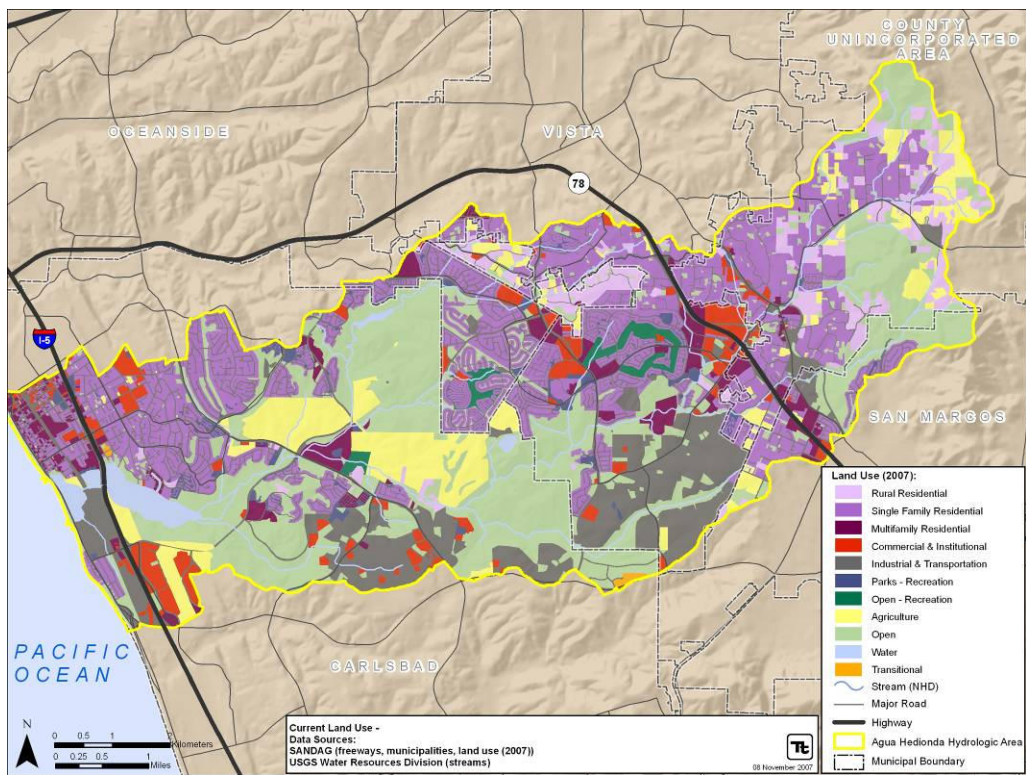


Figure 9. Current Land Use within the Agua Hedionda Watershed

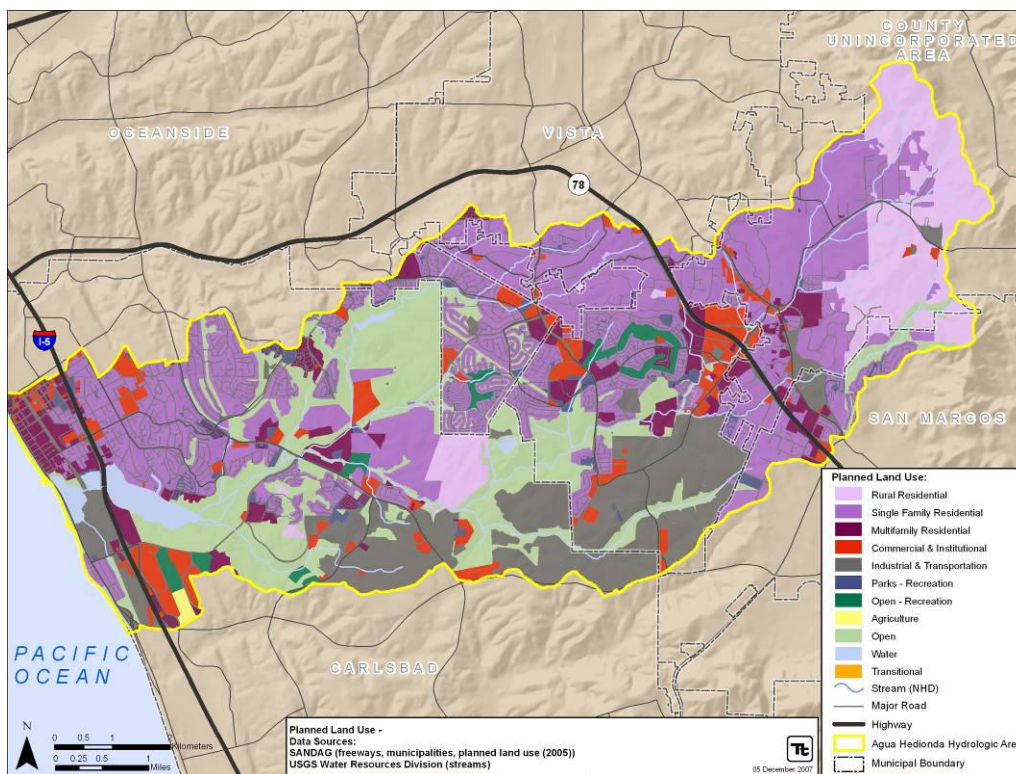


Figure 10. Planned Land Use within the Agua Hedionda Watershed (Final 2030 City/County Forecast)

Impervious Surfaces

Urbanization can have profound influences on watershed health. As land is converted to rooftops, roads, and parking lots, impervious surface area increases leading to increased storm runoff while less surface water is able to infiltrate. These increases in impervious surface lead to greater volume, frequency and magnitude of runoff within the watershed. The Impervious Cover Model (CWP, 2007) indicates that certain zones of stream quality exist, most notably at about 10 percent impervious cover, where sensitive stream elements (e.g. sensitive aquatic species, excellent habitat structure, and excellent water quality) are lost from the system. A second threshold appears to exist at around 25 to 30 percent impervious cover, where most indicators of stream quality consistently shift to a poor condition (e.g., diminished aquatic diversity, water quality, and habitat scores). However, these categories are based heavily upon mid-Atlantic and Puget Sound research and may be less applicable to Southern California watersheds.

Based on 2001 National Land Cover Data (30 m resolution), the upper portion of the watershed generally has a lower percentage of impervious surfaces than the lower watershed. Pockets of low imperviousness are present in the central watershed, especially along Little Encinas Creek (Figure 11). However, conditions within a stream segment are influenced by the entire upstream contributing area. When upstream impervious influences are taken into account, the whole lower watershed is characterized as having greater than second impervious cover threshold contained in the Impervious Cover Model (Figure 12).

Unlike Figure 11, which represents the imperviousness within each individual subbasin, the cumulative percent impervious calculations in Figure 12 take into account upstream imperviousness. This is a useful measure of the potential impact on the mainstem reach in each subbasin. This was determined by taking the average of all cumulative areas upstream of each subbasin. For example, the uppermost subbasin has

a 9.1 percent imperviousness value. To calculate the percent imperviousness for the next subbasin downstream, the combined area of these two subbasins is taken into account. The bottom-most basin (along the beach) represents an average imperviousness of the whole watershed (32.8 percent).

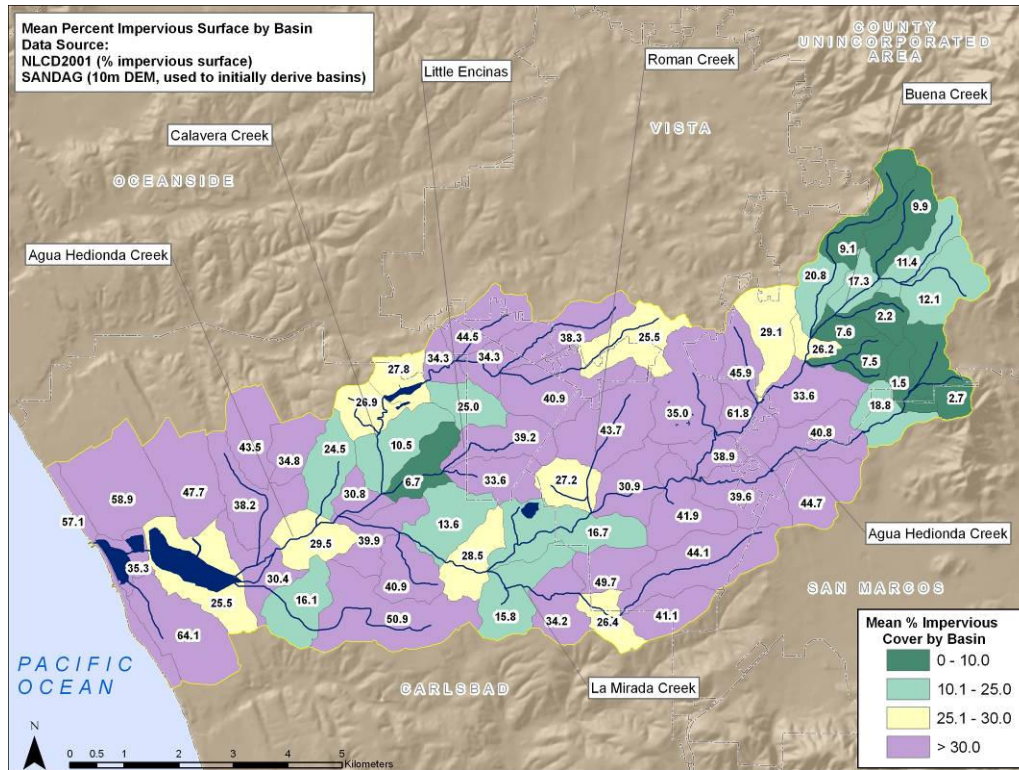


Figure 11. Percent Impervious Surface Cover by Subbasins

Plant Communities

Figure 13 displays the distribution of major Holland vegetation classification system categories within the watershed (SANDAG, 1995). Although most of the watershed is classified as non-native/unvegetated habitat and developed lands, significant areas of scrub/chaparral and herbaceous communities are present (Table 8). Riparian and bottomland habitat is located adjacent to the creek corridors, while bog/marsh and estuary habitat is represented adjacent to the lagoon.

Many of the natural vegetation communities are fragmented due to roads, agriculture, and residential and commercial development. As natural vegetation communities are divided into smaller and smaller parcels, native plant and animal species may be threatened due to reduced mobility. Meanwhile, invasive species often thrive in fragmented habitats. Disturbed wetland communities may be prime candidates for restoration activities.

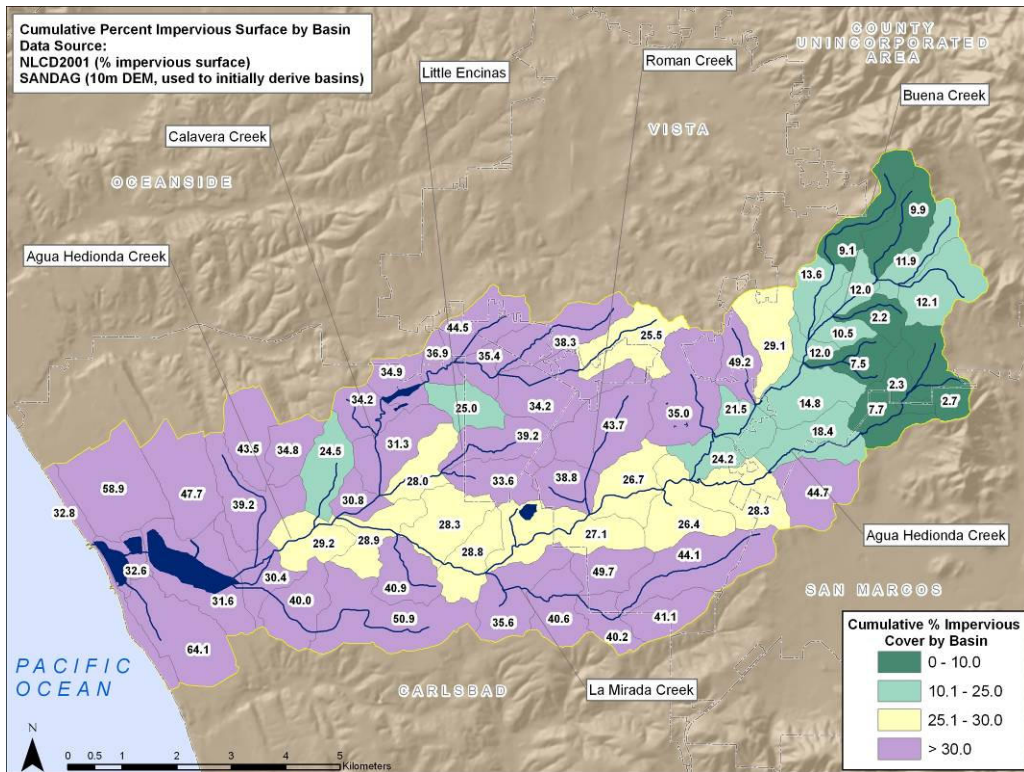


Figure 12. Cumulative Upstream Percent Impervious Surface Cover by Subbasin

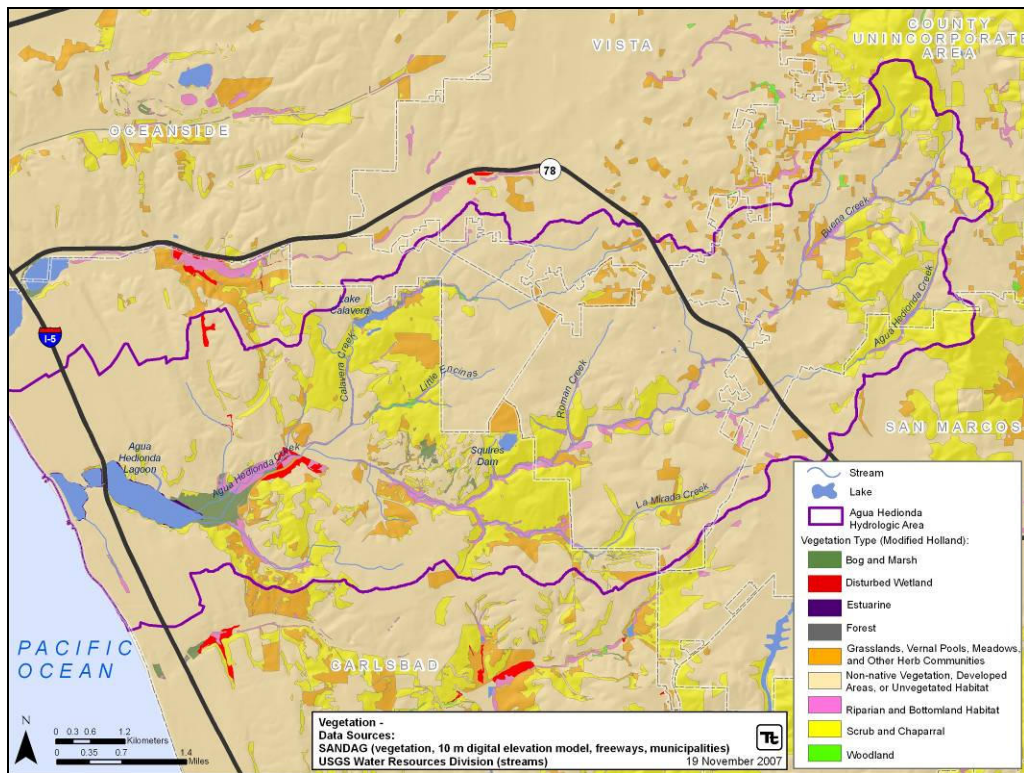


Figure 13. Vegetation Communities Available in the Watershed

Table 8. Vegetation Community Types in Agua Hedionda Watershed

Vegetation Community	Acreage
Non-native Vegetation, Developed Areas, or Unvegetated Habitat	14,087.3
Scrub and Chaparral	3,812.6
Grasslands, Vernal Pools, Meadows, and Other Herb Communities	1,189.9
Riparian and Bottomland Habitat	542.2
Estuarine	272.3
Bog and Marsh	191.9
Disturbed Wetland	52.9
Woodland	26.4
Forest	0.1

Populations of invasive plant species can dominate a plant community by out-competing native species, increasing soil erosion, and altering fire regimes, nutrient cycling, and hydrology. Invasive species data were collected by the SELC (2007) as part of their recent study of restoration of riparian/wetlands habitat in the Carlsbad Hydrologic Unit. They found pampas grass (*Cortaderia selloana*) and giant reed (*Arundo donax*) to be the most dominant invasive species within the Agua Hedionda Watershed (Table 9; Figure 14). However, the presence of periwinkle (*Vinca major*), salt cedar (*Tamarix sp.*), castor bean (*Ricinus communis*), artichoke thistle (*Cynara cardunculus*), palms (*Washingtonia robusta* or *Phoenix canariensis*), and pepperweed (*Lepidium latifolium*) are also a concern.

Table 9. Acreage of Invasive Plant Species Present in the Agua Hedionda Watershed (SELC)

Common Name	Scientific Name	Acreage
Pampas grass	<i>Cortaderia selloana</i>	98.4
Giant reed	<i>Arundo donax</i>	22.9
Periwinkle	<i>Vinca major</i>	6.9
Salt cedar	<i>Tamarix sp.</i>	4.4
Castor bean	<i>Ricinus communi</i>	4.3
Artichoke thistle	<i>Cynara cardunculus</i>	3.6
Palms	<i>Washingtonia robusta</i> or <i>Phoenix canariensis</i>	2.7
Pepperweed	<i>Lepidium latifolium</i>	0.01
Total		143.1

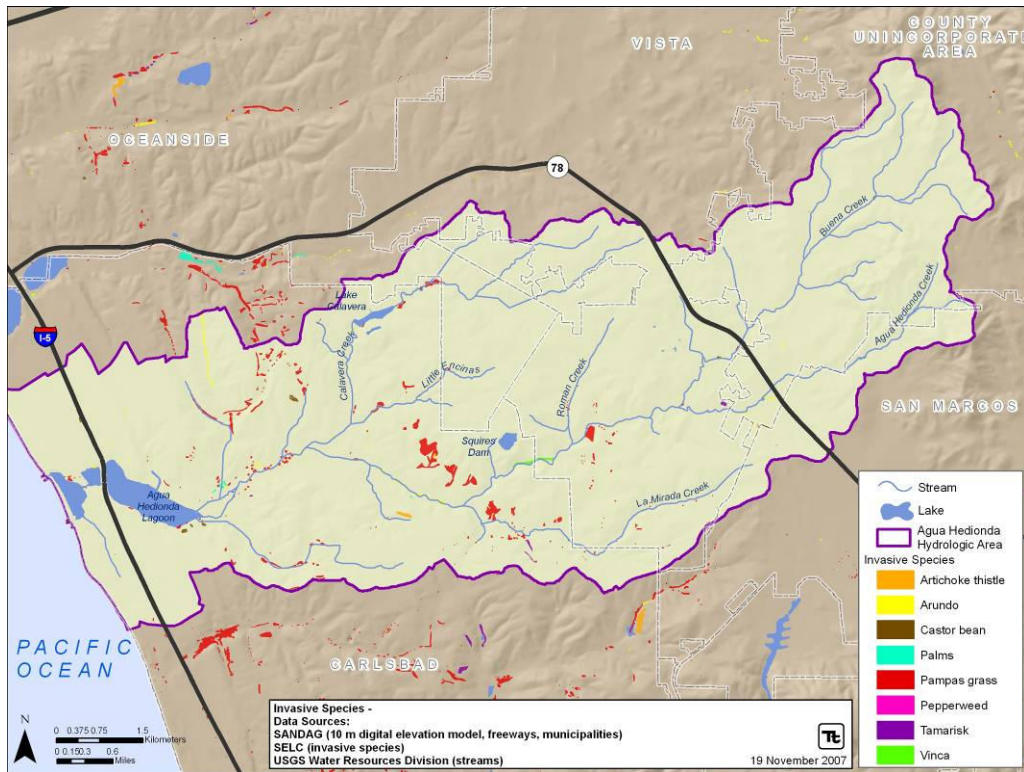


Figure 14. Invasive Plant Species Present in the Watershed

Public Land and Open Space

Several categories of open space are represented in the watershed, including undeveloped natural areas, parks, preserves, and passive beaches. Although the majority of open space is privately owned, there are large tracts of publicly owned open space – especially in the lower half of the watershed. Publicly owned open space may provide prime opportunities for restoration and protection of open space.

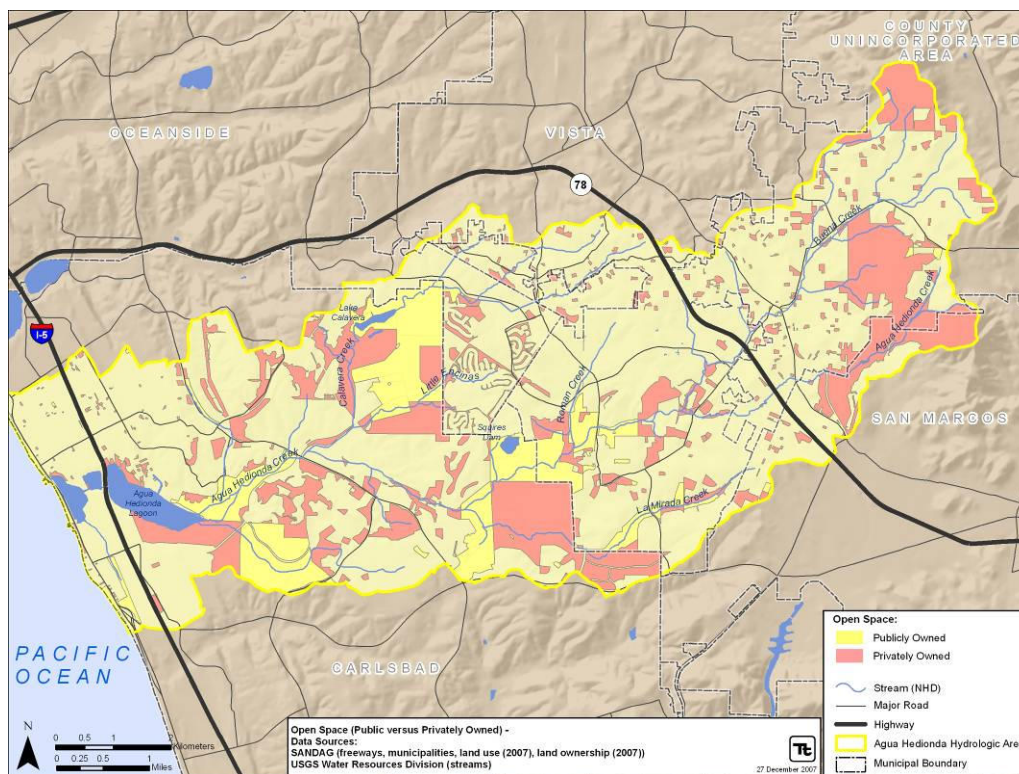


Figure 15. Public and Private Open Space Distribution, 2007

2.2 HUMAN ENVIRONMENT

2.2.1 Point Sources

There are no direct point source discharges from wastewater treatment plants (WWTPs) to waterbodies in the watershed. WWTPs are active in the watersheds; however, all effluent from these facilities is discharged from offshore ocean outfalls. Pollutants are periodically discharged into the water courses as a result of sewage spills.

Other potential sources of pollutants throughout the watershed can be associated with specific facilities if they are not properly managed. Figure 16 shows the distribution of the primary potential sources throughout the watershed according to the Baseline Long Term Effectiveness Report (Weston and others, 2005). This report identifies animal facilities, food facilities, nurseries and water/wastewater publicly owned treatment works (POTWs) to be likely or unknown sources of bacteria and sediment pollution in the watershed. The POTWs are actually lift stations, a potential source of sewage spills due to accidental overflow.

Certain sources of stormwater are also considered point sources. In 1990 USEPA developed rules establishing Phase I of the NPDES stormwater program, designed to prevent harmful pollutants from being washed by stormwater runoff into MS4s (or from being dumped directly into the MS4s) and then discharged from the MS4 into local waterbodies. Phase I of the program required operators of medium and large MS4s (those generally serving populations of 100,000 or more) to implement a stormwater management program as a means to control polluted discharges from MS4s. Phase II of the rule extended coverage of the NPDES stormwater program to certain small municipalities with a population of at least 10,000 and/or a population density of more than 1,000 people per square mile. For the San Diego region,

all discharges of urban runoff are covered by MS4 permits. For the watersheds of San Diego County, the incorporated cities of San Diego County (18 cities), the Airport Authority, and the San Diego Unified Port District, NPDES No. CAS0108758 (referred to in this document as the Municipal NPDES Permit) defines the waste discharge requirements for MS4s. Urban runoff discharges from MS4s contain pollutants that contribute to water quality impairments in the watershed (SDRWQCB, 2007).

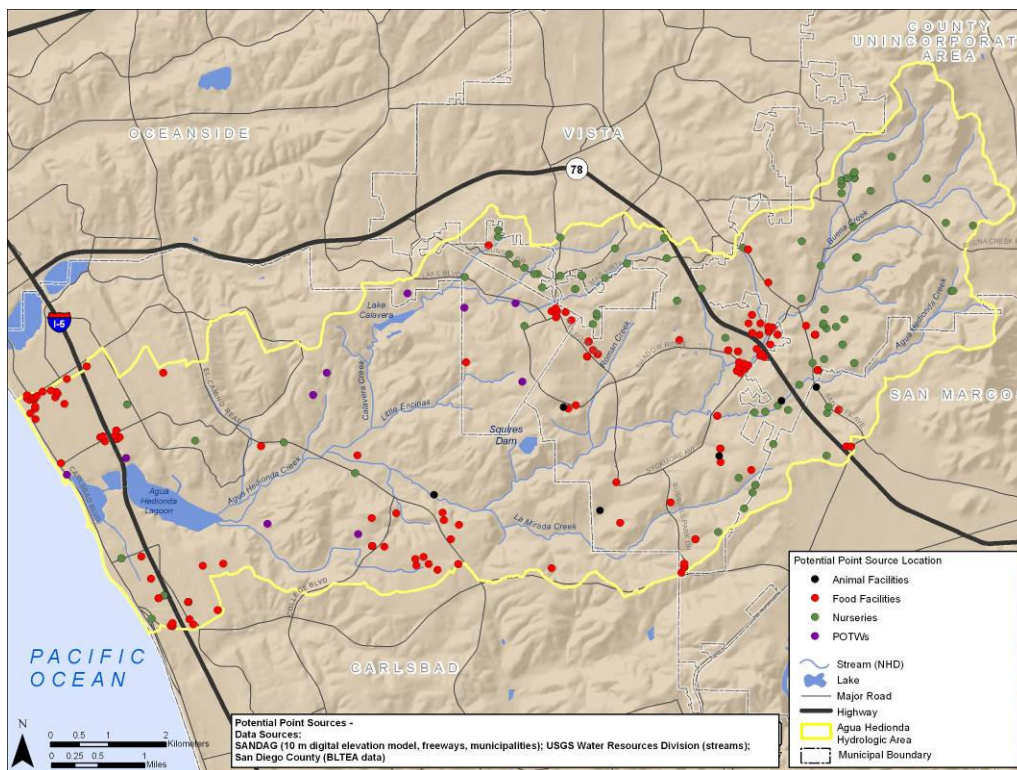


Figure 16. Potential Sources of Pollutants

2.2.2 Sewered/Unsewered Areas

Figure 17 presents data currently available² for the distribution of stormwater and sewer lines throughout the watershed. Although the majority of the watershed is on a sanitary sewer system, some portions of developed lands use septic systems (Figure 18). Figure 18 is based on an analysis of developed parcels with apparent sewer service (i.e., parcels located within 200 ft of the available sewer). Specifically, portions of the upper watershed that are currently low density residential are not on the sewer system.

² City of Vista data is draft for the stormwater system. Also, City of Oceanside data is not available for the watershed.

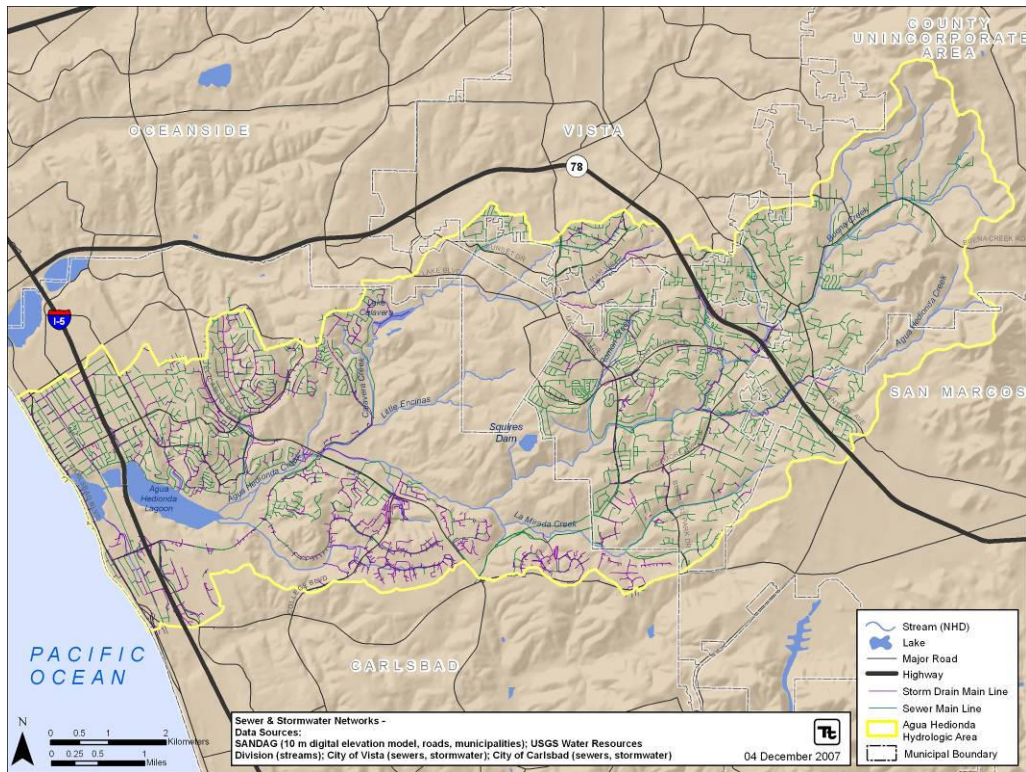


Figure 17. Stormwater and Sewer Line Distribution in the Agua Hedionda Watershed

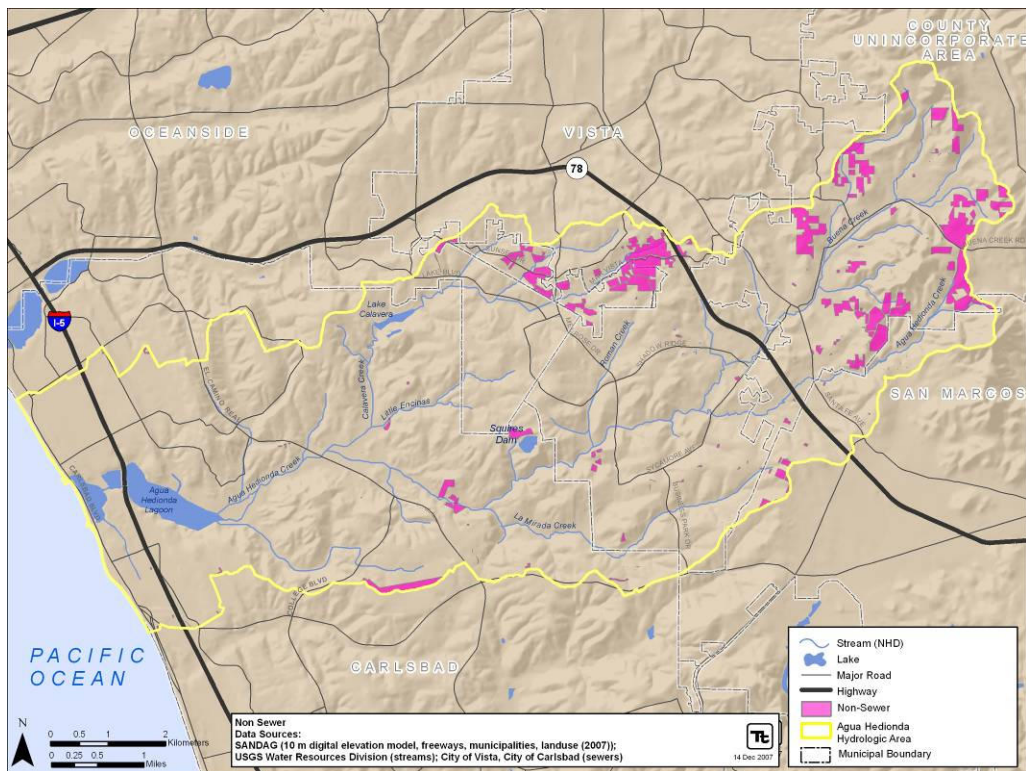


Figure 18. Non-Sewered Development in the Agua Hedionda Watershed

2.2.3 Agriculture

Figure 19 displays agricultural lands within the watershed in three categories: intensive agriculture, field crops, and vineyards/orchards. Field crops, including pasture land, are the most abundant followed by intensive agriculture and vineyards/orchards.

The Agua Hedionda Lagoon also serves as an agricultural environment. The Carlsbad Aquafarm produces scallops, mussels, clams, and oysters. It also raises seahorses, seaweed and octopuses for aquariums. A 22,000 square foot fish hatchery which focuses on white seabass is also located within the lagoon.

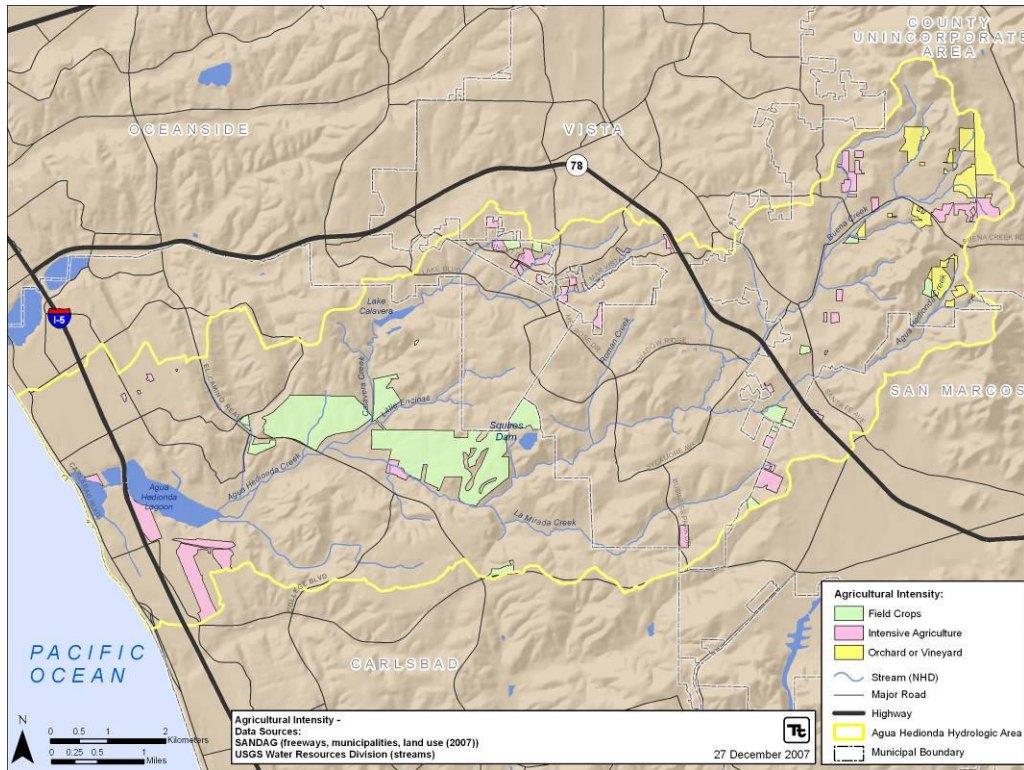


Figure 19. Classification of Agricultural Land Use Intensity in the Agua Hedionda Watershed (SANDAG)

(This page left intentionally blank.)

3 Water Quality Assessment

The following assessment of water quality in the Agua Hedionda Watershed focuses on both impaired and non-impaired waterbodies. Data sets from multiple sources have been used to evaluate existing threats to beneficial uses. In addition, a discussion of trends in pollutant concentrations is presented.

3.1 IMPAIRED WATERS

Section 303(d) of the Clean Water Act requires the Regional Board and State Board to identify waters that do not meet applicable water quality objectives. Those waters not meeting these standards are considered impaired. In the 2006 list of impaired waters, Agua Hedionda Creek is listed as impaired by manganese, selenium, sulfates, and total dissolved solids (TDS) impairment (Table 10). Buena Creek is listed for the pesticide DDT, nitrate and nitrite, and phosphate impairment. The Agua Hedionda Lagoon is listed due to elevated bacteria and sedimentation/siltation. The SDRWQCB is in the process of developing Total Maximum Daily Loads (TMDLs) for Agua Hedionda Creek and Lagoon, supported by ongoing co-permittee monitoring.

Table 10. San Diego Regional Board 2006 Clean Water Act Section 303d List of Water Quality Limited Segments for the Agua Hedionda Watershed³

Waterbody Type	Name	Pollutant/Stressor
Rivers/Stream	Agua Hedionda Creek	Manganese
		Selenium
		Sulfates
		Total Dissolved Solids
Rivers/Stream	Buena Creek	DDT
		Nitrate and Nitrite
		Phosphate
Estuarine	Agua Hedionda Lagoon	Indicator bacteria
		Sedimentation/Siltation

The source for manganese, selenium, and sulfate impairment in Agua Hedionda Creek is unknown according to the 303(d) list for 2006. Likewise, impairments in Buena Creek are attributed to unknown sources. Bacterial and sediment-related impairments have been attributed to urban runoff, storm sewers, and other nonpoint sources.

3.2 LAGOON MONITORING

3.2.1 Lagoon Sediment Monitoring

The Ambient Bay and Lagoon Monitoring (ABLM) program began collecting sediment samples, which included the Agua Hedionda lagoon, as part of the San Diego County Co-permittees' Urban Runoff

³ http://www.waterboards.ca.gov/tmdl/303d_lists2006.html

Monitoring program in 2003. Weston (2007b) examined the program to determine if any linkage was observed between sediment conditions in monitored bays and lagoons and freshwater conditions at upstream mass loading stations (MLS), as stated in the Report of Waste Discharge, County of San Diego Co-permittees. The three years of data are compared to the corresponding three years of wet weather mass loading station (MLS) data from upstream runoff sources.

Results of the ABLM program indicate that the sediment within Agua Hedionda lagoon is relatively healthy. Sediment metals chemistry and mean ERM-Q (Effects Ranged Median-Quotient) values were low. In addition, the levels of pesticides and organics were not detectable in the sediments during any sampling year. Toxicity test results also indicate low toxicity of sediment in 2004 and 2005 and low toxicity of water in all years. Benthic infaunal health was measured by two indices for estuarine conditions (RBI and BRI) and these indices indicated good to fair results. Use of a freshwater index (IBI) resulted in poor scores.

An evaluation of mass loading on Agua Hedionda Creek (monitored just upstream of the lagoon) found high total suspended solids in all three years. On one of three dates in 2003, copper was above the criteria continuous concentrations (CCC) water quality guidelines based on hardness. All other metals were below CCC.

The report concluded that conditions in the lagoon have not changed appreciably over the 3-year study period. The pattern between sediment conditions observed in the lagoon monitoring and upstream stormwater monitoring (at mass loading station) for the 3-year study period is unclear. The report recommends that co-permittees take part in the Bight program, which allows for periodic (5-year) monitoring of sediments within the lagoons.

Sediment samples were collected in Agua Hedionda Lagoon in 2003 to evaluate grain size (MEC, 2004). Sediments in the outer Lagoon consisted primarily of sand (95.1 percent to 96.2 percent) and had a much lower TOC content (0.05 percent to 0.10 percent) than sites in the middle and inner Lagoon. Sediments in the inner Lagoon had a much smaller median grain size consisting primarily of clay, and a higher TOC content than the other sites in the Lagoon.

3.2.2 Co-permittees' Coastal Storm Drain Monitoring

The Co-permittees' Coastal Storm Drain Monitoring (CSDM) program was designed to meet the Municipal NPDES Permit requirements by monitoring bacteria levels in urban runoff from coastal and lagoon outfalls, and evaluating the relationship between storm drain discharges and exceedances of bacteriological water quality standards in the coastal receiving waters. This program included sampling of both storm drains and adjacent receiving waters at coastal beaches and in lagoons. Out of 18 samples collected at site AH-006, four exceeded fecal coliform and enterococcus receiving water standards (one exceeded the total coliform standard) during 2005-2006.

The CSDM Program has been modified (effective in October of 2007) to address new Municipal NPDES Permit requirements (San Diego Co-permittees, 2007). The modifications to the program include a sampling frequency reduction from every other week during the summer months to a monthly frequency year-round. In addition Co-permittees must collect a storm drain outfall sample even when it is not directly discharging to the receiving water. Finally, the program was also modified to increase follow-up sampling based on exceedances of water quality objectives for both receiving water and storm drain samples.

3.3 EXISTING WATERSHED MONITORING DATA

Water quality data have been collected by many organizations (Figure 20; Table 11). Sources include the Co-permittees, San Elijo Lagoon Conservancy, Surface Water Ambient Monitoring Program (SWAMP), and the Citizen's Biomonitoring Program and are summarized below.

3.3.1 Data Sources

Co-permittee Dry Weather Monitoring

Co-permittee dry weather monitoring has been performed in the watershed annually between May 1st and September 30th since 2002 (WURMP, 2003-2007). Data are collected in ambient streams and in storm drains in an effort to identify possible illicit connections and illegal discharges. A total of 61 Co-permittee dry weather data stations have been established, including 10 ambient and 51 storm drain sites.

Co-permittee Wet Weather Monitoring

The Co-permittee wet weather data has been collected since the 1998-1999 storm season (MEC, 2004; MEC, 2005; Weston, 2005; Weston, 2007a). This dataset represents one sample station located at the intersection of Agua Hedionda Creek and the El Camino Real. This site is located downstream of the confluence of Agua Hedionda Creek and Buena Creek. The following parameters have been collected at this site:

- Inorganic Chemicals – Ammonia, Biochemical Oxygen Demand (BOD), Chemical Oxygen Demand (COD), Total and Dissolved Phosphorus, Nitrate, Nitrite, total hardness, Total Kjeldahl Nitrogen (TKN), Total Dissolved Solids (TDS), Total Suspended Solids (TSS), turbidity, and detergents (MBAS).
- Metals (Total and Dissolved) – Antimony, arsenic, cadmium, chromium, copper, lead, nickel, selenium, and zinc.
- Organophosphate Pesticides – Diazinon and chlorpyrifos
- Toxicity Testing – Using *Ceriodaphnia dubia*, *Selenastrum capricornutum*, and *Hyalella azteca*.

In this review, a large focus is on water quality data from the Co-permittee wet weather station. We are able to explore temporal trends because data have been collected for nearly 10 years. It also represents the only wet weather data for this water quality analysis. Furthermore, its location, downstream in the watershed at the confluence of several creeks, provides an integrator site for the majority of the watershed.

Co-Permittee Bioassessment

There are 20 Co-permittee bioassessment monitoring sites throughout San Diego County (Weston, 2007a). However, only two of these sites are located within the Agua Hedionda Watershed. Benthic macroinvertebrate data have been collected at these sites since 2001.

San Elijo Lagoon Conservancy

The San Elijo Lagoon Conservancy (SELCO), on behalf of the Carlsbad Watershed Network, received a grant funded by a Proposition 13 Watershed Protection Program Grant from the California State Water Resources Control Board (Grant Agreement Number 04-083-559-0) for the restoration of riparian and wetland habitat in the Carlsbad Hydrologic Unit (SELCO, 2007). As part of this study, SELCO collected physical habitat, water quality, and benthic macroinvertebrate data between 2004 and 2006. Four sites, located along Agua Hedionda Creek, were monitored as part of this project.

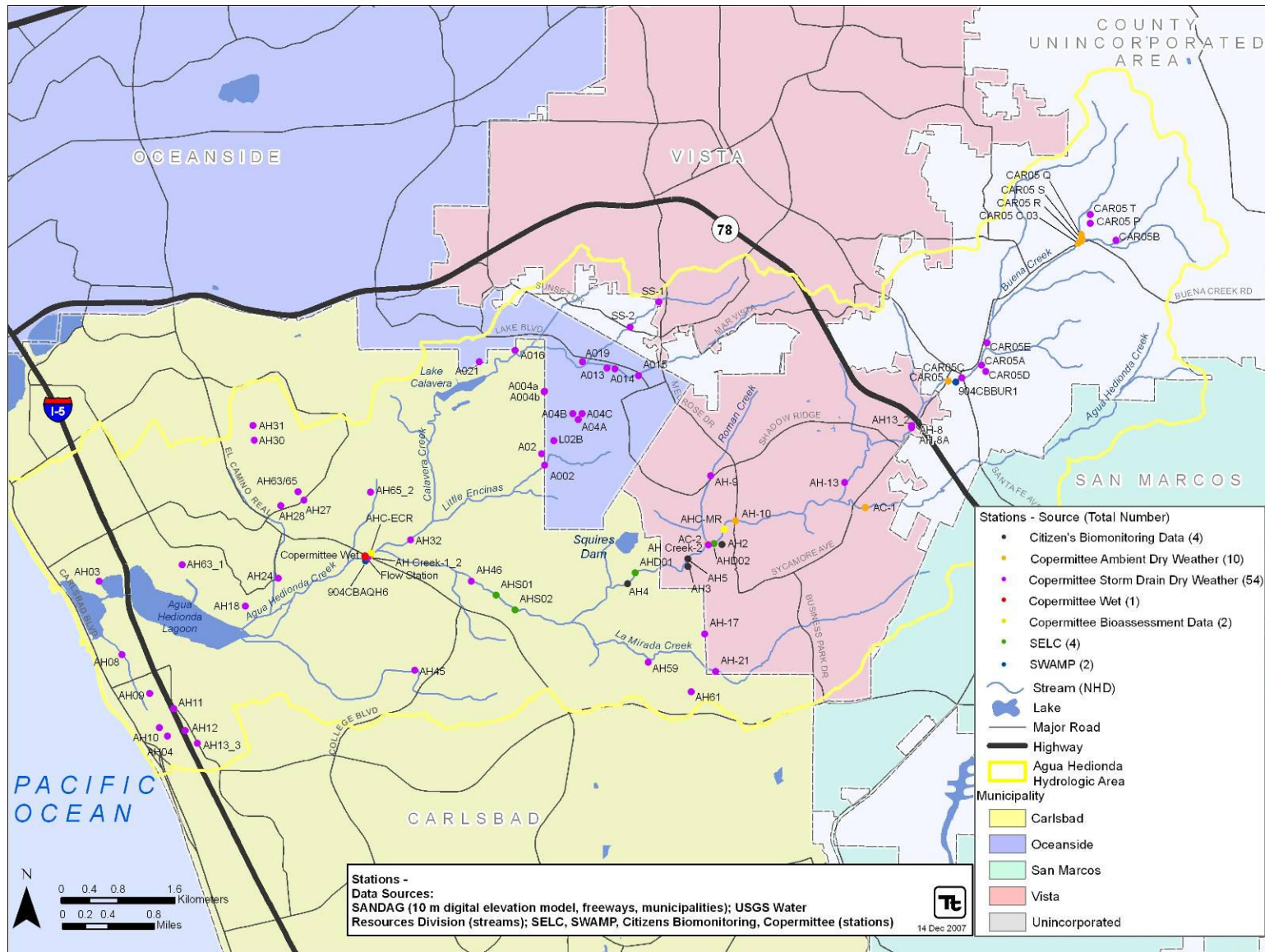


Figure 20. Monitoring Stations in the Agua Hedionda Watershed

Table 11. Summary of Existing Watershed Monitoring

Agency/Organization	Sites	Years Covered	Water Quality	Water Chemistry	Bacteriological	BMI	Toxicity	Physical Habitat	Rain Gauge	Discharge
Co-permittee Dry Weather (ambient & storm drain)	61	2002-2007	X	X	X					
Co-permittee Wet Weather	1	1998 - 2007	X	X	X		X		X	
Co-permittee Bioassessment	2	2002 - 2006		X		X		X		
Citizen's Biomonitoring	4	2001, 2002, 2003, 2005, 2007		X		X		X		
San Elijo Lagoon Conservancy	4	2004 - 2006	X	X	X	X		X		X
SWAMP	2	2002	X	X			X	X		

Surface Water Ambient Monitoring Program (SWAMP)

Data were collected at two stations in the Agua Hedionda Watershed as part of the SWAMP. Water quality, water chemistry, toxicity, and physical habitat data were collected at these sites in 2002.

Citizen’s Biomonitoring

Biomonitoring was conducted by the Watershed Stewards Training for Citizens Monitoring, the Agua Hedionda Lagoon Foundation, and the Carlsbad Watershed Network (Agua Hedionda Lagoon Foundation, 2007). This dataset included four sites located along Agua Hedionda Creek (Table 11). Water chemistry, benthic macroinvertebrate, and physical habitat data were collected at these sites several years between 2002 and 2007.

3.3.2 Water Quality Parameter Summaries

Water quality standards have been established at the federal, state, regional levels. Standards are primarily based on the California Toxic Rule (40 CFR 131 – 65FR 31682, May 18, 2000) and the San Diego Basin Plan (September 8, 1994). The most localized standard available should be used, such that Regional Board standards take precedence over state and federal standards. The San Diego Basin Plan (1994) defines water quality objectives (WQO) for the majority of these parameters. These standards have been established to protect beneficial uses of water and prevent nuisances within a specific area. Each WQO is designated by waterbody type (ocean waters, inland surface waters, enclosed bays and estuaries, coastal lagoons and groundwaters). All data summarized in this section represent inland surface waters.

Data from the sources discussed above were combined by data type (i.e., wet weather, ambient dry, or storm drain) for evaluation. General water quality, chemistry, bacteriological, and pesticide data collected at wet weather, ambient dry weather, and storm drain sites are summarized in Table 12–Table

14 below. Values reported as non-detect were converted to one-half the detection limit for summary purposes. Discussions of individual parameters are provided afterward.

Table 12. Wet Weather Water Quality Summary Statistics

Parameter	Units	WQO	Min	Mean	Max	Count	DL	ND
General								
Electrical Conductivity	umhos/cm	NA	502.00	1,431.85	3,180.00	27	-	0
Oil And Grease	mg/L	15 (a)	0.25	1.16	3.54	27	0.5-5.0	19
pH	pH Units	6.5-8.5 (b)	6.70	7.60	8.22	17	-	0
Chemistry								
Ammonia As Nitrogen	mg/L	NA	0.05	0.38	0.91	27	0.1	3
Un-ionized Ammonia as N	µg/L	25 (b)	0.21	5.31	17.34	15	-	0
Biochemical Oxygen Demand	mg/L	30 (a)	1.00	11.24	49.40	27	2-3	2
Chemical Oxygen Demand	mg/L	120 (a)	2.50	99.13	552.00	27	5	1
Dissolved Organic Carbon	mg/L	NA	7.20	15.24	32.90	15	-	0
Dissolved Phosphorus	mg/L	0.1 (b)	0.03	0.29	1.10	27	0.05-0.1	2
Nitrate As N	mg/L	10 (b)	0.03	1.48	3.20	27	0.05	1
Nitrite As N	mg/L	1 (b)	0.03	0.03	0.09	27	0.05	23
Surfactants (MBAS)	mg/L	0.5 (b)	0.03	0.21	0.33	27	0.05-0.5	22
Total Dissolved Solids	mg/L	500 (b)	10.00	780.00	1,611.00	26	20	1
Total Kjeldahl Nitrogen	mg/L	NA	0.44	3.58	14.10	26	-	0
Total Organic Carbon	mg/L	NA	5.21	22.05	47.50	15	-	0
Total Phosphorus	mg/L	0.1 (b)	0.11	0.67	2.28	27	-	0
Total Suspended Solids	mg/L	100 (a)	5.00	434.42	2,210.00	26	20	2
Turbidity	NTU	20 (b)	6.40	157.14	825.00	26	-	0
Bacteria and Pesticides								
Enterococcus	MPN/100 ml	151 (b)	3,000	56,238	500,000	21	-	0
Fecal Coliform	MPN/100 ml	400 (b)	1	9,787	50,000	27	2	1
Total Coliform	MPN/100 ml	NA	300	58,416	300,000	27	-	0
Chlorpyrifos	µg/L	0.02 (c)	0.001	0.019	0.121	26	0.002-0.5	13
Diazinon	µg/L	0.08 (c)	0.002	0.185	0.464	27	0.004-0.5	11
Malathion	µg/L	0.43 (c)	0.005	0.191	0.622	15	0.01	2

(a) USEPA National Pollutant Discharge Elimination System (NPDES) Storm Water Multi-Sector General Permit for Industrial Activities, 65 Federal Register (FR) 64746 (only used as a benchmark; does not apply to ambient samples);

(b) Water Quality Control Plan for the San Diego Basin; (c) Siepmann and Finlayson. 2000.

; NTU is nephelometric turbidity units; MPN is most probable number

Table 13. Ambient Dry Weather Water Quality Summary Statistics

Parameter	Units	WQO	Minimum	Mean	Maximum	Count	DL	ND
General								
Electrical Connectivity	mS/cm	NA	2.08	2.19	2.33	7	-	0
Specific Conductance	µS/cm	NA	1126	2,3622	5,310	67	-	0
Oil & Grease	mg/L	15 (a)	0.50	3.09	11.00	21	1-5	8
pH	pH Units	6.5-8.5 (b)	6.59	7.94	8.60	70	-	0
Temperature	°C	NA	9.40	17.58	22.70	61	-	0
MBAS	mg/L	0.5 (b)	0.03	0.27	0.50	27	0.05-0.5	7
Chemistry								
Ammonia as N	mg/L	NA	0.05	0.64	8.00	39	0.05-0.1	6
Nitrate as N	mg/L	10 (b)	0.025	5.41	32.96	56	0.05-1.35	1
Nitrate as NO3	mg/L	45 (b)	1.33	13.11	40.30	32	-	0
Nitrite + Nitrate	mg/L	10 (b)	0.48	8.23	19.40	8	-	0
Nitrite as N	mg/L	1 (b)	0.005	0.03	0.19	24	0.01	15
Total Kjeldahl Nitrogen	mg/L	NA	0.05	0.45	1.63	40	0.1-0.5	6
OrthoPhosphate as P	mg/L	NA	0.005	0.20	0.70	58	0.01-0.1	5
Dissolved Oxygen	mg/L	> 5.0 (b)	4.86	8.75	11.26	36	-	0
Phosphate as P	mg/L	0.1 (b)	0.03	0.30	1.62	36	0.06	1
Phosphorus as P	mg/L	0.1 (b)	0.025	0.11	0.20	16	0.02-0.05	2
Salinity	ppt	NA	0.10	0.10	0.11	7	-	0
Sulfate	mg/L	250 (b)	280.00	402.63	522.00	8	-	0
Turbidity	NTU	20 (b)	0.01	6.79	43.00	39	-	0
Bacteria and Pesticides								
Enterococcus	MPN/100 ml	151 (b)	0	463	5,000	54	10-20	5
Fecal Coliform	MPN/100 ml	400 (b)	4	3502	80,000	56	-	0
Total Coliform	MPN/100 ml	NA	50	64,971	3,000,000	56	-	0
Chlorpyrifos	µg/L	0.02 (c)	0.025	0.055	0.500	27	0.05-1	18
Diazinon	µg/L	0.08 (c)	0.010	0.053	0.500	27	0.02-1	17
Malathion	µg/L	0.43 (c)	0.025	0.027	0.050	15	0.05	15

(a) USEPA National Pollutant Discharge Elimination System (NPDES) Storm Water Multi-Sector General Permit for Industrial Activities, 65 Federal Register (FR) 64746 (only used as a benchmark; does not apply to ambient samples); (b) Water Quality Control Plan for the San Diego Basin; (c) Siepmann and Finlayson, 2000; NTU is nephelometric turbidity units; MPN is most probable number

Table 14. Storm Drain Dry Weather Water Quality Summary Statistics

Parameter	Units	WQO	Minimum	Mean	Maximum	Count	DL	ND
General								
Conductivity	µS/cm	NA	0.80	2,199.56	13,000.00	163	-	0
Dissolved Oxygen	mg/L	> 5.0 (b)	0.79	7.18	14.77	24	-	0
Electrical Connectivity	mS/cm	NA	1.67	2.18	2.68	2	-	0
MBAS	mg/L	0.5 (b)	0.03	0.39	5.00	135	0.050.5	34
Oil & Grease	mg/L	15 (a)	0.50	27.62	530.00	62	1-5	27
Temperature	°C	NA	16.00	24.31	220.60	120	-	0
pH	pH Units	6.5-8.5 (b)	5.70	7.71	9.80	166	-	0
Chemistry								
Ammonia as N	mg/L	NA	0.03	0.78	7.65	156	0.05-0.1	1
Nitrate-N	mg/L	10 (b)	0.03	8.56	75.00	142	0.05-1.35	2
OrthoPhosphate	mg/L	NA	0.02	0.81	5.50	109	-	0
Phosphorus	mg/L	0.1 (b)	0.01	0.24	0.98	34	0.02	3
Salinity	ppt	NA	0.07	0.19	0.32	27	-	0
Turbidity	NTU	20 (b)	0.00	13.03	308.00	140	-	0
Bacteriological								
Enterococcus	MPN/100 ml	151 (b)	10	9,545	16,000	68	-	0
Fecal Coliform	MPN/100 ml	400 (b)	20	22,115	300,000	66	-	0
Total Coliform	MPN/100 ml	NA	20	15,5156	1,600,000	67	-	0
Pesticides								
Chlorpyrifos	µg/L	0.02 (c)	0.025	0.124	1.500	57	0.05-3	39
Diazinon	µg/L	0.08 (c)	0.025	0.179	3.000	57	0.05-6	40
Malathion	µg/L	0.43 (c)	0.020	0.047	0.330	15	0.04-0.05	13

(a) USEPA National Pollutant Discharge Elimination System (NPDES) Storm Water Multi-Sector General Permit for Industrial Activities, 65 Federal Register (FR) 64746 (only used as a benchmark; does not apply to ambient samples); (b) Water Quality Control Plan for the San Diego Basin; (c) Siepmann and Finlayson. 2000; NTU is nephelometric turbidity units; MPN is most probable number

pH

Hydrogen ion activity, or pH, is a measure of the acidity/alkalinity of water. The pH scale ranges from 0 to 14, with 7 indicating neutral conditions. The Basin Plan requires that pH levels are maintained between 6.5 and 8.5 in inland surface waters. Storm drain data expressed the greatest range of pH values (5.7 to 9.8) and periodically exceeded both the upper and lower bounds of the WQO. The extremes of the

ambient dry weather data did exceed the upper bounds of this standard. Wet weather samples met this WQO, ranging from 6.70 to 8.22.

Figure 21 presents the distribution of pH measurements collected as part of the Co-permittee storm drain monitoring. Values represent means over all sampling events. Those points exceeding the lower WQO are located in the upper watershed, while those exceeding the upper WQO bounds are located at the base of the watershed. There appears to be a general spatial trend in the watershed: the upper watershed is more acidic than the lower watershed.

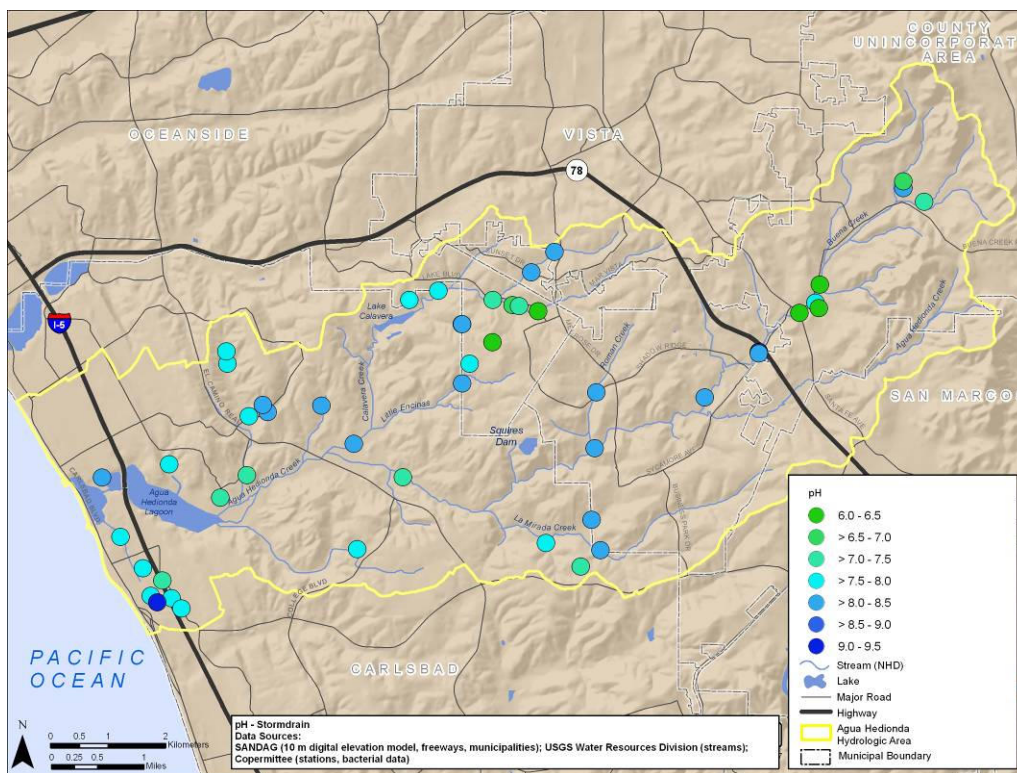


Figure 21. Distribution of pH Measurement Collected as Part of the Co-permittee Dry Weather Storm Drain Monitoring

Turbidity

Turbidity is a measure of light scattering in water or “cloudiness” and is most often a result of suspended fine sediment. It normally increases after heavy rains, as runoff transports increased sediment loads into streams. These increased turbidity levels can harm aquatic life by limiting light penetration.

The Basin Plan lists the water quality objectives for turbidity as not to exceed 20 NTU in inland surface waters. The majority of wet weather samples surpassed this standard and the five samples that did meet this goal were collected prior to 2003 (Figure 22). Wet weather turbidity measured the highest (157 mean) and with the greatest range (6.4 – 825.0) (Table 15).

Twenty-three of the 140 storm drain measurements taken during dry weather (or 16 percent) exceeded the WQO. Similar to the effects of heavy rainfall, these high levels result from increased runoff transporting sediments into the storm drains.

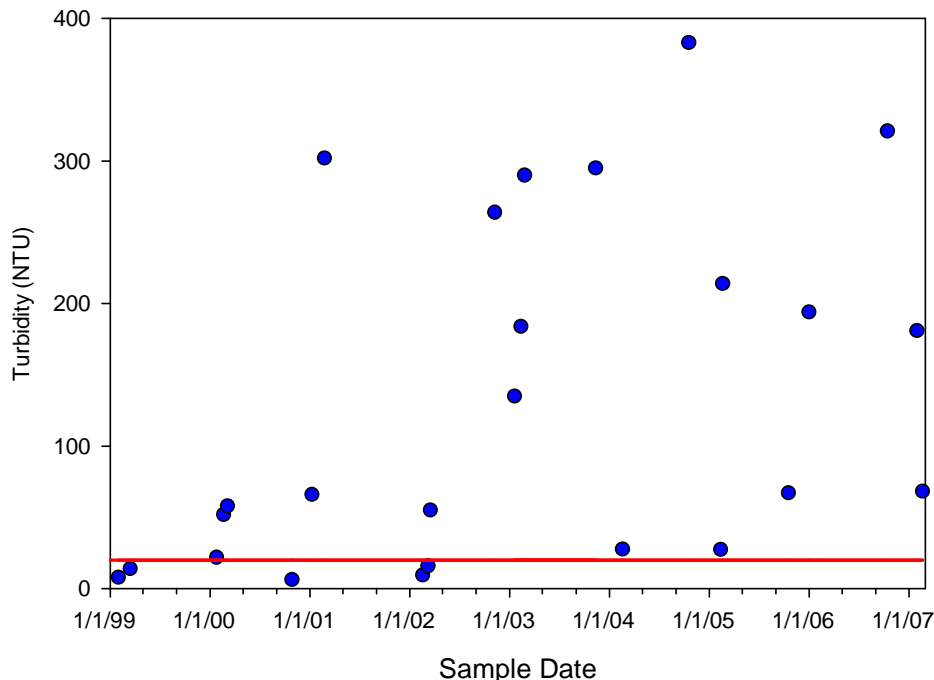


Figure 22. Turbidity Measurements Taken at the Co-permittee Wet Weather Site Between 1999 and 2007 (Line Represents WQO of 20 NTU)

Table 15. Turbidity Measurements (in NTU) Taken at Wet Weather, Ambient, and Storm Drain Sites

Data Type	Minimum	Mean	Maximum	Count
Wet Weather	6.40	157.14	825.00	26
Ambient	0.01	6.79	43.00	39
Storm Drain	0.00	13.03	308.00	140

Total Suspended Solids

Total suspended solids (TSS) can include both organic and inorganic materials including sediments, decaying plant and animal matter, industrial waste, and sewage. Sediment can increase turbidity, clog fish gills, reduce spawning habitat, lower young aquatic organism survival rates, smother bottom-dwelling organisms, and suppress aquatic vegetation growth.

TSS data were only available for the Co-permittee wet weather sample station. Figure 23 presents TSS measurements at this site between 1999 and 2007. Though there is no ambient water quality standard for TSS, 100 mg/L is used as a benchmark (USEPA Multi-Sector General Permit for Industrial Activities). Only seven samples were lower than this benchmark. After 2003 all samples exceeded the benchmark.

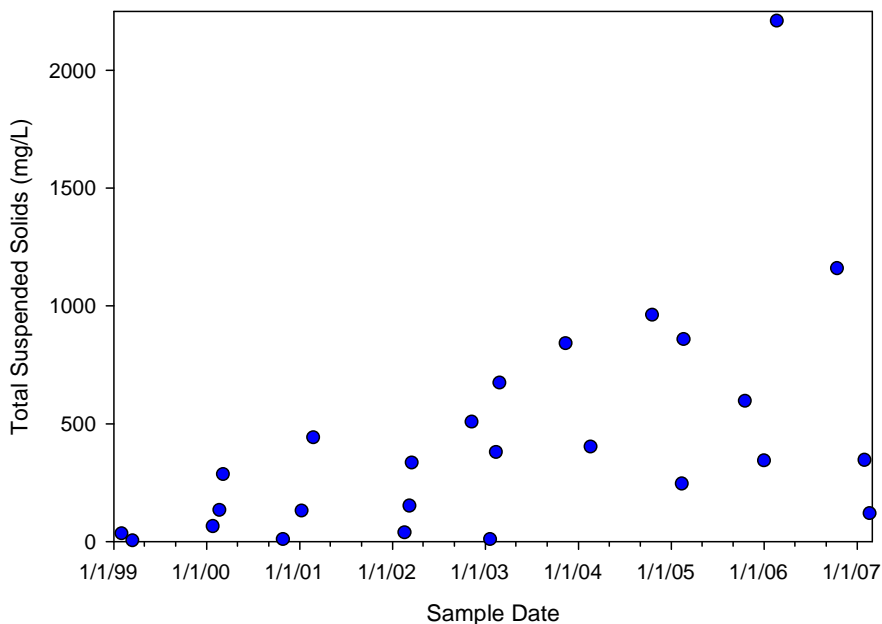


Figure 23. Total Suspended Solids at the Co-permittee Wet Weather Site between 1998 and 2007

Salinity and Total Dissolved Solids

Salinity is a measure of dissolved mineral constituents. Increased salinity can adversely impact aquatic and wildlife habitat and the usability of water for municipal and irrigation supply. Dry weather ambient salinity averaged 0.10 parts per thousand (ppt), while storm drain samples had an average salinity of 0.19 percent. Figure 24 presents the distribution of salinity concentrations throughout the watershed. The central portion of the watershed along the northern boundary represent areas of elevated salinity. In California, elevated salinity often occurs as a result of native geology.

Agua Hedionda Creek was been 303(d) listed for total dissolved solids (TDS) impairment in 2006. TDS is a measure of inorganic salts and small amounts of organic matter present in solution in water. This principally includes calcium, magnesium, sodium, and potassium cations and carbonate, hydrogencarbonate, chloride, sulfate, and nitrate anions along with dissolved organics. Because TDS and salinity measures similar constituents, they are closely related.

According to the Basin Plan, the water quality objective for TDS is 500 mg/L based on beneficial use for municipal and domestic water supply. Nineteen of the 26 wet weather TDS data collected between 1999 and 2007 (or 73 percent) have exceeded this objective (Figure 25). The figure suggests a decrease in TDS concentrations over this time period.

Composition of TDS has not been analyzed in these samples. However, it is not unusual for coastal streams in southern California to exhibit elevated TDS due to mineral soils and geology.

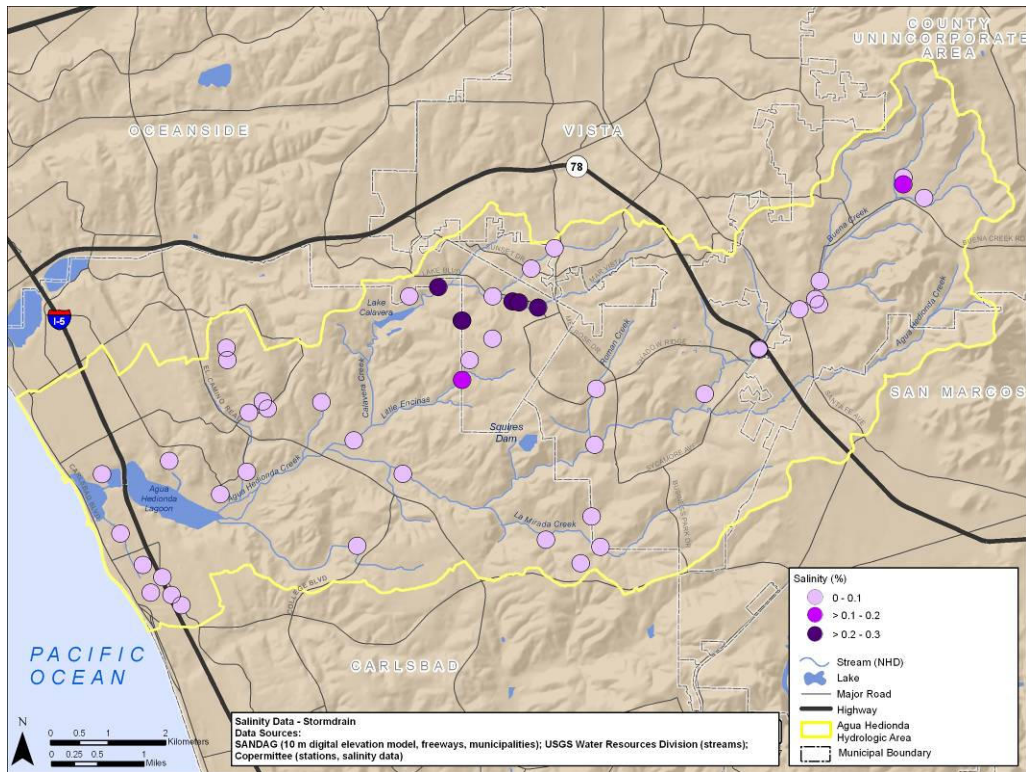


Figure 24. Distribution of Salinity Measurements (ppt) Collected As Part of the Co-permittee Dry Weather Storm Drain Monitoring

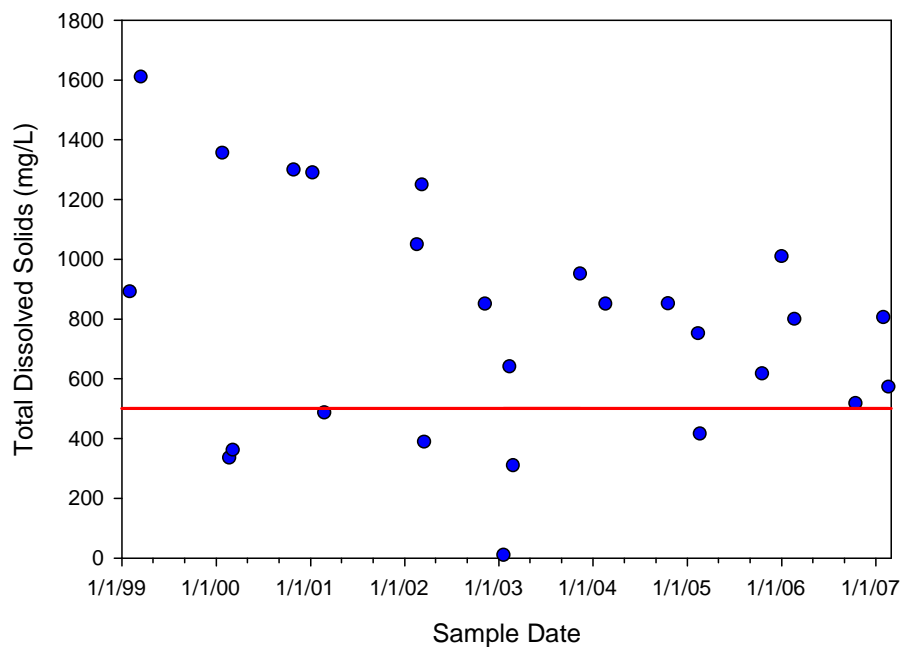


Figure 25. Total Dissolved Solids at the Co-permittee Wet Weather Site (1998-2007) (Line Represents WQO)

Nutrients

Elevated concentrations of nutrients may promote algal blooms and overgrowth of emergent and sub-emergent vegetation, which in turn may cause daily swings in dissolved oxygen (DO) and pH that can harm other aquatic life. Excess plant growth may reduce dissolved oxygen in the water, either on a diurnal basis as a result of night-time algal respiration or on an episodic basis as a result of algal death. Un-ionized ammonia, and perhaps nitrate and nitrite, may also cause direct toxic effects on aquatic life.

Phosphorus, because of its tendency to sorb to soil particles and organic matter, is primarily transported in surface runoff with eroded sediments. Inorganic nitrogen, on the other hand, does not sorb as strongly and can be transported in both particulate and dissolved phases in surface runoff. Dissolved inorganic nitrogen also can be transported through the unsaturated zone (interflow) and ground water. Further, both phosphorus and nitrogen can enter natural waters by both dry fallout and rainfall.

The Basin Plan specifies nitrogen related WQO for un-ionized ammonia (25µg/L), nitrate (10 mg/L), and nitrite (1 mg/L); however, these general criteria were developed for protection of human health and aquatic from direct toxicity and were not developed to control excess algal/plant growth. Wet weather data did not exceed WQO for any of these parameters. Wet weather total nitrogen values were calculated using TKN, nitrate as N, and nitrite as N (Table 16). Figure 26 presents the total nitrogen data. There is some indication of an increasing trend in total nitrogen over these sampling events. This is primarily a result of particularly high samples collected between 2003 and 2005.

Table 16. Wet Weather Nitrogen Summary Statistics

Parameter	Units	WQO	Min	Mean	Max	Count	DL	ND
Ammonia As Nitrogen	mg/L	NA	0.05	0.38	0.91	27	0.1	3
Un-ionized Ammonia as N	µg/L	25 (a)	0.21	5.31	17.34	15	-	0
Nitrate As N	mg/L	10	0.03	1.48	3.20	27	0.05	2
Nitrite As N	mg/L	1	0.03	0.03	0.09	27	0.05	26
Total Kjeldahl Nitrogen	mg/L	NA	0.44	3.58	14.10	26	-	0

(a) Un-ionized Ammonia is a calculated value, non-detectable values calculated at the detection limit. Basin Plan WQO is 0.025 mg/L; values shown here have been converted to µg/L.

Buena Creek is listed on the 2006 303(d) list for nitrate and nitrite. Dry weather samples were high in nitrate. At CAR05 (Figure 20), the mean for 10 samples was almost 12 mg/L.

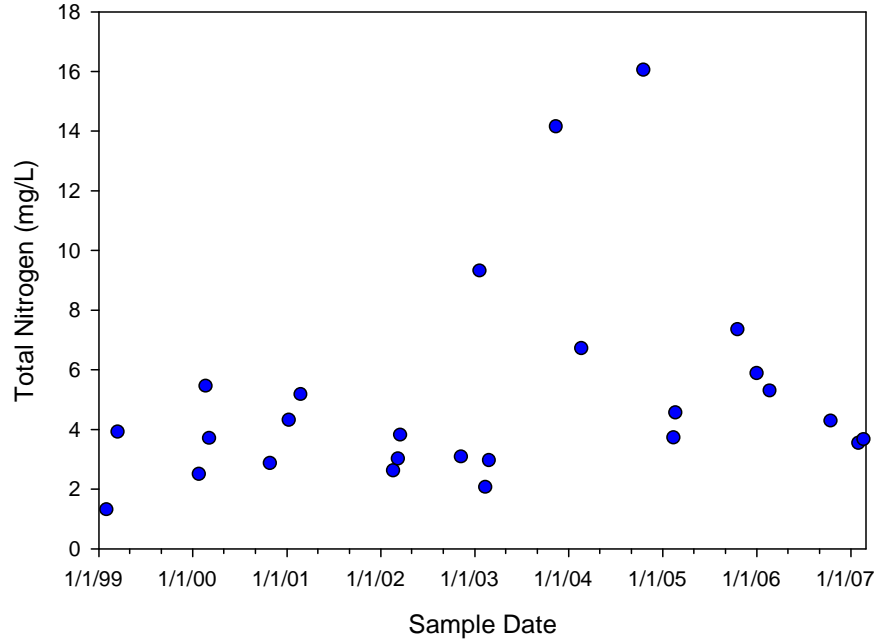


Figure 26. Total Nitrogen Data Collected at the Co-permittee Wet Weather Site (1999-2007)

Phosphorus is often (though not always) the controlling nutrient for algal growth in freshwater systems. The Basin Plan lists the total phosphorus WQO as 0.1 mg/L. The wet weather mean was several times the WQO (Table 17). All wet weather and 50 percent of storm drain phosphorus measurements exceeded this standard (Figure 27).

Table 17. Wet Weather Phosphorus Summary Statistics

Parameter	Units	WQO	Min	Mean	Max	Count	DL	ND
Total Phosphorus	mg/L	0.1	0.11	0.67	2.28	27	-	0
Dissolved Phosphorus	mg/L	NA	0.03	0.29	1.10	27	0.05-0.1	2

Buena Creek was 303(d) listed for phosphorus impairment in 2006. Ambient dry weather phosphate data were available for this watershed. The orthophosphate data averaged 0.16 mg/L.

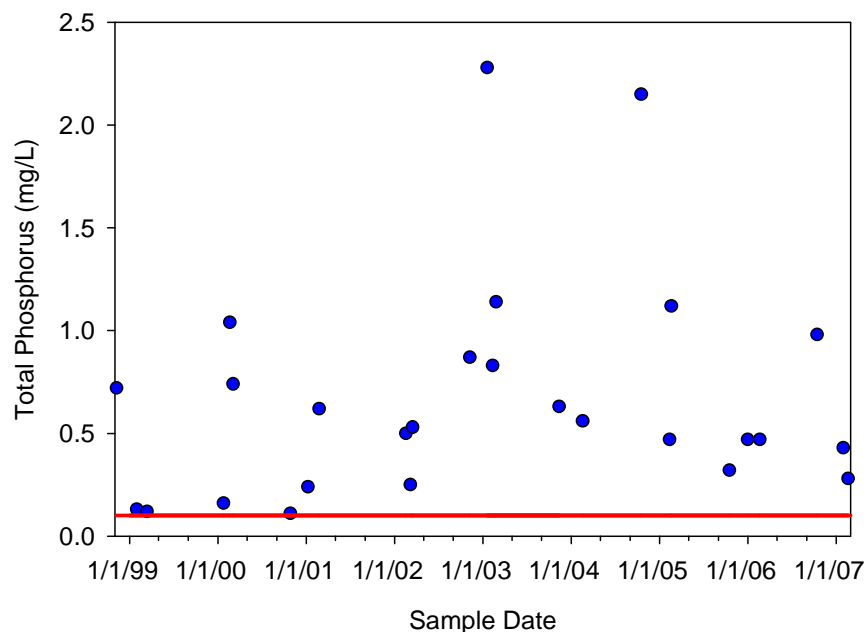


Figure 27. Total Phosphorus Data from the Co-permittee Wet Weather Site Collected Between 1998 and 2007 (Line Represents WQO 0.1 mg/L)

3.3.3 Metals

Although metals occur naturally in the environment, human activity may alter their distribution. Metals can be a significant source of toxicity to aquatic life. Metals criteria vary with hardness, thus each individual sample may have a different concentration objective. The significance of metals can be screened by converting to toxicity units (TU) – the ratio of concentration to the criterion calculated at ambient hardness. A TU > 1 indicates a potential risk of adverse impacts on aquatic life.

Metals criteria are expressed in terms of the dissolved metal concentration as this is the bioactive fraction. However, the rules also provide default equations for converting between dissolved and total recoverable fractions. Both total and dissolved metals (wet weather data) have been converted to toxic units using the California Toxics Rule standards (USEPA Federal Register Doc. 40 CFR Part 131, May 18, 2000). We evaluated metals relative to both acute and chronic aquatic life criteria. Toxicity is a function of the dissolved constituent. The analysis shows that only copper, lead, and zinc may present potential threats to aquatic life (Table 18). However, none exceed 1 TU for the measured dissolved fraction under the acute criteria. Thus, there is little evidence to suggest that ambient metal concentrations present a major risk to aquatic life in the Agua Hedionda Watershed.

Table 18. Criteria Exceedances for Co-Permittee Wet Weather Metals

	Total Metals (Acute Criteria)	Total Metals (Chronic Criteria)	Dissolved Metals (Acute Criteria)	Dissolved Metals (Chronic Criteria)
Arsenic	0.00%	0.00%	0.00%	0.00%
Cadmium	0.00%	0.00%	0.00%	0.00%
Copper	16.70%	34.10%	0.00%	2.70%
Lead	0.00%	8.20%	0.00%	0.00%
Nickel	0.00%	0.00%	0.00%	0.00%
Zinc	0.20%	0.20%	0.00%	0.00%
Chromium	0.00%	0.00%	0.00%	0.00%

Note: table compares metals data with criteria, both in toxicity units

3.3.4 Bacteria

Table 19 through Table 21 provide wet weather, ambient dry weather, and storm drain summary statistics for indicator bacteria. High bacterial concentrations usually result from the presence of animal or human fecal wastes, and may impair aquatic habitat, threaten human health, and promote undesirable organism growth. Total coliform measures include both fecal and non-fecal coliform concentrations. The presence of fecal bacteria, in particular, is an indicator of pollution. Therefore, separate fecal coliform measurements are also reported.

Table 19. Total Coliform (MPN/100ml) Summary Statistics for Wet Weather, Ambient, and Storm Drain Data

Data Type	Min	Mean	Max	Count ¹	DL	ND
Wet Weather	300	58,416	300,000	27	-	0
Ambient Dry Weather	50	64,971	3,000,000	56	-	0
Storm Drain	20	155,156	1,600,000	67	-	0

¹ Refers to number of samples.

Table 20. Fecal Coliform (MPN/100ml) Summary Statistics for Wet Weather, Ambient, and Storm Drain Data.

Data Type	Min	Mean	Max	Count ¹	DL	ND
Wet Weather	1	9,787	50,000	27	2	1
Ambient Dry Weather	4	3,502	80,000	56	-	0
Storm Drain	20	22,115	300,000	66	-	0

¹ Refers to number of samples.

Total coliform concentrations were lowest in the wet weather measurements. However, fecal coliform concentrations were lowest in the ambient dry weather samples. Total and fecal coliform concentrations were highest in storm drain samples.

Table 21. Enterococcus (MPN/100ml) Summary Statistics for Wet Weather, Ambient, and Storm Drain Data.

Data Type	Min	Mean	Max	Count ¹	DL	ND
Wet Weather	3,000	56,238	500,000	21	-	0
Ambient Dry Weather	0	463	5,000	54	10-20	5
Storm Drain	10	9,545	160,000	68	-	0

¹ Refers to number of samples.

In waters designated for contact recreation (REC-1), the fecal coliform concentration based on a minimum of not less than five samples for any 30-day period, shall not exceed a log mean of 200 MPN/100 ml, nor shall more than 10 percent of total samples during any 30-day period exceed 400 MPN/100 ml (SDRWQCB, 2006). The fecal coliform WQO used for comparison of individual samples is 400 MPN/100 ml. The Basin Plan cites USEPA criteria for enterococci WQOs. For waters designated for contact recreation, the freshwater maximum for infrequently used areas is 151 MPN/100 ml.

Figure 28 presents wet and dry weather fecal coliform measurements collected at the Co-permittee wet weather site. Both ambient dry weather samples were below 400 MPN/100 ml, while only two of the wet weather samples met this objective. All wet weather samples collected after 2001 exceeded this value. Figure 29 presents enterococcus data collected from the Agua Hedionda Creek and El Camino Real station between 2000 and 2007. Wet weather samples were consistently greater than those collected in dry weather. The data suggest an increasing bacteria trend in wet weather data.

Figure 30 presents the spatial distribution of fecal coliform concentrations collected as part of the ambient dry weather sampling efforts. The highest mean concentration occurs in Agua Hedionda Creek, just upstream of its confluence with Buena Creek and adjacent to commercial and industrial parcels. The next highest mean fecal coliform concentrations were located in Buena Creek adjacent to single family residential and industrial lands, and in Agua Hedionda Creek downstream of large residential and industrial areas. Enterococcus data exhibited similar patterns.

Figure 31 presents the spatial distribution of dry weather storm drain enterococcus data. Storm drain concentrations were greatest at two stations near the lagoon, several stations in the upper portions of Calavera Creek, and in La Mirada Creek. That pattern was similar in fecal coliform data (not shown). Some of the lowest enterococcus storm drain measurements were located in the upper watershed along Buena Creek, although fecal coliform data (not shown) were high at some stations just above Hwy 78.

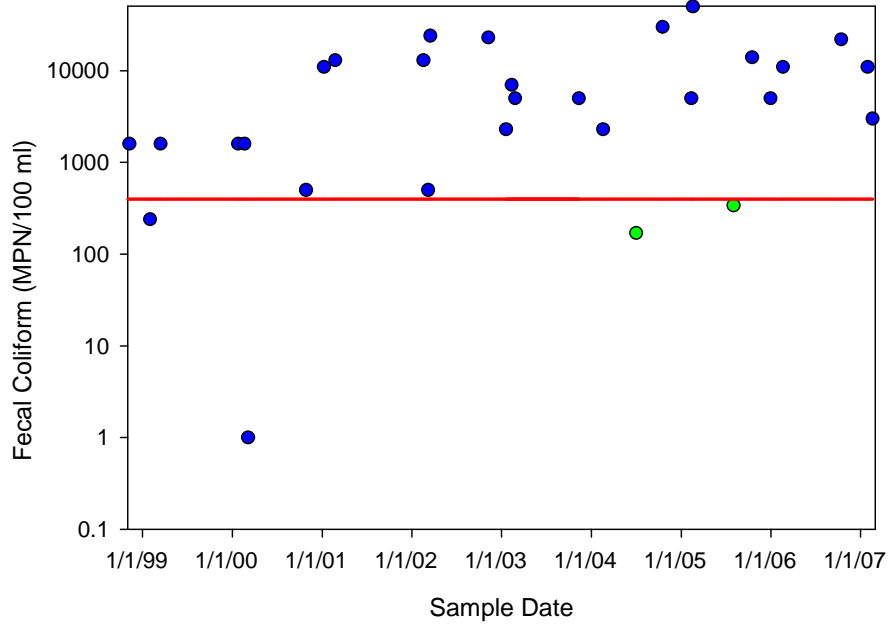


Figure 28. Fecal Coliform Wet (Dark Blue) and Dry (Light Green) Data Collected from Agua Hedionda Creek at the Co-permittee Wet Weather Site (Line Represents WQO)

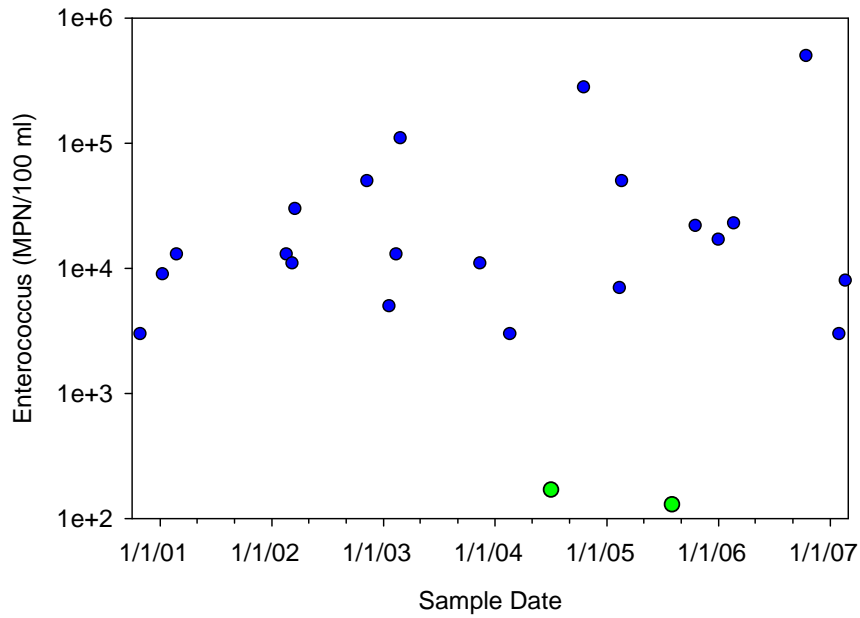


Figure 29. Enterococcus Wet (Dark Blue) and Dry (Light Green) Data Collected from the Agua Hedionda Creek at the Co-permittee Wet Weather Site

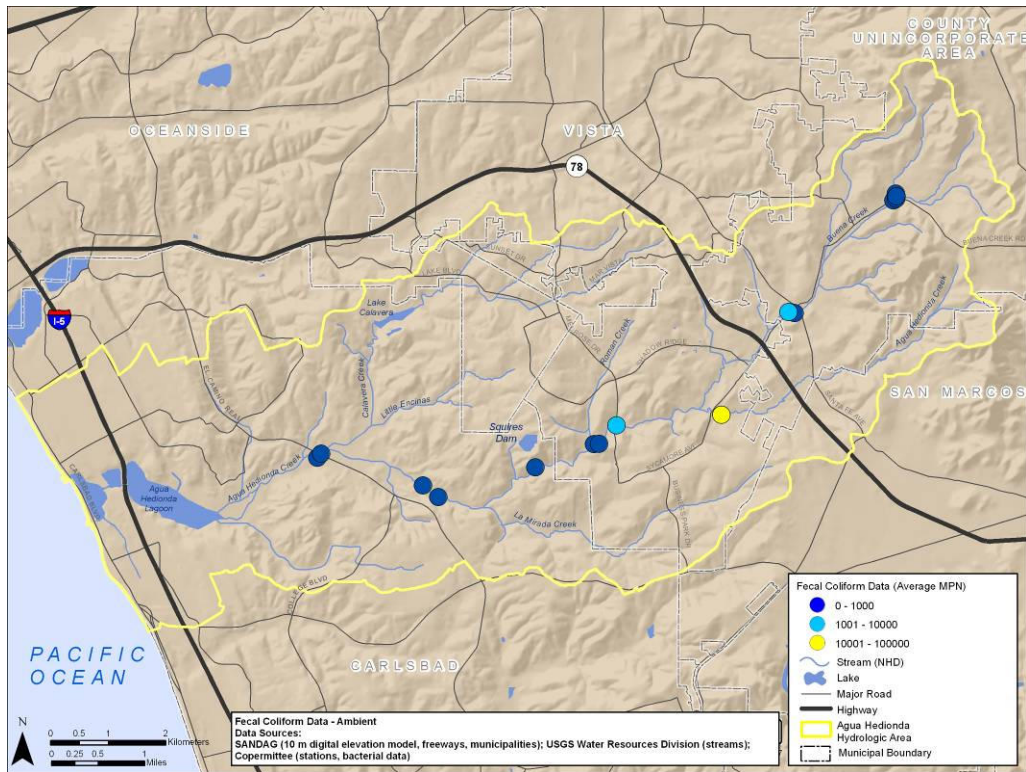


Figure 30. Fecal Coliform Spatial Distribution of Ambient Dry Weather Data (Co-permittee/SELC)

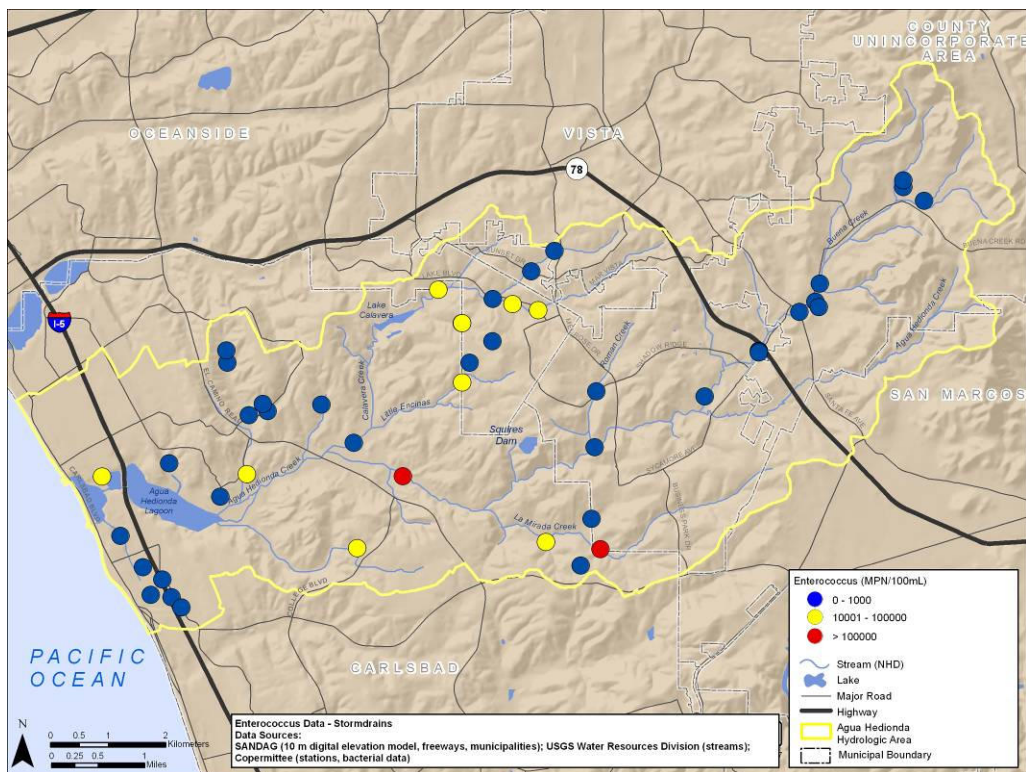


Figure 31. Enterococcus Spatial Distribution of Co-permittee Dry Weather Storm Drain Data (mean values)

3.3.5 Pesticides

Pesticides are synthetic chemicals that are developed to control insect and plants. After application, pesticides can disperse into the environment and contaminate surface and groundwaters. Pesticides are of particular concern because some can persist in an aquatic ecosystem for years and bioaccumulate in aquatic food chains.

Summaries of wet weather, ambient, and storm drain chlorpyrifos, diazinon, and malathion data are provided in Table 22-Table 24. Many of these data were non-detect. However, all three datasets experienced exceedances of these pesticides in comparison to WQOs developed by the California Department of Fish and Game (Table 25). Only the ambient dry and storm drain dry data for malathion did not exceed this WQO in any of its samples. Storm drain samples had the greatest concentrations of all three pesticides. A large number of chlorpyrifos and diazinon samples had detection limits that were greater than the WQOs.

Table 22. Co-permittee Wet Weather Pesticide Summary Statistics

Parameter	Units	WQO	Min ¹	Mean	Max	Count	DL	ND
Chlorpyrifos	µg/L	0.02	0.001	0.019	0.121	26	0.002-0.5	24
Diazinon	µg/L	0.08	0.002	0.185	0.464	27	0.004-0.5	9
Malathion	µg/L	0.43	0.005	0.191	0.622	15	0.01	2

¹minimum levels represent half the lowest detection limit

Table 23. Ambient Dry Weather Pesticide Summary Statistics

Parameter	Units	WQO	Min ¹	Mean	Max	Count	DL	ND
Chlorpyrifos	µg/L	0.02	0.025	0.055	0.500	27	0.05-1	18
Diazinon	µg/L	0.08	0.010	0.053	0.500	27	0.02-1	17
Malathion	µg/L	0.43	0.025	0.027	0.050	15	0.05	15

¹minimum levels represent half the lowest detection limit

Table 24. Storm Drain Dry Weather Pesticide Summary Statistics

Parameter	Units	WQO	Min ¹	Mean	Max	Count	DL	ND
Chlorpyrifos	µg/L	0.02	0.025	0.124	1.500	57	0.05-3	39
Diazinon	µg/L	0.08	0.025	0.179	3.000	57	0.05-6	40
Malathion	µg/L	0.43	0.020	0.047	0.330	15	0.04-0.05	13

¹minimum levels represent half the lowest detection limit

Buena Creek has been added to the 303(d) list for DDT. Of the dataset reviewed for this report, only the SWAMP dataset provided DDT data, which was collected in 2002. DDT was detected in half of the samples. However, the SWAMP dataset did have one aquatic life exceedance for the pesticide Endrin.

3.3.6 Toxicity

Meeting specified criteria for individual chemicals does not guarantee an absence of risks. Multiple chemicals may interact, and unmonitored chemicals (such as polyaromatic hydrocarbons or PAHs) can significantly impact biota. Toxicity tests using well-studied organisms can be used to evaluate the toxicity of a water or sediment sample directly.

Co-permittee Data

Toxicity data have been collected at the mass loading station on Agua Hedionda Creek from 2001 through 2006. While evidence to suggest toxicity was present, there was no evidence of persistent toxicity (Table 25). Persistent toxicity occurs when more than 50 percent of tests have a No Observed Effect Concentration (NOEC) or NOEC of less than 100 percent of the ambient concentration as evaluated through a dilution series.

Table 25. Co-permittee Wet Weather Toxicity Summary Statistics

Parameter	Units	WQO (%)	Percent Below WQO
<i>Ceriodaphnia</i> 96-hr	LC50 (%)	100	7
<i>Ceriodaphnia</i> 7-day Survival	NOEC (%)	100	20
<i>Ceriodaphnia</i> 7-day Reproduction	NOEC (%)	100	13
<i>Hyalella</i> 96-hr	NOEC (%)	100	47
<i>Selenastrum</i> 96-hr	NOEC (%)	100	0

SWAMP Data

SCCWRP (2007) conducted toxicity tests at one site on Agua Hedionda Creek and at one site on Buena Creek under the SWAMP program between 2002 and 2003 (Mazor and Schiff, 2007). Water toxicity was evaluated with 7-day exposures on the water flea, *Ceriodaphnia dubia*, and 96-hour exposures to the alga *Selenastrum capricornutum*. Sediment toxicity was evaluated with 10-day exposures on the amphipod *Hyallella azteca*. Tests showed no toxicity using the *Ceriodaphnia*. Tests using *Selenastrum* and *Hyallella* indicated toxicity 100 percent and 25 percent of the time, respectively.

Buena Creek is on the 303(d) list of impaired waterbodies, which identifies DDT, nitrate and nitrite, and phosphate as known stressors. Although several endpoints indicated toxicity, one sampling date (April 23, 2002) accounted for 75 percent of the toxic hits at this site. Half the sampling dates were not toxic to any endpoint, suggesting that toxicity was not persistent.

3.3.7 Benthic Macroinvertebrates

The Agua Hedionda Lagoon Foundation (AHLF) (2007) sponsored macroinvertebrate bioassessment of the Agua Hedionda Creek at sites located below South Melrose on the border of the cities of Vista and Carlsbad, in the Dawson Reserve located in the city of Vista and through Sunny Creek segment of the creek, and at the wet-weather station near El Camino Real. The protocols for sampling were those specified in the California Department of Fish and Game’s, California Stream Bioassessment Procedure.

The AHLF compared data collected to assessments by the San Diego County Municipal Co-permittees Urban Runoff Monitoring Program and the San Elijo Lagoon Conservancy. Index of Biotic Integrity

(IBI) scores for these surveys are presented in Table 26. The IBI scores from all three efforts are considered Poor to Very Poor.

Table 26. Index of Biotic Integrity Scores for Agua Hedionda Monitoring Sites (table taken from AHLF report)

Program	Site ID	2001		2002		2003		2004		2005		2006
		Spring	Fall	Spring	Fall	Spring	Fall	Spring	Fall	Spring	Fall	Spring
AHLF	AH2		14			3						
	AH3					8						
	AH4			10,8*	7	12						
SELC	AHS01									11	16	15
	AHS02									11	14	9
	AHD01									6	11	3
	AHD02									7	3	6
SD County	AHC-ECR	12	13	3	9	12	21	2	10	12		
	AHC-MR	5	13	2	20	12	12	4	13	5		

*AH4 was sampled in January and June, 2002

3.4 SUMMARY OF WATER QUALITY DATA

The data review suggests that sediment (TSS and turbidity) and bacteria (coliforms and enterococcus) are the greatest threats to watershed function in the Agua Hedionda watershed. Concentrations of these constituents exceed water quality objectives the majority of the time. Moreover, reports of significant upward trends in TSS, turbidity, and fecal coliform at the wet weather monitoring station suggest the problem is getting worse (Weston, 2007a). Turbidity was higher in the receiving water samples, an expected pattern based on the storm-driven nature of this parameter. Impairment from bacteria is, however, both a dry and wet weather problem in the watershed.

While the lack of wet weather sites inhibits the evaluation of spatial patterns, samples collected as part of the dry weather monitoring (storm drains and instream) show particularly high bacteria levels in La Mirada Creek, which drains commercial development, as well as Calavera Creek upstream of Lake Calavera. High salinity (a parameter closely related to TDS) is also found along Calavera Creek in areas draining residential development, suggesting an anthropogenic source though groundwater is likely the chief contributor to TDS levels throughout the watershed.

While nitrogen does not appear to be a significant threat in most of the watershed, the impairment of Buena Creek combined with the significant upward trend of nitrate (Weston, 2007a) suggest that it could become a problem in the future in the watershed. Phosphorus levels in the watershed are a concern: concentrations exceed the Basin Plan WQO and Buena Creek is 303(d)-listed for phosphate.

There is some evidence to suggest that pesticides are a threat in the watershed; however, toxicity tests have not borne out a persistent impact on the biological community. In addition, Weston (2007a) observed that the number of pesticide exceedances have decreased since 2002. There is also little indication that metals present a significant problem for aquatic life in the watershed based on an evaluation of metals toxicity.

Given the lack of evidence for widespread and severe toxicity in the watershed, the poor biological community as seen in biotic integrity indices can likely be attributed to habitat degradation from scour during storms and sediment transport from both upland and instream sources.

(This page left intentionally blank.)

4 Future Monitoring Recommendations

Monitoring has been conducted by multiple organizations in the Agua Hedionda Watershed. Each have their own objectives. The Co-permittees have monitoring requirements for their Municipal NPDES Permit to evaluate program effectiveness. Monitoring to support source assessments and linkage analyses for TMDL development for sediment (TSS and turbidity) and bacterial constituents are ongoing. Progress in meeting the TMDL objectives and to address the remaining impairments will require monitoring in the future in the lagoon and its tributaries. To the extent feasible, monitoring plans should be coordinated to address current as well as anticipated multiple future objectives of the Co-permittees in the Agua Hedionda Watershed and the SDRWQCB.

Given the need to address existing impairments, meet permit requirements, and address other water resource concerns, a comprehensive, watershed-based implementation framework should guide future monitoring efforts. Therefore, the final WMP developed for the Agua Hedionda Watershed will be critical. The goals, objectives, and selected indicators of the final plan should drive future monitoring in the watershed. A comprehensive implementation framework incorporating all of these concerns would result in more efficient and effective management of water resources and increase public support, thereby improving the likelihood of more-successful and rapid overall restoration of beneficial uses.

Many of the sources of the existing and multiple impairments are likely shared. For example, urban stormwater MS4 runoff associated with urban-based activities is a significant source of pollutants in the watershed. Where non-MS4 sources may ultimately also be found to be significant, non-municipal partners can be drawn into the solution development process.

Since stormwater and urban runoff are recognized as a significant contributor to impairments and since both sampling design and sample collection (especially for wet weather) are challenging and labor-intensive activities, efforts to monitor and manage these flows should consider all pollutants of concern. Wet weather monitoring should be extended to additional sites within the watershed to better understand sources and areas requiring treatment. Furthermore, additional monitoring in the lagoon should be conducted.

A more specific monitoring plan should be developed in conjunction with the completion of the WMP and consistent with the final WMP goals and objectives.

(This page left intentionally blank.)

5 References

- Center for Watershed Protection (CWP). 2007. *Impervious Cover Model*. Online at: <http://www.stormwatercenter.net/monitoring%20and%20assessment/imp%20cover/impercovr%20model.htm>. Accessed November 1, 2007.
- Cities of Carlsbad, Encinitas, Escondido, Oceanside, San Marcos, Solana Beach, and Vista, and County of San Diego (WURMP). 2003. Watershed Urban Runoff Management Program Carlsbad Hydrologic Unit.
- Cities of Carlsbad, Encinitas, Escondido, Oceanside, San Marcos, Solana Beach, and Vista, and County of San Diego (WURMP). 2004. Watershed Urban Runoff Management Program 2002-2003 Annual Report for the Carlsbad Hydrologic Unit.
- Cities of Carlsbad, Encinitas, Escondido, Oceanside, San Marcos, Solana Beach, and Vista, and County of San Diego (WURMP). 2005. Watershed Urban Runoff Management Program 2003-2004 Annual Report for the Carlsbad Hydrologic Unit.
- Cities of Carlsbad, Encinitas, Escondido, Oceanside, San Marcos, Solana Beach, and Vista, and County of San Diego (WURMP). 2006. Watershed Urban Runoff Management Program 2004-2005 Annual Report for the Carlsbad Hydrologic Unit.
- Cities of Carlsbad, Encinitas, Escondido, Oceanside, San Marcos, Solana Beach, and Vista, and County of San Diego (WURMP). 2007. Watershed Urban Runoff Management Program 2005-2006 Annual Report for the Carlsbad Hydrologic Unit.
- Federal Emergency Management Agency (FEMA). 1997. *Flood Insurance Study (FIS)*. Vol. 1, 4, Summary of Discharge.
- KTU+A, Merkel & Associates, Inc., and The Rick Alexander Company (KTU+A). 2002. *Carlsbad Watershed Management Plan, A Management Plan for the Coastal Watersheds of the Carlsbad Hydrologic Unit*. Prepared for the Carlsbad Watershed Network.
- Mazor R.D. and K. Schiff. 2007. *Surface Water Ambient Monitoring Program (SWAMP) Report on the Carlsbad Hydrologic Unit*. Prepared for the California Regional Water Quality Control Board, San Diego (Region 9).
- MEC Analytical Systems (MEC). 2004. *San Diego County Municipal Co-permittees 2002-2003 Urban Runoff Monitoring*. Prepared for the County of San Diego.
- MEC Analytical Systems (MEC). 2005. *San Diego County Municipal Co-permittees 2003-2004 Urban Runoff Monitoring*. Prepared for the County of San Diego.
- SANDAG. 1995. *San Diego Holland Vegetation Classification System*. Online at: http://www.sandag.com/resources/maps_and_gis/gis_downloads/downloads/metadata/veg95doc.htm#codes
- SANDAG. 2005. *Final 2030 San Diego Regional Growth Forecast data*. Online at: http://www.sandag.com/resources/maps_and_gis/gis_downloads/downloads/zip/Land/ForecastLand/planludoc.htm#codes
- San Diego County Water Authority, the City of San Diego, and the County of San Diego (IRWMP). 2007. *San Diego Integrated Regional Water Management Plan*.
- San Diego Regional Co-permittees. 2007. Coastal Monitoring Program Final Report. Prepared by Coastal Monitoring Workgroup. September 1, 2007

San Diego Regional Water Quality Control Board (SDRWQCB). 1994 with amendments through 2006. *Water Quality Control Plan for the San Diego Basin (9)*.

San Diego Regional Water Quality Control Board (SDRWQCB). 2007. *San Diego Region 2006 CWA Section 303d List of Water Quality Limited Segment*.
http://www.waterboards.ca.gov/tmdl/303d_lists2006.html .

San Elijo Lagoon Conservancy (SELCO). 2007. *Restoration of Riparian/Wetlands Habitat in the Carlsbad Hydrologic Unit (HU A145904.00)*. Funded by a Proposition 13 Watershed Protection Program Grant from the California State Water Resources Control Board (Grant Agreement Number 04-083-559-0).

Siepmann, S. and B. Finlayson. 2000. Water quality criteria for diazinon and chlorpyrifos. California Department of Fish and Game Pesticide Investigations Unit. Rancho Cordova, CA.

Agua Hedionda Lagoon Foundation (AHLF). 2007. *Bioassessment Monitoring of Agua Hedionda Creek*.

Weston Solutions (Weston). 2005. *San Diego County Municipal Co-permittees 2004-2005 Urban Runoff Monitoring*. Prepared for the County of San Diego.

Weston Solutions (Weston). 2007a. *San Diego County Municipal Co-permittees 2005-2006 Urban Runoff Monitoring*. Prepared for the County of San Diego.

Weston Solutions (Weston). 2007b. *San Diego County Municipal Co-permittees 2003-2005 Ambient Bay and Lagoon Monitoring Review and Recommendations Final Report*

Appendix A. Physicochemical Data

(This page left intentionally blank.)

Table A-1. Ambient Dry Weather Water Chemistry Summary Statistics

Sample Location		Conductivity	Dissolved Oxygen	Electrical Connectivity	MBAS	Oil & Grease	Salinity	Temp	Turbidity	pH
	Units	µS/cm	mg/L	mS/cm	mg/L	mg/L	%	°C	NTU	
	DL	-	-	-	0.05-0.5	1-5	-	-	-	-
AC-1	Min	1,667.0			0.3	2.5		16.0	3.1	7.3
	Mean	3,703.4			0.3	5.8		19.7	13.2	7.9
	Max	5,310.0			0.5	11.0		22.7	26.0	8.4
	Count	5.0	0.0	0.0	7.0	5.0	0.0	3.0	5.0	5.0
	ND	0.0	0.0	0.0	2.0	1.0	0.0	0.0	0.0	0.0
AC-2	Min	1,760.0			0.3	0.5		18.4	0.0	7.6
	Mean	1,960.5			0.3	2.0		20.1	1.3	8.0
	Max	2,300.0			0.5	2.5		21.7	2.0	8.5
	Count	4.0	0.0	0.0	5.0	4.0	0.0	2.0	4.0	4.0
	ND	0.0	0.0	0.0	1.0	2.0	0.0	0.0	0.0	0.0
AH Creek-1_2	Min	2,510.0			0.3	0.5			1.9	8.2
	Mean	2,605.0			0.3	1.5			1.9	8.3
	Max	2,700.0			0.3	2.5			1.9	8.3
	Count	2.0	0.0	0.0	2.0	2.0	0.0	0.0	2.0	2.0
	ND	0.0	0.0	0.0	0.0	0.0	0.0	0.0	0.0	0.0
AH-10	Min	1,790.0			0.3	0.5		18.1	0.4	7.6
	Mean	2,126.3			0.3	2.7		19.6	9.6	8.1
	Max	2,630.0			0.5	5.4		21.0	43.0	8.4
	Count	6.0	0.0	0.0	9.0	6.0	0.0	4.0	6.0	6.0
	ND	0.0	0.0	0.0	3.0	3.0	0.0	0.0	0.0	0.0

Sample Location		Conductivity	Dissolved Oxygen	Electrical Connectivity	MBAS	Oil & Grease	Salinity	Temp	Turbidity	pH
	Units	µS/cm	mg/L	mS/cm	mg/L	mg/L	%	°C	NTU	
	DL	-	-	-	0.05-0.5	1-5	-	-	-	-
CAR05	Min	1,300.0	6.2	2.1	0.0	0.5	0.1	13.5	2.0	7.9
	Mean	1,953.8	7.9	2.1	0.1	2.1	0.1	20.0	8.4	8.1
	Max	2,160.0	9.6	2.1	0.3	5.0	0.1	22.4	17.0	8.3
	Count	8.0	3.0	3.0	4.0	4.0	3.0	8.0	10.0	11.0
	ND	0.0	0.0	0.0	1.0	2.0	0.0	0.0	0.0	0.0
CAR05 C 03	Min		7.3	2.3			0.1	14.7	1.0	7.4
	Mean		7.3	2.3			0.1	14.7	1.0	7.4
	Max		7.3	2.3			0.1	14.7	1.0	7.4
	Count	0.0	1.0	1.0	0.0	0.0	1.0	1.0	1.0	1.0
	ND	0.0	0.0	0.0	0.0	0.0	0.0	0.0	0.0	0.0
CAR05 Q	Min			2.3			0.1	19.0	1.0	7.2
	Mean			2.3			0.1	19.0	1.0	7.2
	Max			2.3			0.1	19.0	1.0	7.2
	Count	0.0	0.0	1.0	0.0	0.0	1.0	1.0	1.0	1.0
	ND	0.0	0.0	0.0	0.0	0.0	0.0	0.0	0.0	0.0
CAR05 R	Min			2.3			0.1	20.1	5.0	7.4
	Mean			2.3			0.1	20.1	5.0	7.4
	Max			2.3			0.1	20.1	5.0	7.4
	Count	0.0	0.0	1.0	0.0	0.0	1.0	1.0	1.0	1.0
	ND	0.0	0.0	0.0	0.0	0.0	0.0	0.0	0.0	0.0

Sample Location		Conductivity	Dissolved Oxygen	Electrical Connectivity	MBAS	Oil & Grease	Salinity	Temp	Turbidity	pH
	Units	µS/cm	mg/L	mS/cm	mg/L	mg/L	%	°C	NTU	
	DL	-	-	-	0.05-0.5	1-5	-	-	-	-
CAR05 S	Min			2.2			0.1	22.0	21.0	7.0
	Mean			2.2			0.1	22.0	21.0	7.0
	Max			2.2			0.1	22.0	21.0	7.0
	Count	0.0	0.0	1.0	0.0	0.0	1.0	1.0	1.0	1.0
	ND	0.0	0.0	0.0	0.0	0.0	0.0	0.0	0.0	0.0
904CBBUR1	Min	1,627						15.41	0.54	6.59
	Mean	1,839						17.71	1.88	7.5575
	Max	1,961						19.19	3.5	8.15
	Count	4						4	3	4
	ND	0						0	0	0
904CBAQH6	Min	2,707						14.44	0.24	7.52
	Mean	2,822.75						17.3375	0.79	7.8125
	Max	3,008						20.65	1.4	8.15
	Count	4						4	4	4
	ND	0						0	0	0
AHD02	Min	1,541.33	4.86					10.00		7.43
	Mean	2,051.38	7.94					16.76		7.65
	Max	2,257.00	9.22					20.60		8.17
	Count	8.00	8.00					8.00		7.00
	ND	0	0					0		0

Sample Location		Conductivity	Dissolved Oxygen	Electrical Connectivity	MBAS	Oil & Grease	Salinity	Temp	Turbidity	pH
	Units	µS/cm	mg/L	mS/cm	mg/L	mg/L	%	°C	NTU	
	DL	-	-	-	0.05-0.5	1-5	-	-	-	-
AHD01	Min	1,408.33	5.12					9.40		7.80
	Mean	1,971.83	8.51					15.90		7.96
	Max	2,139.67	9.92					19.37		8.20
	Count	8.00	8.00					8.00		7.00
	ND	0	0					0		0
AHS01	Min	1,980.67	8.22					9.60		7.87
	Mean	2,521.33	9.64					15.74		8.15
	Max	2,751.67	11.26					19.60		8.60
	Count	8.00	8.00					8.00		8.00
	ND	0	0					0		0
AHS02	Min	1,126.33	7.52					9.70		7.77
	Mean	2,394.58	9.43					16.48		8.15
	Max	2,726.00	10.68					20.70		8.50
	Count	8.00	8.00					8.00		8.00
	ND	0	0					0		0
AH2	Min	1,946	9.7					21		7.7
	Mean	1,946	9.7					21		7.7
	Max	19,46	9.7					21		7.7
	Count	1	1					1		1
	ND	0	0					0		0

Sample Location		Conductivity	Dissolved Oxygen	Electrical Connectivity	MBAS	Oil & Grease	Salinity	Temp	Turbidity	pH
	Units	µS/cm	mg/L	mS/cm	mg/L	mg/L	%	°C	NTU	
	DL	-	-	-	0.05-0.5	1-5	-	-	-	-
AH3	Min	1,933	8					18.5		7.7
	Mean	1,933	8					19.25		7.8
	Max	1,933	8					20		7.9
	Count	1	1					2		2
	ND	0	0					0		0
AH4	Min	848	7					13.1		8
	Mean	12,41.5	8.5					15.45		8.05
	Max	1,635	9.5					17.8		8.1
	Count	2	3					2		2
	ND	0	0					0		0

(This page left intentionally blank.)

Appendix B. Nutrient Data

(This page left intentionally blank.)

Table B-1. Ambient Dry Weather Nutrient Summary Statistics

Sample Location		Ammonia as N	Nitrate as N	Nitrate as NO3	Nitrite	Nitrite + Nitrate	TKN	Orthophosphate	Phosphate as P	Phosphorus
	Units	mg/L	mg/L	mg/L	mg/L	mg/L	mg/L	mg/L	mg/L	mg/L
	DL	0.05-0.1	0.05-1.35	-	0.01	0.01	0.1-0.5	0.01-0.1	0.06	0.02-0.05
AC-1	Min	0.40	0.10					0.10		0.07
	Mean	2.75	0.52					0.25		0.07
	Max	8.00	1.00					0.40		0.07
	Count	7.00	5.00	0.00	0.00	0.00	0.00	4.00	0.00	1.00
	ND	0.00	0.00	0.00	0.00	0.00	0.00	0.00	0.00	0.00
AC-2	Min	0.10	0.30					0.07		
	Mean	0.20	3.26					0.41		
	Max	0.30	7.50					0.70		
	Count	5.00	5.00	0.00	0.00	0.00	0.00	5.00	0.00	0.00
	ND	0.00	0.00	0.00	0.00	0.00	0.00	0.00	0.00	0.00
AH Creek-1_2	Min	0.10	1.25					0.03		
	Mean	0.20	1.25					0.03		
	Max	0.30	1.25					0.03		
	Count	2.00	2.00	0.00	0.00	0.00	0.00	2.00	0.00	0.00
	ND	0.00	0.00	0.00	0.00	0.00	0.00	0.00	0.00	0.00
AH-10	Min	0.05	0.03					0.07		0.07
	Mean	0.19	3.25					0.32		0.11
	Max	0.30	7.50					0.60		0.16
	Count	6.00	6.00	0.00	0.00	0.00	0.00	4.00	0.00	2.00
	ND	0.00	1.00	0.00	0.00	0.00	0.00	0.00	0.00	0.00

Sample Location		Ammonia as N	Nitrate as N	Nitrate as NO3	Nitrite	Nitrite + Nitrate	TKN	Orthophosphate	Phosphate as P	Phosphorus
	Units	mg/L	mg/L	mg/L	mg/L	mg/L	mg/L	mg/L	mg/L	mg/L
	DL	0.05-0.1	0.05-1.35	-	0.01	0.01	0.1-0.5	0.01-0.1	0.06	0.02-0.05
CAR05	Min	0.10	8.13					0.16	0.15	0.15
	Mean	0.21	11.65					0.18	0.16	0.18
	Max	0.40	16.03					0.23	0.16	0.23
	Count	10.00	10.00	0.00	0.00	0.00	0.00	3.00	3.00	4.00
	ND	0.00	0.00	0.00	0.00	0.00	0.00	0.00	0.00	0.00
CAR05 C 03	Min	0.30	32.96						0.15	
	Mean	0.30	32.96						0.15	
	Max	0.30	32.96						0.15	
	Count	1.00	1.00	0.00	0.00	0.00	0.00	0.00	1.00	0.00
	ND	0.00	0.00	0.00	0.00	0.00	0.00	0.00	0.00	0.00
CAR05 Q	Min		11.74							
	Mean		11.74							
	Max		11.74							
	Count	0.00	1.00	0.00	0.00	0.00	0.00	0.00	0.00	0.00
	ND	0.00	0.00	0.00	0.00	0.00	0.00	0.00	0.00	0.00
CAR05 R	Min		15.58							
	Mean		15.58							
	Max		15.58							
	Count	0.00	1.00	0.00	0.00	0.00	0.00	0.00	0.00	0.00
	ND	0.00	0.00	0.00	0.00	0.00	0.00	0.00	0.00	0.00

Sample Location		Ammonia as N	Nitrate as N	Nitrate as NO3	Nitrite	Nitrite + Nitrate	TKN	Orthophosphate	Phosphate as P	Phosphorus
	Units	mg/L	mg/L	mg/L	mg/L	mg/L	mg/L	mg/L	mg/L	mg/L
	DL	0.05-0.1	0.05-1.35	-	0.01	0.01	0.1-0.5	0.01-0.1	0.06	0.02-0.05
CAR05 S	Min		27.09							
	Mean		27.09							
	Max		27.09							
	Count	0.00	1.00	0.00	0.00	0.00	0.00	0.00	0.00	0.00
	ND	0.00	0.00	0.00	0.00	0.00	0.00	0.00	0.00	0.00
904CBBUR1	Min	0.05				10.10	0.25	0.13		0.12
	Mean	0.13				15.38	0.55	0.15		0.15
	Max	0.38				19.40	1.44	0.17		0.18
	Count	4.00				4.00	4.00	4.00		4.00
	ND	3.00				0.00	3.00	0.00		0.00
904CBAQH6	Min	0.05				0.48	0.25	0.01		0.03
	Mean	0.07				1.09	0.32	0.03		0.07
	Max	0.13				1.36	0.52	0.05		0.14
	Count	4.00				4.00	4.00	4.00		6.00
	ND	3.00				0.00	3.00	1.00		2.00
AHD02	Min		1.38	6.11	0.01		0.10	0.08	0.15	
	Mean		4.63	22.78	0.07		0.62	0.30	0.51	
	Max		9.00	40.30	0.13		1.63	0.49	1.62	
	Count		6.00	8.00	6.00		8.00	8.00	8.00	
	ND		0.00	0.00	1.00		0.00	0.00	0.00	

Sample Location		Ammonia as N	Nitrate as N	Nitrate as NO3	Nitrite	Nitrite + Nitrate	TKN	Orthophosphate	Phosphate as P	Phosphorus
	Units	mg/L	mg/L	mg/L	mg/L	mg/L	mg/L	mg/L	mg/L	mg/L
	DL	0.05-0.1	0.05-1.35	-	0.01	0.01	0.1-0.5	0.01-0.1	0.06	0.02-0.05
AHD01	Min		0.48	2.12	0.01		0.05	0.09	0.16	
	Mean		2.55	13.64	0.01		0.44	0.24	0.41	
	Max		5.60	32.40	0.03		0.76	0.47	1.14	
	Count		6.00	8.00	6.00		8.00	8.00	8.00	
	ND		0.00	0.00	4.00		1.00	0.00	0.00	
AHS01	Min		0.30	1.33	0.01		0.05	0.01	0.08	
	Mean		1.26	7.73	0.04		0.39	0.11	0.18	
	Max		2.50	23.80	0.19		0.73	0.24	0.43	
	Count		6.00	8.00	6.00		8.00	8.00	8.00	
	ND		0.00	0.00	5.00		2.00	1.00	0.00	
AHS02	Min		0.37	1.64	0.01		0.05	0.01	0.03	
	Mean		1.29	8.29	0.01		0.38	0.12	0.18	
	Max		2.50	27.60	0.01		0.77	0.27	0.46	
	Count		6.00	8.00	6.00		8.00	8.00	8.00	
	ND		0.00	0.00	5.00		1.00	3.00	1.00	

Appendix C. Bacterial Data

(This page left intentionally blank.)

Table C-1. Ambient Dry Weather Bacteriology Data

Sample Location	Units	Enterococcus	Fecal Coliform	Total Coliform
		MPN/100 ml	MPN/100 ml	MPN/100 ml
DL		10-20	-	-
AC-1	Min	110	1300	50000
	Mean	2,947.25	2,7140	65,8000
	Max	5,000	80,000	300,0000
	Count	4	5	5
	ND	0	0	0
AC-2	Min	110	40	700
	Mean	173.33	116.67	1166.67
	Max	300	170	1700
	Count	3	3	3
	ND	0	0	0
AH Creek-1_2	Min	130	170	14,000
	Mean	150	255	32,000
	Max	170	340	50,000
	Count	2	2	2
	ND	0	0	0
AH-10	Min	62	170	1,600
	Mean	458.4	1,134	3,960
	Max	800	3,000	8,000
	Count	5	5	5
	ND	0	0	0
CAR05	Min	25	555	3,000
	Mean	840.63	4,472.78	16,262.78
	Max	1,300	13,000	40,005
	Count	8	9	9
	ND	0	0	0
AHD02	Min	2.00	8.00	50.00
	Mean	125.36	472.25	3,743.75
	Max	669.90	1,600.00	16,000.00
	Count	8.00	8.00	8.00
	ND	1	0	0

Sample Location		Enterococcus	Fecal Coliform	Total Coliform
	Units	MPN/100 ml	MPN/100 ml	MPN/100 ml
	DL	10-20	-	-
AHD01	Min	0.00	4.00	50.00
	Mean	114.19	459.25	4,543.75
	Max	685.50	1,700.00	16,000.00
	Count	8.00	8.00	8.00
	ND	1	0	0
AHS01	Min	5.00	13.00	500.00
	Mean	112.23	424.13	3,612.50
	Max	552.00	1,400.00	16,000.00
	Count	8.00	8.00	8.00
	ND	2	0	1
AHS02	Min	5.00	8.00	800.00
	Mean	70.84	351.00	2,237.50
	Max	298.00	1,700.00	5,000.00
	Count	8.00	8.00	8.00
	ND	0	0	1

Table C-2. Co-permittee Dry Weather Storm Drain Bacteria Summary Statistics

Sample Location		Enterococcus	Fecal Coliform	Total Coliform
	Units	MPN/100 ml	MPN/100 ml	MPN/100 ml
	DL	10-200	20-200	20-2000
A002	Min	10	230	3,000
	Mean	2,620.5	1,182.5	67,000
	Max	9,520	2,300	240,000
	Count	4	4	4
	ND	0	0	0
A004a	Min	1,300	5,000	300,000
	Mean	55427.2	122400	600,000
	Max	160,000	300,000	1,600,000
	Count	5	5	5
	ND	1	1	0
A004b	Min	52	40	17000
	Mean	1,920.5	1,685	56,250
	Max	6,130	5,000	110,000
	Count	4	4	4
	ND	0	0	0
A013	Min	74	110	2,800
	Mean	8,366	6202.5	128,200
	Max	30,000	22,000	240,000
	Count	4	4	4
	ND	0	0	0
A015	Min	41	5,000	23,000
	Mean	1,810.25	10,500	50,750
	Max	2,800	24,000	80,000
	Count	4	4	4
	ND	0	0	0
A016	Min	1,133	300	50,000
	Mean	2,053.25	12,325	495,000
	Max	3,080	24,000	900,000
	Count	4	4	4
	ND	0	0	0

Sample Location		Enterococcus	Fecal Coliform	Total Coliform
	Units	MPN/100 ml	MPN/100 ml	MPN/100 ml
	DL	10-200	20-200	20-2000
A04C	Min	516	500	16,000
	Mean	516	500	16,000
	Max	516	500	16,000
	Count	1	1	1
	ND	0	0	0
AH Creek-2	Min	170	5,000	8,000
	Mean	170	5,000	8,000
	Max	170	5,000	8,000
	Count	1	1	1
	ND	0	0	0
AH03	Min	40	500	7,000
	Mean	3,968	11,360	61,600
	Max	9,000	50,000	170,000
	Count	5	5	5
	ND	0	0	0
AH08	Min	70	300	1300
	Mean	246	13,868	38,860
	Max	500	50,000	90,000
	Count	5	5	5
	ND	0	0	0
AH10	Min	80	110	800
	Mean	320	9,777.5	202,200
	Max	800	23,000	50,0000
	Count	4	4	4
	ND	0	0	0
AH-21	Min	40	20	230
	Mean	16,089.5	35,764	42,926
	Max	50,000	160,000	160,000
	Count	6	5	5
	ND	0	0	0

Sample Location		Enterococcus	Fecal Coliform	Total Coliform
	Units	MPN/100 ml	MPN/100 ml	MPN/100 ml
	DL	10-200	20-200	20-2000
AH24	Min	230	70	8,000
	Mean	1,632.5	2,192.5	16,2750
	Max	5,000	5,000	500,000
	Count	4	4	4
	ND	0	0	0
AH28	Min	170		20
	Mean	170		20
	Max	170		20
	Count	1	0	1
	ND	0	0	0
AH32	Min	170	1,300	2,400
	Mean	170	1,300	2,400
	Max	170	1,300	2,400
	Count	1	1	1
	ND	0	0	0
AH45	Min	1,300	3,000	50,000
	Mean	3,400	43,250	202,500
	Max	8,000	160,000	300,000
	Count	4	4	4
	ND	0	0	0
AH46	Min	10	270	22,000
	Mean	40,282.5	41,317.5	285,500
	Max	160,000	130,000	900,000
	Count	4	4	4
	ND	1	0	0
AH59	Min	1,300	220	386
	Mean	1,300	220	386
	Max	1,300	220	386
	Count	1	1	1
	ND	0	0	0

Sample Location		Enterococcus	Fecal Coliform	Total Coliform
	Units	MPN/100 ml	MPN/100 ml	MPN/100 ml
	DL	10-200	20-200	20-2000
CAR05A	Min	300	3,000	5,000
	Mean	300	3,000	5,000
	Max	300	3,000	5,000
	Count	1	1	1
	ND	0	0	0
CAR05B	Min	340	1,400	2,800
	Mean	340	1,400	2,800
	Max	340	1,400	2,800
	Count	1	1	1
	ND	0	0	0
CAR05C	Min	270	800	1,300
	Mean	270	800	1,300
	Max	270	800	1,300
	Count	1	1	1
	ND	0	0	0
CAR05D	Min	300	3,000	7,000
	Mean	300	3,000	7,000
	Max	300	3,000	7,000
	Count	1	1	1
	ND	0	0	0
CAR05E	Min	800	13,000	24,000
	Mean	800	13,000	24,000
	Max	800	13,000	24,000
	Count	1	1	1
	ND	0	0	0
L02B	Min	388	700	11,000
	Mean	388	700	11,000
	Max	388	700	11,000
	Count	1	1	1
	ND	0	0	0

Appendix D. Pesticide Data

(This page intentionally left blank.)

Table D-1. Co-permittee Dry Weather Ambient Pesticide Summary Data

Sample Location		Chlorpyrifos	Diazinon	Malathion
	Units	µg/L	µg/L	µg/L
	DL	0.05-1	0.02-1	0.05
AC-1	Min	0.025	0.025	0.025
	Mean	0.025	0.025	0.025
	Max	0.025	0.025	0.025
	Count	5	5	2
	ND	3	3	2
AC-2	Min	0.025	0.025	0.025
	Mean	0.025	0.04125	0.025
	Max	0.025	0.09	0.025
	Count	4	4	2
	ND	2	2	2
AH Creek-1_2	Min	0.025	0.025	
	Mean	0.025	0.025	
	Max	0.025	0.025	
	Count	2	2	0
	ND	0	0	0
AH-10	Min	0.025	0.025	0.025
	Mean	0.12	0.12	0.025
	Max	0.5	0.5	0.025
	Count	5	5	2
	ND	3	3	2
CAR05	Min	0.025	0.025	0.05
	Mean	0.108333333	0.108333333	0.05
	Max	0.25	0.25	0.05
	Count	3	3	1
	ND	2	2	1
904CBBUR1	Min	0.025	0.01	0.025
	Mean	0.025	0.01	0.025
	Max	0.025	0.01	0.025
	Count	4	4	4
	ND	4	4	4

Sample Location		Chlorpyrifos	Diazinon	Malathion
	Units	µg/L	µg/L	µg/L
	DL	0.05-1	0.02-1	0.05
	904CBAQH6	Min	0.025	0.01
	Mean	0.025	0.0155	0.025
	Max	0.025	0.032	0.025
	Count	4	4	4
	ND	4	3	4

Table D-2. Co-permittee Dry Weather Storm Drain Pesticide Summary Data

Sample Location		Chlorpyrifos	Diazinon	Malathion
	Units	µg/L	µg/L	µg/L
	DL	0.05-3	0.05-6	0.04-0.05
A002	Min	0.025	0.025	0.020
	Mean	0.025	0.173	0.023
	Max	0.025	0.470	0.025
	Count	3	3	2
	ND	2	2	2
A004a	Min	0.025	0.025	0.025
	Mean	0.170	0.063	0.038
	Max	0.460	0.140	0.050
	Count	3	3	2
	ND	1	2	1
A004b	Min	0.025	0.025	0.025
	Mean	0.025	0.025	0.025
	Max	0.025	0.025	0.025
	Count	3	3	2
	ND	2	2	2
A013	Min	0.025	0.025	0.025
	Mean	0.025	0.025	0.178
	Max	0.025	0.025	0.330
	Count	2	2	2
	ND	2	2	1
A015	Min	0.025	0.025	0.025
	Mean	0.025	0.025	0.025
	Max	0.025	0.025	0.025
	Count	2	2	2
	ND	2	2	2
A016	Min	0.025	0.025	0.025
	Mean	0.025	0.025	0.025
	Max	0.025	0.025	0.025
	Count	3	3	3
	ND	3	3	3

Sample Location		Chlorpyrifos	Diazinon	Malathion
	Units	µg/L	µg/L	µg/L
	DL	0.05-3	0.05-6	0.04-0.05
A02	Min	0.250	0.250	
	Mean	0.250	0.250	
	Max	0.250	0.250	
	Count	1	1	0
	ND	1	1	0
A04A	Min	1.500	3.000	
	Mean	1.500	3.000	
	Max	1.500	3.000	
	Count	1	1	0
	ND	1	1	0
A04B	Min	1.500	3.000	
	Mean	1.500	3.000	
	Max	1.500	3.000	
	Count	1	1	0
	ND	1	1	0
A04C	Min	0.250	0.250	
	Mean	0.250	0.250	
	Max	0.250	0.250	
	Count	1	1	0
	ND	1	1	0
AH Creek-2	Min	0.025	0.025	
	Mean	0.025	0.025	
	Max	0.025	0.025	
	Count	1	1	0
	ND	1	1	0
AH03	Min	0.025	0.025	
	Mean	0.070	0.070	
	Max	0.250	0.250	
	Count	5	5	0
	ND	3	3	0

Sample Location		Chlorpyrifos	Diazinon	Malathion
	Units	µg/L	µg/L	µg/L
	DL	0.05-3	0.05-6	0.04-0.05
AH08	Min	0.025	0.025	
	Mean	0.070	0.070	
	Max	0.250	0.250	
	Count	5	5	0
	ND	3	3	0
AH10	Min	0.025	0.025	
	Mean	0.081	0.081	
	Max	0.250	0.250	
	Count	4	4	0
	ND	3	3	0
AH-21	Min	0.025	0.025	0.025
	Mean	0.104	0.104	0.025
	Max	0.500	0.500	0.025
	Count	6	6	2
	ND	4	4	2
AH24	Min	0.025	0.025	
	Mean	0.025	0.025	
	Max	0.025	0.025	
	Count	4	4	0
	ND	2	2	0
AH28	Min	0.250	0.250	
	Mean	0.250	0.250	
	Max	0.250	0.250	
	Count	1	1	0
	ND	1	1	0
AH32	Min	0.250	0.250	
	Mean	0.250	0.250	
	Max	0.250	0.250	
	Count	1	1	0
	ND	1	1	0

Sample Location		Chlorpyrifos	Diazinon	Malathion
	Units	µg/L	µg/L	µg/L
	DL	0.05-3	0.05-6	0.04-0.05
AH45	Min	0.025	0.025	
	Mean	0.025	0.025	
	Max	0.025	0.025	
	Count	4	4	0
	ND	2	2	0
AH46	Min	0.025	0.025	
	Mean	0.025	0.025	
	Max	0.025	0.025	
	Count	4	4	0
	ND	2	2	0
AH59	Min	0.250	0.250	
	Mean	0.250	0.250	
	Max	0.250	0.250	
	Count	1	1	0
	ND	1	1	0
L02B	Min	0.025	0.025	
	Mean	0.025	0.025	
	Max	0.025	0.025	
	Count	1	1	0
	ND	0	0	0

Appendix E. Metals Data

(This page left intentionally blank.)

Table E-1. Co-permittee Wet Weather Metals Summary Data

Parameter	Units	Min	Mean	Max	Count	DL	ND
Hardness							
Total Hardness	mg CaCO3/L	35.3	395	680	27	-	0
Total Metals							
Antimony	mg/L	7.50E-04	1.59E-03	3.00E-03	26	0.0015-0.006	21
Arsenic	mg/L	1.47E-06	1.91E-05	5.29E-05	26	0.001-0.002	4
Cadmium	mg/L	1.20E-05	9.92E-05	3.38E-04	26	0.0003-0.001	21
Chromium	mg/L	2.88E-07	2.13E-06	1.60E-05	26	0.005	15
Copper	mg/L	2.93E-05	6.38E-04	3.81E-03	26	0.005	4
Lead	mg/L	1.07E-06	1.66E-05	1.15E-04	26	0.001-0.005	7
Nickel	mg/L	1.78E-06	9.84E-06	7.36E-05	26	0.005	3
Selenium	mg/L	5.00E-04	2.00E-03	6.00E-03	26	0.001-0.005	22
Zinc	mg/L	1.64E-05	2.58E-04	1.01E-03	26	0.02	3
Dissolved Metals							
Antimony	mg/L	1.00E-03	2.44E-03	7.50E-03	24	0.0015-0.006	21
Arsenic	mg/L	1.47E-06	6.31E-06	3.24E-05	24	0.001-0.002	10
Cadmium	mg/L	5.16E-05	1.01E-04	1.79E-04	24	0.00025- 0.001	24
Chromium	mg/L	9.13E-07	2.12E-06	1.03E-05	24	0.005	24
Copper	mg/L	3.06E-05	1.52E-04	8.89E-04	24	0.005	12
Lead	mg/L	1.70E-06	4.86E-06	2.45E-05	24	0.001-0.002	24
Nickel	mg/L	8.68E-07	3.02E-06	1.29E-05	24	0.002-0.005	4
Selenium	mg/L	5.00E-04	2.13E-03	1.00E-02	24	0.001-0.02	23
Zinc	mg/L	2.94E-06	7.39E-05	8.20E-04	24	0.001-0.02	19

P

National Weather Service
Daily Climate Reports

<http://www.wrh.noaa.gov/sgx/obs/rtp/carlsbad.html>

Q

David L. Mayer, Ph.D.

President / Principal Scientist

Education

Ph.D. Fisheries and Quantitative Sciences, University of Washington, 1973

M.S.C. Environmental Biology, California State University, Hayward, 1970

B.A. Biology and Chemistry, California State University, San Jose, 1965

Experience

Dr. Mayer has extensive experience in marine, estuarine, and freshwater environmental studies. He directed and provided overview of entrainment studies for two full-scale (100 mgd) desalination projects in Southern California and one pilot desalination project in San Francisco Bay. Dr. Mayer provided expert witness testimony before the Santa Ana and San Diego Regional Water Quality Control Board hearings during the National Pollutant Discharge Elimination System (NPDES) permit process for the Southern California desalination facilities. He also provided expert witness testimony before the cities of Huntington Beach and Carlsbad throughout the CEQA process. Both projects were approved by the cities. He directed and provided overview of entrainment and source water studies to assess the effects of candidate desalination projects located in the San Francisco Bay Area. He is currently directing ongoing entrainment studies of the Bay Area Regional Desalination Facility and the recently initiated entrainment and intake screen studies for the Santa Cruz and Soquel Water Districts' pilot desalination facility. NPDES permits were granted to both facilities. Dr. Mayer is assisting West Basin Water District in their efforts to design and permit a demonstration desalination facility in Redondo Beach; and his recently completed research plan to investigate the benefits of wedgewire screen intakes to eliminate impingement and reduce entrainment effects is in the final stages of agency review and comment.

Dr. Mayer specializes in aquatic temperature and flow regimes and their effects on ecological systems beginning with his doctoral research analyzing and modeling the relationships of water temperatures and hydrodynamics in northern Puget Sound aquatic communities. He has participated in the San Francisco Bay/Delta's Interagency Ecological Program's estuarine ecology work team since the group's founding. Dr. Mayer has devoted a majority of his professional career and expertise to studies of the thermal and hydraulic discharge effects of the majority most of California's major utility companies. He has also applied his expertise and experience in research the assessment and problem solving of issues related to the entrainment and impingement effects of marine, estuarine and freshwater water intakes and the location and screening technologies associated with these water intakes.

Dr. Mayer's project results and conclusions, several involving multiple years of research, have been submitted to the State and Regional Water Resources Boards and the California Energy Commission (CEC). In addition to his testimony before the Santa Ana and San Diego Regional Water Quality Control Boards, he has also provided professional testimony before Central Coast, San Francisco, and Los Angeles Water Boards in formal hearings and workshops on the results of aquatic resources impact studies, water quality, and thermal and ecological modeling. He appeared as an expert witness on the biological effects resulting from expansion of the Moss Landing Power Plant.

1975 – Present *President, Tenera Environmental Inc. Lafayette, California*

Poseidon Resources - Intake and Discharge Effects of the Huntington Beach and Carlsbad Desalination Project

Dr. Mayer designed and directed the yearlong entrainment abundance and entrainment survival studies for the Poseidon's Huntington Beach and Carlsbad Desalination Projects. He collaborated with Scripps professors Drs. Jenkins and Graham and the potential effects of the facilities' hypersaline discharges. He provided expert witness

testimony, which ultimately led to the issuance of NPDES permits and project approvals by cities of Huntington Beach and Carlsbad.

Marin Municipal Water District – Entrainment Effects of a Pilot Desalination Plant

Dr. Mayer designed and directed studies for determining entrainment effects of a pilot desalination facility to be used to estimate effects of a full-scale facility. He also designed source water studies, mainly for assessing effects to Pacific herring.

Moss Landing, Morro Bay, Huntington Beach, Encina, Diablo Canyon, Potrero, South Bay, Scattergood, Haynes, Alamitos, Redondo Beach, El Segundo, Harbor, San Onofre, Honolulu, Kahe, Waiiau, Cabras (Guam) power plant entrainment and impingement investigations.

Dr. Mayer designed and directed entrainment and impingement studies at the majority of California's power plants, and power plants in Hawaii and Guam in response to the recent Clean Water Act 316(b) Phase II Rule and the California Energy Commission's Application for Certification of new generating units.

Diablo Canyon, San Luis Obispo County, PG&E Diablo Canyon Power Plant

Dr. Mayer designed and directed the ongoing Diablo Canyon thermal effluent studies of discharge water effects on natural populations and habitats of the surrounding area. These studies incorporate *in situ* temperature recording instruments; the construction of a preliminary predictive mathematical model; a 1:75 scale hydraulic model at the University of California, Richmond Hydraulic Field Station; a final three-dimensional computer simulation of the operating prototype; and intertidal and subtidal observations of the distribution and abundance of fishes, invertebrates, and algae.

The study represents California's longest and most comprehensive study of discharge effects on marine organisms. In addition to this ongoing study that began in 1975, he is currently directing discharge effects studies for ConocoPhillips in San Pablo Bay, Mirant Corporation in Antioch, Pittsburg and Potrero California, and recently completed a highly detailed study of Dynergy's South San Diego Bay Power Plant for the San Diego Regional Water Quality Control Board. In conjunction with other studies of repowering this facility, Dr. Mayer consulted with the power plant's former owner Duke Energy of North America on the feasibility and potential impacts of using the offshore international discharge located at the Mexican American border to discharge to rerouting the plant's in-San-Diego-Bay discharge to the offshore diffuser.

Expert Witness Testimony

Dr. Mayer conducted water quality modeling efforts in assessment of EBMUD's planned water diversions and prepared expert testimony of the plaintiff's water quality modeling evidence. The water contract was upheld and environmental assessments were continued under the authority of a court-appointed Special Master. Dr. Mayer provides expert witness testimony as part of the NPDES permit renewal process, the California Energy Commission's Application for Certification process, and during hearings before city councils. He has also received additional EPA training and certification in the use and interpretation of the EPA's QUAL-2e and is familiar with other commonly employed thermal and hydraulic models, including USFWS IFIM series models and the Better model.

1973 – 1975 Senior Biologist, Marine Biological Consultants, Costa Mesa, California

Designed and conducted studies for compliance with California State Thermal Plan for the Control of Temperature in Inland and Marine Waters – Southern California Edison

Selected Publications and Technical Reports

Steinbeck, J., J. Hedgepeth, P. Raimondi, G. Cailliet, and David Mayer. 2007. Assessing power plant cooling water intake system entrainment impacts. California Energy Commission Consultant Report, CEC-700-2007-010, 130 pages.

Tenera Environmental. 2006. Draft Marin Municipal Water District Desalination Facility Intake Effects. Prepared for URS Corporation, Oakland, CA. **Contributor.**

Tenera Environmental. 2006. ConocoPhillips Technology Installation and Operation Plan. Prepared for ConocoPhillips, Rodeo, CA. **Contributor.**

Tenera Environmental. 2005. Huntington Beach Desalination Facility Intake Effects Assessment. Prepared for Poseidon Resources Corporation. August 2005. **Contributor.**

Tenera Environmental. 2005. Carlsbad Desalination Facility Feedwater Intake Effects Assessment. Prepared for Poseidon Resources Corporation. November 2005. **Contributor.**

Professional Affiliations

Estuarine Ecology Team of the Sacramento/San Joaquin Interagency Ecological Program, American Society of Naturalists, Western Society of Naturalists, Pacific Fisheries Biologists, American Institute of Fisheries Research Biologists